



**British
Geological Survey**
NATURAL ENVIRONMENT RESEARCH COUNCIL

STARS 
Soils Training And Research Studentships



The University of
Nottingham

UNITED KINGDOM • CHINA • MALAYSIA

Investigation of zinc nanoparticles in soil environments

Beckie Draper

MSc (Analytical science), BSc (Chemistry)

**Thesis submitted to the University of Nottingham for the degree of
Doctor of Philosophy, 2021**

Abstract.....	VI
List of tables and figures.....	VII
Abbreviations.....	X
Chapter 1: Review – zinc nanoparticles in soil environments.....	1-52
1.1 Defining nanoparticles	
1.2 Zinc nanoparticles	
1.3 Processes affecting zinc nanoparticles in soil environments	
1.3.1 Aggregation and agglomeration	
1.3.2 Dissolution	
1.3.2.1 Thermodynamic solubility	
1.3.2.2 Kinetic dissolution rate	
1.3.3 Chemical transformation	
1.3.4 Adsorption	
1.4 Experimental variables	
1.4.1 Important factors	
1.4.1.1 pH	
1.4.1.2 Coatings	
1.4.1.3 Humic substances	
1.4.1.4 Ionic zinc	
1.4.1.5 Size	
1.4.2 Commonly used unrepresentative experimental parameters	
1.4.2.1 Unrealistic concentration	
1.4.2.2 Pristine nanoparticles	
1.4.2.3 Simplified matrix	
1.5 Applied ecotoxicology and environmental fate studies	
1.5.1 Waste water treatment plants	
1.5.2 Toxicity to plants	
1.6 Modelling	
1.7 Analytical techniques and instruments used for nanoparticle analysis in soil environments	
1.7.1 Sample preparation techniques for soil experiments	
1.7.1.1 Spiking procedure	
1.7.1.2 Extraction procedure	
1.7.2 Characterisation and measurement of nanoparticles	
1.7.2.1 Counting methods	
1.7.2.2 Ensemble methods	
1.7.2.3 Separation methods	
1.7.3 Inductively coupled plasma	
1.7.4 Mass spectrometry	
1.7.4.2 Isotopic labelling	
1.8 Aims and objectives of this thesis	
Chapter 2: Materials and methods.....	53-59
2.1 Producing and characterising zinc sulphide nanoparticles	
2.2 Soil sampling and preparation	
2.3 Spiking soil with zinc species	
2.4 Preparing seeds	

- 2.5 Experimental set up
- 2.6 Harvesting and processing
- 2.7 DTPA-extractable zinc
- 2.8 Soil characterisation
- 2.9 Microwave digestion of grass and roots
- 2.10 Hydrofluoric acid digestion of soil
- 2.11 ICP-MS analysis
- 2.12 Statistical analysis

Chapter 3: Development of characterisation methods.....60-104

3.1 Monitoring the dissolution of zinc nanoparticles in the presence of humic acid speciation using size exclusion chromatography

3.1.1 Introduction

3.1.1.1 Zinc nanoparticles in soils

3.1.1.2 Methods for analysing nanoparticle dissolution

3.1.1.2.1 Size exclusion chromatography

3.1.1.3 Aims of work

3.1.2 Materials and methods

3.1.2.1 Zinc species

3.1.2.2 Humic acid preparation

3.1.2.3 Size exclusion chromatography

3.1.2.4 Sample preparation

3.1.3 Initial results

3.1.4 Method development

3.1.4.1 Addition of surfactants to the mobile phase

3.1.4.1.1 Sample preparation

3.1.4.1.2 Results

3.1.4.2 Further adjustments

3.1.4.2.1 Change of column

3.1.4.2.2 Addition of complexing reagents

3.1.4.2.3 Trialling different eluents

3.1.4.2.4 Trialling labelled nanoparticles

3.1.4.2.5 Set up

3.1.4.2.6 Results

3.1.5 Conclusions

3.2 Monitoring zinc nanoparticle dissolution in soils using dialysis

3.2.1 Introduction

3.2.1.1 Aims of work

3.2.2 Materials and methods

3.2.2.1 Zinc species

3.2.2.2 Dialysis tubing

3.2.2.3 Set up

3.2.3 Initial results

3.2.4 Method development

3.2.4.1 Comparison with ionic samples

3.2.4.1.1 Sample preparation

3.2.4.1.2 Results

3.2.4.1.2.1 ⁷⁰Zn spike

3.2.4.1.2.2 Zinc nitrate samples

3.2.4.1.2.3 Isotopically labelled zinc sulphide nanoparticle samples

- 3.2.4.2 Assessing nanoparticle adsorption to equipment
 - 3.2.4.2.1 Sample preparation
 - 3.2.4.2.2 Results
- 3.2.4.3 Eliminating zinc contamination from the dialysis tubing
 - 3.2.4.3.1 Sample preparation
 - 3.2.4.3.2 Results
- 3.2.5 Conclusions
- 3.3 Producing working solutions of a ^{68}ZnS nanoparticle sample for experimental use
 - 3.3.1 Introduction
 - 3.3.1.1 Nanoparticle adsorption onto equipment
 - 3.3.1.2 Sonication
 - 3.3.1.3 Aims of work
 - 3.3.2 Materials and methods
 - 3.3.3 Initial results
 - 3.3.4 Method development
 - 3.3.4.1 Investigating nanoparticle adsorption onto equipment
 - 3.3.4.1.1 Sample preparation
 - 3.3.4.1.2 Results
 - 3.3.4.2 Producing a stable working solution of the required concentration
 - 3.3.4.2.1 Sample preparation
 - 3.3.4.2.2 Results
 - 3.3.5 Conclusions
- 3.4 Overall conclusions

Chapter 4: Effects of different zinc nanoparticles on soil and ryegrass.....105-142

- 4.1 Background
- 4.2 Materials and methods
 - 4.2.1 Zinc species
 - 4.2.2 Soil sampling, preparation and characterisation
 - 4.2.3 Preparing seeds
 - 4.2.4 Experimental set up
 - 4.2.5 DTPA-extractable zinc
 - 4.2.6 Harvesting
 - 4.2.7 Microwave digestion of grass and roots
 - 4.2.8 Hydrofluoric acid digestion of soil
 - 4.2.9 Sequential extraction
 - 4.2.10 ICP-MS analysis
 - 4.2.11 Statistical analysis
- 4.3 Results and discussion
 - 4.3.1 Nanoparticle characterisation
 - 4.3.2 Soil characteristics
 - 4.3.3 Available zinc in soils
 - 4.3.4 Weight and length of grass samples
 - 4.3.5 Zinc concentration of grass samples
 - 4.3.6 Zinc offtake
 - 4.3.7 Zinc concentration of roots
 - 4.3.8 Total zinc in soils
 - 4.3.9 Sequential extraction
- 4.4 Conclusions

Chapter 5: Effects of different zinc nanoparticles on mycorrhizal fungi and wheat.....143-179

- 5.1 Background
- 5.2 Materials and methods
 - 5.2.1 Zinc species
 - 5.2.2 Arbuscular mycorrhizal fungi species
 - 5.2.3 Soil sampling, preparation and characterisation
 - 5.2.4 Preparing seeds
 - 5.2.5 Experimental set up
 - 5.2.6 Harvesting and processing
 - 5.2.7 AMF staining
 - 5.2.8 AMF counting
 - 5.2.9 Microwave digestion of plant material
 - 5.2.10 DTPA-extractable zinc of soil
 - 5.2.11 Soil *E* values
 - 5.2.12 Statistical analysis
- 5.3 Results and discussion
 - 5.3.1 Nanoparticle characterisation
 - 5.3.2 Soil characteristics
 - 5.3.3 Weight of wheat samples
 - 5.3.4 Stem length of wheat samples
 - 5.3.5 Number of heads
 - 5.3.6 AMF colonisation
 - 5.3.7 Zinc concentration of plant samples
 - 5.3.8 Zinc offtake
 - 5.3.9 Soil pH
 - 5.3.10 DTPA-extractable zinc of soil
 - 5.3.11 Soil *E* values
 - 5.3.12 Biological concentration ratio
- 5.4 Conclusions

Chapter 6: Discussion, conclusions, future research needs.....180-191

- 6.1 Current issues and project conclusions
- 6.2 New avenues for future research
 - 6.2.1 Long term low dose exposures
 - 6.2.2 Poly nanoparticle systems
 - 6.2.3 Different soil types
 - 6.2.4 Trans-generational transfer
 - 6.2.5 Trophic transfer
- 6.3 Promising analytical techniques
 - 6.3.1 Field flow fractionation
 - 6.3.2 Single particle ICP-MS
 - 6.3.3 Multi collector ICP-MS
- 6.4 Overall conclusions

References

Appendix

Abstract

Nanoparticles (NPs) are materials that have at least one dimension between 1 – 100 nm. Zinc oxide (ZnO) NPs have properties such as UV-light absorption that make them suitable for adding to personal care products. Many ZnO NP-containing products are routinely rinsed into household wastewater and the resulting zinc NP-containing biosolids frequently used to fertilise agricultural soils.

This thesis aimed to investigate potential methods to detect and analyse zinc NPs in natural soil environments as a result of biosolid application. For this, two different strategies were used. The first intended to look at the mechanism of zinc NP dissolution and fixation in soils by developing methods based on dialysis and size exclusion chromatography (SEC). The second aimed to grow plants on soils spiked with different zinc NPs in order to observe differences in various parameters.

Preliminary experimental work focused on method development and determined that NPs can exhibit different behaviours in different solutions and can readily adsorb to equipment surfaces. It was also found that SEC suffered severely from zinc NP column adsorption which persisted despite many attempts to rectify the issue and attempts to use dialysis experienced similar issues.

Following this, experimental work shifted focus to investigate the different behaviours of ZnO NPs, ZnSO₄, ZnS NPs and Zn₃(PO₄)₂ in soil and ryegrass. Pristine ZnO NPs were shown to dissolve quickly in soil and followed a similar pattern to ZnSO₄ for Zn_{DTPA}, but sequential fractionation results revealed that they behaved differently to ZnSO₄. ZnO NPs also reacted differently to aged ZnS NP and Zn₃(PO₄)₂ particles, which did dissolve, but very slowly. This experiment indicated that ZnS NPs could potentially be safe for crops while still providing nutrition, which would make them useful as a potential method of fertilisation.

The next experiment examined the same four zinc species with AMF and wheat. Results suggested that ZnS NPs could potentially provide a long-term supply of zinc that supports the biofortification of cereal grains while also avoiding issues of toxicity that can be associated with ZnSO₄ or ZnO NP fertilisers.

Overall, both these experiments highlighted that it is not applicable to test ZnO NPs and subsequently apply the results to aged particles. Studies using ZnO NPs are likely to observe fast NP dissolution and high zinc availability, potentially leading to concerns over zinc toxicity that may not have been raised if appropriately aged particles had been used instead.

List of tables and figures

Figures

- 1.1 - Size comparison of nanoparticle range with some common biological entities
- 1.2 - Factors that affect nanoparticle behaviour
- 1.3 - Potential routes of zinc nanoparticles into soil environments
- 1.4 - Transformations of zinc nanoparticles during sewage treatment and disposal
- 1.5 - Processes governing nanoparticle fate, behaviour and toxicity in soil environments
- 1.6 - Diagram of Derjaguin-Landau-Verwey-Overbeek theory
- 1.7 - Mechanism of dissolution
- 1.8 - Brownian motion
- 1.9 - Hydrodynamic diameter of particle
- 1.10 - Analyte separation in ion exchange chromatography
- 1.11 - Mechanism and order of analyte separation in size exclusion chromatography
- 1.12 - Molecular structures of surfactants Triton X-100 and sodium dodecyl sulphate
- 1.13 - Surfactant molecules with their hydrophobic tails (A) and hydrophilic heads (B) can form structures such as: bilayers (C), micelles (D) and liposomes (E)
- 1.14 - Nanoparticles without surfactant can aggregate and become adsorb to the stationary phase (A). The addition of surfactants to the mobile phase can suppress adsorption (B)
- 1.15 - Diagram of ICP torch
- 1.16 - Sector Field mass analyser
- 1.17 - Quadrupole mass analyser
- 1.18 - Inductively coupled plasma-mass spectrometry
- 2.1 - Transmission electron microscopy images of synthesised ZnS NPs at different magnifications
- 2.2 - Diethylenetriaminepentaacetic acid (DTPA) forming a coordination complex with a zinc ion
- 3.1 - Mechanism and order of analyte separation in size exclusion chromatography
- 3.2 - TEM images of ZnS NPs at different magnifications
- 3.3 - SEC-ICP-MS chromatogram showing elution of ZnS nanoparticles at day 1

- 3.4 - SEC-ICP-MS chromatogram showing injection of 0.005 M EDTA
- 3.5 - Molecular structures of surfactants Triton X-100 and sodium dodecyl sulphate
- 3.6 - Surfactant molecules with their hydrophobic tails (A) and hydrophilic heads (B) can form structures such as: bilayers (C), micelles (D) and liposomes (E).
- 3.7 - Nanoparticles without surfactant can aggregate and become adsorb to the stationary phase (A). The addition of surfactants to the mobile phase can suppress adsorption (B)
- 3.8 - ZnS (10 mg L⁻¹ Zn) in SDS eluent at pH 4
- 3.9 - ZnS (10 mg L⁻¹ Zn) in Triton X-100 eluent at (A) pH 4 and (B) pH 6
- 3.10 - Zn(NO₃)₂ (10 mg L⁻¹ Zn) in Triton X-100 eluent
- 3.12 - Concentration of (A) ⁶⁶Zn, (B) ⁶⁸Zn and (C) ⁷⁰Zn in blank samples, internal and external dialysis tubing solutions
- 3.13 - Equilibration of ⁷⁰Zn spike across dialysis tubing in ⁶⁸Zn samples
- 3.14 - Equilibration of ⁶⁶Zn across dialysis tubing in Zn(NO₃)₂ samples
- 3.15 - Equilibration of ⁶⁸Zn across dialysis tubing in ⁶⁸ZnS samples
- 3.16 - Average concentration of ⁶⁸Zn under different conditions
- 3.17 - Sonicating water bath (A) and sonicating probe (B)
- 3.18 - Concentration of ⁶⁸Zn in working solution before and after sonication
- 3.19 - Average ⁶⁸Zn concentration over time in (A) Milli-Q water and (B) calcium nitrate working solutions
- 3.20 - Average ⁶⁸Zn concentration over minutes (A) and days (B) in working solutions
- 4.1 - Orthogonal contrasts of the five different treatments (control, soil spiked with ZnS NPs, ZnO NPs, ZnSO₄ and Zn₃(PO₄)₂)
- 4.2 - TEM images of ZnO NPs at A – 50 nm and B – 20 nm, and ZnS NPs at C – 50 nm and D – 5 nm
- 4.3 - Available zinc (Zn_{DTPA}) from unvegetated soils spiked with different zinc species over time
- 4.4 - Zinc storage in soils, in solution, exchangeable and non-exchangeable
- 4.5 - Average available zinc (Zn_{DTPA}) concentration of soil from vegetated and unvegetated samples following 20 weeks of incubation
- 4.6 - Average dry weight of harvested grass
- 4.7 - Average length of harvested grass
- 4.8 - Average total zinc (Zn_{Total}) concentration of harvested grass
- 4.9 - Total zinc (Zn_{Total}) concentration of grass compared to available zinc (Zn_{DTPA}) concentration of soil
- 4.10 - Total zinc (Zn_{Total}) concentration of grass compared to available zinc (Zn_{DTPA}) concentration of soil
- 4.11 - Average zinc offtake (Zn_{Offtake}) of harvested grass
- 4.12 - Zinc offtake (Zn_{Offtake}) of grass compared to available zinc (Zn_{DTPA}) concentration of soil
- 4.13 - Zinc offtake (Zn_{Offtake}) of grass compared to available zinc (Zn_{DTPA}) concentration of soil
- 4.14 - Average total zinc (Zn_{Total}) concentration of roots
- 4.15 - Average root to shoot zinc translocation %
- 4.16 - Average total zinc (Zn_{Total}) spike of unvegetated soil samples
- 4.17 - Average % of zinc in fractions of unvegetated soils.
- 4.18 - Average total zinc (Zn_{Total}) concentration of sequential extraction fractions of unvegetated soils.
- 5.1 - AMF forms symbiotic associations with plant roots and develops extensive, branching networks of extraradical hyphae that facilitate nutrient transfer between plant roots and soil
- 5.2 - Zinc storage in soils, in solution, exchangeable and non-exchangeable

- 5.3 - Orthogonal contrasts of the five different treatments (control, soil spiked with ZnS NPs, ZnO NPs, ZnSO₄ and Zn₃(PO₄)₂)
- 5.4 - TEM images of ZnO NPs at A – 50 nm and B – 20 nm, and ZnS NPs at C – 50 nm and D – 5 nm
- 5.5 - Average dry weight of harvested wheat
- 5.6 - Average lengths of harvested wheat
- 5.7 - Average number of heads of harvested wheat
- 5.8 - Wheat root segment colonised with stained mycorrhizal fungi
- 5.9 - Average % wheat root colonisation
- 5.10 - Average total zinc (Zn_{Total}) concentration of harvested wheat
- 5.11 - Average zinc offtake (Zn_{Offtake}) of harvested wheat
- 5.12 - Average soil pH
- 5.13 - Soil pH verses grain zinc offtake (Zn_{Offtake})
- 5.14 - Post harvest average available zinc (Zn_{DTPA}) of soil
- 5.15 - Average *E* value of soil
- 5.16 - Soil *E* value vs grain zinc offtake (Zn_{Offtake}).
- 5.17 - Soil *E* value vs soil available zinc (Zn_{DTPA})
- 5.18 - Average biological concentration ratio (BCR)
- 6.1 - Field Flow Fractionation (FFF)
- 6.2 - Single particle ICP-MS – effect of dwell and settling times.

Tables

- 1.1 - Methods for monitoring zinc nanoparticle transformation in the presence of humic substances
- 1.2 - Recommended minimum nanoparticle characterisation
- 1.3 - Stable isotopes of zinc
- 3.1 - Sample running order
- 3.2 - Average mass (µg) of ⁶⁸Zn in samples
- 4.1 - Average pH of unvegetated soils from beginning to end of the experiment
- 4.2 - Significant orthogonal contrasts of grass weight data.
- 4.3 - Significant orthogonal contrasts of stem length.
- 4.4 - Significant orthogonal contrasts of grass total zinc
- 4.5 - Results of analysis of variants (ANOVA) tests comparing grass total zinc (Zn_{Total}) concentration of ZnS NP spiked samples with that of control samples.
- 4.6 - Orthogonal contrasts of grass zinc offtake
- 4.7 - Average sequential extraction recovery rates (%)
- 5.1 - Significant orthogonal contrasts of stem/leaf weight
- 5.2 - Significant orthogonal contrasts of grain weight
- 5.3 - Significant orthogonal contrasts of root weight
- 5.4 - Significant orthogonal contrasts of stem length
- 5.5 - Significant orthogonal contrasts of number of heads
- 5.6 - Significant orthogonal contrasts of AMF colonisation.
- 5.7 - Significant orthogonal contrasts of stem/leaf total zinc
- 5.8 - Significant orthogonal contrasts of grain total zinc
- 5.9 - Significant orthogonal contrasts of root total zinc
- 5.10 - Significant orthogonal contrasts of stem/leaf zinc offtake
- 5.11 - Significant orthogonal contrasts of grain zinc offtake
- 5.12 - Significant orthogonal contrasts of root zinc offtake (Zn_{Offtake}).
- 5.13 - Significant orthogonal contrasts of soil pH.
- 5.14 - Significant orthogonal contrasts of average available zinc (Zn_{DTPA}).
- 5.15 - Significant orthogonal contrasts of soil *E* values

Abbreviations

AAS	atomic absorption spectrometry
AGNES	absence of gradients and Nernstian equilibrium stripping
AMF	arbuscular mycorrhizal fungi
ANOVA	analysis of variance
ASV	anodic stripping voltammetry
AUC	analytical ultracentrifugation
$C_2H_3NaO_2$	sodium ethanoate
$C_2H_7NO_2$	ammonium ethanoate
$CaCl_2$	calcium chloride
$Ca(NO_3)_2$	calcium nitrate
CH_3CO_2H	ethanoic acid
cm	centimetre
DI	deionised
DTPA	diethylenetriaminepentaacetic acid
DLS	dynamic light scattering
DLVO	Derjaguin-Landau-Verwey-Overbeek
EC	electrical conductivity
EDTA	ethylenediaminetetraacetic acid
FA	fulvic acid
H_2	hydrogen
HA	humic acid
$HClO_4$	perchloric acid
He	helium
HF	hydrofluoric acid
HNO_3	nitric acid
hr	hours
HS	humic substance
ICP	inductively coupled plasma
IEC	ion exchange chromatography
K_d	distribution coefficient
kg	kilogram
KOH	potassium hydroxide
LOI	loss on ignition
MS	mass spectrometer/spectrometry
μg	microgram
min	minutes
mL	millilitre
mm	millimetre
nm	nanometre
NP	nanoparticle
rpm	revolutions per minute
SDS	sodium dodecyl sulphate
SEC	size exclusion chromatography
SEM	scanning electron microscopy
TEOA	triethanolamine
TEM	transmission electron microscopy
TOF	time-of-flight
WHC	water holding constant
WWTP	wastewater treatment plant
w/v	weight/volume

XRD	X-ray diffraction
Zn	zinc
Zn(NO ₃) ₂	zinc nitrate
ZnO	zinc oxide
Zn ₃ (PO ₄) ₂	zinc phosphate
ZnSO ₄	zinc sulphate
ZnS	zinc sulphide

Chapter 1

Review – zinc nanoparticles in soil environments

1.1 Defining nanoparticles

The term 'nanotechnology' refers to a broad range of different fields all concerned with the engineering of functional systems at the molecular scale [1]. In recent decades, nanotechnology has been used to develop and produce a large number of products that have been brought to the market and so the description of 'nanoproduct' covers many things, including: products with nanosized pores, products with nanometer (nm) coatings or products containing nanoparticles (NPs).

In order to assess, monitor and regulate the possible environmental and health risks associated with nanoproducts, the terms that describe them need to be universally defined so that policy makers are able to produce clear regulations and risk assessments, and companies are able to correctly label their products [2].

In a recent review of scientific writings and policy documents, Boholm and Arvidsson identified 36 different definitions of the terms 'nanomaterial', 'nanoparticle' or 'nano-object' [3]. Another review from the same year collated all of the varying definitions of 'nanomaterial' from 14 different regulatory authorities around the world [4]. The lack of parity in classification can cause scientific work to be based on an inconsistent understanding of the nature of the substances being assessed, and mean that communication between scientists, regulatory agencies and companies becomes obscured.

In 2011, the European Commission published its recommendations on the definition of nanomaterials [5]:

“Nanomaterial” means a natural, incidental or manufactured material containing particles, in an unbound state or as an aggregate or as an agglomerate and where,

for 50% or more of the particles in the number size distribution, one or more external dimensions is in the size range 1 nm – 100 nm.

In specific cases and where warranted by concerns for the environment, health, safety or competitiveness the number size distribution threshold of 50% may be replaced by a threshold between 1 and 50%.'

However, the recommendation contains the acknowledgement that:

'there is no scientific evidence to support the appropriateness of this (100 nm) value.'

While most regulatory authorities have also defined the nanoscale as 1 – 100 nm [4, 6], this lack of scientific justification for defining nanomaterials predominantly by their size has led to concern that other potentially hazardous attributes may be overlooked, or that some materials may display nano-related risks but not be categorised as a nanomaterial [2, 7, 8]. Others have argued that it is the sizing scale that is unsuitable, advocating for an upper limit of 30 [9], 500 [10, 11] or 1000 nm [12], a lower limit of 0.2 nm [13], or for an additional definition based on volume-specific surface areas [14].

The European Commission's recommendation also highlighted the fact that despite this focus on size, validated analytical characterisation and sizing techniques were needed to be developed in order to put this into practice and, at the time of writing, this is still the case:

'Measuring size and size distributions in nanomaterials is challenging in many cases and different measurement methods may not provide comparable results.

Harmonised measurement methods must be developed with a view to ensuring that the application of the definition leads to consistent results across materials and over time. Until harmonised measurement methods are available, best available

alternative methods should be applied' [5].

Although some methods exist for the characterisation of nanomaterials in simple matrices, the assessment of nanomaterials in complex media such as soil is currently extremely analytically challenging and prohibitively expensive as a routine analytical procedure, making adhering to legislation difficult and dependent on suitable measuring methods and reference materials being developed.

Despite all of this, NPs are generally referred to as materials that have at least one dimension between 1 – 100 nm [15] (**Figure 1.1**). Their small size means that they have a much larger proportion of their atoms on the particle surface than their bulk counterparts. Atoms on a particle's surface are exposed to the surrounding environment and so tend to be more reactive than internal atoms. NPs' large surface area-to-volume ratio can affect their behaviour, as can other features such as their size, shape and surface coating. NPs are also highly affected by their own concentration [16] and by the chemistry of the medium in which they are dispersed [17] (**Figure 1.2**).

All of these different factors interact with one another making NP behaviour difficult to predict. Studies looking into NP reactions can often only report on the specific particle type under the specific conditions that have been examined and are not currently able to extrapolate results to cover other situations. It is important not to make assumptions about NPs' toxicity and health impacts under conditions that have not been studied based on knowledge of their behaviour under alternative conditions or on the known behaviour of bulk particles of the same substance.

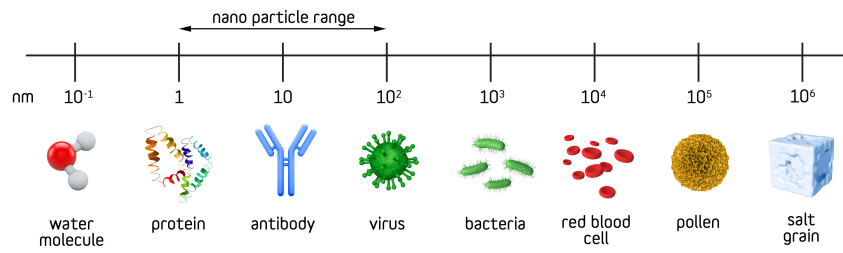


Figure 1.1 Size comparison of the nanoparticle range with some common biological entities. Source: author

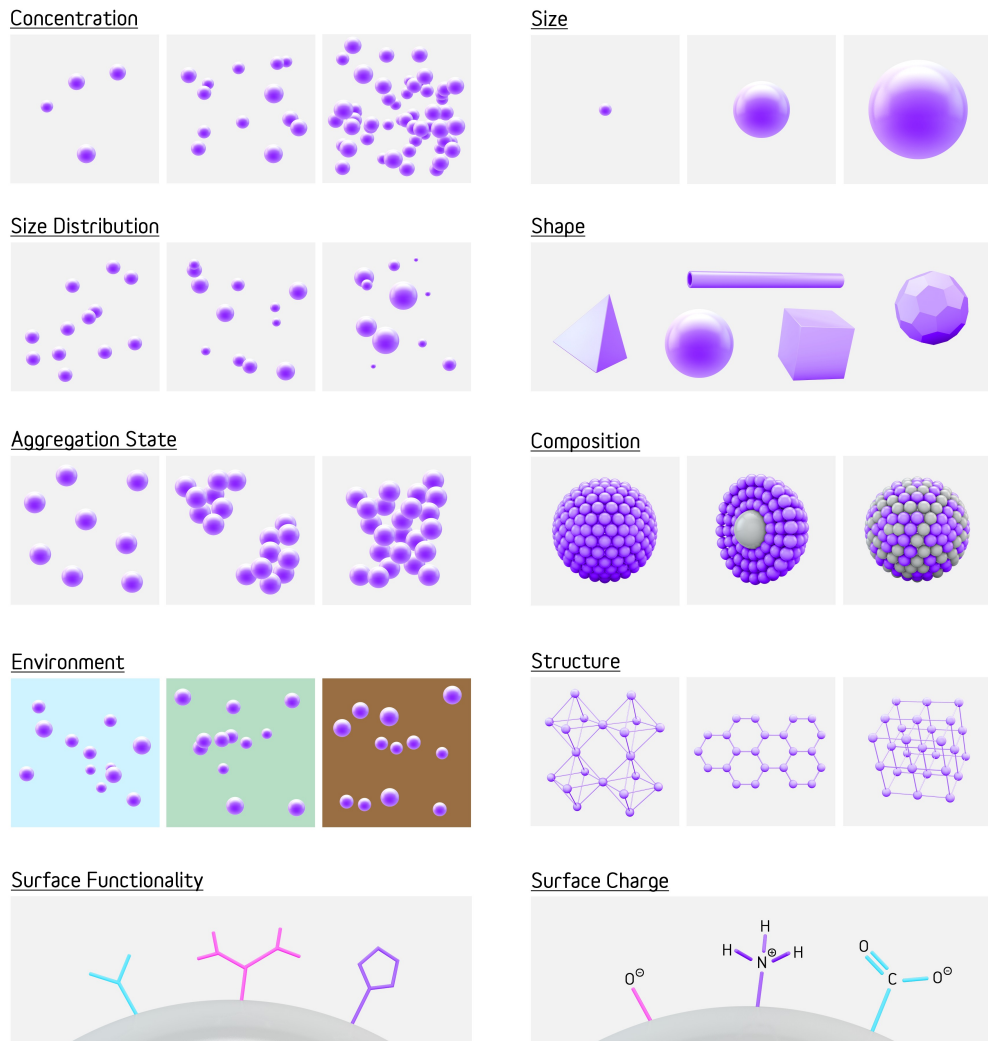


Figure 1.2 Factors that affect nanoparticle behaviour. Source: author

1.2 Zinc nanoparticles

Zinc oxide (ZnO) has properties that have long been harnessed to produce useful products and ZnO NPs have been shown to enhance many of these properties even further. ZnO NPs demonstrate heightened anti-bacterial and anti-fungal characteristics compared to bulk ZnO [18, 19] and so are used for many purposes, including: textile production to produce clothes with anti-microbial properties [20-22]; in rubber production [23] which is then used to manufacture mould-resistant medical equipment; in anti-bacterial oral care products [24] and in anti-microbial food packaging [25, 26].

ZnO has high UV-light absorption properties which makes it suitable for adding to sunscreens and cosmetics. However, bulk ZnO is opaque and people are often reluctant to use products that leave a white residue on the skin. ZnO NPs with a particle size of < 70 nm are visible-light transparent and the particle size for optimum UV-absorbance has been shown to be around 40 nm [27, 28] so a great many common personal care products now contain ZnO NPs [29-31]. The number and variety of products available that utilise ZnO NPs means that there are many potential routes for their release into the environment (**Figure 1.3**): cosmetics and sunscreens can be washed into lakes and rivers when people swim [32]; factories can accidentally release NPs into the atmosphere or nearby waterways during production or through their waste streams; zinc NPs are increasingly being introduced directly onto fields as fertilisers and pesticides [33, 34] and discarded products end up on landfill sites where NPs can leach into the surroundings [35, 36]. One major route is via household wastewater. Many ZnO NP-containing products, including paints, mouthwashes, creams and shampoos, are rinsed into sinks and ZnO NPs in clothes are leached into water during laundering [37].

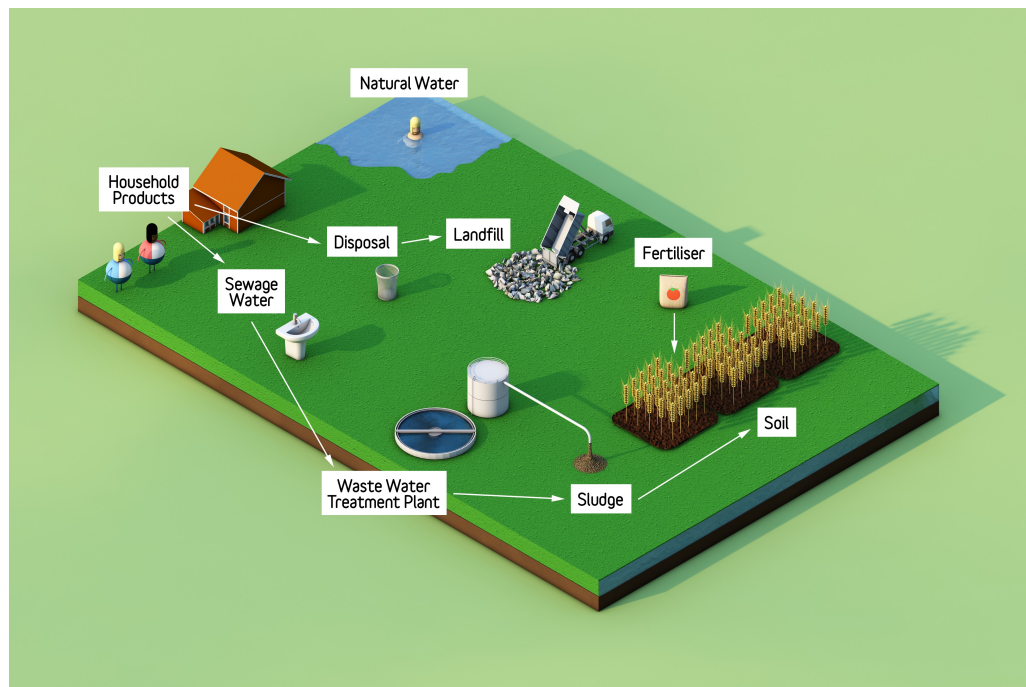


Figure 1.3 Potential routes of zinc nanoparticles into soil environments. Source: author

The resulting sewage is transported to wastewater treatment plants (WWTPs) but none of the sanitisation treatment stages are specifically designed to remove NPs so they can remain in the purified water and accumulate in the sludge [38], where ZnO NPs tend to undergo anaerobic sulfidation [39-42]. Composting the sludge causes further zinc transformations, most notably into zinc phosphate ($Zn_3(PO_4)_2$) [39, 40] (**Figure 1.4**). Treated sewage sludge contains high concentrations of nutrients and organic matter and so is often spread onto agricultural fields to fertilise the soil [43, 44]. Properties such as the ability to absorb UV radiation or inhibit bacteria that make zinc NPs desirable as product ingredients could become harmful if applied in the environment. For example, it has been suggested that ZnO NPs inhibit *Azotobacter*, P-solubilizing and K-solubilizing bacteria in soils [45] and causes coral bleaching in oceans [46].

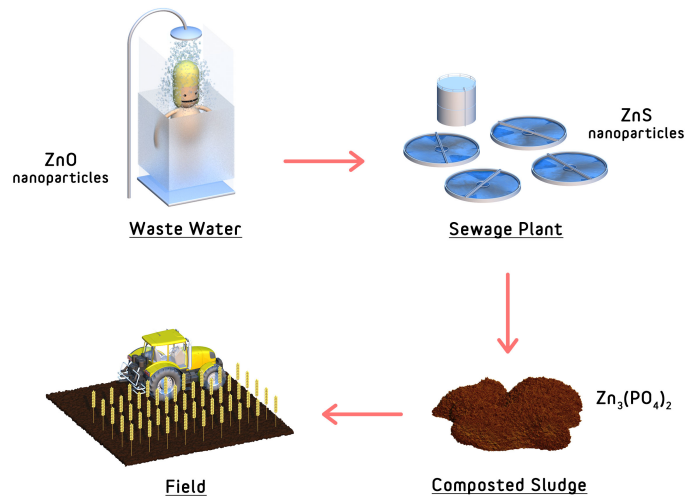


Figure 1.4 Transformations of zinc nanoparticles during sewage treatment and disposal. Source: author

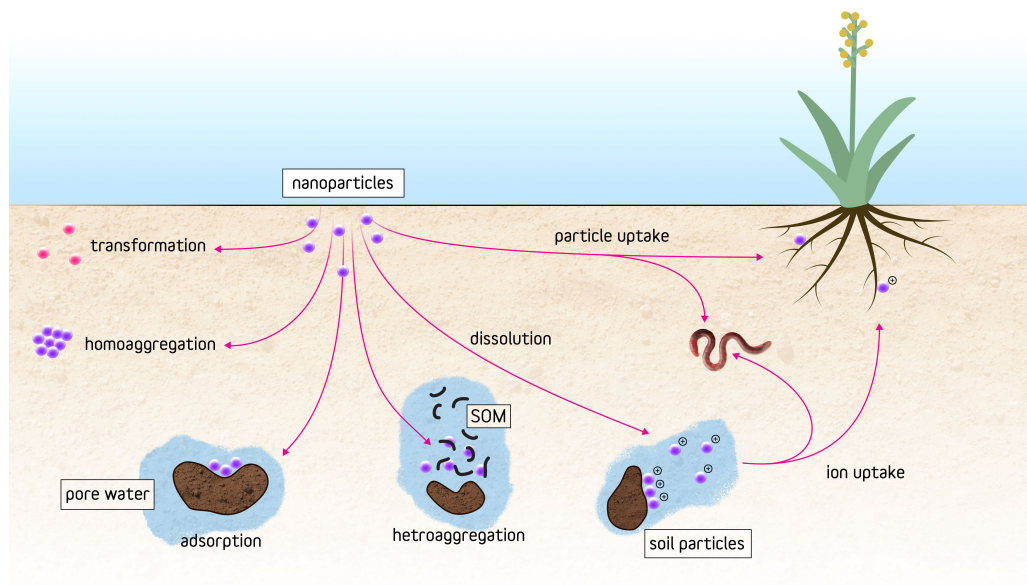


Figure 1.5 Processes governing nanoparticle fate, behaviour and toxicity in soil environments. SOM: Soil organic matter. Source: author

The main processes that control zinc NP mobility, availability, bioaccumulation and toxicity in soil are chemical transformation, aggregation/agglomeration, adsorption and dissolution (**Figure 1.5**), and these must all be investigated, understood and monitored in order to establish robust risk assessments for both acute and chronic zinc NP exposure resulting from environmental release. In addition, for foods to be certified as organic in the UK, the Soil Association specifies that materials containing manufactured NPs where the mean particle size is < 200 nm and the minimum particle size is < 125 nm, must not be used [47]. At present, obtaining this information is analytically problematic, so for all of this to be undertaken requires much more work to be done in developing relevant experimental approaches before proven protocols and certified reference materials can become universally available.

1.3 Processes affecting zinc nanoparticles in soil environments

By the time NPs are discharged from WWTPs into terrestrial ecosystems they will have fundamentally different chemical and physical properties than the pristine particles from which they originated [48]. Once NPs are present in soil environments there are many further transformations that may take place (**Figure 1.5**) and NP interactions with solid and solution phase species can interfere with the extent and timescales of processes that affect soil nutrients and minerals. Understanding these processes requires the establishment of methods that can detect and analyse NP under actual environmental conditions. Looking at some of these processes in simplified systems can sometimes improve understanding of potential environmental outcomes, however, extrapolating results for a specific pristine NP in a simplified system to other NPs in complex natural soil systems is probably unviable [49].

1.3.1 Aggregation and agglomeration

In scientific publications, the terms 'aggregate' and 'agglomerate' are regularly used interchangeably. In 2002, a review of the nomenclature recommended that 'agglomerate' should be used to describe all assemblages of NPs and 'aggregate' reserved only for pre-nucleation structures [50] but, despite this, both terms are still regularly used as synonyms. When they are differentiated, it is most commonly by following the International Organization for Standardization definitions of 'aggregate' meaning fused or irreversibly attached primary particles and 'agglomerate' as particles which are weakly bound or subject to a reversible attachment [51]. In practice however, it is very difficult to measure or even estimate the strength of NP attachment [52], making adhering to classifications difficult. Most powdered NP samples contain both agglomerates and aggregates [50, 53, 54] which further explains their common use as exchangeable terms, although it has also been suggested that below a diameter of 1 μm , most NP clumps will only be comprised of strongly bonded particles [55].

However it is described, the clumping together of NPs plays an important role in determining NP behaviour, bioavailability, transport, fate, reactivity and toxicity in environmental matrices. Aggregation and agglomeration decreases the available NP surface area which can inhibit dissolution and reduce reactivity. NP transport can also be affected because larger agglomerates are potentially more hindered in their movement through soil than individual NPs [48].

Studies often apply colloidal science principles based around the Derjaguin-Landau-Verwey-Overbeek (DLVO) theory, to try to model NP agglomeration behaviour under various conditions. DLVO theory takes account of two types of force: attractive van der Waals' forces, and electrostatic repulsion. NP stability is attained when these

two forces balance one another, which is dependent on the distance between NPs (**Figure 1.6**) [56]. Particles located in the primary minimum area are regarded as being irreversibly aggregated, while particles in the secondary minimum area are reversibly agglomerated [57].

DVLO theory assumes that particle surface charges remain constant and that their surfaces are infinitely flat. NPs' small size means that their surface curvature is too pronounced to fit this assumption, but DVLO theory has still been shown to frequently fit experimental results [58-63].

Both matrix chemistry and NP characteristics such as size, shape, structure, composition and surface coatings, acting simultaneously affect NP clumping [64]. It has been found that pH [65], ionic strength [65] and organic matter [66] alter the electrostatic repulsion between NPs, while NP concentration changes the collision frequency between particles [67], and NP morphology alters diffusion and attachment, all of which have an impact on NP agglomeration kinetics.

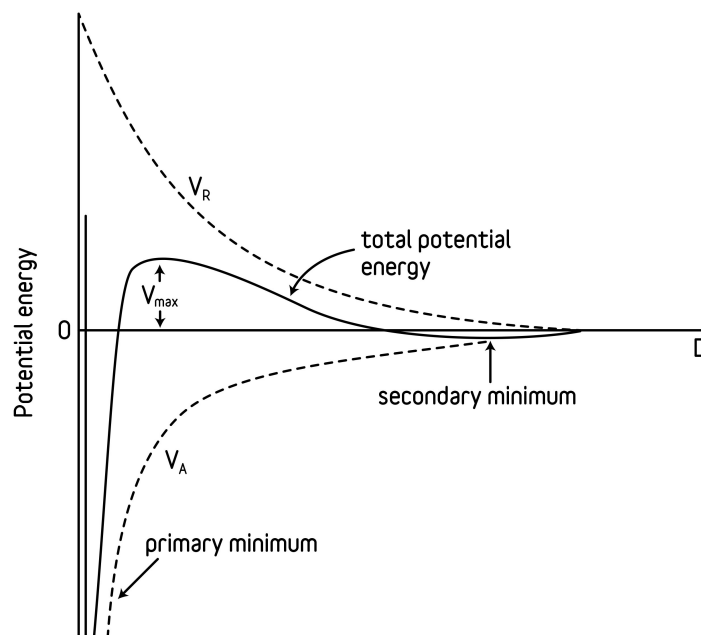


Figure 1.6 Diagram of Derjaguin-Landau-Verwey-Overbeek theory. D: Separation distance; V_A : Attractive van de Waals potential; V_R : Repulsive electrostatic potential. Source [56]

In one study, Majedi et al. designed an orthogonal array experiment to assess the impact of six different environmental factors (NP concentration, organic acid type, organic acid concentration, pH, salt content and electrolyte type) on the agglomeration of ZnO NPs and found that the concentration of organic acid was the most significant factor [68]. It has also been found that the smallest attainable aggregate size of NPs is not altered by the solvent type used or by the NP concentration [69] and that ZnO NPs are most prone to aggregation at the isoelectric point of pH 8.7 [70].

1.3.2 Dissolution

ZnO NPs will dissolve to some degree under most conditions. Soil pore waters provide an aqueous environment for NPs to undergo dissolution and so dissolution is a potentially very important aspect of zinc NP bioavailability and toxicity in soils [17]. The mechanism of dissolution involves components of a solid particle migrating from its surface, through a saturated diffusion layer into a solution phase (**Figure 1.7**) and NP surfaces possess a large proportion of edge, corner and terrace atoms which have been shown to be preferred detachment sites [71].

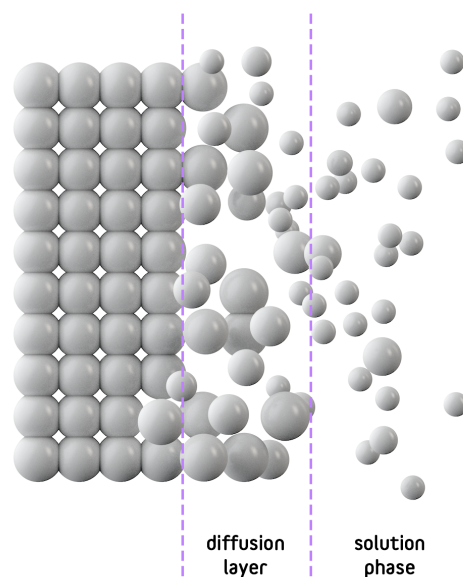


Figure 1.7. Mechanism of dissolution. Components of a solid particle migrate from its surface, through a saturated diffusion layer into a solution phase. Source: author

There have been a number of studies looking at the effects of zinc NPs in soil environments on plants and animal species, with the vast majority of these experiments looking at the short-term toxicity of ZnO NPs at high concentrations [72-74]. Some studies have concluded that observed effects are due to ionic zinc [75-77] some have concluded that toxicity cannot be adequately explained by NP dissolution alone [78-81] and others have not examined dissolution at all. In general, there is uncertainty as to whether results are due to the particles themselves [82], dissolved ions [75-77, 83-85] or a combination of both [86] and a major reason for this is down to the lack of available methods for both extracting zinc species from soils and distinguishing between dissolved zinc and very small zinc NPs.

Recently, following an experiment to identify and characterize zinc sulphide (ZnS) NPs in sewage sludge, Kim et al. [42] recommended that future studies looking at ZnS NP dissolution as a function of size, aggregation state and soil type after biosolid application were needed, but as yet this has not happened.

1.3.2.1 Thermodynamic solubility

In an ideal system, the solubility (S_R) of a small solid spherical particle (γ with radius R) in solution (α) is described by the Ostwald–Freundlich equation [87].

$$k_B T \ln \frac{S_R}{S_\infty} = \frac{2\sigma^{\alpha\gamma} v_2^\gamma}{R}$$

Where S_∞ is the solubility of bulk material (with the radius taken as infinity), T is the temperature, v_2^γ is the volume per molecule in the particle and $\sigma^{\alpha\gamma}$ is the surface tension of particle at its boundary with the solution phase α .

Theoretically, as particle size decreases, the net surface area exposed to the solution phase increases and so the solubility equilibrium should also increase, making NPs theoretically more soluble than bulk particles. However, in reality so-called 'spherical' NPs tend to have highly faceted surfaces rather than being perfect spheres [17, 88]. The complexity of the matrix interactions, the variation in zinc NP properties and behaviours and the difficulties in detection and analysis, means that experimental results can be inconsistent and conflicting, for example, Bandyopadhyay et al. [89] actually found lower dissolution rates in ZnO NPs compared to bulk particles.

Franklin et al. [76] looked at dissolution equilibria of bulk and 30 nm ZnO using dialysis tubing with a pore size of 1 nm at pH 7.6. No difference was found between them and it was suggested that this was due to agglomeration of the NPs. Another study looking at zinc coated onto macronutrient fertilisers also found no difference between NP and bulk ZnO dissolution [90].

David et al. [91] used the electroanalytical technique 'absence of gradients and nernstian equilibrium stripping' (AGNES) to measure the Zn^{2+} concentration in aqueous 0.1 M KCl solutions with three types of ZnO NPs of different sizes and it was found that solubility only increased once the particle diameter was < 20 nm. Above this, the solubility was found to be indistinguishable from that of bulk ZnO dispersions. For ZnS NPs, Zhang et al. found that that in weak ethylenediaminetetraacetic acid (EDTA), the smaller the ZnS particle size, the greater the solubility and that particles with a radius > 3 nm did not dissolve, whereas particles with radius < 1 nm did [92]. Mudunkotuwa et al. [93] focused on dissolution of ZnO NPs in the range of 4 – 130 nm at pH 7.5. It was found that dissolution was indeed size dependent but that classical theoretical models were not accurate enough to enable quantitative

predictions as they do not take agglomeration state or NP surface properties into account.

1.3.2.2 Kinetic dissolution rate

In theory, the dissolution rate of a particle is proportional to its solubility. The rate of dissolution can be described by the Nernst–Brunner equation [94] which indicates that, like solubility, dissolution rate (dC/dt) is also dependent on the surface area (S) of the particle.

$$\frac{dC}{dt} = \frac{DS}{Vh} (C_s - C)$$

Where C is the concentration in solution phase, C_s is the saturation solubility (concentration in the diffusion layer), D is the diffusion coefficient, h is the thickness of the diffusion layer, t is the time and V is the volume of the solution phase.

NPs would therefore be expected to dissolve faster than larger sized materials of the same mass due to their larger surface area-to-volume ratio. As the concentration in the solution phase reaches equilibrium, the dissolution rate should slow down. Other factors such as the surface curvature and texture of the particle, the temperature and the degree of agitation also play important roles. AGNES allows fast *in situ* measurements of zinc ions to be taken and was used to find that the kinetic approach to zinc NP dissolution equilibrium is dependent on the NP concentration and the radius of the agglomerates [91]. However, it has been shown that NP corner, edge and terrace atoms all have different dissolution coefficients and so dissolve at different rates [71], meaning that kinetic studies based on a spherical model that do not take different surface sites into account cannot accurately predict NP dissolution.

The difficulty in interpreting results from all of the many studies is that NP dissolution behaviour in the environment is governed by a complex amalgamation of many

different physiochemical factors (**Figure 1.2**) [17, 68] and current theoretical models do not take all of these factors into account. The complexity is further increased because heterogeneous environments such as soils have constantly changing parameters such as temperature and ionic content, which also play important roles [95]. A mechanistic understanding of all of these processes and how they intersect is a key part of assessing the toxicity and risk of NP release into ecosystems.

1.3.3 Chemical transformation

Sulphidation is an important process that will potentially affect zinc NP persistence and toxicity in the environment. Zinc has a strong affinity for sulphide ligands and ZnO NPs will react with inorganic sulphur present in WWTPs [39, 40] and in terrestrial environments [48]. It has been shown that in the presence of enough sulphide, such as in anaerobic sewage sludge, ZnO NPs will transform into much smaller ZnS NPs [42, 96], which indicates that the mechanism of action is via dissolution and subsequent re-precipitation. A recently published study that looked at the speciation of zinc present in pig manure found that 100% was present as ZnS, and was believed to be entirely composed of agglomerated ZnS NPs [97]. The manure was spread onto soil over a period of 11 years and the resultant zinc speciation monitored. Despite an almost 2-fold increase in the zinc concentration in the amended soil, no remaining ZnS was detected within the soil, indicating that the ZnS had dissolved or transformed.

Phosphate-induced transformation of zinc NPs has also been shown to be a significant process especially during composting, [39, 40, 98, 99] resulting in products that are much larger than the original zinc NP species [98, 99].

Despite this, the literature is overwhelmingly focused on ZnO NPs. This is pertinent when studies are considering the effect of ZnO NP-containing fertilisers and pesticides [90], factory spills or waste from batteries [100], but when the focus of the study is on

the fate of zinc in soil as a result of biosolid application [43, 101] it is more valuable to look at NP ZnS and $Zn_3(PO_4)_2$ because these are the main species that are present [40, 102, 103]. Metal oxides are generally more soluble than the equivalent sulphide, indeed the approximate solubility constants of ZnS and $Zn_3(PO_4)_2$ are 2×10^{-25} and 9×10^{-33} , respectively, whereas ZnO is 4×10^{-10} [104] and it has been shown that bulk ZnO dissolves faster than ZnS in soils [105]. Examining the effects of biosolid application using ZnO NPs is therefore likely to give an over estimation of dissolution rates and ionic zinc availability. There is a growing consensus that research into the release of NPs into the environment needs to begin to focus on realistic conditions and relevant aged species rather than “pristine, as-produced particles” as has often been the case in the past [48, 106-110].

1.3.4 Adsorption

Particle adsorption to soil components such as clays is an important process that is responsible for much of the retention of substances in terrestrial environments. Adsorption isotherm equations are used to describe how particles distribute between liquid pore water phases and solid phases when the sorption process reaches equilibrium and this approach has been used for NPs [79, 84, 111]. The simplest method of estimating NP adsorption is based on the distribution coefficient (K_d). The K_d is the ratio of the NP concentration associated with solid phases to the NP concentration in the aqueous pore water when the system is at equilibrium [112].

$$x = K_d C$$

Where x is the amount adsorbed onto solid phases and C is the solution concentration. For zinc NP adsorption in soils the most commonly fitted models are the Freundlich (K_f) isotherm equation:

$$x = K_f C^n$$

and the Langmuir (K_l) isotherm equation:

$$x = \frac{x_m K_l C}{1 + K_l C}$$

where x_m is the maximum adsorption per unit mass.

In order to improve the determination of the fraction of NPs retained onto solid phases, Cornelis et al. [113] developed a method to calculate retention values (K_r). The method is based on the K_d but takes dissolution into account. The soils were spiked with NPs then the pore waters were extracted and filtered by micro- and ultrafiltration. The unknown retained concentration (M_{solid}) was defined as the amount of added NP, minus the amount that passed through the 0.45 μm microfiltration:

$$M_{\text{solid}} = M_{\text{add}} - M_{\text{NP}} - M_{\text{NP_diss}}$$

Metal that passed through microfiltration was defined as the NP fraction plus the ionic fraction. Metal that passed through the 1 kDa ultrafiltration was defined as the ionic fraction.

$$K_r = (M_{\text{solid}}/M_{\text{NP}}) \times L/S \text{ (L kg}^{-1}\text{)}$$

$$K_r = (M_{\text{add}} - M_{\text{MF}} + M_{\text{geo}}/M_{\text{MF}} - M_{\text{UF}}) \times L/S \text{ (L kg}^{-1}\text{)}$$

Where M_{solid} is the metal NP retained on solid phases (mg kg^{-1}), the M_{NP} is the metal NP fraction (mg kg^{-1}), $M_{\text{NP_diss}}$ is the ionic fraction (mg kg^{-1}), M_{add} is the added metal NP (mg kg^{-1}), M_{MF} is the metal NP that passes through a 0.45 μm filter (mg kg^{-1}), M_{geo} is the geogenic metal (mg kg^{-1}), M_{UF} is the metal NP that passes through a 1 kDa filter (mg kg^{-1}), K_r is the retention (L kg^{-1}), L is the liquid and S is the solid.

This method was used on Ag and CeO_2 NPs in five different soils and it was found that NP retention was different to that of the corresponding bulk particle and soluble salt.

1.4 Experimental variables

Reviewing the growing number of studies examining zinc NPs in the environment highlights a number of factors that have been shown to be central to their behaviour in soil environments. It also exposes a number of experimental parameters that are repeatedly applied but are unrepresentative of the environmental systems that they are purporting to model. This is generally because researchers are forced to set up systems that will work with analytical equipment available and within the viable limits of instrument detection. In addition, there are other variables that have tended to be overlooked and require investigation.

1.4.1 Important factors

1.4.1.1 pH

pH has been shown to be an extremely important variable that affects the agglomeration, dissolution and dispersion of zinc NPs [62, 114, 115]. Waalewijn-kool et al. [116] investigated the effect of time on ZnO NP dissolution in soil and compared it to bulk ZnO and ionic zinc. It was found that pH was the main factor with no NP size dependent effects observed. A later study looking at the toxicity of ZnO NPs compared to bulk ZnO and ionic zinc in earthworms also found no size-dependent effects and that soil pH was the main influencing factor in particle toxicity [117].

Watson et al. [118] looked at the phytotoxicity of ZnO NPs to wheat (*Triticum aestivum*) seedlings in a calcareous and an acid soil and found that exposure caused dose-dependent inhibition of root elongation in the acidic soil but not in the calcareous soil. Another study looking at ZnO NPs in acid and alkaline soils also found that pH was the key factor in zinc availability and ZnO NP phytotoxicity to crops [119]. It has been shown that ZnO NPs are more toxic to *F. candida* [79], and have higher toxicity to soil

microorganisms [120] and soil bacterial communities [121] in acidic soils, and that the toxicity decreases as the soil pH increases.

1.4.1.2 Coatings

Coatings have been shown to be an important factor affecting NP behaviour [63, 122-125], but having an effect on so many different processes can mean that it is not easy to predict how behaviour will be altered. When designing experiments to look at the effects of coated NPs, it is of vital importance to verify that any observed alteration in toxicity or stimulation has not been caused by the coating itself.

Waalewijn-kool et al. [116] assessed the effect of long-term dissolution on bioavailability and toxicity, using triethoxyoctylsilane-coated and uncoated ZnO NPs. The coated ZnO NPs were found to be more toxic to *F. candida* than uncoated, with reduced toxicity at 12 and 3 months equilibration, respectively. In another study, ZnO NPs coated in sodium dodecyl sulphate (SDS) were shown to be protected against dissolution for 2 weeks [126].

In an attempt to evaluate what effects surface coating and lattice doping had on ZnO NP interactions with plants, Mukherjee et al. [124] exposed green pea (*Pisum sativum*) plants to 3 types of ZnO NPs (10 nm bare, 15 nm alumina doped ($\text{Al}_2\text{O}_3@\text{ZnO}$) and 20 nm aminopropyltriethoxysilane coated), bulk ZnO and ionic zinc. Particles were spiked into soil as a dry powder, at concentrations of 250 and 1000 mg kg⁻¹. $\text{Al}_2\text{O}_3@\text{ZnO}$ NPs had a greater negative effect on plant and seed quality than the bare or coated ZnO NPs.

Merdzan et al. [125] looked at the uptake of 3 different ZnO NPs (bare, polyacrylic acid coated and sodium hexametaphosphate coated) in algae to test the hypothesis that bioaccumulation is solely dependent on the concentration of dissolved zinc ions and

concluded that extrapolating results for a given NP to other NPs with dissimilar surface coatings is not possible.

1.4.1.3 Humic substances

Soil humic substances (HS) are made up of humic acids (HA) which are soluble in alkali, fulvic acids (FA) which are soluble over a wider pH range (2 – 12) and humins which are insoluble at any pH [127]. HAs and FAs have similar structures but FAs have lower molecular weights and a larger number of carboxylic and phenolic functional groups than HAs. These oxygen-containing functional groups have high complexation capacities for trace metals. It has been shown that the mobility of bulk zinc in soil environments is influenced by HS sorption [128]. Therefore, HS are likely to have significant control over the fate and bioavailability of zinc NPs in soils.

The majority of research into the interaction of zinc NPs and HS has been carried out in aqueous media using ZnO NPs [115, 129-131], with very few papers focusing on soil environments, or transformed particles [66, 132]. It has been shown that HA is able to stabilise zinc NPs by imparting negative charge to the NPs' surfaces and preventing them from agglomerating because of the increase in repulsive forces between them [66, 115, 133-135]. It has also been found that pH and ionic strength are very important variables for zinc NP adsorption to HS [66, 132], with ionic strength being positively correlated with adsorption inhibition and homoagglomeration [133], and pH 8 being optimum for ZnO–HA adsorption. At environmentally realistic concentrations of ZnO NPs (1 – 30 mg L⁻¹) [44], a near complete electrostatic and steric stabilisation has been observed using high concentrations of FA (30 – 40 mg L⁻¹) [114], however, at low FA concentrations agglomeration actually increased. In other studies, ZnO NP dissolution rate was shown to be positively correlated with the quantity of

Analysis used	How adsorption/aggregation/dissolution was defined/monitored	Reference
UV-Vis at 420 nm	HA concentration in the presence of ZnO NPs measured and control (HA solution with no NPs) subtracted.	[133]
UV-Vis at 372 nm	ZnO aggregation determined by monitoring sedimentation of NP aggregates.	[136]
DLS	Particle size measured – the larger the particle size, the larger the degree of aggregation and the lower the degree of HA adsorption, and vice versa.	[66, 115, 132]
FCS for aggregation SSCP for dissolution	Particle size measured – the larger the particle size, the larger the degree of aggregation and the lower the degree of FA adsorption, and vice versa.	[114]

Table 1.1 Methods for monitoring zinc nanoparticle transformation in the presence of humic substances
DLS: Dynamic light scattering; FCS: Fluorescence correlation spectroscopy; NPs: Nanoparticles; SSCP: Scanned stripping chronopotentiometry.

aromatic FA content [129, 137] and HAs were more effective than FAs at promoting dissolution [129].

The monitoring of zinc NP adsorption to HS and dissolution in the presence of HS has been carried out in different ways. Often more than one type of assay has been carried out in order to determine the different NP states (**Table 1.1**).

1.4.1.4 Ionic zinc

Zinc NP toxicity and fate studies do not always include ionic zinc comparisons which makes the effects of NP dissolution difficult to identify. When controls are included, many papers looking into the toxicity of ZnO NPs on a range of species conclude that effects are due to ionic zinc [75-77, 85], but many others conclude that toxicity cannot be adequately explained by NP dissolution alone [78, 79]. A meta-analysis of studies looking at ZnO NP toxicity compared to ionic zinc found that in most cases nanomaterials are far less toxic than the dissolved metal even when matrix, test organism and particle characteristics are taken into account [138].

1.4.1.5 Size

Studies comparing NP and bulk ZnO particles sometimes find size-dependent effects [18, 86, 102, 134, 139, 140] and sometimes do not [76, 90, 116, 117]. When differences are found, some studies have concluded that the NP toxicity is due to the same dissolution mechanism as bulk zinc but exacerbated by smaller particle size resulting in increased ion release, and some have concluded that NP toxicity is due to a different mechanism such as ZnO NPs producing reactive oxygen species that cause oxidative stress within cells, although this is unlikely to be the case for organisms that live in soil below the depth that UV radiation is able to penetrate.

It is important to work towards resolving these uncertainties and uncovering the underlying mechanisms in order to accurately assess whether separate risk assessments are needed for zinc NPs or if current bulk zinc exposure and risk assessments are adequate to cover NPs.

1.4.2 Commonly used unrepresentative experimental parameters

1.4.2.1 Unrealistic concentration

The modelled ZnO NP concentration in sludge-treated soils in the USA in 2012 is 22 mg kg⁻¹ [44] but a great many studies use concentrations of zinc species that far exceed expected environmental levels [141]. While sometimes this is in order to obtain lethal dose measurements, it is more often due to restrictions caused by the detection limits of the analytical instruments available. Using high concentrations of NPs can alter their behaviour; for instance, if concentration-dependent sedimentation occurs then the NPs under investigation could be misinterpreted as non-toxic rather than unavailable. Test systems containing high concentrations of one type of NP are likely to undergo homoaggregation, but this process is expected to be insignificant under realistic environmental conditions [142]. Therefore, looking at a realistic NP

concentration range is vital [16, 143] and applied experiments using excessive dosing are likely to be unrepresentative of what is actually occurring in the environment [49]. For example, ZnO NPs in soil at a concentration of 5 mg kg⁻¹ were found to undergo rapid dissolution and displayed comparable behaviour to ionic zinc [144]. Whereas studies that have used much higher concentrations of ZnO NPs [89, 145] have found ZnO NPs to show lower effects than ionic zinc, most likely due to the excessive concentrations used leading to NP dissolution being inhibited by increased homoaggregation.

Isotopic labelling of atoms in NPs used in experimental systems provides increased sensitivity [146], as does using high mass accuracy mass spectrometry instruments (see section 6.3.3) [147]. As analytical techniques and instruments such as these become more affordable and are used more routinely, it will be possible to carry out a greater proportion of experiments at environmentally relevant concentrations, allowing true exposure and toxicity mechanisms to be confirmed.

1.4.2.2 Pristine nanoparticles

To date, the main focus of environmental investigations of zinc NPs has been in assessing the transport, fate and toxicity of pristine ZnO NPs. Section 1.3.3 describes some of the transformations that ZnO NPs have been shown to undergo during their life cycle under different environmental conditions. Exposure to zinc NPs in environmental settings is unlikely to be to pristine ZnO NPs but to aged, transformed particles [48, 106-110] such as ZnS NPs or Zn₃(PO₄)₂ [39-42, 99, 103], and so it is these transformed species that should be tested for their environmental and/or biological risk. However, while this is the proposed objective, in practice it is currently difficult to carry out. ZnS NPs are not readily available for purchase whereas ZnO NPs are, and synthesising ZnS NPs by sulfidising larger ZnO NPs has been shown to

result in ZnS NPs with a primary particle size of around 6 nm [96] which makes analysis very challenging.

1.4.2.3 Simplified matrix

The testing matrix is likely to be a key factor in influencing NP dissolution and aggregation. Reed et al. [123] stated that if Zn NP solubility in a matrix is not known, then caution should be exercised in attributing toxicity to NPs. Despite this, studies are often carried out without sufficiently characterising NPs to establish their physical state in the test media being used. This can potentially cause misinterpretations of bioavailability and toxicity, and observed effects to be inaccurately attributed to either dissolved or particulate matter. Full characterisation of NPs prior to, during and after exposure to experimental media would allow these potential errors to be avoided.

It is common in NP phytotoxicity testing to use a hydroponic growth system with agar [86, 134, 148], perlite [149, 150], polyurethane foam [151] or filter paper [152, 153] as a supporting material. While this means that the chemical composition of the nutrient solution applied can be strictly controlled and will not be altered by soil components, as well as allowing the roots and shoots to be clearly visible, it may give very different results to the same experiment carried out using soil [141, 154]. Hydroponic media often have high ionic strengths which is likely to affect NP dissolution or agglomeration state and is not representative of realistic environmental conditions.

Joško et al. found that ZnO NPs stimulated the growth of cress (*Lepidium sativium*) in a hydroponic system but exhibited toxicity when exposed to the same species in a soil matrix [155]. Wang et al. [156] compared cowpea (*Vigna unguiculata*) plant growth in soil and solution cultures spiked with ZnO NPs and ionic zinc. It was found that there was no difference between ZnO NP and ionic zinc toxicity when grown in soil, but in

solution culture the ionic zinc was more phytotoxic than the NPs. Thunugunta et al. [157] observed that aubergine (*Solanum melongena*) seed germination was negatively affected by ZnO NPs in Murashige and Skoog plant growth medium, but germination was enhanced by ZnO NPs in soil, highlighting that different matrices should not be treated as analogous.

Studies endeavouring to simulate the transport and retention of zinc NPs in soils often use well-defined systems containing columns packed with uniform, spherical glass beads [61, 158] or saturated sand [159-161] in place of soil. These systems do not contain silts and clays and lack the meso- and micropores of soils. This means that they cannot replicate NP transport by the movement and storage of soil porewaters or retention on the huge variety of soil sorption sites [49].

1.5 Applied ecotoxicology and environmental fate studies

1.5.1 Waste water treatment plants

There have been a number of studies addressing what happens to ZnO NPs at various stages in WWTPs. Brunetti et al. [41] set up a scaled-down simulation of a sewer which was filled with wastewater. The system was run for 3 months and then spiked with ZnO NPs. In order to obtain a high enough signal for the added zinc to be detected against the naturally occurring background concentration using X-ray absorption spectroscopy (XAS), a target concentration of $700 \mu\text{g L}^{-1}$ was used. The influent and effluent were analysed and it was determined that all of the spiked ZnO NPs had transformed to sulphidic forms by the end of the process. It is also notable that no detectable presence of zinc bound to HA was found in any of the samples. Following this, Ma et al. [96] investigated the process of ZnO NP sulphidisation. It was found that in the presence of enough sulphide, 30 nm ZnO particles will undergo almost complete

conversion to 2.5 – 5 nm ZnS, a decrease in surface charge and an increase in agglomeration.

Kim et al. [42] used XAS and transmission electron microscopy (TEM) to identify and characterise zinc NPs in sewage sludge material. It was found that ZnS NPs with a size range of 2.5 – 7.5 nm present as agglomerates of a few hundred nanometres were the dominant species and it was proposed that future studies to investigate ZnS NP dissolution as a function of size, agglomeration state and soil type after biosolid application were needed.

Lombi et al. [39] also set up benchtop sewage digesters filled with wastewater sludge to examine the fate of spiked ZnCl₂, bulk ZnO and three ZnO NP suspensions, one of which was dispersed in vegetable oil to mimic the conditions of household sewage. In the fresh biosolids all of the zinc species tested were found to have largely transformed into sulphides and because no size-dependent differences were found it was suggested that risk assessments in place for bulk zinc would be sufficient for zinc NPs too. Once the biosolids were aged to mimic the composting process, sulphides were found to no longer dominate, with significant levels of Zn₃(PO₄)₂ and zinc ions adsorbed to iron mineral surfaces also present. This has also been found for bulk particles [103] and was corroborated by a study investigating zinc NPs in a pilot WWTP and in processed biosolids [40]. ZnO NPs were transformed to Zn₃(PO₄)₂, ZnS and zinc associated with iron oxy/hydroxides with the ratio of the latter two being dependent on the redox state and water content of the biosolids; no size-specific differences in the zinc speciation products were exhibited.

Lv et al. examined the phosphate-induced transformations of pristine ZnO NPs and showed that much larger tetrahydrate zinc phosphate products are formed [98]. A later study looked at the transformation of 30 nm ZnO particles to Zn₃(PO₄)₂ and found that

this process is pH dependent [99]. At pH 6, ZnO dissolution was enhanced and μm -sized crystals of $\text{Zn}_3(\text{PO}_4)_2 \cdot 4\text{H}_2\text{O}$ predominated, whereas at pH 8, it was suggested that 30 nm-sized ZnO particles with amorphous $\text{Zn}_3(\text{PO}_4)_2$ shells were produced. Increased phosphate concentration and reaction time were also found to increase the percentage of $\text{Zn}_3(\text{PO}_4)_2$ formed. It was noted that these NP core-shell structures are unlikely to be formed in WWTP because previous studies [39, 40] have not detected any ZnO remaining in the sludge. However, it was also noted that they are unlikely to ever form from bulk particles, which emphasises the premise that NPs may undergo unique size-dependent transformations under different environmental conditions which all require independent investigation.

1.5.2 Toxicity to plants

Plants generally form the base of terrestrial food webs and so NP bioavailability and toxicity to plants could have far reaching affects and impact wider ecosystems. Zinc is an essential micronutrient that is required for the normal growth, development, and reproduction of plants. However, when present in high concentrations, zinc can have detrimental consequences for plant cells. In recent years, a number of studies have looked into zinc NP bioaccumulation and phytotoxicity in a variety of different plant species, including wheat [118, 145, 162], maize (*Zea mays*) [74, 81, 163-165], soybean (*Glycine max*) [166-169], courgette (*Cucurbita pepo*) [170], buckwheat (*Fagopyrum esculentum*) [171], alfalfa (*Medicago sativa*) [89], tomato (*Solanum lycopersicum*) [72, 172], mouse-ear cress (*Arabidopsis thaliana*) [86], radish (*Raphanus raphanistrum*) [81, 145], vetch (*Vicia sativa*) [145], cowpea [156], Chinese cabbage (*Brassica rapa*) [152], rice (*Oryza sativa*) [153], onion (*Allium cepa*) [173], ryegrass (*Lolium perenne*) [81], lettuce (*Lactuca sativa*) [81], mung bean (*Vigna radiata*) [148], cucumber (*Cucumis sativus*) [81, 134, 174], blue palo verde (*Parkinsonia florida*) [175], tumble-weed [175], velvet mesquite

(*Prosopis velutina*) [151, 175], mustard (*Sinapsis alba*) [176, 177], rapeseed (*Brassica napus*) [81, 149, 150], aubergine [157] and green pea [73, 124, 140]. The results of these studies can often be conflicting [178, 179], although given the wide range of experimental conditions and analytical methods used, this is to be expected. Studies being carried out using mediums other than soil is a particular issue in phytotoxicity studies [86, 148-150]. Other common issues include: failure to investigate ionic and bulk particles for comparison, using excessive concentrations of NPs and failing to adequately examine NP dissolution in the medium used. The lack of experimental consistency means despite data being available for many different plant species the results can be difficult to compare with one another.

Judy et al. [102, 180] looked at the effect of growing barrel clover (*Medicago truncatular*, a small annual legume) in soil amended with biosolids generated with ZnO NPs introduced into the influent wastewater. It was found that plants grown in the NP-amended media exhibited a > 8 fold decrease in nodulation frequency compared to the bulk metal treatment. This suggested a significant difference in metal bioavailability between the NP and bulk-amended soils. The soil extraction procedures used did not find this to be the case, highlighting a pressing need for zinc NP-specific extraction procedures to be developed.

Even if ZnO NPs are observed inside a plant this is not enough evidence to be able to determine whether they are there as a result of direct uptake, or from the plant synthesising them from dissolved zinc [74]. Yoon et al. [169] reported that adverse effects on soybean plant growth were mainly caused by ZnO NPs rather than dissolved zinc, but without tracking the zinc transformation, transport and fate this is not possible to confirm. It was stated that the levels of ionic zinc were very low, but it was acknowledged that because the dissolved zinc measurements were taken after the

plants were harvested, they may not have been an accurate representation of the growing conditions. Indeed, their method of making high concentration stock soils with dry ZnO NP powder to spike into testing soils is likely to cause rapid and increased ionisation compared to other spiking methods [181]. Use of isotopically labelled NPs [182] is one way of being able to follow transport and transformation of NPs; but to establish definitive mechanisms of action or toxicity would require *in situ* NP characterisation.

1.6 Modelling

Predicting environmental concentrations of NPs using modelling approaches should be based on data calculated using NP production and NP release volumes, and life cycle assessments. At present, researching zinc NP life cycles are limited by the inability to detect and track them *in situ* under real conditions. Instead, predicting the passage of NPs into the environment has been carried out using material flow analysis. Gottschalk et al. [44] modelled the flow of ZnO NPs from production to environmental release in Europe and the USA. The modal concentration predicted to be present in WWTP sludge for the EU in 2008 was 17.1 mg kg^{-1} and the predicted modal concentration change in sludge-treated soils was $3.25 \text{ } \mu\text{g kg}^{-1} \text{ year}^{-1}$. However, these calculations did not take transformations such as sulphidation into account. Sun et al. [183] carried out the same modelling analysis for 2012, but factored in the loss of ZnO NPs due to chemical transformation during the WWTP anaerobic digestion process. The modal concentration of ZnO NPs predicted to be present in STP sludge was 24 mg kg^{-1} and the predicted modal concentration change in sludge treated soils was $0.01 \text{ } \mu\text{g kg}^{-1} \text{ year}^{-1}$. Concentrations of other zinc NP species such as ZnS or $\text{Zn}_3(\text{PO}_4)_2$ were not calculated. The total native zinc concentration in soil was predicted to be 7 orders of magnitude higher than the NP concentration, making zinc NP detection and analysis a challenging task.

A recent review of nanomaterial flow modelling asserted that:

'the main limitation faced by all modellers is that the information needed to feed those models is almost inexistent' [184].

The same review stated that the models usually overlook NP transformations and mainly describe the flow of pristine NPs; this mirrors the current state of NP fate and toxicity research.

1.7 Analytical techniques and instruments used for nanoparticle analysis in soil environments

Investigating NPs in the environment first requires experimental and analytical methods to be developed. Currently, applied studies aiming to qualitatively and quantitatively analyse NPs in soil environments are hindered by a lack of established robust methods [185, 186] especially ones that are able to measure *in situ* samples in real time. Difficulties in detection and analysis have led to the experimental issues described in section 1.4.2. Studies are usually lab-based and often use exaggerated concentrations of NPs [16, 187], synthetic or simplified mediums [49] and short time-scales [141, 188]. It is generally the case that multiple methods are needed in order to obtain all of the necessary information [189, 190]. The aim should be to optimise these methods for detection and characterisation with realistic concentrations of NPs and using naturally occurring media and conditions, which greatly increases the experimental complexity but is necessary for gaining an accurate understanding of their behaviour in the environment [16]. Conflicting experimental results can often be due to differences such as detection limits or biases in the analytical techniques and instruments used and unsystematic experimentation [154, 191, 192]. Indeed, in a recent mini review of nanosafety, Valsami-Jones et al. state that:

'A lot of publications produce "low-value results" due to lack of harmonized experimental protocols, incomplete or problematic nanomaterial characterization and lack of reference materials and media that would allow comparisons between studies' [191].

Establishing universal analytical methods for NP characterisation and detection is vital for current knowledge gaps to be filled and both acute and chronic NP toxicity risk to be understood.

1.7.1 Sample preparation techniques for soil experiments

1.7.1.1 Spiking procedure

In order to carry out fate and ecotoxicity testing of zinc NPs in soil it is often necessary to spike test soils with known quantities of characterised NPs. Establishing a uniform NP distribution throughout the soil sample is important and there are three main procedures that are used to do this; adding the NPs as an aqueous suspension, as a suspension in an aqueous soil extract or as a dry powder.

To produce a stock aqueous soil extract, control soil is mixed with Milli-Q water and then filtered. NPs are then added to the aqueous filtrate and shaken to produce a homogenous concentrated stock suspension which can then be mixed with dry soil samples [84, 116, 121, 193, 194]. Alternatively, dry NP powder can be mixed directly into dry soil and Milli-Q water added [79, 111, 195-197]. This method can be preferable if NPs with a hydrophobic coating are being applied [116].

These methods were compared using ZnO NPs and it was found that spiking the soil with an aqueous suspension or a dry powder did not alter the resulting distribution of the NPs in the soil [198]. However, when the spiking methods were looked at in terms of dissolution it was found that spiking procedure had an effect [181] with dry spiking

producing the highest level of dissolution. This could be because the ZnO NPs had no protection mechanism and so were quickly ionised. NPs suspended in pure Milli-Q water tended to agglomerate and so were slower to dissolve when spiked into soil. ZnO NPs suspended in soil pore water extract exhibited the lowest availability of NPs and zinc ions, probably due to the extra stability that comes from being adsorbed onto organic matter present in the matrix [199].

Tuoriniemi et al. [200] reported a protocol for dispersing NPs into soil without causing aggregation. Aqueous NP dispersions were added to soil as 10 µL drops and the soil stirred with a glass rod in between each droplet addition, however, this was only carried out using gold NPs.

1.7.1.2 Extraction procedure

Once NPs have been spiked into soil, it is necessary to be able to extract them again in order to ascertain whether they have partitioned between the soil solution and solid phases, adsorbed onto other species or whether their speciation has altered. However, separating NPs from soil suspensions or sediment slurries is difficult and existing methods run the risk of introducing contaminants and losing or transforming the NPs [201].

Of the studies looking at zinc NPs in soils [79, 84, 111, 116, 194, 196, 198] most have initially found the total soil zinc concentration by digesting spiked soil with a solution of Milli-Q:HCl:HNO₃ (1:1:4 by volume), placing the slurry in an oven for 7 hr at 140°C and then analysing. Another technique has been soil pore water extraction in order to measure its zinc NP and ion content. There are a range of methods available for sampling soil pore waters [202], but most studies concerning zinc NPs have done this by saturating the soil with Milli-Q water and equilibrating for at least a week, centrifuging the soil over microfilters and then analysing. There are concerns that

membrane filtration can lead to a serious underestimation of the total mass of colloidal matter in soil suspensions [203, 204] and an underestimation of NP partitioning and dissolution [113] due to the loss of analyte on membranes and subsequent filter clogging [201]. Van Koetsem et al. [205] found significant NP retention by filters with pore sizes both smaller and larger than the particle size, with retention increasing as initial NP concentration decreases and being mainly dependent on particle characteristics.

Another study assessed the capability of cloud point extraction to separate ZnO NPs from water samples and the method was subsequently applied directly to waste water effluents [206].

1.7.2 Characterisation and measurement of nanoparticles

There is no agreed upon universal list of NP properties that require characterisation, but comprehensive characterisation is crucial for verifying the properties of synthesised NPs, confirming manufacturers' claims for purchased NPs and identifying any transformations of NPs during or after experimentation. An exhaustive list of the NP physicochemical properties that could potentially be assessed would be extensive, leading to time consuming, expensive and complex analysis. However, insufficient or inadequate NP characterisation can mean that observed effects are ascribed to the wrong species and produce inconsistent results [192, 207]. There have been a few proposals for a set of minimum physicochemical parameters required to adequately describe NPs. **Table 1.2** shows the combined minimum characterisation recommendations resulting from a workshop of the European Network on the Health and Environmental Impact of Nanomaterials (NanoImpactNet) held in June 2008 [208], a workshop on ensuring appropriate material characterization in nanotoxicology studies held in the USA, in October 2008 [209] and a recent review paper [210].

Size	Primary particle size distribution Average particle size
Composition	Chemical composition Purity Crystal structure Morphology
Surface	Composition Area Charge Oxidation state Coating agents
Agglomeration/aggregation	Aggregate size distribution Morphology Kinetics and mechanisms of (dis)aggregation
Stability	Solubility Dissolution rate UV-stability Thermal-stability

Table 1.2 Recommended minimum nanoparticle characterisation. Taken from European Network on the Health and Environmental Impact of Nanomaterials (NanoImpactNet) [208], material characterization in nanotoxicology studies [209] and review paper [210].

There are a great many techniques and instruments that can potentially be used for NP characterisation. Every characterisation technique gives subtly different information and presents unique difficulties and limitations, meaning that characterisation should be carried out using a combination of different methods [190]. Indeed, it has been recommended that multiple methods are used to describe each physicochemical parameter [208, 210, 211]. Most methods can be broadly categorised as either a counting method (also known as a single particle method), an ensemble method (also known as particle population method) or a separation method.

1.7.2.1 Counting methods

Single particle counting techniques such as TEM, scanning electron microscopy (SEM) and nanoparticle tracking analysis (NTA) are excellent for obtaining specific information about NPs, however, the limited number of particles analysed means that

these techniques can easily lead to errors or bias due to the potentially poor statistical representation of a sample.

TEM and SEM are frequently used to determine particle size, shape and/or size distribution. They can also make it possible to visualise the degree of aggregation/agglomeration. TEM and SEM use electron beams to provide rapid direct images of NPs. In TEM, the electron beam passes through (transmits) a thin sample to a detector below. It does this at high resolution and so can be used to image individual NPs and NP aggregates at scales approaching a single atom [212].

1.7.2.2 Ensemble methods

Ensemble methods measure large numbers of particles simultaneously. In dynamic light scattering (DLS), particle size is determined by illuminating a suspension or solution with a laser and then measuring the rate of the intensity fluctuations of the resulting scattered light. These fluctuations occur because random collisions with the surrounding solvent molecules causes the particles to be in constant motion. This is known as Brownian motion and the crucial feature of this phenomenon is that the speed of a particle is correlated to its size, with smaller particles moving more rapidly than larger ones [213] (**Figure 1.8**).

The relationship between the particle size and speed due to Brownian motion is modeled by the Stokes-Einstein equation:

$$D_h = \frac{k_B T}{3\pi\eta D_t}$$

where D_h is the hydrodynamic diameter, D_t is the translational diffusion coefficient, k_B is Boltzmann's constant, T is thermodynamic temperature and η is dynamic viscosity.

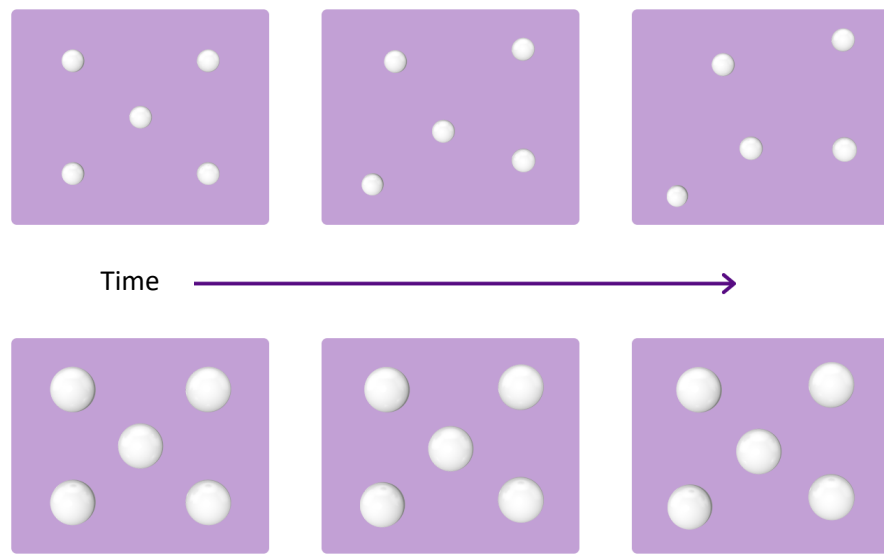


Figure 1.8 Brownian motion. Smaller particles move more rapidly than larger ones. This process is the basis of dynamic light scattering as an analytical technique. Source: author

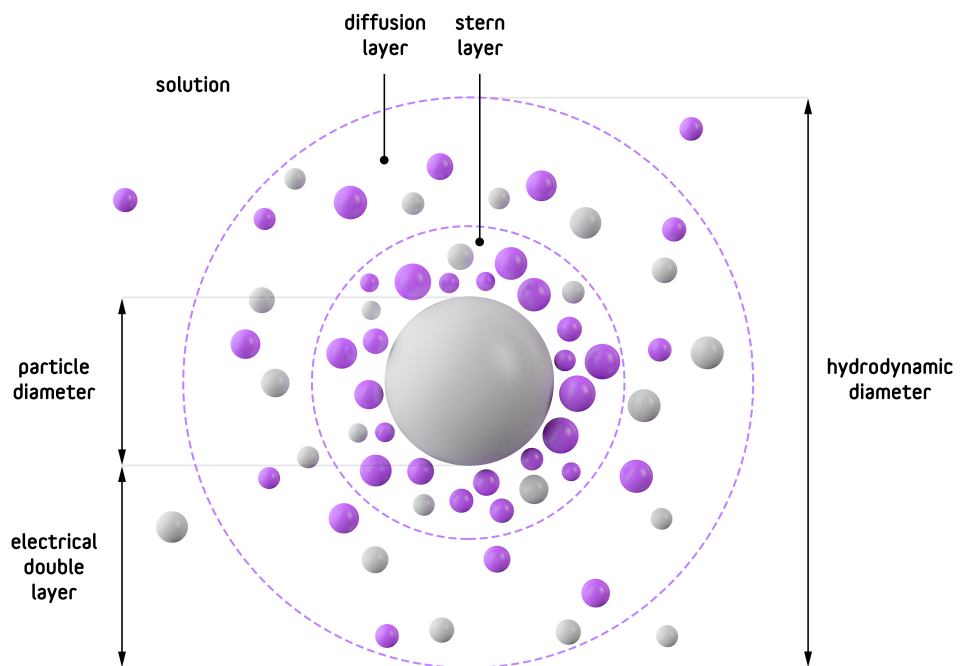


Figure 1.9 Hydrodynamic diameter of particle. Source: author

As the analyte is dispersed in liquid and this model assumes particles to be spherical, the value obtained by this technique is the hydrodynamic diameter (**Figure 1.9**) of a hypothetical perfect sphere with the same translational diffusion speed as the particle. The equation also highlights that it is important for the temperature to be kept stable in order to stop thermal currents causing non-random particle motion and to keep a constant solvent viscosity.

DLS can be used to ascertain the size distribution of suspended NPs, the average hydrodynamic diameter and zeta potential of NPs [214] although measurement can be difficult when NP samples are agglomerated and results can be limited by an inherent bias toward the largest particles present which can skew the reported size distribution [215, 216].

X-ray diffraction (XRD) is a commonly used method that can establish crystal structure. Sometimes the average NP diameter is then estimated using the Scherrer equation [42, 90], however, because this assumes translational symmetry of the NP crystal structure it is unsuitable for exact sizing if the NP shape is not known [217].

1.7.2.3 Separation methods

In order to successfully detect specific analytes, it is often desirable to separate them from other interfering species. For zinc NP fate and toxicity testing, separate observation of the ionic zinc and particulate fractions is often required. There have been attempts to do this with zinc NPs using a variety of methods.

Some studies have used ultrafiltration to separate the free Zn^{2+} ions from the NP fraction in extracted soil pore waters [79, 84, 116]. These filtering steps may add contaminants and cause analyte to be lost [113] so it is important to carry out recovery experiments for each filtering step if this method is to be used. Alternatively, issues of extraneous sample exposure can be avoided if separation is obtained using analytical

ultracentrifugation (AUC). Using speeds of < 300,000 g, NPs will sediment into fractions according to their size [218]. As part of a study looking at the potential effects of ZnO NPs on *Daphnia magna*, Wiench et al. used AUC to assess the size distribution of agglomerated NPs in different test dispersions using a modified ultracentrifuge with the capacity for online detection and recording of sedimentation [219]. Jiang and Hsu-Kim [137] compared anodic stripping voltammetry (ASV) with AUC (370,000 g for 1 hr at 25°C) followed by inductively coupled plasma-mass spectrometry (ICP-MS, see sections 1.7.3-1.7.4) to quantify dissolved zinc in the presence of ZnO and found that the results from both methods were comparable.

Merdzan et al. [125] compared different methods to measure the ionic zinc content of samples spiked with ZnO NPs and found that 3 kDa ultrafiltration allowed dissolved zinc and zinc phosphate to pass through. Ion exchange chromatography (IEC) coupled with ICP-MS, and ASV were also investigated. Each method gave slightly different results and all had their own benefits so using a variety of methods in tandem was recommended.

AGNES has been used to determine the total soluble zinc in a dispersion of 20 nm ZnO NPs [91]. The results were compared to centrifugation of the same dispersion. It was reported that while the AGNES method gave results that mirrored predicted values, the centrifugal method gave a concentration five times larger. This was put down to small NPs remaining in the supernatant after centrifugation being detected as ionic metal and highlights how greatly the analytical methods used can impact on the data obtained. One benefit of ASV and AGNES over other methods is that the short time resolution allows kinetic studies to be carried out on the dissolution rates.

Dialysis using a membrane with a 1 nm pore size has also been used so that only dissolved zinc ions were able to pass through, allowing the ionic and particulate

fractions to be separated and identified [76]. However, another study found that the method cannot be applied to accurately quantify the dissolved fraction of a NP suspension because of the continuous dissolution that occurs while the technique is being carried out [220].

For the isolation and detection of ZnO NPs, coupling an IEC column containing a strong metal binding chelex resin (**Figure 1.10**) to an ICP-MS in single particle (sp, see section 6.3.2) mode was shown to greatly decrease the background signal that arose due to dissolved zinc ions [221]. Without the IEC column the baseline signal meant that only large particles could be observed, but by hyphenating with the IEC the size detection limit was reduced and the sensitivity increased enough to allow the characterisation of ZnO NPs at low concentrations in environmental water samples.

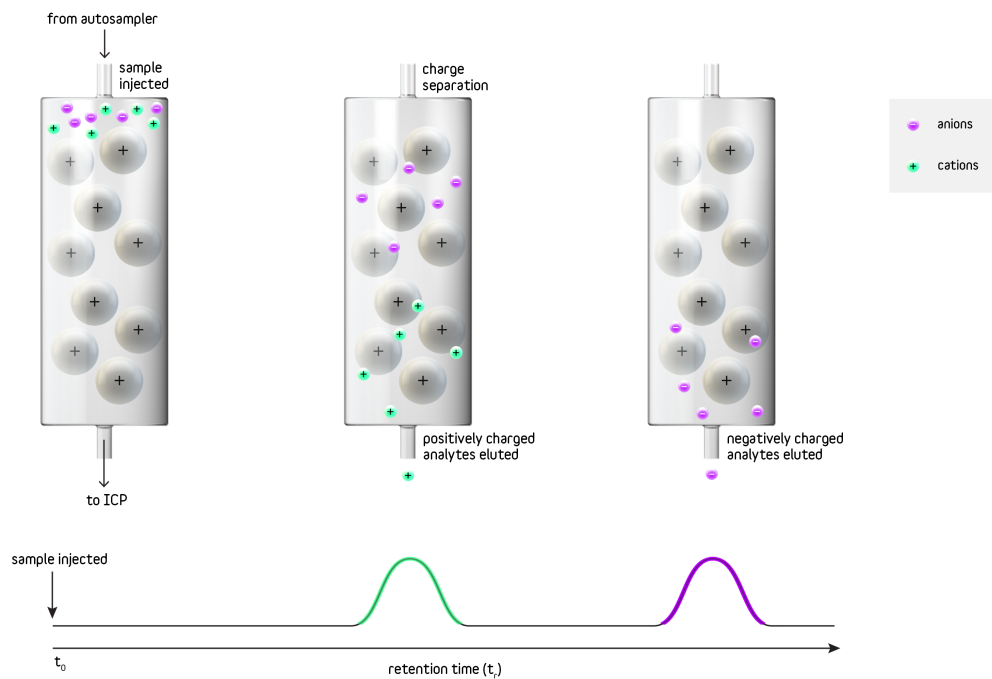


Figure 1.10 Analyte separation in ion exchange chromatography. Source: author

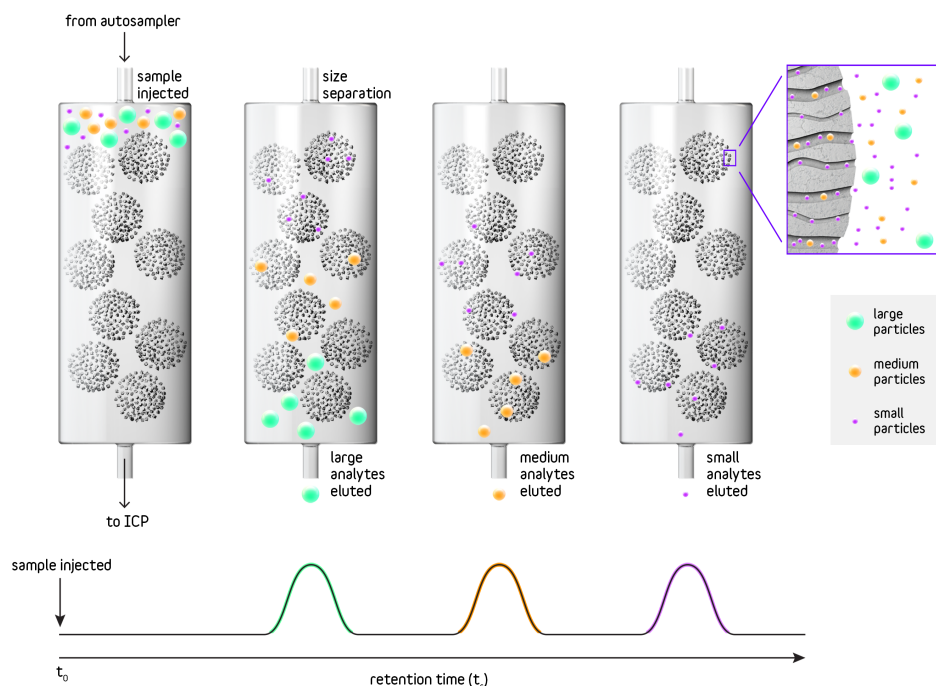


Figure 1.11 Mechanism and order of analyte separation in size exclusion chromatography. Source: author

Size exclusion chromatography (SEC) is a technique that separates analytes based on their hydrodynamic volume (**Figure 1.11**). Species that are able to access the full pore volume of the porous solid phase within the column are retained for longer, whereas larger species are excluded and are eluted faster, resulting in analyte separation [222].

In theory there should be no interaction between analyte and column stationary phase, however, a major issue that researchers have repeatedly encountered when attempting to analyse NPs using SEC is NP adsorption onto the stationary phase [222]. Column retention prevents quantitative analysis due to low analyte recoveries and can cause carryover from one sample to the next. The lack of research available on NP analysis using SEC is likely to be largely due to this problem.

One tactic that has been used to try to overcome the issue is to increase the pore size of the stationary phase, which reduces the overall stationary phase surface area, giving less capacity for adsorption [222]. However, the main approach has been to incorporate

additives to the eluent (mobile phase). Lui and Wei looked at the effect of three different mobile phase additives on the separation of two different sizes of gold NPs using SEC. It was found that the anionic surfactant SDS (**Figure 1.12**) was most effective [223] and that the optimum SDS eluent concentration was 5 mM [224], which is close to its critical micelle concentration of $\sim 7 - 8$ mM [225, 226]. Surfactants or 'surface-active-agents' are molecules that have hydrophilic heads and hydrophobic tails and can form different structures as well as coatings around other species [227] (**Figure 1.13**). Their dual nature means that they can potentially disperse the NPs in the mobile phase and block unwanted interfacial interactions between the NPs and the stationary phase [222] (**Figure 1.14**).

Lui and Wei consequently repeatedly used SDS in the separation of gold NPs by SEC [228-234] and recently, SEC has been carried out with nanomagnetite [235] and a number of metal oxide NPs including ZnO NPs [236], with both of these studies using SDS as a mobile phase additive. However, a method cannot necessarily be successfully replicated in different systems. Altering the specific combination of the analyte, mobile phase formulation and column stationary phase material can cause different interactions to occur. For example, despite using stationary phases with the same pore size, trisodium citrate was shown to be an effective stabiliser of gold NPs using a column with silica packing material [237] whereas the same method carried out on a polymer-based column suffered from severe adsorption [224].

Hydrodynamic chromatography (HDC) is similar to SEC but uses non-porous stationary phases. Despite the lack of pores, HDC can still suffer from NP retention within the column. SDS has been used in combination with the non-ionic surfactant Triton X-100 (**Figure 1.12**) as a surfactant addition to eluents in HDC to suppress NP agglomeration and adsorption, and therefore increase analyte recovery [238-242].

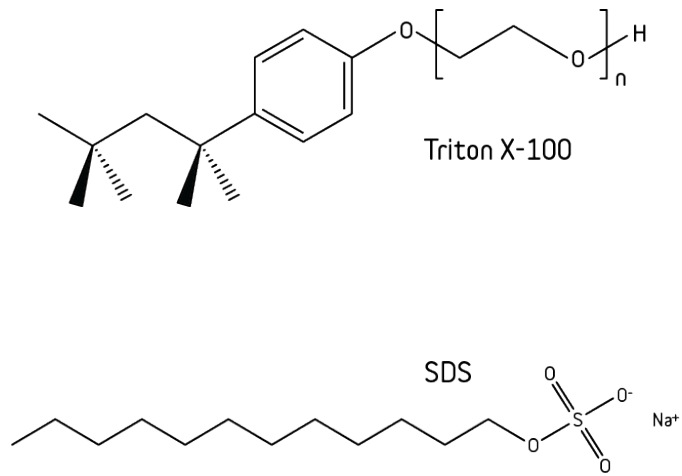


Figure 1.12 Molecular structures of surfactants Triton X-100 and sodium dodecyl sulphate (SDS).
Source: author

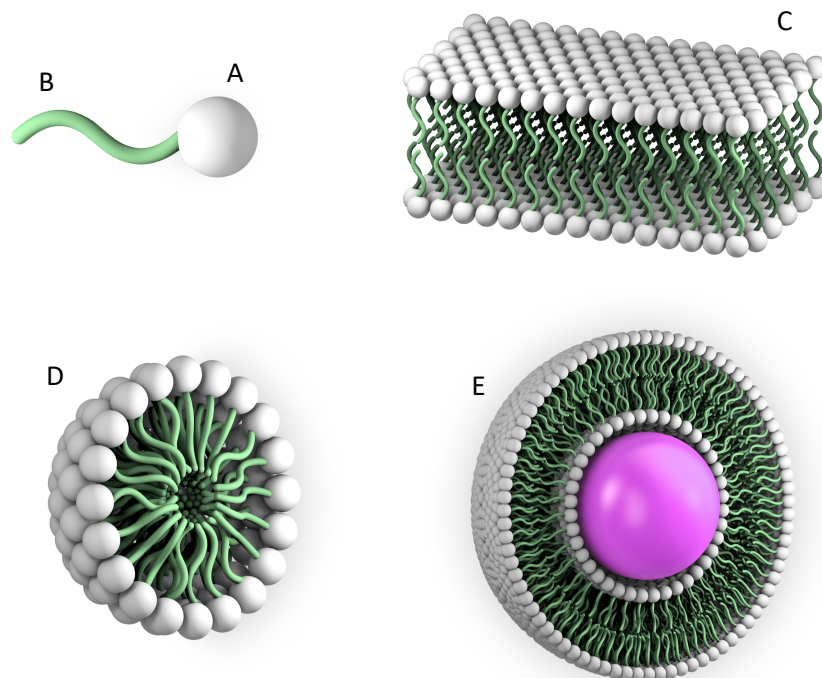


Figure 1.13 Surfactant molecules with their hydrophobic tails (A) and hydrophilic heads (B) can form structures such as: bilayers (C), micelles (D) and liposomes (E). Source: author

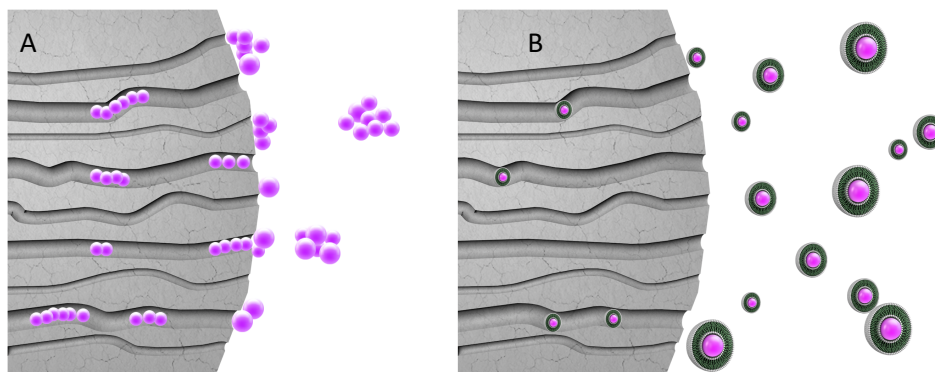


Figure 1.14 Nanoparticles without surfactant can aggregate and become adsorbed to the stationary phase (A). The addition of surfactants to the mobile phase can suppress adsorption (B). Source: author

HDC coupled to ICP-MS [243] has been successfully used to analyse metal NPs spiked into sewage sludge, however, high concentrations had to be added for the signal to be over the limit of detection. HDC-ICP-MS has also been used in sp mode [240, 244] (see section 6.3.2).

Establishing whether observed effects are due to NPs, dissolved ions or a combination of both is an important aim for any investigation of NP fate or toxicity. With this in mind, it is of great importance that experimental methods used for ion and NP separation are fit for purpose. Difficulties in detection and analysis means that experimental results can be inconsistent and conflicting. Robust protocols for tracking and assessing NPs have not yet been established, so the rigorous interrogation and testing of experimental systems is still a continual necessity to ensure that NP fate and toxicity are not misreported or misinterpreted.

1.7.3 Inductively coupled plasma

At high temperatures a gas will lose electrons from its atoms and become charged plasma. Plasma is the fourth state of matter and will conduct electricity. ICP is method of hard ionisation that uses high temperature plasma discharge to ionise samples in order for them to undergo elemental and isotopic analysis. The ICP torch has a high

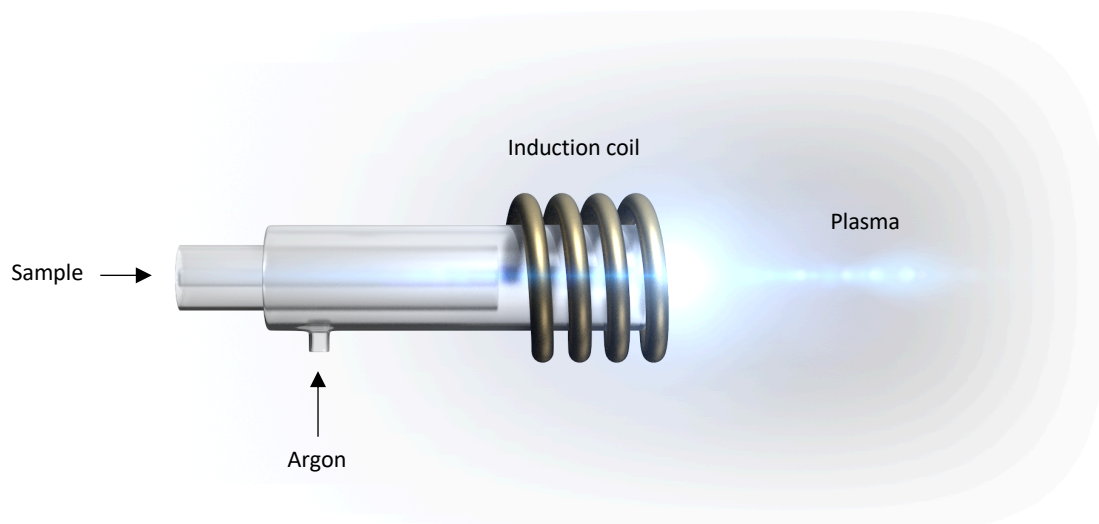


Figure 1.15 Diagram of ICP torch. Source: author

ionisation efficiency which is ideal for generating elemental ions (**Figure 1.15**) so it is a very useful tool for the ionisation of metal NPs.

For sample detection and analysis, ICP can be coupled with an optical emission spectrometer (also known as an atomic emission spectrometer) [123, 131, 164], however this often leads to complicated spectra, spectral interferences and high background noise [245]. Coupling an ICP torch with an MS (see section **1.7.4**) gives greatly increased sensitivity and, although there is no universal MS that will perform all types of analyses, the choice of MS instruments available allows a range of different applications to be undertaken due to the variety of functions and sensitivities that they offer.

1.7.4 Mass spectrometry

MS are instruments that separate ions based on their mass-to-charge (m/z) ratio. Different types of MS instruments do this in different ways. For example, Time-of-Flight (TOF) instruments guide ions into a flight tube where they drift along and are separated due to their differing velocities, and in high mass accuracy Orbitraps, ions oscillate at different frequencies according to their m/z around an electrode.

The most commonly used MS instruments for zinc NP analysis are Sector Field (SF) and Quadrupole (Q) instruments.

In SF MS ions are accelerated through a flight tube, where they are separated by passing through a magnetic field which is applied in a perpendicular direction (**Figure 1.16**).

A Q-based MS consists of 4 parallel rods which have alternating DC/RF potentials applied (**Figure 1.17**). This causes ions to spiral at a rate proportional to their m/z value so that only selected ions have a stable trajectory to the detector. These MS instruments can be coupled to an ICP giving different options and possibilities for analysis (**Figure 1.18**).

1.7.4.2 Isotopic labelling

One problem with analysing zinc NP fate in soil samples is that zinc is already naturally present at fluctuating concentrations in the environment. This means that analytical methods employed to trace zinc NPs need to be sensitive and selective enough to differentiate between naturally occurring background zinc and the spiked NPs of interest, and ideally should be able to do so at environmentally relevant levels. Simulating real environmental conditions and concentrations to study behaviour or bioaccumulation is crucial because NPs can be significantly affected by both [16].

Using isotopically enriched particles as tracers [246] (whereby a stable isotope of zinc with an abundance that differs from its natural incidence is introduced into a sample and any transfer that may occur identified) is a technique that has been applied to many different assessments of NP exposure monitoring and environmental fate studies, including: ZnO NP uptake in molluscs and ragworms from sediment [247];

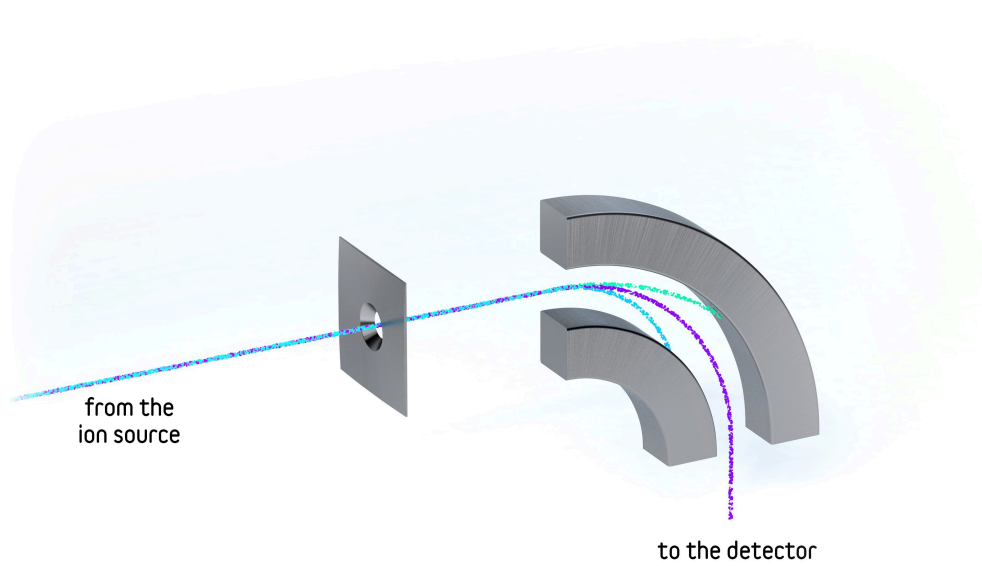


Figure 1.16 Sector Field mass analyser. Source: author

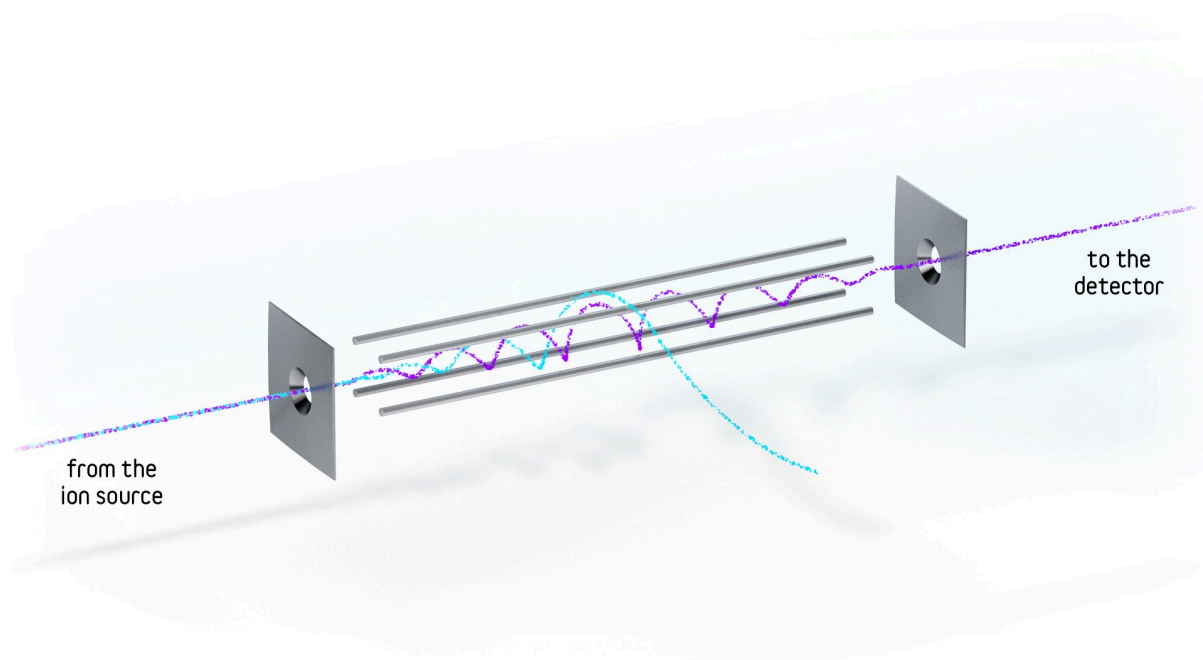


Figure 1.17 Quadrupole mass analyser. Source: author

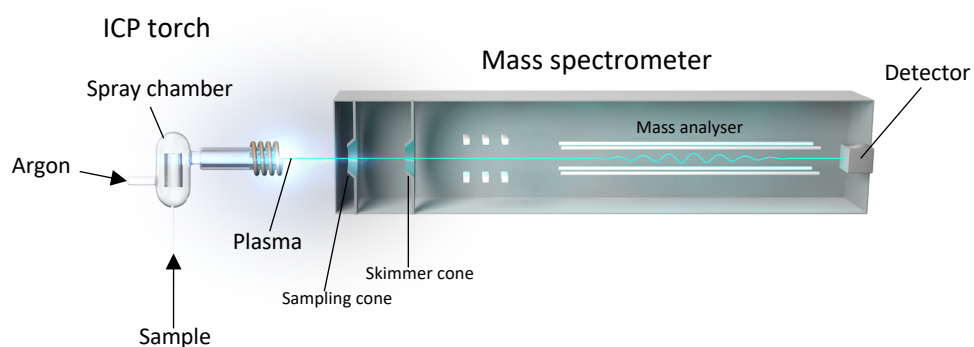


Figure 1.18 Inductively coupled plasma-mass spectrometry. Example shows quadrupole as the mass analyser. Source: author

assessing the bioavailability of zinc to earthworms at different concentrations of salt [248]; tracing dermal absorption of zinc from sunscreen [249] and investigating the isotopic composition of zinc available to plants in soil [182]. The movement of ionic zinc to wheat grains was investigated by spiking the growth medium with ^{70}Zn , and then studying the spatial distribution of zinc within the grains by laser ablation-ICP-MS [162].

Analysis can be carried out on Q-based ICP-MS instruments although simultaneous detection is not possible [247, 248, 250-255]. Standards are used to calibrate the instrument and then the relative abundance of the chosen tracer isotope is determined using the signal intensities of each isotope (from [253]):

$$p^i = \left(\frac{\text{Intensity}^i E}{\sum_j^{jj} \text{Intensity}^j E} \right)$$

p^i = the relative abundance of the natural isotope $^i E$

$^i E$ = the tracer isotope

E = the element (metal)

j = the lightest isotopes of E

jj = the heaviest isotopes of E

Concentrations of tracer in the sample are then calculated as the product of p^i and the total metal concentrations inferred by the ICP-MS software from the tracer intensity:

$$[{}^iE]_{\hat{e}} = p^i \times [T^iE]$$

$[{}^iE]_{\hat{e}}$ = concentration of tracer in sample / total experimental metal concentration

$[T^iE]$ = tracer intensity

Total metal concentrations inferred from the intensity of the most abundant isotope are then used to derive the original load of tracer that occurred in each sample in the absence of a spike:

$$[{}^iE]_{\hat{e}}^0 = p^i \times [T^kE]$$

$[{}^iE]_{\hat{e}}^0$ = original load of tracer

k = most abundant isotope of E

Finally, the net tracer uptake is derived from the total experimental tracer concentration minus the pre-existing concentration of tracer:

$$\Delta [{}^iE]_{\hat{e}} = [{}^iE]_{\hat{e}} - [{}^iE]_{\hat{e}}^0$$

$\Delta [{}^iE]_{\hat{e}}$ = net tracer uptake

Factors such as the purity of the spiked isotope tracer and the instrument sensitivity dictate the effectiveness of this approach. There are a number of ways of improving the methodology if sensitivity proves to be an issue. Zinc has five stable isotopes (**Table 1.3**) that are normally present in the environment at the following natural relative isotopic abundances:

Zn isotope	Zn ⁶⁴	Zn ⁶⁶	Zn ⁶⁷	Zn ⁶⁸	Zn ⁷⁰
% Relative abundance	48.9	27.8	4.1	18.6	0.62

Table 1.3 Stable isotopes of zinc

Buying isotopic tracers with lower natural abundance is more expensive but increases sensitivity and using an MS that offers higher ion transmission than a Q-based MS such as a SF instrument will also enhance sensitivity.

The wide variety of techniques and instruments available for NP analysis means that there are many options to choose from, but the drawbacks to each method must be recognised and taken into account when data is reported.

1.8 Aims and objectives of this thesis

As described in this review, there is currently a pressing need for validated methods that can detect and analyse zinc NPs in natural soil environments. This gap in analytical capability means that many zinc NP environmental fate studies are not currently able to mimic what they intend or purport to represent. Common approaches to overcoming analytical problems include: using unrealistically high concentrations of zinc NPs, using pristine ZnO NPs rather than aged species and using simplified mediums rather than soil. The aims of this thesis were to avoid these methodological issues and investigate potential methods that could eventually become useful for overcoming problems associated with current research of NPs in soil environments as a result of biosolid application. For this, two different strategies were used. The first intended to look at the mechanism of zinc NP dissolution and fixation in soils by developing methods based on dialysis and SEC. The second aimed to grow plants on soils spiked with different zinc NPs in order to make detailed observations about differences in various parameters. In both cases the final goal was to enhance knowledge about the

application of biosolids containing zinc NPs onto soils. The main objectives of the thesis were the following:

1 – Develop a method to monitor zinc NPs in the presence of soil humic acid using SEC, in order to track the levels of NP dissolution and fixation that occur;

2 – Develop a method to sample pore waters of soils spiked with zinc NPs using dialysis tubing, in order to determine the levels of zinc in the available, exchangeable and fixed soil fractions;

3 – Set up a growth experiment using grass and soil spiked with different NPs. Monitor soil zinc availability over time, as well as plant biomass and zinc content;

4 – Set up a growth experiment using wheat, arbuscular mycorrhizal fungi (AMF) and soil spiked with different NPs. Monitor any effects on AMF, as well as plant biomass and zinc content.

The thesis consists of 7 chapters:

Chapter 1 describes the processes affecting zinc NPs in soil environments and explains the types of experiment that are frequently carried out. It includes a description of analytical techniques, instruments and approaches most commonly found in literature.

Chapter 2 covers the materials and methods that have been used throughout the thesis as a whole, including producing ZnS NPs, setting up experiments and sample analysis.

Chapter 3 describes the development of NP characterisation methods. It begins with a description of experiments carried out using SEC, continues onto experiments carried out using dialysis and finishes with an investigation into NP sonication.

Chapter 4 reports on an experiment looking at the effects of different zinc NPs on soil and ryegrass.

Chapter 5 reports on an experiment looking at the effects of different zinc NPs on AMF and wheat.

Chapter 6 begins with a discussion about the general conclusions of the thesis and follows on with some suggestions for future directions and work.

Chapter 7 contains additional statistical information for chapters 4 and 5.

Chapter 2

Materials and methods

This chapter describes general methods and approaches that have been used throughout this thesis, including field sampling protocols for soil, plant sample preparation and harvesting methods, and soil and plant material analysis. Materials and methods that are specific to individual experiments are described in their own chapters.

2.1 Producing and characterising zinc sulphide nanoparticles

Zinc sulphide (ZnS) nanoparticles (NPs) were synthesised using the method described by Ganguly et al. [256]. Briefly, 1 M Na₂S (VWR, UK) was added dropwise to 1 M ZnCl₂ (Honeywell Fluka) with continuous stirring using a magnetic stirrer at 70°C for 2 hr. The resulting ZnS NPs were collected by centrifugation at 3000 g for 15 min and the precipitate suspended in Milli-Q water. The morphology and size distribution were examined using transmission electron microscopy (TEM) analysis (JEOL, JEM-2100F FEG-TEM, **Figure 2.1**).

2.2 Soil sampling and preparation

An arable Wick series sandy loam soil was collected from a field at the University of Nottingham Sutton Bonington campus (52°49'48.6"N, 1°14'24.2"W). Soil was collected with a stainless-steel spade and sealed in plastic bags for transport. It was then

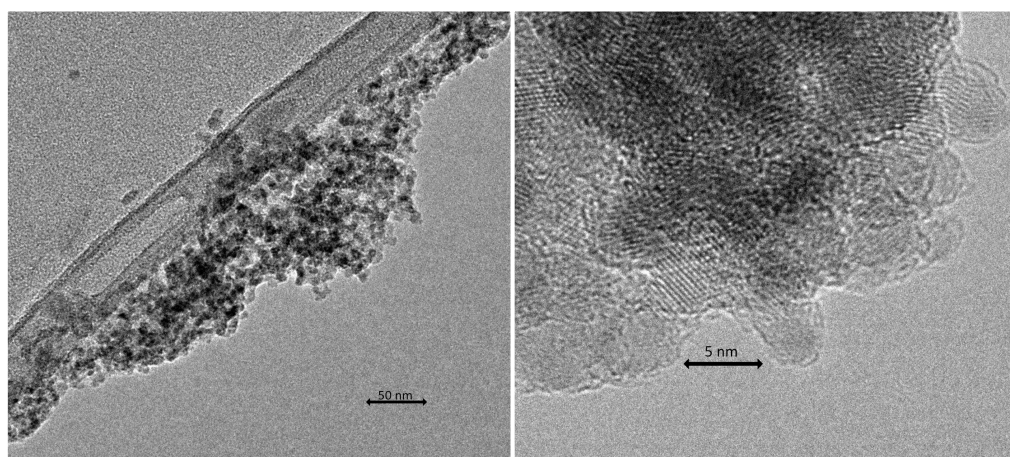


Figure 2.1 Transmission electron microscopy images of synthesised ZnS NPs at different magnifications.

homogenised by sieving to < 4 mm while field-moist and stored at 4°C before use. A small subsample of soil (~ 100 g) was separated in order to carry out characterisation (section 2.8). This was air dried at room temperature in an aluminium tray and sieved to < 2 mm.

2.3 Spiking soil with zinc species

Zinc species were added to soil fractions as aqueous solutions. The ZnS NPs, zinc oxide (ZnO) NPs and zinc phosphate ($Zn_3(PO_4)_2$) solutions were dispersed by sonication (Bandolin Sonoplus HD2070) on pulse mode for 10 min at 30% power in an ice bath. Each soil fraction was mixed in a stainless-steel mixer while the spiking solution was added and then for a further 10 min to homogenise the added zinc throughout the soil.

2.4 Preparing seeds

Seeds were inspected and any damaged or discoloured ones were removed [257]. Seeds were immersed in 3% H_2O_2 solution (v/v) for 10 min to sterilise them [152], rinsed 3 times, soaked in Milli-Q water for 1 hr and then dried. A small batch was germinated to determine the germination rate. The remaining stock was stored in dry conditions in the dark to avoid any potential loss of viability.

2.5 Growth experiments set up

Experiments were undertaken in a glasshouse at the University of Nottingham under full sunlight. Shade temperature was recorded using a Tinytag (Gemini Data Loggers, UK). Replicates were arranged in randomised block formation. An online random number generator (random.org) was used to randomise the arrangement of pots within each block.

Deionised (DI) water was used to water all of the pots every 2 – 3 days depending on the weather conditions to maintain a steady soil moisture content of ~ 80% water holding capacity (WHC).

2.6 Harvesting and processing

Grass was harvested by cutting at 1 cm above the soil surface; grass length and fresh weight were recorded [145]. After the final harvest the pots were left to dry for 3 days until the roots could be gently separated from the soil. Roots were then washed with DI water in order to remove as much soil as possible. Grass, root and grain samples were dried in an oven at 50°C for 3 days and the dry weights recorded before samples were ground using an ultra-centrifugal mill (ZM200, Retsch, Germany).

2.7 DTPA-extractable zinc

DTPA is a polydentate ligand or chelating agent consisting of an aminopolycarboxylic acid with diethylene triamine backbone and five carboxymethyl groups that forms complexes with available zinc ions (**Figure 2.2**).

Available zinc concentrations in soils were determined using an extractant solution of 0.005 M diethylenetriaminepentaacetic acid (DTPA, Fisher scientific), 0.1 M triethanolamine (TEOA) and 0.1 M calcium chloride (CaCl₂, Fisher scientific), adjusted to pH 7.3 with concentrated HCl [258]. Airdried soil (5 g) was placed in a centrifuge tube before DTPA extraction solution (10 mL) was added and the tubes shaken on a rotary shaker for 2 hr. Each suspension was then centrifuged (3000 g, 10 min) and the supernatant syringe-filtered (< 0.2 µm). Samples were diluted with Milli-Q water and acidified to 2% HNO₃ before analysis by ICP-MS (see section **2.11**).

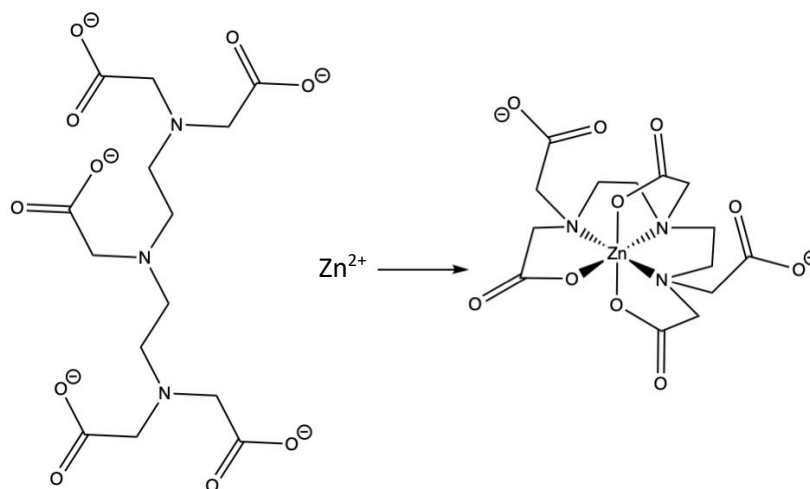


Figure 2.2 Diethylenetriaminepentaacetic acid (DTPA) forming a coordination complex with a zinc ion.

2.8 Soil characterisation

Approximately 100 g of fresh soil was air dried and sieved (< 2 mm) to use for characterisation. Soil pH was measured using a combined glass electrode (HI 209 pH meter, Hanna instruments Ltd, UK) after equilibrating soil (5 g) in Milli-Q water (12.5 mL) and shaking on a rotary shaker for 30 min. Prior to each set of pH readings the electrode was calibrated using pH 7.00 and pH 4.01 buffers. Loss on ignition (LOI) was determined by heating oven dried soil (5 g) in a muffle furnace at 550 °C for 8 hr. The % LOI was calculated from the difference between the pre-ignition and post-ignition masses. Water holding capacity (WHC) was determined by drying saturated soil in an oven at 105°C for 12 hr. The % WHC was calculated from the difference between the pre-drying and post-drying mass.

Total elemental concentrations were assayed following hydrofluoric acid (HF) digestion (see section 2.10) and analysis by ICP-MS (see 2.11). All analyses were carried out in triplicate and the data averaged.

2.9 Microwave digestion of grass and roots

Approximately 200 mg of each grass or root sample was placed into pressurised PFA digestion vessels. Concentrated (> 67%) HNO₃ (6 ml, Fisher 'trace analysis grade') was

added to each vessel and the material digested via microwave heating (Multiwave; Anton Paar, 3000 platform fitted with a 24-vessel 24HVT50 rotor). The digestate was diluted to 20 mL with Milli-Q water and transferred to a universal sample tube before dilution with Milli-Q water into ICP tubes prior to analysis by ICP-MS (see section 2.11).

2.10 Hydrofluoric acid digestion of soil

Soil was air-dried and ground using a ball mill (Retsch, Model PM400). In order to confirm the total zinc content of the soils, approximately 200 mg of each homogenized sample was digested using concentrated (67%) HNO₃ (2 mL) and perchloric acid (HClO₄, 1 mL, analytical grade, Fisher Scientific, UK) in a teflon-coated graphite block digester (Model 3, Analysco Ltd., UK) containing places for 48 PFA digestion vessels. Samples were heated at 80°C for 8 hr and then at 100°C for a further 2 hr. HF (2.5 mL, 40% trace element grade) was then added and the samples were heated to 120°C for 8 hr. A further 2.5 mL of HNO₃ and 2.5 mL Milli-Q water were then added to the dry residue and the vessels heated at 50°C for 30 min. After the digestion was complete the final volume was made up to 50 mL using Milli-Q water followed by 1-in-10 mL dilution with Milli-Q water into ICP tubes prior to analysis by ICP-MS (see section 2.11).

2.11 ICP-MS analysis

Multi-element analysis was undertaken using an ICP-MS system (Thermo-Fisher Scientific X-Series^{II}) with a 'hexapole collision cell' operating in 'collision cell with kinetic energy discrimination' mode (7% H₂ in He) upstream of the analytical quadrupole to prevent isobaric interferences. Samples were introduced from an autosampler (Cetac ASX-520 with 4 x 60-place sample racks) through a concentric glass venturi nebuliser (Thermo-Fisher Scientific; 1 mL min⁻¹). External multi-element calibration standards (Claritas-PPT grade CLMS-2, Certiprep/Fisher) which included Zn, were diluted in 2% HNO₃ (Fisher 'trace analysis grade') to provide a calibration range

of 0–100 $\mu\text{g L}^{-1}$. Sample processing was undertaken using Plasmalab software (version 2.5.4; Thermo-Fisher Scientific).

For each digestion batch, data was corrected using 2 blank digestions and concentrations converted to mg kg^{-1} :

$$X_S = \frac{(X_{\text{sol}} - X_{\text{blank}}) \times V \times 0.001}{W}$$

where X_S is the elemental concentration (mg kg^{-1}) in the soil or plant tissue; X_{sol} and X_{blank} are the concentrations ($\mu\text{g L}^{-1}$) in the sample and blank digests, corrected for dilution, V is the digest volume (L) and W is the mass (kg) of soil or plant tissue digested.

2.12 Statistical analysis

Orthogonal contrasts for analysis of variance are an *a priori* (before the fact) statistical approach that makes independent linear comparisons between treatments [259]. This means that this approach takes data with multiple factors and partitions them by making 1 degree of freedom comparisons, but these comparisons must be specified prior to the analysis. Each null hypothesis is a linear combination of treatment means, and the set of linear combinations must satisfy two mathematical properties:

- the sum of the coefficients in each linear contrast equal zero
- the sum of the products of the corresponding coefficients in any two contrasts must equal zero

In order to identify any significant differences between treatments, orthogonal contrasts were carried out in R [260]. Following this, the significant data was examined in Excel.

Chapter 3

Development of characterisation methods

3.1 Monitoring the dissolution of zinc nanoparticles in the presence of humic acid speciation using size exclusion chromatography

3.1.1 Introduction

3.1.1.1 Zinc nanoparticles in soils

As described in section 1.2, many ZnO NP-containing products are transported to WWTPs via household wastewater and can accumulate in the sludge [38], where ZnO NPs tend to undergo anaerobic sulfidation to ZnS NPs [39-42, 96]. Treated sewage sludge is then spread onto agricultural fields to fertilise soil [43, 44], however, the long-term fate of the NPs once they have entered soils is not currently known.

The importance of understanding NP dissolution within soils is described in section 1.3.2. Studies looking at the effects of zinc NPs in soil environments on plants and animal species have presented mixed conclusions, with some attributing effects to dissolved zinc [75-77], some to dissolution plus other factors [78, 79] and others not examining dissolution at all. In general, there is uncertainty as to whether results are due to the particles themselves [82], dissolved ions from the particles [75-77, 83-85] or a combination of both [86]. A major reason for this uncertainty is due to the lack of available methods for (i) extracting zinc species from soils and (ii) distinguishing between dissolved zinc and intact zinc NPs.

Recently, following an experiment to identify and characterize ZnS NPs in sewage sludge, Kim et al. [42] recommended that future studies examining ZnS NP dissolution as a function of size, aggregation state and soil type after biosolid application were needed; as yet the investigations proposed have not occurred.

3.1.1.2 Methods for analysing nanoparticle dissolution

To assess zinc NP dissolution, separate observations of the ionic zinc and particulate fractions are required; several methods intended to achieve these objectives have been explored. Some studies have used ultrafiltration to separate the free Zn^{2+} ions from the NP fraction in extracted soil pore waters [79, 84, 116]. Others have looked at IEC coupled with ICP-MS [125] or analytical ultracentrifugation (AUC) [137, 219] where speeds of $< 300,000$ g are applied to cause NPs to sediment into fractions according to their size [218]. The electroanalytical techniques, 'absence of gradients and Nernstian equilibrium stripping' (AGNES) [91] and 'anodic stripping voltammetry' (ASV) [125, 137] have also both been investigated and offer the benefit of short time resolution.

Dialysis with a membrane of a 1 nm pore size has also been used so that only dissolved zinc ions were able to pass through, allowing the ionic and particulate fractions to be separated and assayed [76].

3.1.1.2.1 Size exclusion chromatography

Size exclusion chromatography (SEC) is a technique that separates analytes based on their hydrodynamic volume (**Figure 3.1**). Species that are able to access the full pore volume of the porous solid phase within the column are retained for longer, whereas larger species are excluded and are eluted faster, resulting in analyte separation [222].

Zhou et al. [236] attempted to carry out speciation analysis of a number of metal oxide NPs and metal ions, including ZnO NPs and Zn^{2+} , using a SEC column coupled with ICP-MS, and described it as a powerful tool for studying the fate and toxicity of metal oxide NPs in the environment. While Zhou et al. attempted to apply their method to environmental water samples, the goal of this experiment was to produce a method to analyse soil pore waters.

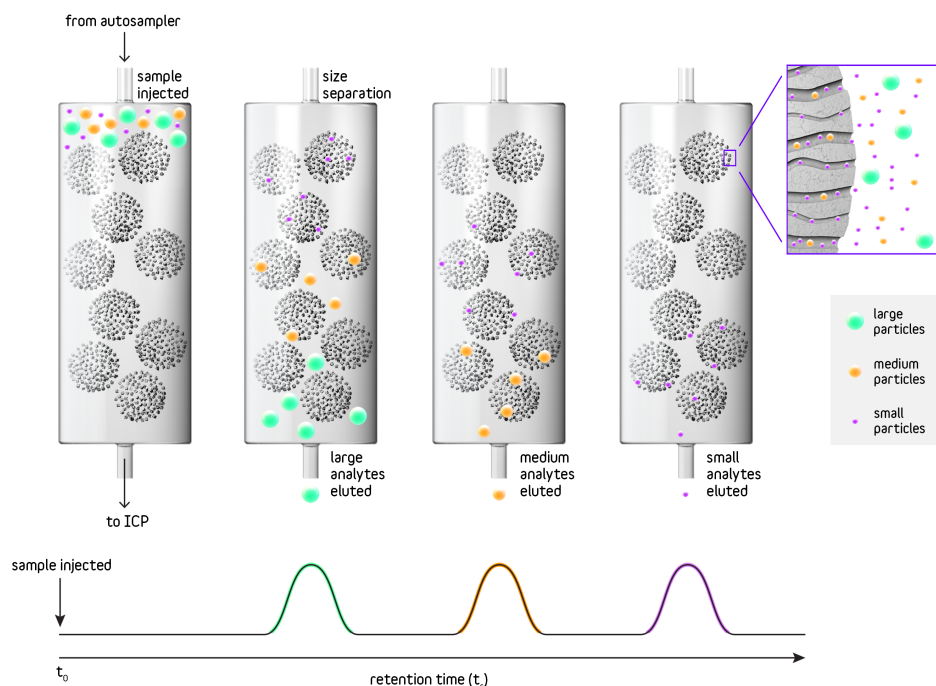


Figure 3.1 Mechanism and order of analyte separation in size exclusion chromatography

Currently, there is a lack of knowledge about the behaviour of aged zinc NPs from biosolids in soil environments, but in order for significant data to be obtained, research into this area must attempt to represent environmental conditions [48, 106-110]. As described in section **1.4.1.3**, humic acid (HA) is an operationally defined component of soil that supports many processes, including soil aggregation, trace metal mobility and water retention [261-263]. Looking at the interaction of ZnS NPs with HA could help to understand some of the processes that control their transport and fixation within soils. SEC-ICP-MS could enable NP-HS adsorption, NP aggregation and dissolution in environmental samples to be monitored within the same assay [235] and be an efficient method of obtaining information on the changing state of zinc NPs exposed to HA over time.

3.1.1.3 Aims of work

This aim of this experimental work was to monitor ZnS NP aggregation, dissolution and adsorption to HA within the same assay. It was hoped that once an operational method had been established, samples of isotopically labelled ZnS NPs and HA could be monitored over time in order to obtain information on the changing state of NPs when exposed to HA.

3.1.2 Materials and methods

3.1.2.1 Zinc species

Zn(NO₃)₂ and ZnO NPs (< 100 nm particle size, 35 nm average particle size, 50% weight dispersion in water) were purchased from Sigma Aldrich.

In order to produce ZnS NPs the method proposed by Ma et al. was followed. ZnO NPs (15 mM) were combined with NaNO₃ (10 mM) in N₂-purged Milli-Q water and sonicated in an ice bath. Na₂S (30 mM) was added and the mixture left for 5 days. After centrifuging at 6000 g for 20 min, the supernatant was discarded and the precipitate washed with Milli-Q water. This was repeated and the precipitate suspended in Milli-Q water [96].

The ZnS NPs were characterised by X-ray diffraction (XRD) and the Scherrer equation applied to estimate the average NP diameter [42, 90]. TEM analysis (JEOL, JEM-2100F FEG-TEM) was undertaken to corroborate the estimate of size.

3.1.2.2 Humic acid preparation

Humic acid was extracted and purified from a peat soil following the procedure suggested by the International Humic Substances Society (IHSS) [264]. Peat soil (300 g) was added to a large carboy container and 1 M NaOH (800 mL) was added, followed

by 0.1 M NaOH (8 L) under an atmosphere of N₂. The suspension was left overnight and the resulting supernatant collected. The supernatant was acidified with 6 M HCl and constant stirring to pH 1 and again left to stand overnight. After centrifuging, the HA precipitate was separated and redissolved by adding a minimum volume of 0.1 M KOH under N₂. Solid KCl (0.3 M [K⁺]) was added and then the mixture centrifuged to remove any suspended solids. The HA was reprecipitated by adding HCl with constant stirring to pH 1.0 and the suspension again left overnight.

After further centrifugation the supernatant was discarded. The precipitate was transferred into dialysis tubing and dialyzed against Milli-Q water. The purified HA was freeze dried and stored in the dark.

3.1.2.3 Size exclusion chromatography

Analysis was carried out using SEC with a Superose 12 10/300 GL column (GE Healthcare) with a separation range of 1000 – 300,000 Da, meaning that NPs with a diameter larger than approximately 20 nm should be excluded. Samples were injected into a 0.1 M Tris eluent at a flow rate of 1 ml min⁻¹.

The SEC column outflow was connected to the nebuliser of an ICP-MS (Thermo-Fisher Scientific X-Series^{II}) with a 'hexapole collision cell' operating in 'collision cell with kinetic energy discrimination' mode (7% H₂ in He) upstream of the analytical quadrupole to prevent isobaric interferences. ⁶⁶Zn was measured and chromatographic data were collected for 36 min.

3.1.2.4 Sample preparation

Freeze dried HA (0.2 g) was dissolved in NaOH (2 mL, 1 M) and made up to 200 mL in Milli-Q water with stirring under an N₂ atmosphere. The HA solution was separated

(3 x 30 mL) into beakers. The 3 solutions were adjusted to pH 4, 6, 8 using HNO₃ or NaOH (both 0.1 M, Fischer scientific) and left overnight. Adjustment of the pH was repeated until stable for 24 hr. Samples of ZnS NPs, ZnO NPs and Zn(NO₃)₂ at a concentration of 20 mg Zn L⁻¹ were prepared. One sample of HA at a concentration of 0.5 g L⁻¹ was produced for each pH. Mixed samples of HA (0.5 g L⁻¹) and zinc species (20 mg L⁻¹) were prepared so that there was one HA sample at every pH level for each zinc species. Samples were injected into a 0.1 M Tris eluent at a flow rate of 1 ml min⁻¹. Each SEC run took 40 minutes, so in order for all of the mixed samples to be equilibrated for 1 hr before analysis, the production of the samples was staggered.

3.1.3 Initial results

Using XRD and the Scherrer equation, the ZnS NPs were found to have a diameter of approximately 6 nm and this was confirmed by TEM (**Figure 3.2**). However, despite sonicating, it is likely that they would be present in the sample as much larger aggregates and therefore should have been excluded. Any NPs present as aggregates smaller than 20 nm or as individual particles should have been retained within the column for longer and eluted later in the run. The first injection of ZnS NPs at day 1 showed a large NP peak at around 400 s. However, the peak demonstrated such sustained tailing that the baseline was never restored (**Figure 3.3**). This indicated that a large portion of the NPs became stuck in the SEC column and by the end of the run were still not fully eluted. These trapped particles likely underwent slow dissolution and therefore distorted data by affecting not only the subsequent sample, but all samples in the following sequence.

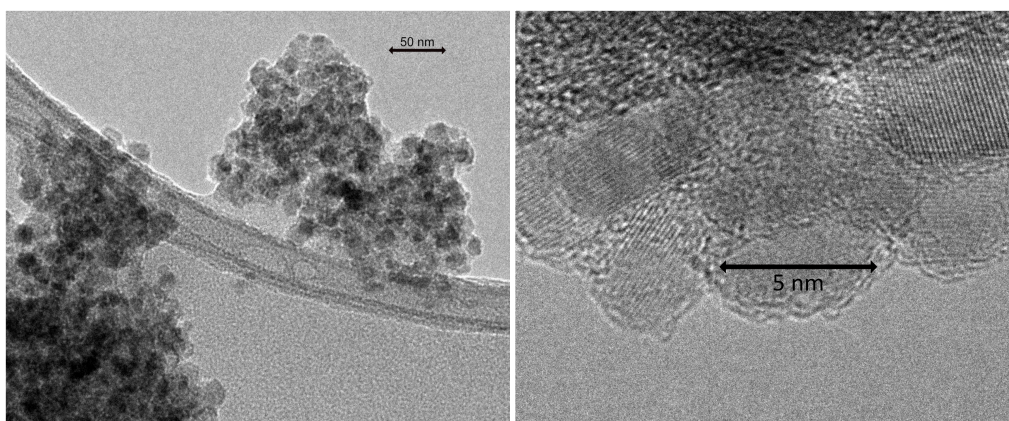


Figure 3.2 TEM images of ZnS NPs at different magnifications.

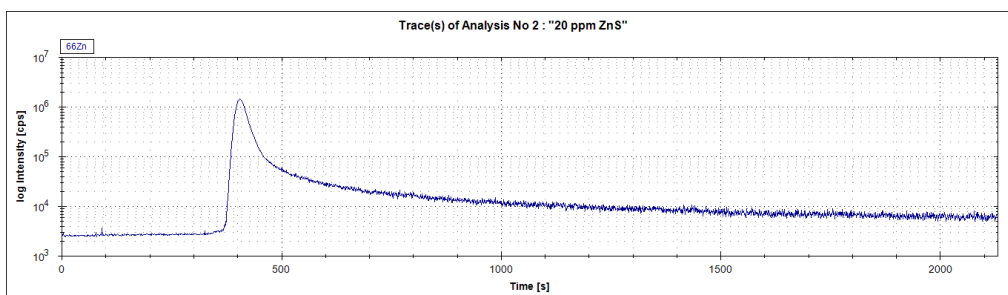


Figure 3.3 SEC-ICP-MS chromatogram showing elution of ZnS nanoparticles at day 1

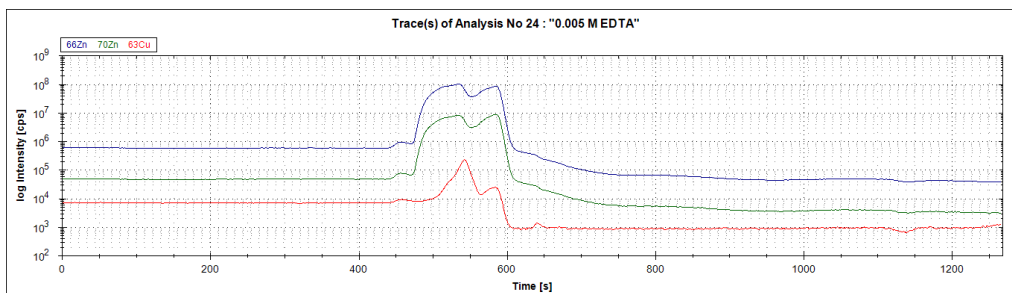


Figure 3.4 SEC-ICP-MS chromatogram showing injection of 0.005 M EDTA

Despite taking steps to reduce carryover [265] and running blanks between samples, the tailing and carryover not only continued but increased, indicating that each successive injection was causing more NPs to become trapped in the column. A final injection of 0.005 M EDTA at the end of the analysis washed a large amount of zinc out of the column and highlighted how much sample was being retained (**Figure 3.4**). The method was further developed using several different strategies.

3.1.4 Method development

The initial intention was to run the samples and then analyse them again on day 4, 11 and 36, however, once the day 1 analysis was complete it was evident that NPs were being retained by the stationary phase. The original plan for the experiment was therefore put on hold in order to focus on eliminating this sample-specific carryover.

3.1.4.1 Addition of surfactants to the mobile phase

Lui and Wei [223] looked at the effect of three different mobile phase additives on the separation of two different sizes of gold NPs using SEC. It was found that the anionic surfactant SDS (**Figure 3.5**) was most effective [223] and that the optimum SDS eluent concentration was 5 mM [224], which is close to its critical micelle concentration of $\sim 7 - 8$ mM [225, 226]. Surfactants or ‘surface-active-agents’ are molecules that have hydrophilic heads and hydrophobic tails and can form different structures as well as coatings around other species [227] (**Figure 3.6**). Their dual nature means that they can potentially disperse the NPs in the mobile phase and block unwanted interfacial interactions between the NPs and the stationary phase [222] (**Figure 3.7**).

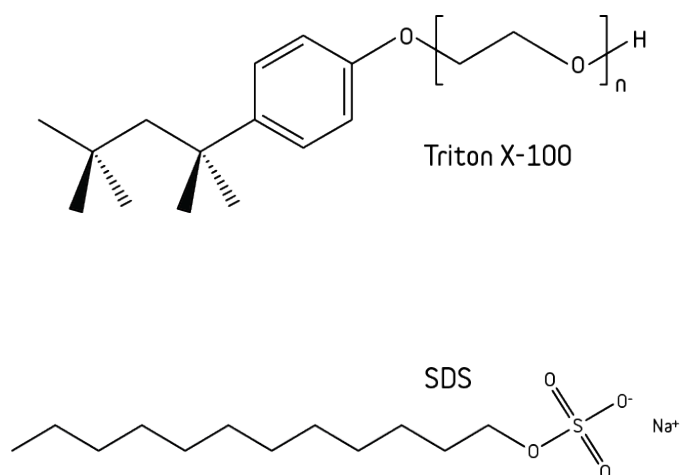


Figure 3.5 Molecular structures of surfactants Triton X-100 and sodium dodecyl sulphate (SDS). Source: author

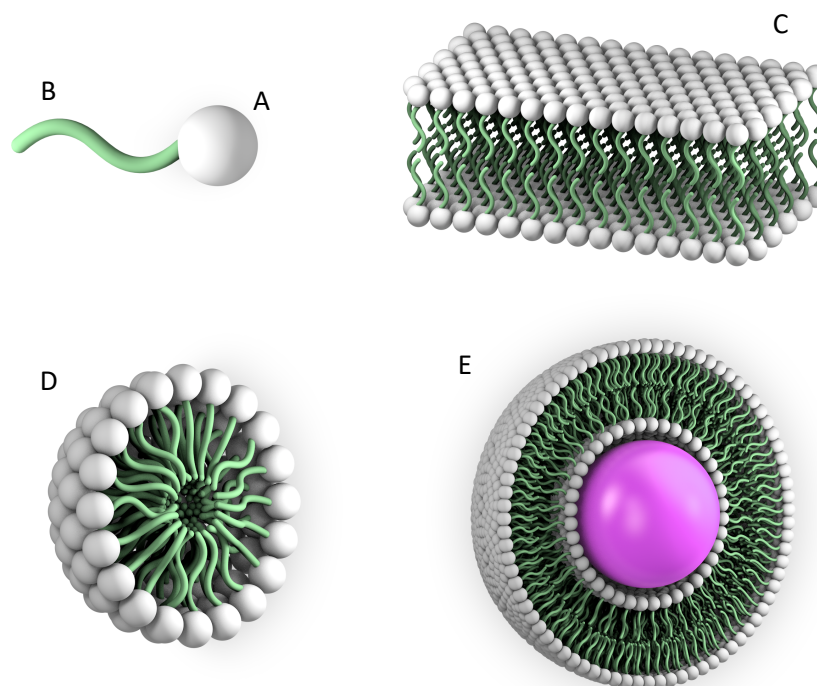


Figure 3.6 Surfactant molecules with their hydrophobic tails (A) and hydrophilic heads (B) can form structures such as: bilayers (C), micelles (D) and liposomes (E). Source: author

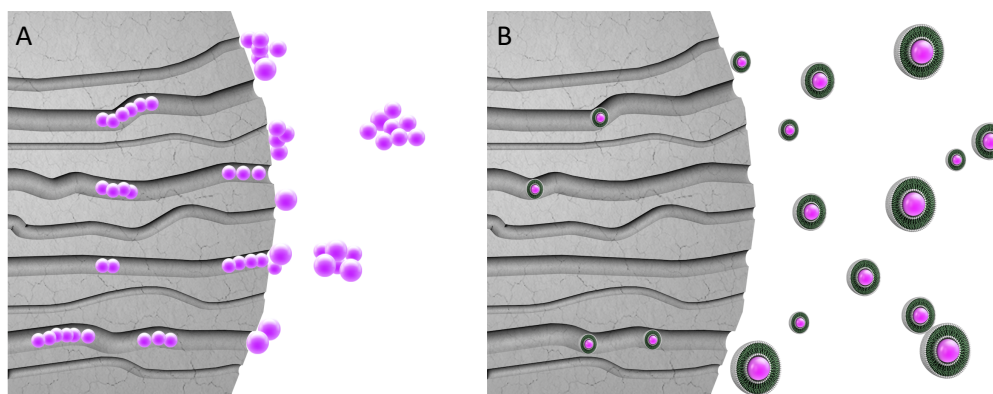


Figure 3.7 Nanoparticles without surfactant can aggregate and become adsorb to the stationary phase (A). The addition of surfactants to the mobile phase can suppress adsorption (B). Source: author

Lui and Wei consequently repeatedly used SDS in the separation of gold NPs by SEC [228-234]. SEC has also been carried out with nanomagnetite [235] and a number of metal oxide NPs including ZnO NPs [236]; both of these studies used SDS as a mobile phase additive.

Hydrodynamic chromatography (HDC) is similar to SEC but uses non-porous stationary phases. Despite the lack of pores, HDC can still suffer from NP retention within the column. SDS has been used in combination with the non-ionic surfactant Triton X-100 (**Figure 3.5**) as a surfactant addition to eluents in HDC to suppress NP agglomeration and adsorption, and increase analyte recovery [238-242].

Therefore, the aim of this experiment was to investigate the effectiveness of the surfactants SDS and/or Triton X-100 as eluent additives in the analysis of ZnS NPs using SEC.

3.1.4.1.1 Sample preparation

Samples of ZnS NPs and $\text{Zn}(\text{NO}_3)_2$ (100 mL, 50 mg L⁻¹) were prepared from stock solutions. These were each separated into 2 solutions (50 mL) and pH adjusted using HNO_3 or NaOH (both 0.1 M, Fischer scientific) to produce solutions of pH 4 and 6 of each species. From each of these, samples of 10 mg L⁻¹ of zinc were produced. Concentrations were made lower than in the previous experiment in an attempt to reduce column adsorption.

Two different surfactants were tested. For the first run, samples were injected into a 0.1 M Tris eluent containing 0.1% Triton X-100 and for the second run, the 0.1 M Tris eluent contained 0.01 M SDS. Both eluents were run at a flow rate of 1 ml min⁻¹. SEC analysis was carried out as described in section **3.1.2.3**.

3.1.4.1.2 Results

For the ZnS NP samples, the addition of SDS to the eluent was not successful, with the chromatograms still showing significant NP retention and carryover (**Figure 3.8**). The addition of Triton X-100 to the eluent resulted in an improvement in peak shape for

the ZnS NP samples at both pH 4 and 6 at the higher concentrations (**Figure 3.9**). Unfortunately, the method did not work with the ionic samples (**Figure 3.10**) so further method development was carried out.

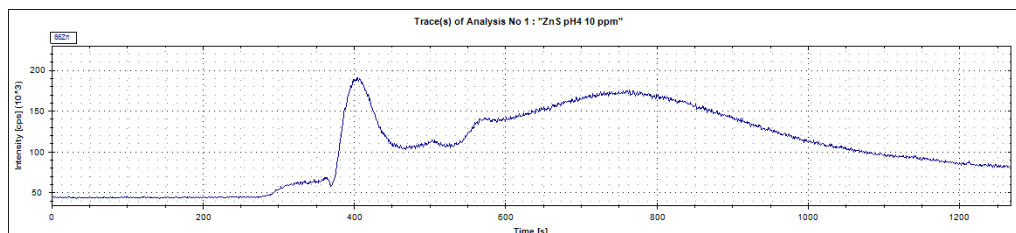


Figure 3.8 ZnS ($10 \text{ mg L}^{-1} \text{ Zn}$) in SDS eluent at pH 4

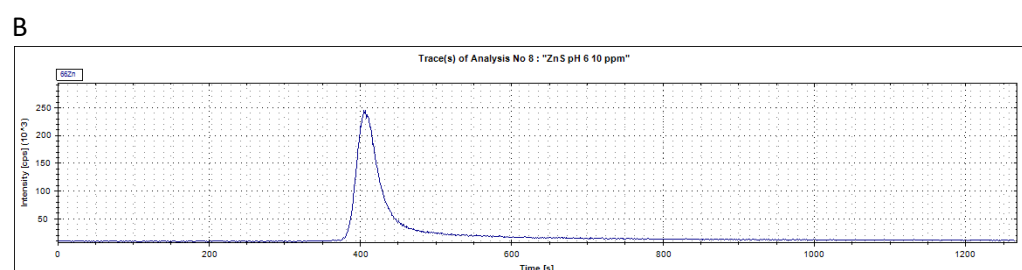
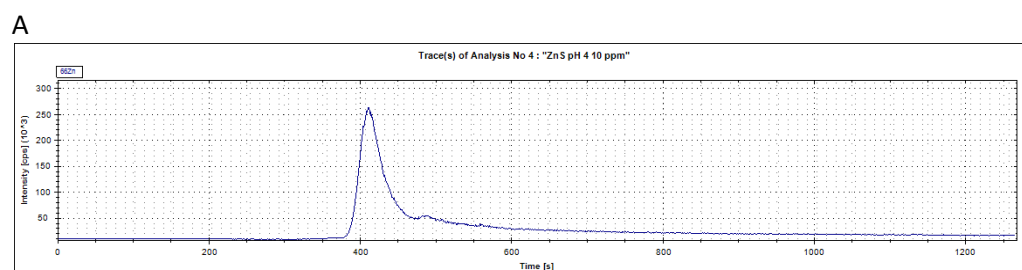


Figure 3.9 ZnS ($10 \text{ mg L}^{-1} \text{ Zn}$) in Triton X-100 eluent at (A) pH 4 and (B) pH 6

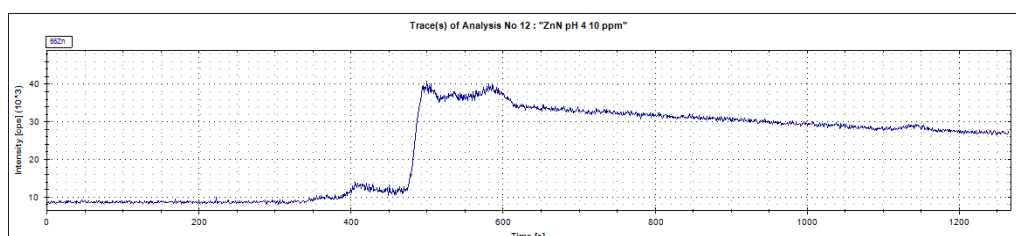


Figure 3.10 $\text{Zn}(\text{NO}_3)_2$ ($10 \text{ mg L}^{-1} \text{ Zn}$) in Triton X-100 eluent

3.1.4.2 Further adjustments

3.1.4.2.1 Change of column

Following the surfactant trials using the Superose column, it was decided that a new column would be tested. A Nucleosil column that has been used in experiments looking at Ag NPs [266] and Fe₃O₄ NPs [235] and has the same dimensions and pore size as the column used with ZnO NPs by Zhou et al. [236], was selected.

3.1.4.2.2 Addition of complexing reagent

Many published chromatography studies have added complexing reagents to either the eluent or the sample to increase the analyte separation selectivity. Zhou et al. [236] added the complexing reagent ethylenediaminetetraacetic acid (EDTA) to the mobile phase in order to dissolve any large NPs and clean out the column. For zinc analysis, EDTA has been a common choice [267-269], so it was decided that this would be added to some samples in an attempt to improve the resolution of the ionic zinc.

3.1.4.2.3 Trialling different eluents

In an attempt to improve resolution for all samples, two eluents from the literature were trialed as well as the Tris containing Triton X eluent method that had been developed previously.

3.1.4.2.4 Trialling labelled nanoparticles

It was decided to include ⁶⁸ZnS NPs in the system to monitor their response.

3.1.4.2.5 Set up

A reversed-phase Nucleosil C18 column with a particle size of 7 μm, a pore size of 1000 Å, a length of 250 mm and an inner diameter of 4.6 mm was chosen (Macherey-

Nagel GmbH & Co. KG, Düren, Germany) as this had been used in previous studies using Ag NPs [266, 270].

The eluents chosen were:

- eluent 1 - ammonium acetate (10 mM), SDS (10 mM), sodium thiosulfate 1 mM which has been used with Ag NPs on a Nucleosil column with a pore size of 1000 Å, a particle size of 7 µm and with length and diameter of 250 and 4.6 mm, respectively [266]
- eluent 2 - SDS (15 mM), NaNO₃ (10 mM), sodium citrate tribasic dehydrate (5 mM) which has been used with Fe₃O₄ NPs on 2 linked Nucleosil columns with a pore size of 4000 Å, a particle size of 7 µm and with length and diameter of 250 and 4.6 mm, respectively [235]
- eluent 3 - 0.1 M Tris containing 0.1% Triton X-100

1 – EDTA	11 – EDTA + ZnO NPs
2 – EDTA	12 – HA + ⁶⁸ ZnS NPs
3 – HA	13 – HA + Zn(NO ₃) ₂
4 – ⁶⁸ ZnS NPs	14 – HA + ZnO NPs
5 – Zn(NO ₃) ₂	15 – ⁶⁸ ZnS NPs + Zn(NO ₃) ₂
6 – ZnO NPs	16 – EDTA
7 – EDTA	17 – EDTA + HA + ⁶⁸ ZnS NPs
8 – EDTA + HA	18 – EDTA + HA + Zn(NO ₃) ₂
9 – EDTA + ⁶⁸ ZnS NPs	19 – EDTA + HA + ZnO NPs
10 – EDTA + Zn(NO ₃) ₂	

Table 3.1 Sample running order. EDTA - 5 mM; HA - 50 mg L⁻¹; Zn(NO₃)₂, ZnO NPs and ⁶⁸ZnS NPs - 100 µg Zn L⁻¹

Freeze dried HA (0.2 g) was dissolved in NaOH (2 mL, 1 M) and made up to 200 mL with Milli-Q water with stirring under an N₂ atmosphere. The HA solution was adjusted to pH 6 using HNO₃ (0.1 M) and left overnight. Adjustment of the pH was repeated until stable for 24 hr. The resulting HA stock solution had a concentration of 0.75 g L⁻¹.

Powdered ⁶⁸ZnS NPs (9 mg, Imperial College) were produced using a method from Panda et al. [271] with modifications from Chae [272] and dispersed in 10 mL of Milli-Q water to produce a stock NP solution (611.64 mg L⁻¹ of ⁶⁸Zn in 10 mL solution).

Solutions of EDTA (5 mM, Fischer scientific), HA (50 mg L⁻¹), Zn(NO₃)₂, ZnO NPs and ⁶⁸ZnS NPs (all 100 µg L⁻¹ Zn) were produced in the following combinations and run in the following order (**Table 3.1**).

3.1.4.2.6 Results

The samples of ⁶⁸ZnS generally gave very low concentrations of ⁶⁸Zn. This was thought to be mainly due to column retention, but further examination led to the realisation that there was also an issue with the concentration in the working solution which was then investigated (see section **3.3**).

For all samples containing individual species combined with EDTA, although the EDTA was added at as late a stage as possible, it chelated all the zinc present, not just the ionic fractions as was hoped. Many samples also contained significant amounts ⁶⁶Zn, ⁶⁸Zn and Cu but the levels and ratios varied. This could have been due to material being carried over in the SEC column and subsequently washed out by the EDTA, or zinc and copper contamination coming from the EDTA itself or from the mobile phase, or a combination of both (**Figure 3.11**).

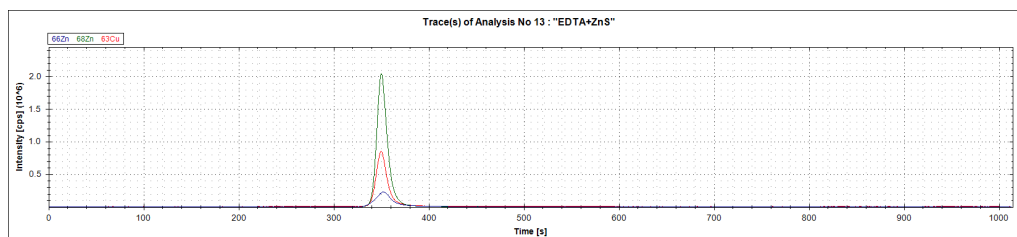


Figure 3.11 Sample run in eluent 2. EDTA + ^{68}ZnS NPs

Injections of EDTA were run between samples to check for carryover. For all 3 eluents these injections showed significant zinc peaks after all zinc samples and also significant copper peaks following samples containing HA, indicating that both the zinc NPs and the HA were being retained in the column.

3.1.5 Conclusions

In theory there should be no interaction between analyte and column stationary phase in SEC, however, a major issue that researchers have repeatedly encountered when attempting to analyse NPs using SEC is NP adsorption onto the stationary phase [222]. Sorption of NPs onto SEC column stationary phases is a problem which has been observed in previous studies [236]. Indeed, a recent review of SEC of metal NPs stated that:

“The most significant challenge in the SEC analysis of metal NPs and quantum dots is their adsorption to the column packing material” [222].

Column retention prevents quantitative analysis due to low analyte recoveries and can cause carryover from one sample to the next. The lack of research available on NP analysis using SEC is likely to be largely due to this problem.

One tactic that has been used to try to overcome the issue is to increase the pore size of the stationary phase, which reduces the overall stationary phase surface area, giving less capacity for adsorption [222]. However, the main approach has been to incorporate

additives to the mobile phase. Zhou et al. [236] found that metal oxide NPs were completely adsorbed to the column. They therefore decided to quantify ion concentration directly by SEC-ICP-MS, whereas NPs were indirectly quantified by determining the total metal concentration by direct aspiration ICP-MS and subtracting the ion content.

This experiment attempted to develop a method that could separate zinc NPs from dissolved ionic zinc and to use it to look at interactions with HA. Unfortunately, the system suffered from column retention of both NP species and HA. The addition of non-ionic surfactant Triton X-100 to a Tris eluent resulted in improved resolution and reduced tailing for some species, but not all. Furthermore, the system still exhibited NP adsorption to the column stationary phase. The next experiment attempted to rectify this NP adsorption by adding surfactants to the mobile phase. In an attempt to make further improvements, a further experiment was carried out with complexing agents added to the samples and two new methods were trialed using a new column. These experiments also highlighted that the ^{68}Zn concentration was considerably lower than expected which was subsequently investigated as described in section **3.3**.

Testing three eluents with a different column and the addition of EDTA had both positive and negative effects, but overall the issues of analyte adsorption were never resolved. Altering the specific combination of the analyte, mobile phase formulation and column stationary phase material can cause different interactions to occur and so a method cannot necessarily be successfully replicated in different systems. For example, despite using stationary phases with the same pore size, trisodium citrate was shown to be an effective stabiliser of gold NPs using a column with silica packing material [237] whereas the same method carried out on a polymer-based column exhibited severe adsorption [224].

SEC has the potential to be a good technique for monitoring zinc NP aggregation, dissolution and HA adsorption within the same assay. However, to overcome the problem of NPs being retained in the SEC column, the method has to be further developed. This has been attempted previously by adding agents such as surfactants to the mobile phase to reduce interactions between the NPs and the stationary phase as was attempted in this experiment, and also by using columns with large pore sizes which reduces the stationary phase surface area [222]. Despite this, more progress needs to be made for this to become a viable method of NP separation.

3.2 Monitoring zinc nanoparticle dissolution in soils using dialysis

3.2.1 Introduction

As described in section 1.3.2, dissolution is one of the main factors affecting NP speciation, bioavailability and toxicity [17] and section 1.6.2.3 describes some of the methods that have been used to try to differentiate between dissolved zinc and particulate fractions. In a study published in 2007, Franklin et al. [76] used dialysis tubing with 1 nm pores to compare the dissolution equilibrium of 30 nm ZnO NPs and bulk ZnO but, since then, monitoring NP dissolution using dialysis has not been pursued. Dialysis involves the diffusion of solutes from a high concentration solution across a membrane along a concentration gradient according to Fick's 1st law of diffusion [273]:

$$J_x = -D_x \frac{\partial C}{\partial x}$$

Where J is the mass flux of solute ($\text{kg s}^{-1} \text{m}^{-2}$), D is the diffusion coefficient in ($\text{m}^2 \text{s}^{-1}$), and C is the concentration (kg m^{-3}) and co-ordinate in the diffusion direction (m). Therefore, with a suitable membrane, dialysis could be used to separate dissolved ions from NPs.

3.2.1.1 Aims of work

The aim of this experiment was to monitor the dissolution of zinc NPs in soil by developing a method that could allow soil pore waters to be sampled using dialysis tubing after soil has been spiked with ^{68}ZnS NPs.

3.2.2 Materials and methods

3.2.2.1 Zinc species

Powdered ^{68}ZnS NPs (9 mg, Imperial College) were produced using a method from Panda et al. [271] with modifications from Chae [272] and dispersed in 10 mL of Milli-Q water to produce a stock NP solution (611.64 mg L^{-1} of ^{68}Zn in 10 mL).

The stock NP solution was sonicated using a Bandolin Sonoplus HD2070 at 30% power on pulse mode for 10 min. Stock ^{68}ZnS NP solution (0.1635 mL) was diluted to produce a NP working solution (1 mg L^{-1} of ^{68}ZnS in 100 mL).

3.2.2.2 Dialysis tubing

Dialysis tubing with a pore size of 2.4 nm and a diameter of 6.3 mm was purchased from Medicell Membranes. The tubing was cut into 10 cm lengths and wetted thoroughly in Milli-Q water.

3.2.2.3 Set up

An equilibrating solution ($\text{Ca}(\text{NO}_3)_2$, 0.01 M, 2 mL) was pipetted into dialysis tubing and any trapped air excluded. Three different methods of securing the dialysis tubing samples were tested: knotting, clipping the tubing using polypropylene clips (WeLoc PP 30) without folding the ends, and clipping the tubing after folding the ends.

Calcium nitrate ($\text{Ca}(\text{NO}_3)_2$, Fisher Chemicals) was used to produce a stock equilibrating solution (0.1 M) and 2 mL was added to each of 12 jars (high density polyethylene, Ampulla). Excluding the blanks, ^{68}ZnS NP stock solution (6 mL) was spiked into the jar equilibrating solutions to give an end concentration of 300 ppb of ^{68}Zn . The solution volume in each jar was made up to 20 mL using Milli-Q water.

Dialysis tubing balloons were then fully submerged into the jars of equilibrating solution. Samples were left to equilibrate on a slow shaking platform for either 1, 2 or 3 days. All samples were run in triplicate.

After equilibration, dialysis bags were removed from jars and washed in Milli-Q water. A 1 mL aliquot of the contents was removed from the tubing with a syringe and put into an ICP tube. Equilibrating solution from outside of the dialysis bag (1 mL) was removed from the jar with a pipette and put into an ICP sample tube. The samples were acidified with 0.5 mL of 40% nitric acid (HNO₃) and diluted to a final volume of 10 mL with Milli-Q water. They were then analysed by ICP-MS as described in section 2.11, in order to obtain ⁶⁶Zn, ⁶⁸Zn and ⁷⁰Zn concentrations.

3.2.3 Initial results

The 'clipped with folding' technique proved to be unsuitable because many of the samples popped open during equilibration. Both knotting and clipping appeared to be adequate methods for securing the dialysis tubing but clipping was easier to implement and there was a lower risk of damaging the tubing.

The blanks showed that there was zinc contamination in the system and that most of this zinc was in the internal dialysis tubing solution. The equilibrating solutions inside and outside of the dialysis tubing were the same when they were set up, so this contamination appeared to come from the tubing itself. The patterns and proportions of the three isotopes showed that the zinc contamination was of natural isotopic abundance. The fact that the zinc was concentrated in the internal dialysis tubing solution and had not equilibrated was notable. Either the contamination was ionic zinc but not able to pass across the dialysis membrane, or it was zinc compounds trapped inside the tubing.

The ^{68}ZnS NP samples contained only trace amounts of ^{68}Zn , a large proportion of which came from the zinc contamination. One possibility for the lack of ^{68}Zn was that the ^{68}ZnS NPs in the working solution were not dispersed well enough. In an attempt to develop the method, the system was altered in a number of ways.

3.2.4 Method development

3.2.4.1 Comparison with ionic samples

3.2.4.1.1 Sample preparation

After establishing that securing the dialysis tubing with clips was a viable method and in order to establish that ionic zinc was able to pass across the membrane, the experimental set up was repeated using ^{68}ZnS NPs, samples containing $\text{Zn}(\text{NO}_3)_2$ and a ^{70}Zn spike. The same ^{68}ZnS NPs stock solution and $\text{Ca}(\text{NO}_3)_2$ stock equilibrating solution from section 3.2.2.3 were used. In an attempt to improve the dispersion of the ^{68}ZnS NPs, the NP solutions were sonicated for longer (15 min).

An aliquot of $\text{Ca}(\text{NO}_3)_2$ (0.1 M, 2 mL) was added to 9 jars, ^{68}ZnS NPs (6 mL) were added to three of the jars and $\text{Zn}(\text{NO}_3)_2$ (6 mL, Fisher Chemicals) to another three to give a final concentration of $300 \mu\text{g L}^{-1}$ of zinc. The remaining three blanks were left unspiked. The solution volume in each jar was made up to 20 mL using Milli-Q water, as before.

The dialysis tubing was prepared in the same way as in section 3.2.2.2. For the zinc species samples, equilibrating solution ($\text{Ca}(\text{NO}_3)_2$, 0.01 M, 2 mL) spiked with ^{70}Zn ($300 \mu\text{g L}^{-1}$) was pipetted into the dialysis tubing and sealed with polypropylene clips (WeLoc PP 30). The tubing for the blank samples contained only equilibrating solution. The dialysis tubing balloons were then fully submerged into the equilibrating solution

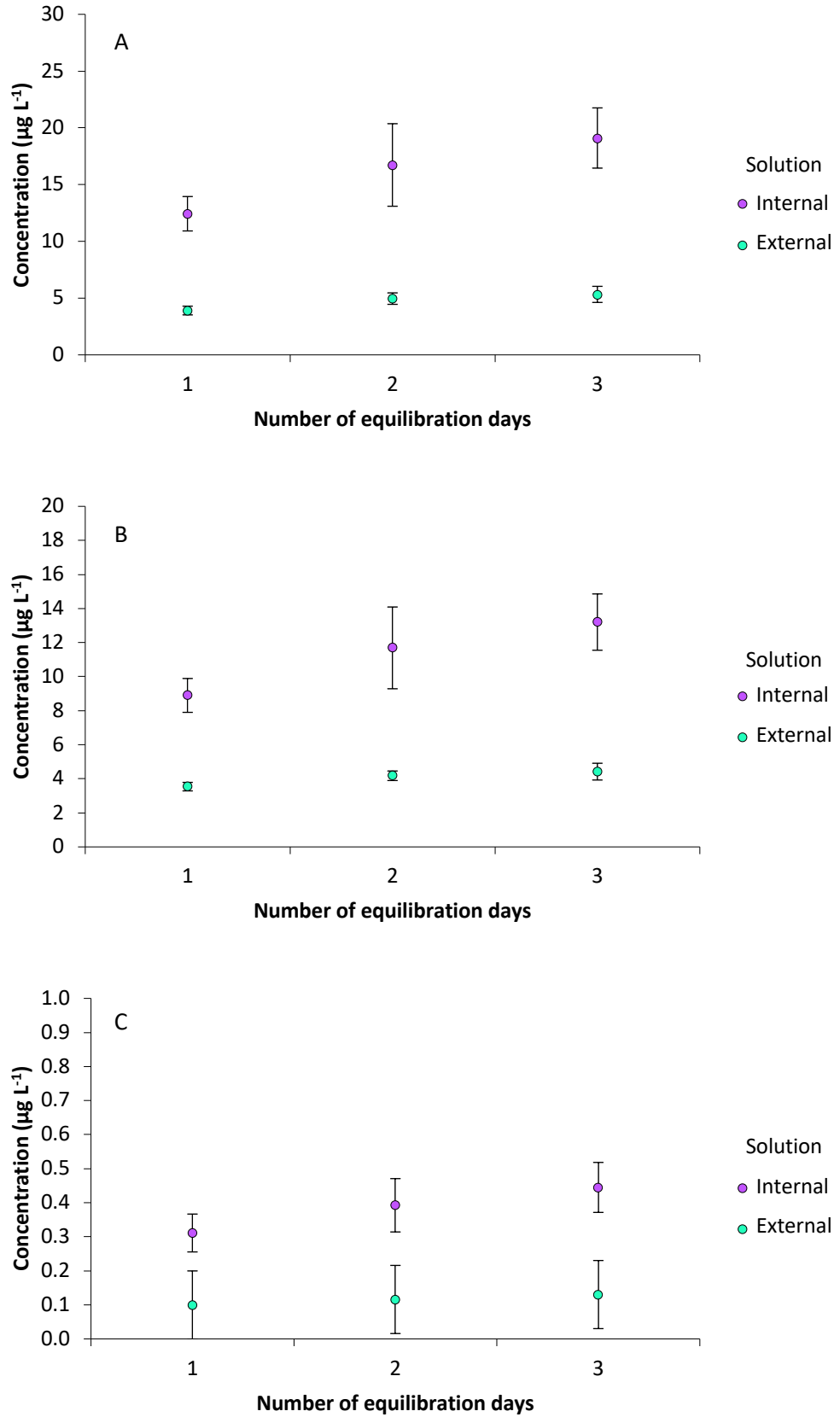


Figure 3.12 Concentration of (A) ^{66}Zn , (B) ^{68}Zn and (C) ^{70}Zn in blank samples, internal and external dialysis tubing solutions. Bars show standard deviation of the 3 replications of each sample.

in the jars. The samples were left to equilibrate on a slow shaking platform for either 1, 2 or 3 days and again all samples were run in triplicate. Samples were extracted and analysed as in section 3.2.2.3.

3.2.4.1.2 Results

As in section 3.2.3, the blanks showed that there was zinc contamination of natural isotopic abundance in the system and that there was a higher concentration of this contamination in the internal dialysis tubing solution than the external (Figure 3.12).

3.2.4.1.2.1 ^{70}Zn spike

The ^{70}Zn (2 mL, $300 \mu\text{g L}^{-1}$) spike in the samples equilibrated across the tubing (22 mL, $27 \mu\text{g L}^{-1}$), showing that ionic zinc was able to pass across the membrane and confirmed that the contamination was a result of zinc compounds from the dialysis tubing (Figure 3.13).

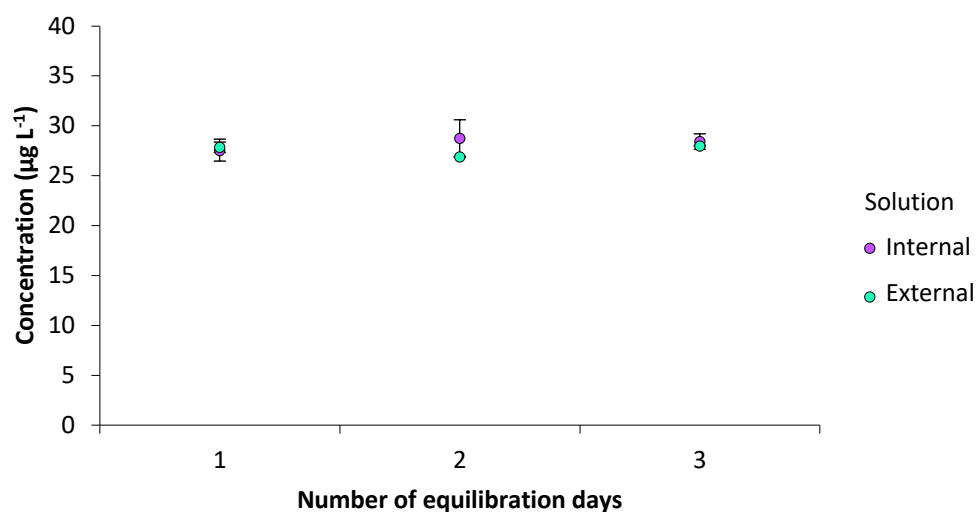


Figure 3.13 Equilibration of ^{70}Zn spike across dialysis tubing in ^{68}Zn samples. Bars show standard deviation of the 3 replications of each sample.

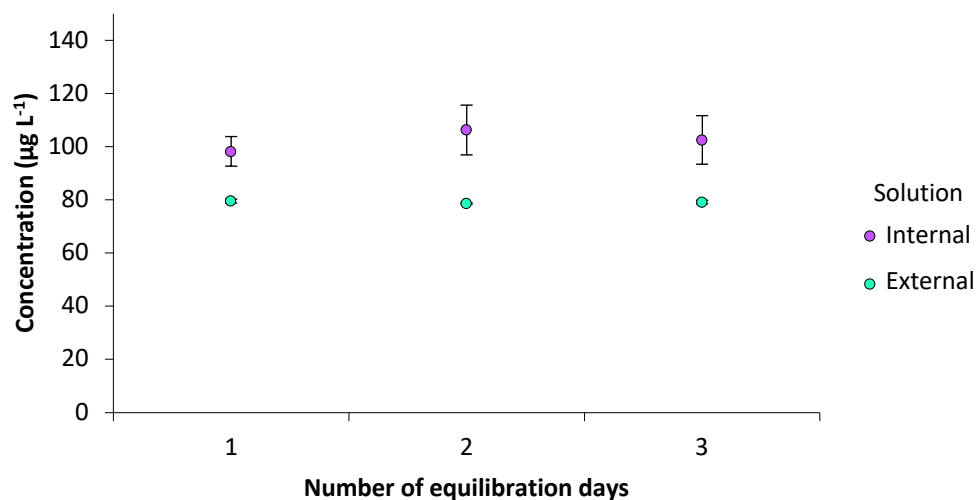


Figure 3.14 Equilibration of ^{66}Zn across dialysis tubing in $\text{Zn}(\text{NO}_3)_2$ samples. Bars show standard deviation of the 3 replications of each sample.

3.2.4.1.2.2 Zinc nitrate samples

The ^{66}Zn from the $\text{Zn}(\text{NO}_3)_2$ samples equilibrated across the tubing between the 20 mL of external equilibrating solution and 2 mL of internal (**Figure 3.14**). The $\text{Zn}(\text{NO}_3)_2$ was of normal isotopic abundance and the expected concentration of zinc was $273 \mu\text{g L}^{-1}$. The natural isotopic abundance of ^{66}Zn is 27.7%, so the expected concentration of this isotope was $75.6 \mu\text{g L}^{-1}$. Taking the average external solution ^{66}Zn concentration in the blank from the average external solution ^{66}Zn concentration in the $\text{Zn}(\text{NO}_3)_2$ samples gave a concentration of $74.4 \mu\text{g L}^{-1}$. Repeating this for the internal dialysis tubing solution shows that the concentration was slightly higher than expected at $86.3 \mu\text{g L}^{-1}$.

3.2.4.1.2.3 Isotopically labelled zinc sulphide nanoparticle samples

The ^{68}ZnS samples showed only a very slightly higher concentration of ^{68}Zn than the blanks (**Figure 3.15**). The expected concentration of ^{68}Zn was $273 \mu\text{g L}^{-1}$. Taking the average concentration of ^{68}Zn in the external solution in the blank from the average

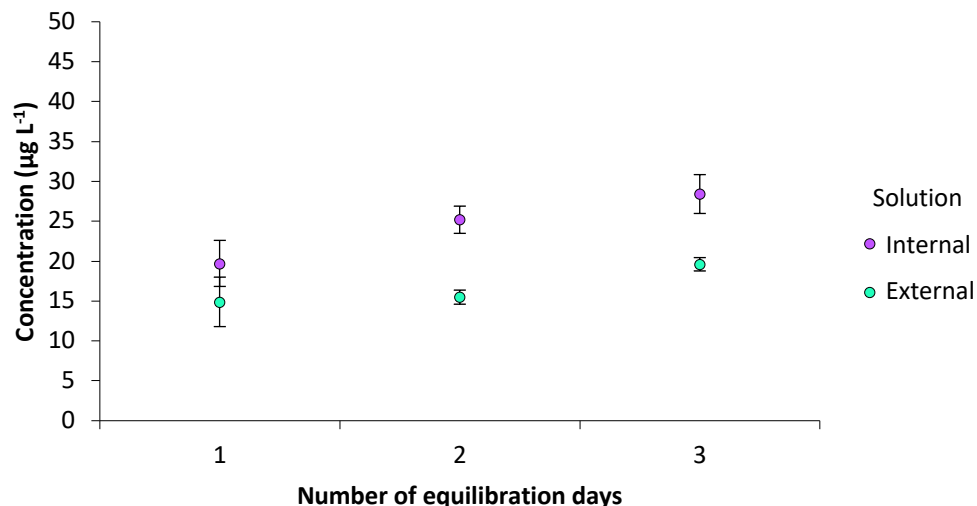


Figure 3.15 Equilibration of ⁶⁸Zn across dialysis tubing in ⁶⁸ZnS samples. Bars show standard deviation of the 3 replications of each sample.

concentration of ⁶⁸Zn in the external solution in the ⁶⁸ZnS samples gave a concentration of only 12.6 µg L⁻¹. Repeating this for the in the internal solution gave a concentration of 13.2 µg L⁻¹. The lack of ⁶⁸Zn in the samples could have been due to the NPs being inadequately dispersed during sonication and therefore not present in the working solution at the expected concentration, or from NPs adsorbing to the sides of the containers and the dialysis tubing.

This experiment found that although ionic zinc was able to pass across the membrane, the issues of zinc contamination and low concentration of ⁶⁸ZnS NP analyte continued to be a problem.

3.2.4.2 Assessing nanoparticle adsorption to equipment

3.2.4.2.1 Sample preparation

After establishing that there were major issues concerning the concentrations of ⁶⁸Zn in the equilibrated samples, an experiment was set up to assess whether the issue was due to ⁶⁸ZnS NP adsorption to dialysis tubing and jar surfaces. The same ⁶⁸ZnS NPs stock solution and Ca(NO₃)₂ stock equilibrating solution from section 3.2.2.3 were used.

Stock equilibrating solution (2 mL of 0.1 M $\text{Ca}(\text{NO}_3)_2$) was added to 2 jars and made up to 14 mL using Milli-Q water. A further 2 jars were each filled with 14 mL of 2% HNO_3 . ^{68}ZnS NPs (6 mL) were added to each jar to give an expected concentration of $300 \mu\text{g L}^{-1}$ of zinc.

Dialysis tubing was cut into 5 cm lengths and wetted thoroughly in Milli-Q water. A piece of dialysis tubing and a polypropylene clip was added to 1 jar containing $\text{Ca}(\text{NO}_3)_2$ and one containing HNO_3 . Again, all samples were set up in triplicate.

The samples were left overnight on a slow shaking platform. One mL of solution was taken from each jar and placed in an ICP tube. As with the previous experiments, the samples were acidified with 0.5 mL of 40% HNO_3 and diluted to a final volume of 10 mL with Milli-Q water. They were then analysed by ICP-MS in order to obtain ^{66}Zn , ^{68}Zn and ^{70}Zn concentrations.

3.2.4.2.2 Results

Results showed that the NPs were adsorbing to container surfaces, clips and the dialysis tubing. When dissolved in HNO_3 the average ^{68}Zn concentration in the samples with and without tubing was shown to be 44.9 and 45.2 $\mu\text{g L}^{-1}$, respectively (**Figure 3.16**). Using a $\text{Ca}(\text{NO}_3)_2$ solution caused the average concentration to be reduced to 28.6 $\mu\text{g L}^{-1}$. The addition of dialysis tubing and clips caused an additional loss, giving an average concentration of only 22.5 $\mu\text{g L}^{-1}$. Comparing the average concentration in the HNO_3 samples to the $\text{Ca}(\text{NO}_3)_2$ sample containing tubing showed that 50% of the ^{68}Zn had been lost to surface adsorption and/or sedimentation.

This experiment also highlighted that the overall maximum ^{68}Zn concentration of 45 $\mu\text{g L}^{-1}$ was significantly lower than expected, suggesting that there were serious issues with producing working reliable working solutions at intended concentrations.

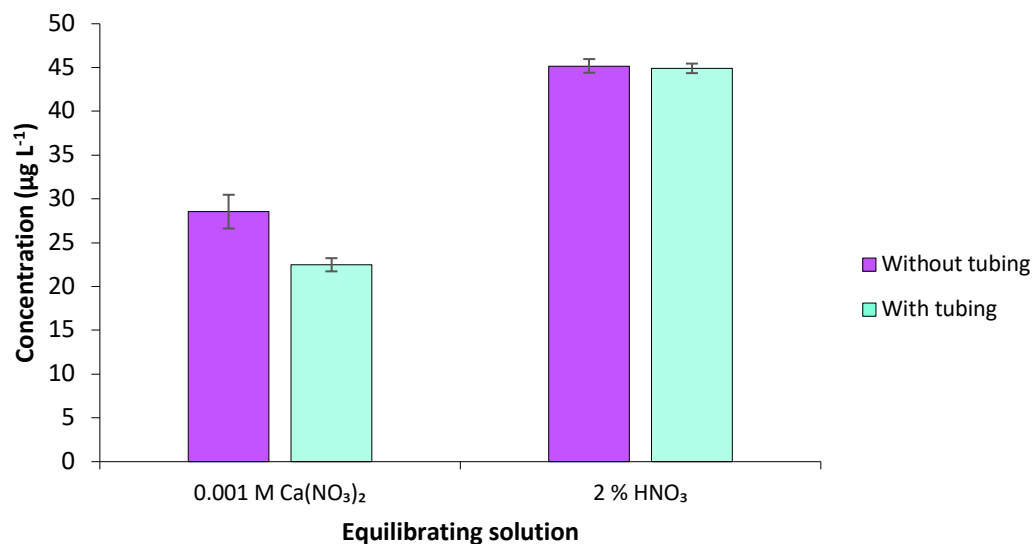


Figure 3.16 Average concentration of ⁶⁸Zn under different conditions. Ca(NO₃)₂: calcium nitrate; HNO₃: nitric acid. Bars show standard deviation of the three replications of each sample.

3.2.4.3 Eliminating zinc contamination from the dialysis tubing

3.2.4.3.1 Sample preparation

After establishing that the concentrations of ⁶⁸ZnS NPs in the working solutions being used were unpredictable and problematic, an investigation into methods for producing working solutions from the ⁶⁸ZnS NP stock solution was carried out and is described in section 3.3. The working solution for this experiment was produced by sonicating the ⁶⁸ZnS NP stock solution, using a concentration 10 times the calculated amount needed to produce a 1000 µg L⁻¹ working solution, and then checking the actual concentration of the working solution before use. This was done by taking a 1 mL aliquot of the working solution, placing into an ICP tube, dissolving the NPs in 0.5 mL of 40% HNO₃, diluting to a volume of 10 mL in Milli-Q water and analysing using ICP-MS.

Focus was then on the issue of zinc contamination from the dialysis tubing. Prior to setting up the experiment, the dialysis tubing was cut to length and washed in 0.1% HNO₃ overnight. The tubing was washed repeatedly in Milli-Q water to flush

out any remaining acid. The equipment was then set up as described in section **3.2.2.3**, using ^{68}ZnS NP, $\text{Zn}(\text{NO}_3)_2$ and blank samples.

3.2.4.3.2 Results

The aim of this experiment was to attempt to eradicate the zinc contamination from the dialysis tubing. Contamination of dialysis tubing with heavy metals, and by zinc in particular, has been previously identified as an issue [274]. Before setting up this experiment, the dialysis tubing was washed in 0.1% HNO_3 and then washed repeatedly in Milli-Q water. Analysis showed that this had been successful in eradicating the contamination because the blank samples contained only trace levels of zinc and there was no longer a significant difference between the internal and external dialysis tubing solutions with concentrations of ^{66}Zn at 1.77 and 1.43 $\mu\text{g L}^{-1}$, respectively.

Despite using a concentration 10 times the calculated amount needed to produce a 1000 $\mu\text{g L}^{-1}$ ^{68}Zn working solution, the average concentration of the 3 aliquots of working solution was shown to be only 434 $\mu\text{g L}^{-1}$. This was unexpected because for the sonication experiments (see section **3.3**) solutions of between 800 – 2400 $\mu\text{g L}^{-1}$ had been produced using the same method.

The analysis showed that the ^{68}Zn in the ^{68}ZnS samples had equilibrated across the dialysis tubing membrane, with average internal and external concentrations of 24.9 and 26.3 $\mu\text{g L}^{-1}$, respectively. If the average concentration of ^{68}Zn in the ^{68}ZnS working solution was taken to be 434 $\mu\text{g L}^{-1}$, then the anticipated concentration in the samples would be 118 $\mu\text{g L}^{-1}$. It could be that the intact NPs all stuck to the tubing and containers and/or sedimented and so were not sampled.

The sampled ^{68}Zn could be the dissolved fraction in the samples that had equilibrated across the tubing, but it is also possible that washing the dialysis tubing in acid caused

damage [274] that then allowed any suspended NPs to cross the membrane. If the membrane was functioning correctly and the NPs were suspended in solution then it would be expected that the external solution would contain a much larger proportion of ^{68}Zn than the internal solution, which would contain only the dissolved fraction of ^{68}Zn .

3.2.5 Conclusions

A number of experiments were carried out with the aim of developing a method for sampling soil pore waters using dialysis tubing after the soil has been spiked with ^{68}ZnS NPs. Experiments were carried out without soil using only solutions, with the intention of introducing soil into the system once a viable method was established.

The initial trial was carried out in order to determine how to secure the ends of the dialysis tubing. After this, the experimental set up was repeated using samples of ^{68}ZnS NPs and ionic zinc. These experiments highlighted two major issues: that the ^{68}Zn concentration in the end samples was considerably lower than expected, and that the system had a zinc contamination source. Further experiments were set up in an attempt to rectify these problems. The zinc contamination was eliminated, but it is possible that the dialysis tubing was damaged in the process. The low concentration of ^{68}Zn was subsequently investigated as described in section 3.3.

The aim of these experiments was to try to develop a method that could allow soil pore waters to be sampled using dialysis tubing after the soil has been spiked with ^{68}ZnS NPs. The idea was that soil would be spiked with a known amount of ^{68}ZnS NPs, some of which would become adsorbed to soil solid phases. Dialysis tubing would be submerged in the porewater and any dissolved ^{68}Zn would equilibrate across the membrane. The concentration would be found from sampling the internal dialysis tubing solution. The external solution should contain the same concentration of

dissolved ^{68}Zn plus the fraction of intact ^{68}ZnS NPs that remained suspended in the pore water. However, trials of this method came up with significant issues. The ^{68}ZnS NPs adsorbed to equipment to such an extent that producing samples at an expected concentration was impossible. It was found that NPs in the samples also adsorbed to the container surfaces and dialysis tubing. The tubing itself was shown to be a source of zinc contamination. Washing the tubing in dilute HNO_3 prior to set up was successful in eradicating the contamination, however, it is possible that it also damaged the membrane, allowing NPs to pass into the tubing. This method has the potential to be a useful cheap way of monitoring the dissolution of zinc NPs, but a number of issues with the particular NPs and tubing prevented trials being carried out using soils. This has also been found previously, with Misra et al. [17] stating in a review paper focused on the complexity of NP dissolution:

“use of dialysis membrane alone remains a non-trivial task, as the efficiency of recovery of dissolved species is often compromised due to adsorption of the metal ions onto the membrane”

3.3 Producing working solutions of a ⁶⁸ZnS nanoparticle sample for experimental use

3.3.1 Introduction

3.3.1.1 Nanoparticle adsorption onto equipment

As described in section 1.3.1, one of the processes that plays an important role in determining NP behaviour is their tendency to form clumps. Studies using NPs in working or test dispersions can be hindered when they clump together within the solution or with other NPs that are adsorbed onto the surfaces of equipment, causing the effective particle size to be larger and the concentration to be lower than expected or reported [67]. Indeed, it has been found that breaking apart clumps of NPs down to primary particles that are < 50 nm may not actually be possible [53, 275, 276], meaning that the primary NP diameter cited by suppliers and in scientific publications may be much lower than the effective particle size used in test suspensions [54, 67]. Pradhan et al. [67] emphasised the necessity of measuring the actual NP concentration in each individual sample due to the fact that, of the multiple samples of the 4 different NPs types that they investigated, incomplete disaggregation caused them all to have a significantly lower concentration than was intended.

One study looking into the synthesis of ZnS NP clumps found that significant analyte losses were caused by their adsorption to containers, both plastic (polypropylene, polytetrafluoroethylene Teflon and fluorinated ethylene propylene Teflon) and borosilicate glass [277]. It was shown that after 2 days, 21% of the 5 µM ZnS NPs in Milli-Q water had adsorbed onto the sides of the glass container. When the concentration of ZnS NPs was reduced to 0.03 µM in synthetic hard water the loss of analyte onto the glass container sides after 2 days was 85%. Analyte adsorption onto the sides of polytetrafluoroethylene containers from a 5 µM ZnS NP solution in

Milli-Q water was found to be 73% after 3 days. A review of environmental NP analysis and characterization methodologies recommended that [201]:

'Adsorption (of NPs) to sample bottles needs to be investigated for both inorganic and carbon-based nanoparticles on a case-by-case basis until new experience-based knowledge has been accrued. Similar concerns apply to all other materials to which the sample is being exposed (e.g., tubing, filter materials, pipettes, amongst others).'

This poses significant issues when attempting to make working solutions and/or dilutions of NPs or conduct experiments that require the concentration of NPs to be monitored over time.

3.3.1.2 Sonication

Ultrasonication is the harnessing of sound energy at ultrasonic frequencies (> 20 kHz) to agitate particles in liquid samples in order to produce a homogeneous dispersion but is generally just referred to as sonication. The sound waves disseminate around the solution causing alternating high-pressure and low-pressure cycles. These create microscopic bubbles in the solution which then collapse, causing rapid localized temperature and pressure changes, generating waves of vibration that can break apart clumped NPs [54, 278].

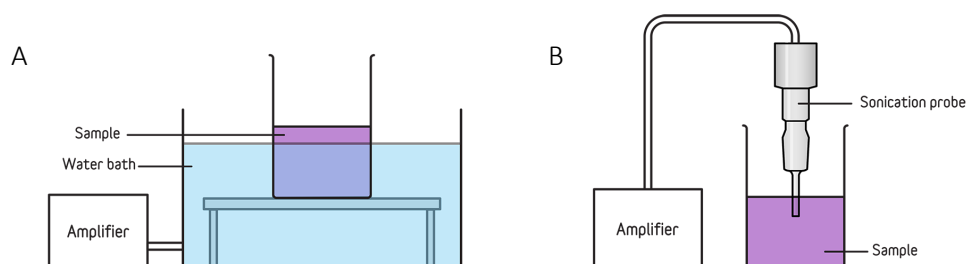


Figure 3.17 Sonicating water bath (A) and sonicating probe (B). Source: author

Sonication can be carried out using a water bath or a probe [54] (**Figure 3.17**), with probes generally generating a more monodisperse, homogeneously sized particle dispersion than baths [67].

Although sonication is regularly used to prepare test suspensions by dispersing powdered NPs through solutions or re-dispersing stock suspensions, inconsistent application has been found to actually increase sample variability [279]. A study looking at the effect of sonication on aluminium oxide NPs found that an optimum amplitude and sonication time were reached [280]. Using higher amplitudes does not improve NP dispersion and sonicating for longer time periods can actually itself cause agglomeration [275, 280], thermally-induced chemical aggregate formation [54] or increased NP dissolution [67]. Under optimal conditions, using continuous or pulsed sonication over the same time period produced no significant difference in this study, with the use of pulsed mode favoured due to the slower increase in temperature and therefore reduced solution evaporation. Although failure to follow a standardised sonication method for dispersing NPs [281] can induce physicochemical effects that cause the properties of the NPs to be altered [54], previous studies looking into harmonising the technique have found that:

'specifying the optimum sonication conditions is both critical and difficult to accomplish' [279].

3.3.1.3 Aims of work

Attempts to carry out experiments using a stock solution of ^{68}ZnS NPs were unsuccessful due to analyte concentrations being much lower than anticipated in all of the final solutions (as described in sections **3.1.4.2.6** and **3.2.4.2**, and in further experiments not covered in this thesis). It was decided that the process of producing

working solutions from the stock solution should be investigated, to make sure that the purported concentration being used to make the experimental samples was correct.

3.3.2 Materials and methods

Powdered ^{68}ZnS NPs (9 mg, Imperial College) were produced using a method from Panda et al. [271] with modifications from Chae [272] and dispersed in 10 mL of Milli-Q water to produce a stock NP solution (612 mg L^{-1} of ^{68}Zn , 10 mL). The stock NP solution was sonicated using a Bandolin Sonoplus HD2070 on pulse mode for 10 min at 30% power in an ice bath. The sonicator had a maximum power output and frequency of 70 W and 20 kHz, respectively. The ultrasonic horn that was submerged in the solution had a tip diameter of 3 mm and the sonication amplitude was in the range of 245 μm . A 50 mL centrifuge tube was filled with approximately 20 mL of Milli-Q water and 65.4 μL ^{68}ZnS stock solution added using a pipette. The Milli-Q water was added before the NPs in order to prevent them from immediately adsorbing to the sides of the container. The pipette tip was rinsed three times with Milli-Q water into the centrifuge tube working solution, which was then made up to 40 mL with Milli-Q water to give an expected concentration of 1 mg L^{-1} ^{68}Zn .

Aliquots (1 mL) of the unsonicated working solution were taken in triplicate at 1, 2, 3, 5, 10 and 20 min, and put into ICP tubes.

The working solution was then sonicated on pulse mode for 10 min at 100% power in an ice bath, and then aliquots (1 mL) taken in triplicate at 1, 2, 3, 5, 10 and 20 min, and dispensed into ICP tubes, as before.

All of the samples were acidified with 0.5 mL of 40% HNO_3 (Fisher 'trace analysis grade'), diluted with 8.5 mL Milli-Q water and analysed for ^{68}Zn by ICP-MS, as described in section **2.11**.

3.3.3 Initial results

The expected concentration of ^{68}Zn in the working solution was $1000 \mu\text{g L}^{-1}$, however, analysis showed that a large proportion of the analyte was lost during the process of preparing this solution from the primary stock solution. Initially, the ^{68}ZnS NPs could be seen sedimented at the bottom of the stock solution container. After sonication, the solution appeared to be mainly homogenised, although an oily film could be seen at the solution surface. It could be that despite sonicating the stock solution, much of the ^{68}ZnS NP material was not successfully dispersed and so was not pipetted into the working solution at the correct concentration to start with, causing the first source of analyte loss.

Prior to sonication, the working solution gave an average concentration of $105 \mu\text{g L}^{-1}$ which fell to only $94.3 \mu\text{g L}^{-1}$ over a period of 20 min (**Figure 3.18**). This suggested that despite the lower than expected concentration, the NPs that were present in the working solution were at least stable enough in suspension to be used for a short time after the working solution was produced. The standard deviations of the replications showed that the concentration of the aliquot repeats were consistent.

Applying sonication to the working solution increased the ^{68}Zn concentration to an average of $239 \mu\text{g L}^{-1}$, which then also remained fairly stable over a period of 20 min. Applying a line of best fit to the average concentrations showed that the rate of decline was very similar for both before and after sonication, but with the R^2 value showing that the 'before sonication' data was a closer fit.

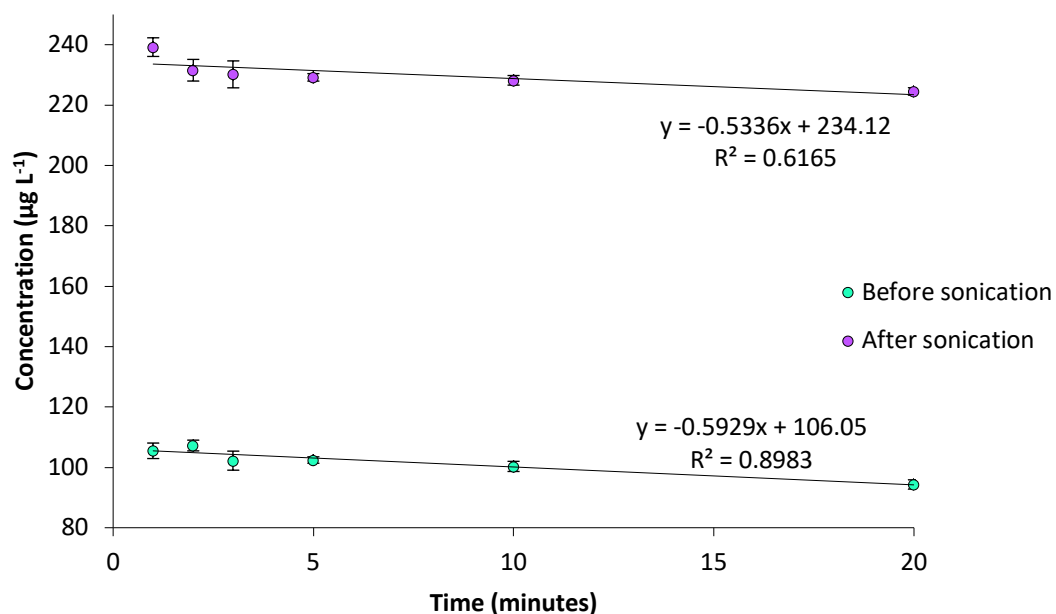


Figure 3.18 Concentration of ⁶⁸Zn in working solution before and after sonication. Bars show standard deviation of the 3 replications of each sample.

These results indicated that, at the point of production of the working solution some of the NPs were adsorbed onto the solution container, a proportion of which were then liberated upon sonication. Therefore, another source of analyte loss appeared to be the hydrophobic nature of the NP aggregates which caused adsorption to equipment such as the plastic surfaces of the containers and pipette tips. This was investigated in the next experiment.

3.3.4 Method development

3.3.4.1 Investigating nanoparticle adsorption onto equipment

3.3.4.1.1 Sample preparation

The same stock solution of ⁶⁸ZnS NPs was used to prepare a working solution with an expected concentration of 1000 µg L⁻¹ ⁶⁸Zn, as before. The pipette tip used to dispense the stock solution was rinsed three times with Milli-Q water into the centrifuge tube working solution, which was then made up to 40 mL with Milli-Q water to give an expected concentration of 1000 µg L⁻¹ ⁶⁸Zn. The pipette tip was left soaking overnight

in another centrifuge tube containing 40 mL of 10% HNO₃, in order to assess how much NP analyte had remained adsorbed to the tip. This process was repeated using 0.01 M Ca(NO₃)₂ (Fisher chemicals) instead of Milli-Q to see if a different solvent had any effect.

The working solution was then sonicated on pulse mode for 10 min at 30% power in an ice bath and transferred to a second 50 mL centrifuge tube. The original centrifuge tube was filled with 10 mL of 10% HNO₃ in order to assess how much analyte had remained stuck onto the container sides.

The pipette tip samples and the container residue samples were all left on a slow shaking platform for 3 days. A 1 mL aliquot of the working solution was removed and put into an ICP tube immediately after sonication, again every 30 min over a period of 3 hr. The aliquots were acidified with 0.5 mL of 40% HNO₃.

The aliquot samples were diluted with 8.5 mL of Milli-Q water and 1 mL of each of the pipette tip and container residue samples were diluted with 9 mL of Milli-Q water. All of the samples were then analysed for ⁶⁸Zn by ICP-MS as before. The whole process including the production of working solutions and all samples were carried out in triplicate.

3.3.4.1.2 Results

Total average ⁶⁸Zn concentration in three working solutions were taken after production, sonication and transfer into a new container. Results showed that again the average concentration was considerably lower than the expected value of 1000 µg L⁻¹, in both Milli-Q water and 0.01 M Ca(NO₃)₂. Aliquots were taken over a period of 3 hr and during this time the average ⁶⁸Zn concentration in all of the working solutions remained close to the initial concentration.

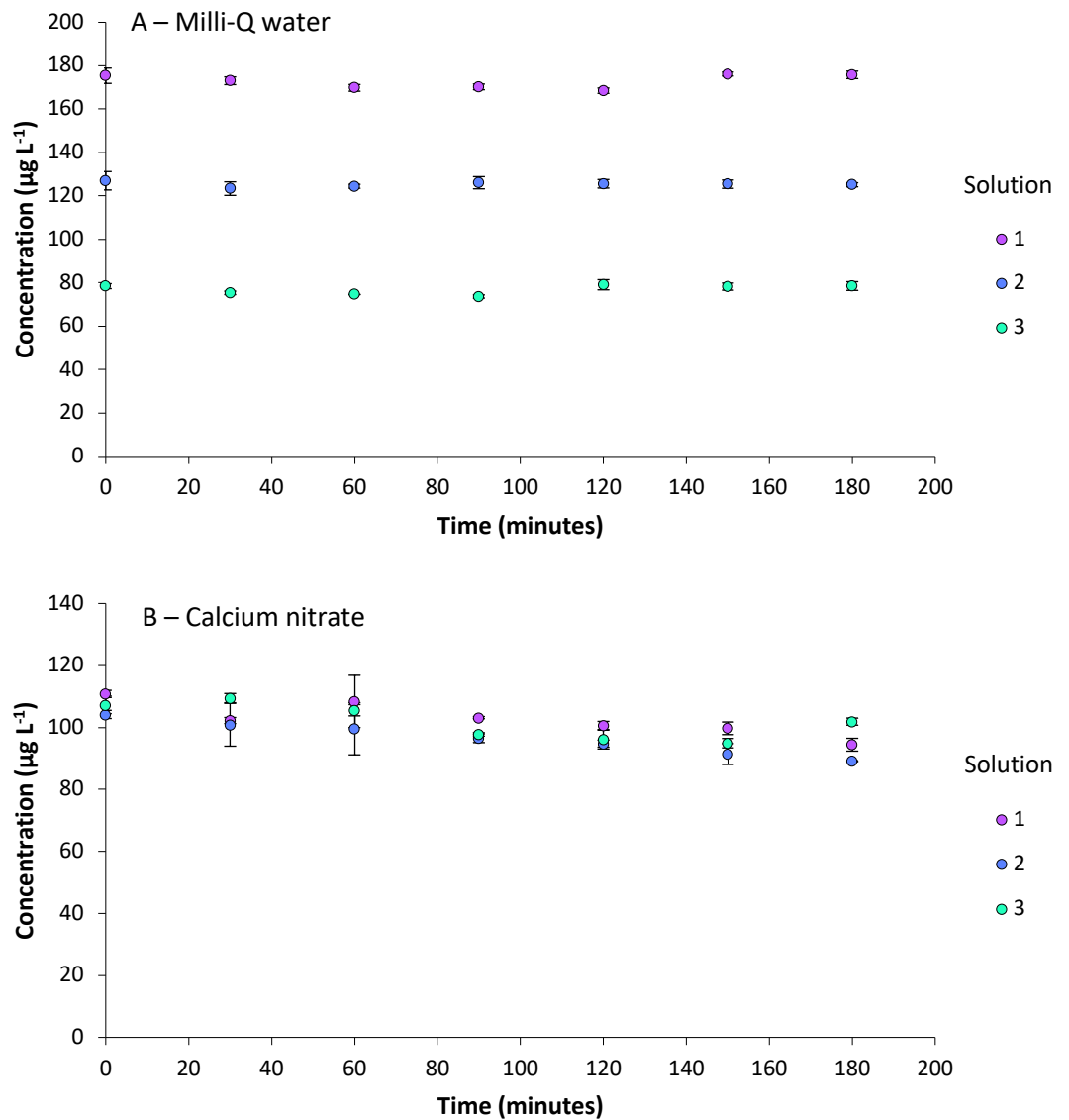


Figure 3.19 Average ⁶⁸Zn concentration over time in (A) Milli-Q water and (B) calcium nitrate working solutions. Bars show standard deviation of the three replications of each sample

Replication was very consistent, with the standard deviation of < 2 µg L⁻¹ for the majority of triplicate aliquots (black bars). The initial average ⁶⁸Zn concentrations in the working solutions produced in 0.01 M Ca(NO₃)₂ were close to one another, but the ones produced in Milli-Q water varied considerably (**Figure 3.19**).

A – Milli-Q water

Average mass ⁶⁸ Zn (µg)	Working solution 1	Working solution 2	Working solution 3
Solution	7.02	5.08	3.14
Pipette tip	1.58	3.88	2.66
Container	3.11	2.63	2.71
Unaccounted for	28.3	28.4	31.5

B – Calcium nitrate

Average mass ⁶⁸ Zn (µg)	Working solution 1	Working solution 2	Working solution 3
Solution	4.43	4.17	4.29
Pipette tip	6.17	3.64	3.21
Container	2.33	2.67	2.59
Unaccounted for	27.1	29.5	29.9

Table 3.2 Average mass (µg) of ⁶⁸Zn in samples. A: Milli-Q samples; B: calcium nitrate samples

The mass of ⁶⁸Zn in the solutions, pipette tip and container samples are shown in **Table 3.2**. The ratios for each working solution varied, but all of them had a large proportion of the total 40 µg of ⁶⁸Zn unaccounted for. Some of this could be due to insufficient dispersal of the original stock solution, and another portion a result of NP sedimentation.

3.3.4.2 Producing a stable working solution of the required concentration

3.3.4.2.1 Sample preparation

The same stock solution of ⁶⁸ZnS NPs was used to prepare a working solution with an expected concentration of 10 mg L⁻¹ ⁶⁸Zn, in triplicate.

The working solution was then sonicated on pulse mode for 10 min at 30% power in an ice bath and transferred to a second 50 mL centrifuge tube.

A 1 mL aliquot of the working solution was removed and put into an ICP tube immediately after sonication, and again every 30 min over a period of 3 hr. Further aliquots were taken at 2, 4 and 7 days. The aliquot samples were acidified with 0.5 mL of 40% HNO₃, diluted with 8.5 mL of Milli-Q water and analysed for ⁶⁸Zn by ICP-MS, as before. All samples were taken in triplicate.

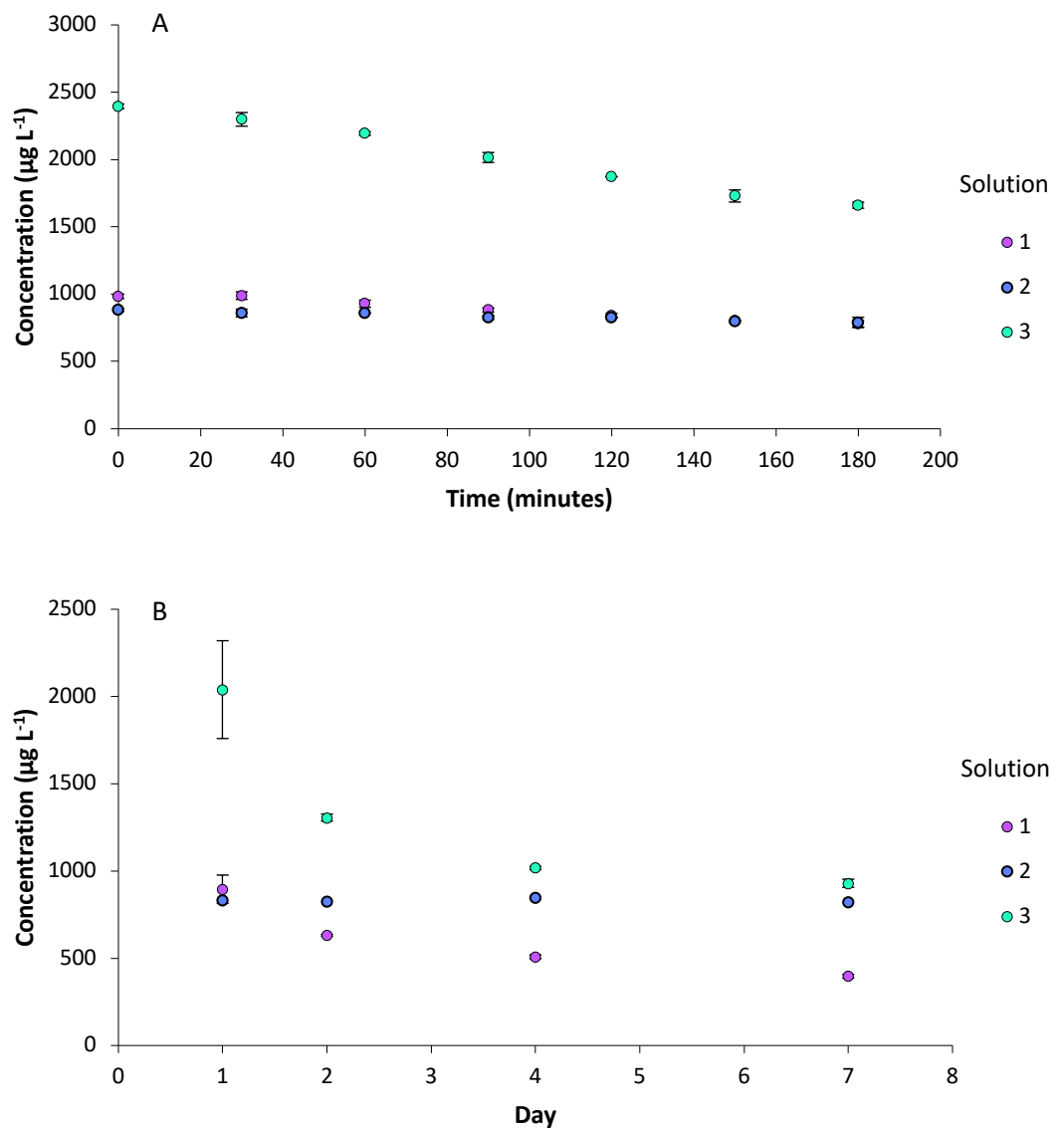


Figure 3.20 Average ⁶⁸Zn concentration over minutes (A) and days (B) in working solutions. Bars show standard deviation of the three replications of each sample

3.3.4.2.2 Results

The working solutions of an expected concentration of 10 mg L^{-1} demonstrated similar behaviour to the solutions of an expected concentration of 1 mg L^{-1} . Both sets of working solution samples gave initial concentrations between 7 – 24% of the expected concentration. As before, although the initial effective concentration varied between the working solution replicates, each remained fairly stable over a period of 3 hr (**Figure 3.20**).

These results suggest that it is possible to make a stable working solution of around $1000 \text{ } \mu\text{g L}^{-1}$ of this batch of ^{68}ZnS NPs, accepting a large amount of loss during its production.

3.3.5 Conclusions

The stabiliser used in the production of the ^{68}ZnS NPs was polyvinylpyrrolidone (PVP). It is the stabiliser that dictates the surface chemistry and therefore their stability in a given solvent [282]. The synthesis used zinc nitrate and thioacetamide with the PVP, heated under reflux and then washed with isopropanol and water. PVP controls the NP dispersion through steric repulsion, so NPs should not aggregate because PVP provides a physical barrier inhibiting this process. However, some reports suggest that dispersions of PVP-stabilised NPs are sensitive to both pH and ionic strength of the solvation medium and this would imply there is also some element of stabilisation through electrostatic repulsion [283, 284]. If electrostatic repulsion does modulate NP stability, then changes to pH or ionic strength could cause NPs to be harder to disperse. The intention was to check the NPs' point of zero charge using DLS, however, that required a solution that was concentrated enough for the DLS to recognise, and this was not possible to produce.

The first experiment was carried out in order to investigate what the concentration of a ^{68}ZnS NP working solution calculated to be $1000 \mu\text{g L}^{-1}$ actually was, and what effect sonicating the working solution had. The second experiment was looking at ^{68}ZnS NP losses that occurred during the process of making working solutions and the third experiment attempted to produce a working solution of approximately $1000 \mu\text{g L}^{-1}$ and tested its stability over time.

Although it could be anticipated that using a higher NP concentration in a suspension could cause a greater fraction of the NPs to be successfully dispersed, or conversely a greater degree of aggregation and sedimentation, it has been shown here that the proportion of ^{68}ZnS NP availability remained similar whether a working solution of 10 mg L^{-1} or 1 mg L^{-1} was produced, although it must be stated that the concentration of solution replicates produced was variable and unpredictable. Between 80 – 90% of the NP analyte was lost during the process of making the working solutions, some of which was a result of adsorption to the surfaces of equipment. Dispersing the NPs in a dilute salt rather than water did not reduce the analyte loss. In order to produce a working solution of ^{68}ZnS NPs at approximately $1000 \mu\text{g L}^{-1}$ for future experiments, a concentration of 10 times the calculated amount needs to be used, steps need to be taken to reduce NP loss via adsorption onto equipment surfaces and then the actual concentration of the working solution produced needs to be checked before use.

3.4 Overall conclusions

Environmental fate and toxicity of NPs is an area of research still very much in its infancy. This means that the majority of the literature to date has focused on gold NPs in simple systems. Analytical methods for assessing zinc NPs have not been established and reference material is not yet available. This being the case, the original project concept to monitor the behaviour and transformations of zinc NPs in soils at

environmentally expected levels was ambitious and extensive. Monitoring zinc NPs in soils has been carried out, but using pristine ZnO NPs [116, 285] rather than aged zinc NPs, excessively high NP concentrations are frequently used [89, 145] and soil is often replaced with a simplified matrix [61, 158-161].

This project aimed to monitor the transport and fate of aged zinc NPs in soils and plants using systems that accurately represent environmental processes. Specifically, the intention was to investigate zinc NP dissolution in soils. This chapter documents some of the attempts that were made to develop a method that could distinguish between zinc NPs and dissolved ions so that zinc NP dissolution in soils could be monitored. It was hoped that this could be achieved by using isotopically labelled ^{68}ZnS , allowing low concentrations of NPs to be differentiated from native zinc and tracked. Different methods were investigated and developed. However, the labelled NPs proved very challenging to use. The main difficulty was their proclivity for adsorbing to equipment. Their high initial cost of production meant that only 20 mg of powdered sample could be purchased, but the losses to equipment surfaces at every stage of every experimental trial meant that the effective amount obtained once in solution was significantly lower than 20 mg. Method development used up a large proportion of the ^{68}ZnS NP stock and was unsuccessful in producing any viable methods capable of achieving the initial aims. Thus, despite many different methods being explored, it was not possible to develop effective working protocols with the time and equipment available.

The review paper on NP dissolution by Misra et al. [17] highlights that the majority of potential analytical methods to assess dissolution first require the separation of the dissolved fraction, but that:

'it should be noted that evaluating dissolution of NPs, is not trivial.....the effective separation of particulates from truly dissolved species and maintaining an optimal recovery of the dissolved fraction remains the main challenge'

After devoting a large portion of time and resources to method development, it was decided that for the remaining time the project should take a different focus. Rather than continuing to examine mechanistic processes, the experiments would now be centred around observational data derived from growing plants on soils spiked with different zinc NP species.

Chapter 4

Effects of different zinc nanoparticles on soil and ryegrass

4.1 Background

Zinc is an essential plant micronutrient that is necessary for the function of many enzymes used in nitrogen and carbohydrate metabolism, energy transfer and protein synthesis [286, 287]. Zinc deficiency in plants can result in stunted and deformed growth, vulnerability to infection and crop yield reduction [288]. However, excessive uptake of zinc can affect cell membrane permeability and disrupt cell energy-producing functions leading to enzyme inhibition, oxidative stress and toxicity in plants [288, 289]. This manifests as wilting, leaf chlorosis and necrosis, biomass decline, and a reduction in the mitotic activity of roots, with the toxicity threshold varying between plant species [287].

Zinc NPs contained in personal care products can enter soil environments as a result of biosolid application onto agricultural fields, potentially affecting crop health. As described in section 1.5.2, many studies have investigated zinc NP bioaccumulation and phytotoxicity in a variety of different plant species. Despite it being shown that the species present in biosolids are ZnS NPs and $(Zn_3(PO_4)_2)$ [39-42], these studies have typically examined ZnO NPs [72, 74, 81, 85, 86, 290-296] and some have included bulk ZnO and ionic zinc for comparison.

A wide range of phytotoxic effects have been shown to occur in plants as a result of ZnO NP exposure. It has been reported that ZnO NPs significantly reduced the germination rate and biomass of alfalfa plants [89], stunted root length in rice [153], and prevented soybean from producing seed [169]. Studies have often focused on germination and seedling development, harvesting plants somewhere between a few days [81, 118, 153] and a few weeks [85, 86, 89, 102, 119], with studies extending to eight weeks described as 'long-term' [149, 150]. The effect of ZnS NPs has been investigated

on mung bean [297] using filter paper as a substrate and sunflower [298], employing foliar applications.

In contrast to any potential phytotoxicity, many other studies have focused on the effectiveness of ZnO NPs as a potential alternative to conventional fertilisers [299-302].

It is well documented that fertilisers with high release rates can overwhelm plants' nutritional needs and result in excess nutrients being transformed, lost in leachate away or 'fixed' in soils, leading to limited fertiliser efficiency and sustainability. The high solubility and therefore low environmental stability of ZnO NPs could mean that they present some of the same issues. It has been suggested that the solubility of ZnO NPs could be controlled by sulphidising a thin ZnS layer on the ZnO NP surface to inhibit the ZnO dissolving process in water [303]. However, it has also been found that with foliar application, both ZnO NPs and ZnS NPs are more easily absorbed by plants than ZnSO₄ [304]. Therefore, it is possible that the application of zinc as poorly soluble ZnS NPs could provide a strategy to feed plants gradually, possibly in a controllable manner. If effective, the benefits could include an increase in fertilizer use efficiency and a reduction in environmental hazards [305, 306]. If it was found that applying biosolids containing ZnS NPs offered similar advantages, rather than simply assuming toxicity from ZnO NPs that may not be present, this could further improve nutrient delivery efficiency and sustainability.

Lolium perenne (ryegrass) is a monocot plant in the Poaceae family that has a rapid growth rate and regrows when cut [307], allowing repeated harvests in the same season to be studied. The phytotoxicity of ZnO NPs on *Lolium perenne* has been investigated using a hydroponic culture system [80] and filter paper [81] but not using soil as a growth substrate. Ryegrass has also been investigated using gold NPs in a hydroponic system [308] and hydroxyapatite NPs in soil [309].

This study aimed to investigate how *Lolium perenne* was affected when grown on soil spiked, for comparative purposes, with ZnO NPs, ZnS NPs, Zn₃(PO₄)₂ particles and ionic zinc, over a period of 18 weeks. The objectives were: (i) to assess whether there is a significant difference in the effect of ZnS NPs and Zn₃(PO₄)₂ particles with ZnO NPs and ionic zinc on the growth of *Lolium perenne*, (ii) to evaluate changes in zinc availability using DTPA extractions and (iii) to evaluate changes in zinc uptake.

4.2 Materials and methods

4.2.1 Zinc species

ZnS NPs were synthesised by the method developed by Ganguly et al. [256] and characterised as described in section 2.1. ZnO NPs (advertised average particle size ≤ 40 nm, 20% wt in H₂O) and Zn₃(PO₄)₂ were purchased from Sigma-Aldrich, and ZnSO₄ was purchased from Fisher Scientific.

Solutions (35 mL) of all of the zinc species (ZnS NPs, ZnO NPs, Zn₃(PO₄)₂ and ZnSO₄) were suspended in Milli-Q water at concentrations calculated to provide a spike of either 100, 300 or 600 mg Zn kg⁻¹ to each soil fraction on a dry weight basis.

4.2.2 Soil sampling, preparation and characterisation

Soil was collected and treated as described in section 2.2 and characterised as described in section 2.8.

Thirteen aliquots of soil were weighed out (1.8 kg each on a dry weight basis), one aliquot for each zinc spiking species (ZnS NPs, ZnO NPs, Zn₃(PO₄)₂ and ZnSO₄) at each concentration level (100, 300 and 600 mg Zn kg⁻¹), with one for the un-spiked control. Zinc species were added to soil fractions as aqueous solutions (35 mL), as described in section 2.3.

Plant pots (65 large (1 L) and 39 small (0.36 L)) were prepared by covering the draining holes with filter paper. Thirteen large plant pots were filled with 300 g (dry weight) of spiked (ZnS NPs, ZnO NPs, $Zn_3(PO_4)_2$ and $ZnSO_4$ at 100, 300 and 600 mg of Zn kg^{-1}) or un-spiked (control) soil, with five replicates made of each. Thirteen small plant pots were filled with 100 g (dry weight) of spiked (ZnS NPs, ZnO NPs, $Zn_3(PO_4)_2$ and $ZnSO_4$ at 100, 300 and 600 mg of Zn kg^{-1}) or un-spiked (control) soil, with three replicates made of each. Milli-Q water was added to bring each pot up to approximately 80% WHC. Pots were then left to equilibrate in the dark for 24 hr before sowing seeds.

4.2.3 Preparing seeds

Dwarf ryegrass seeds (*Lolium perenne*) were treated as described in section 2.4. A small batch was germinated and the average germination rate was > 90%. Seeds were sown in each 1 L (13 cm diameter) pot at a rate of 1 $kg\ ha^{-1}$ which corresponded to 13 g per pot. Potassium nitrate (KNO_3 , 0.02 M, Fischer chemicals) was then added to each pot at a rate of N equivalent to 200 $kg\ ha^{-1}$ [310, 311], and again at each harvest.

4.2.4 Experimental set up

The experiment was set up in a glasshouse as described in section 2.5. Throughout the experiment the temperature fluctuated between a maximum of 63°C and a minimum of 18°C, with an average of 28°C. This maximum was much higher than expected, however it only occurred on a few occasions at the peak of summer when the ventilation system temporarily broke down and did not appear to significantly impact the grass.

There were five replicates of each vegetated treatment and three replicates of each unvegetated treatment. The unvegetated pots were set up in order to monitor soil zinc availability over time. Carrying this out using the vegetated pots would not have been possible because it would have disturbed the plants. These pots were arranged in a

split-plot randomised block formation. The vegetated pots were placed into five blocks and the unvegetated pots were placed into three blocks, each of which contained one pot of each treatment. Pots were arranged and watered as described in section 2.5.

4.2.5 DTPA-extractable zinc

The unvegetated samples were tipped out onto plastic sheeting and homogenised. Approximately 8 g of each sample was placed into a universal tube. The remaining soil was returned to the pot. The soil sampled was air-dried overnight and available zinc content (Zn_{DTPA}) was determined as described in section 2.7. This process was carried out weekly on the unvegetated samples for six weeks, and then fortnightly until the final harvest in week 18.

By week 20, the harvested vegetated sample pots had undergone the separation of the roots from the soil. At this point, DTPA-extractions were carried out on soil from all of the samples in order to compare Zn_{DTPA} in soil from the vegetated sample pots to the unvegetated sample pots.

4.2.6 Harvesting

Grass was germinated and grown for 18 weeks with harvests taken at weeks 6, 12 and 18 as described in section 2.6. Root mass was not recorded because the majority of the roots were too fine and fragile to be successfully removed.

4.2.7 Microwave digestion of grass and roots

Grass and root samples were dried and ground as described in section 2.6 and digested as described in section 2.9.

4.2.8 Hydrofluoric acid digestion of soil

At week 18 the remainder of the unvegetated soil samples were airdried and ground using a ball mill (Retsch, Model PM400). The total zinc content of the soils was determined using the method described in section 2.10.

4.2.9 Sequential extraction

In order to determine the effect treatments had on the fractionation of zinc, sequential extraction was carried out on each of the unvegetated soils after 18 weeks. A modified version of the 5-step sequential soil extraction described by Li and Thornton [312] was carried out. At the end of every step the suspension was centrifuged (3000 g, 10 min) and the solution retained for analysis. The residue was then washed using Milli-Q water and the washing discarded before moving on to the next step.

Step 1: Exchangeable metal

Soil (1 g) was added to centrifuge tubes and extracted with 8 ml of 0.5 M MgCl_2 at pH 7.0 for 20 min, with continuous agitation in a rotary shaker at room temperature.

Step 2: Carbonate-bound and specifically adsorbed metal

The residue from step 1 leached with 8 ml of 1 M sodium ethanoate ($\text{C}_2\text{H}_3\text{NaO}_2$) adjusted to pH 5.0 with ethanoic acid ($\text{CH}_3\text{CO}_2\text{H}$) with continuous agitation in a rotary shaker for 5 hr at room temperature.

Step 3: Metal bound to Fe–Mn oxides

The residue from step 2 was extracted with 20 ml of 0.04 M $\text{NH}_2\text{OH}\cdot\text{HCl}$ in 25% (v/v) $\text{CH}_3\text{CO}_2\text{H}$ for 6 hr. The extraction was performed in a fume cupboard and kept at 96°C using a water bath with occasional agitation. The samples were then placed on a rotary shaker at room temperature for 10 min.

Step 4: Metal bound to organic matter and sulphide

The residue from step 3 was extracted with a solution of 3 ml of 0.02 M HNO₃ and 5 ml of 30% H₂O₂ adjusted to pH 2.0 with HNO₃. The sample was heated progressively to 85°C and maintained at this temperature for 2 hr with occasional agitation. A second 3 ml aliquot of 30% H₂O₂ (adjusted to pH 2.0 with HNO₃) was then added, and the mixture was heated again at 85°C for 3 hr with intermittent agitation. After cooling, 5 ml of 3.2 M ammonium ethanoate (C₂H₇NO₂) in 20% (v/v) HNO₃ was added, followed by dilution to a final volume of 20 ml with Milli-Q water. The tubes were then continuously agitated for 30 min at room temperature.

Step 5: Residual metal fraction

Approximately 200 mg of the homogenized residue from step 4 was digested by HF digestion (see section **2.10**).

4.2.10 ICP-MS analysis

Multi-element analysis was undertaken using ICP-MS as described in section **2.11**.

4.2.11 Statistical analysis

As described in section **2.12**, orthogonal contrasts for analysis of variance are an *a priori* (before the fact) statistical approach that makes independent linear comparisons between treatments with at least three fixed levels to obtain main effects and interaction effects [34].

There were five different treatments (control, soil spiked with ZnS NPs, ZnO NPs, ZnSO₄ and Zn₃(PO₄)₂) and therefore four possible independent variables (degrees of freedom) that could be partitioned into simple contrasts (**Figure 4.1**). Orthogonal contrasts were carried out as described in section **2.12**. Data from this experiment was partitioned as follows:

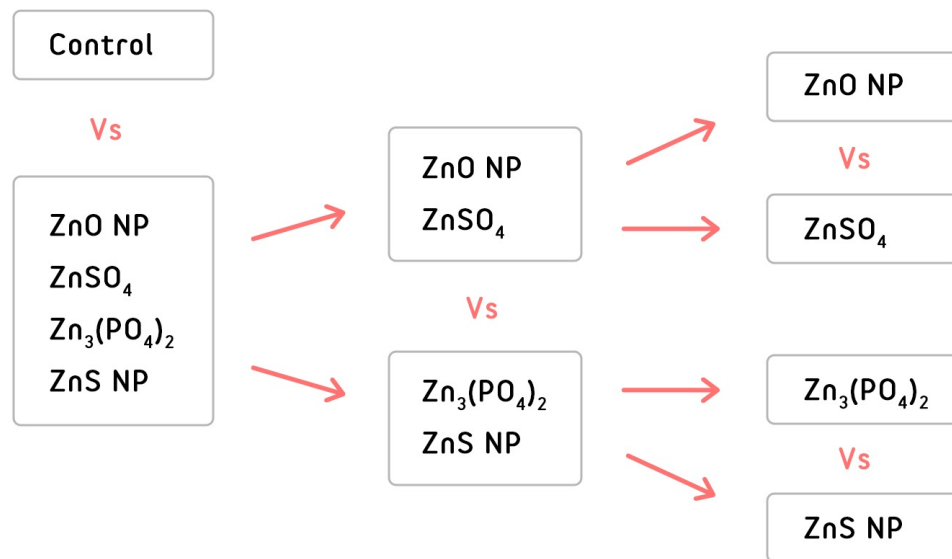


Figure 4.1 Orthogonal contrasts of the five different treatments (control, soil spiked with ZnS NPs, ZnO NPs, ZnSO₄ and Zn₃(PO₄)₂)

Class comparisons pairs

- C1 – Control vs all Zn treatments
- C2 – (ZnO NPs and ZnSO₄) vs (Zn₃(PO₄)₂ and ZnS NPs)
- C3 – ZnO NPs vs ZnSO₄
- C4 – Zn₃(PO₄)₂ vs ZnS NPs

Trend comparisons

- C5 – Harvest effect vs no harvest effect
- C6 – Linear concentration vs non-linear concentration
- C7 – Quadratic concentration vs non-quadratic concentration

Contrasts are orthogonal if the products of their coefficients sum to zero, and a set of more than two contrasts are orthogonal if each and every pair within the set are orthogonal. Contrasts were chosen on the basis that the groups were expected to be different to one another, to assess whether there was a significant average treatment effect and whether treatments were significantly different from one another. For example, ZnO NPs and ZnSO₄ were expected to behave differently to one another (C3),

as were $\text{Zn}_3(\text{PO}_4)_2$ and ZnS NPs (C4), however, previous experiments showed that ZnO NPs can dissolve rapidly, and so were expected to behave more similarly to ZnSO_4 than $\text{Zn}_3(\text{PO}_4)_2$ and ZnS NPs (C2). Contrast 5 was included to see whether there was a significant difference between harvests. The trend comparison contrasts 6 and 7 were to see whether or not the concentration of the soil spike caused the response to have a significant linear or quadratic trend, respectively. With a linear trend, values tend to rise or fall at a constant rate, whereas with a quadratic trend, values tend to rise or fall at a rate that is not constant. If both are shown to be significant that would mean that there was an overall linear trend with some non-linear components. Contrasts with $P < 0.05$ are taken to be significant.

If these comparisons are shown to be significant, then they can be combined to look at the interaction comparisons EG – C2:C6, will show whether the linear component to the response differs between the groups.

4.3 Results and discussion

4.3.1 Nanoparticle characterisation

The morphology and size distribution of the NP species were examined using TEM analysis (JEOL, JEM-2100F FEG-TEM); the ZnS NPs were shown to be broadly spherical with a diameter of approximately 5 nm and results for the ZnO NPs corroborated the advertised average particle size of ≤ 40 nm (**Figure 4.2**).

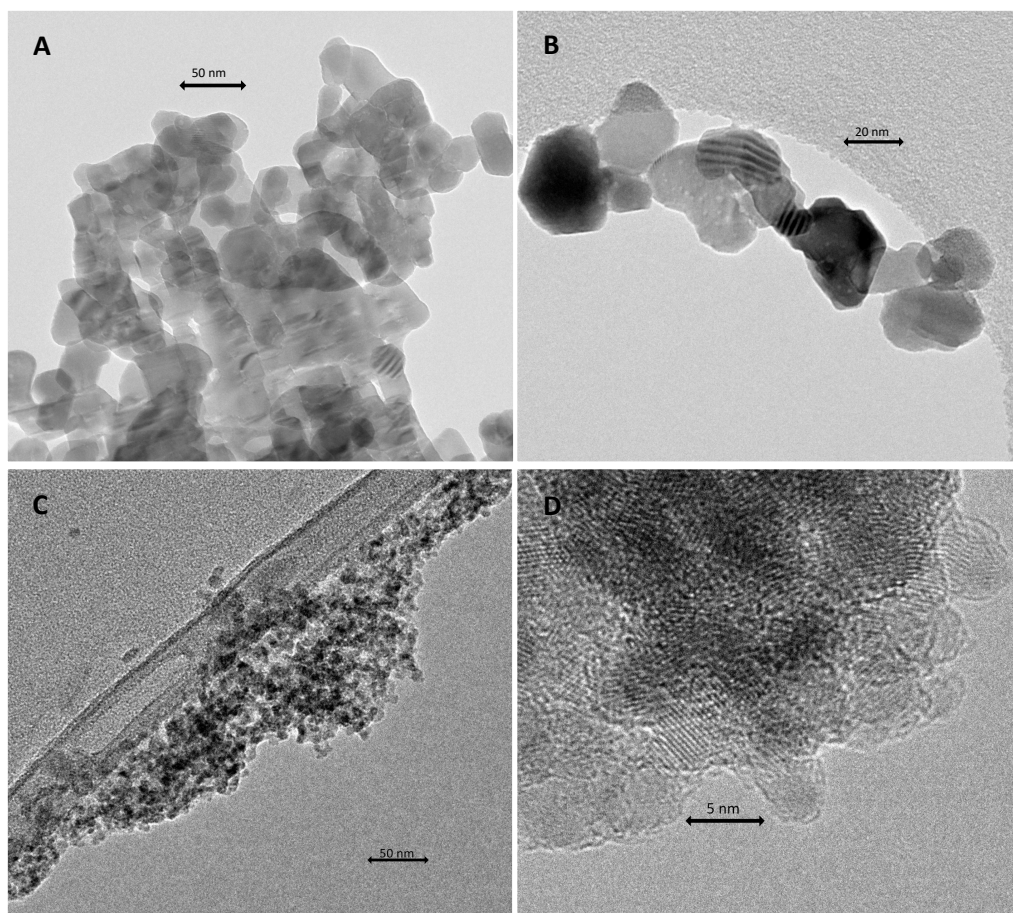
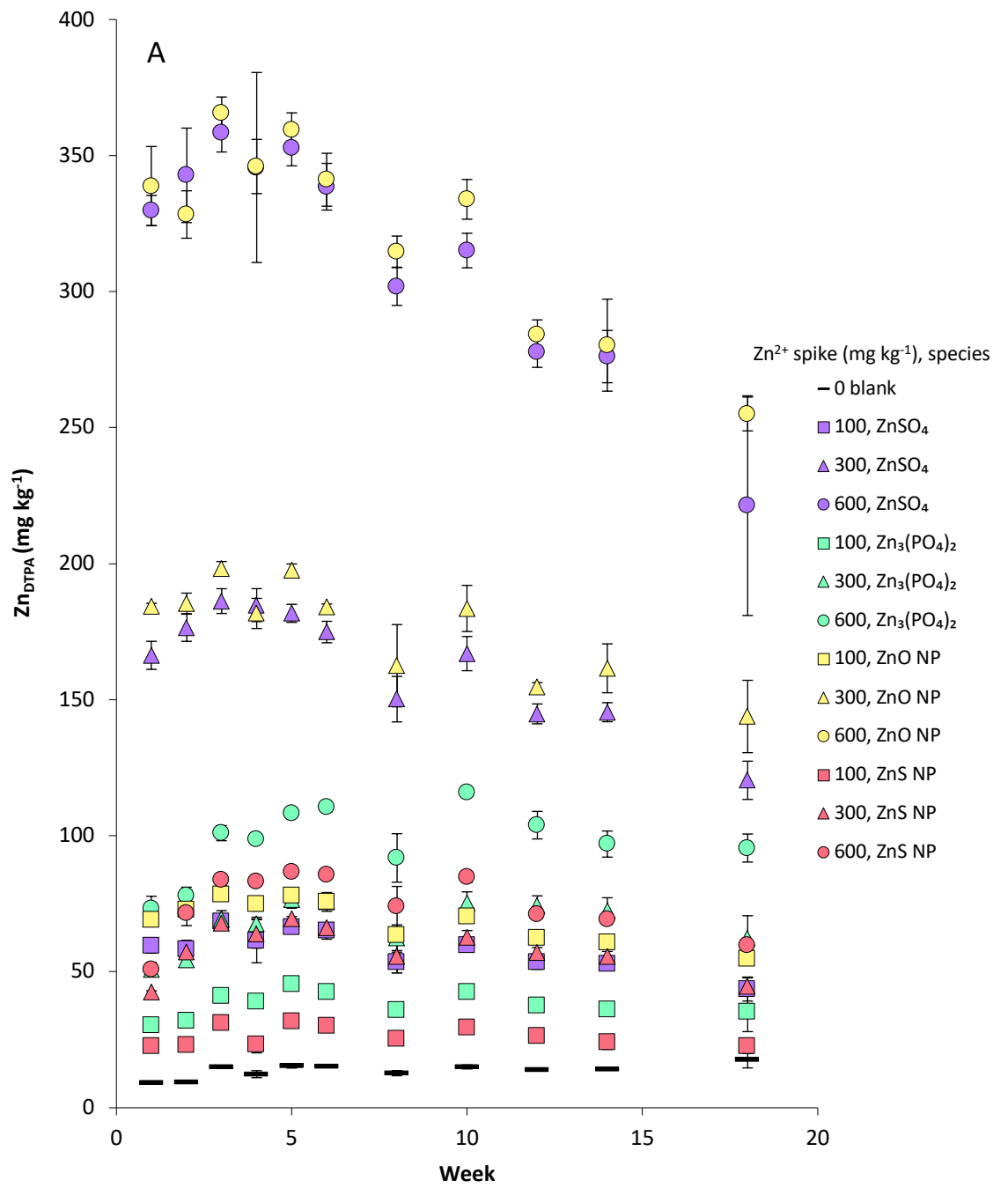


Figure 4.2 Transmission electron microscopy (TEM) images of ZnO NPs at A – 50 nm and B – 20 nm, and ZnS NPs at C – 50 nm and D – 5 nm

4.3.2 Soil characteristics

The soil was an arable Wick series sandy loam and the main physiochemical characteristics of the soil were as follows: pH (water, 1 : 2.5 soil : water ratio) 6.57; LOI of 8.6%; and an average total zinc concentration of 112 mg kg^{-1} . The soil water holding capacity (WHC) was found to be 25.7%.



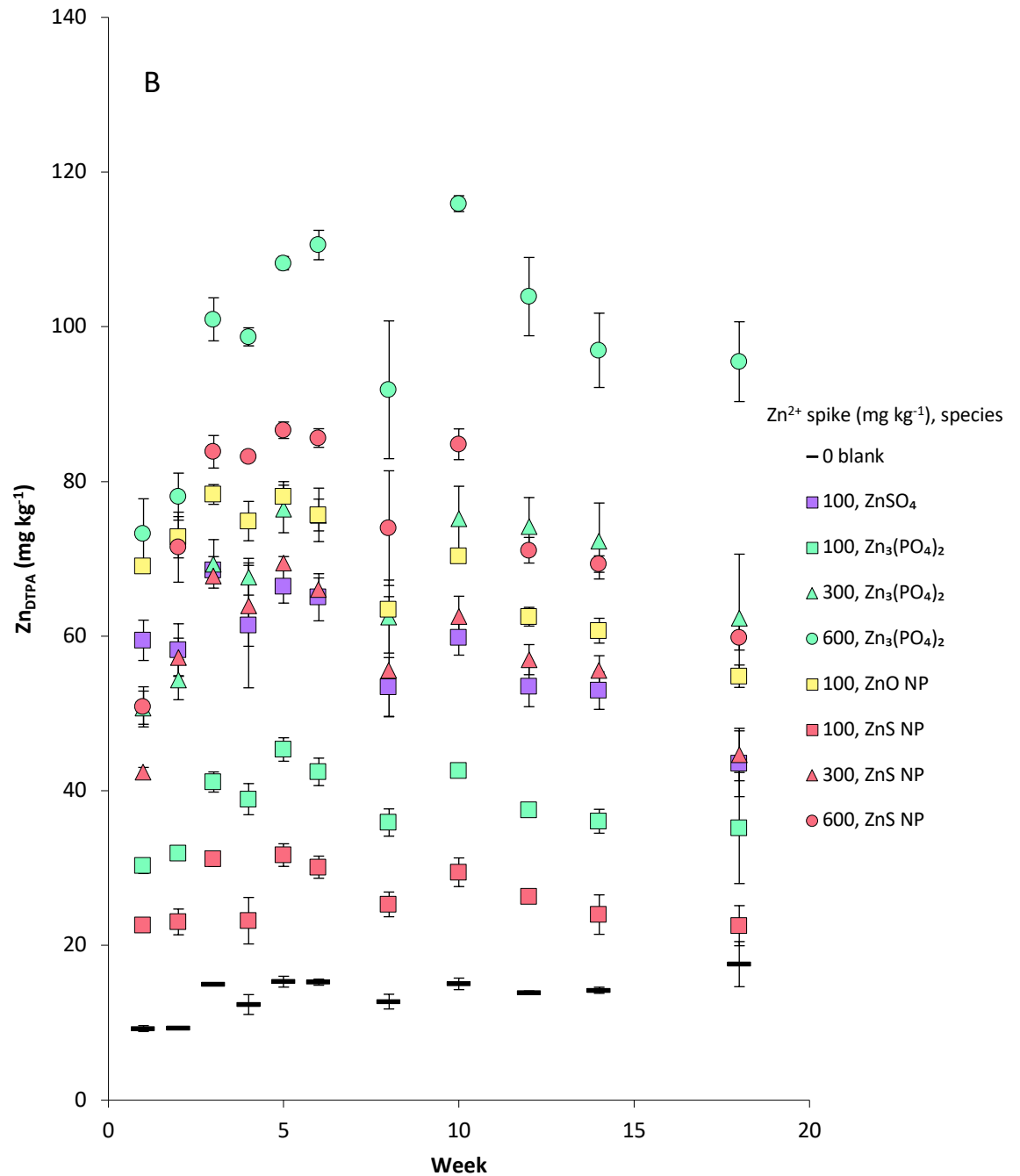


Figure 4.3 Available zinc (Zn_{DTPA}) from unvegetated soils spiked with different zinc species over time. A – all samples, B – samples with a Zn_{DTPA} concentration < 120 $mg\ kg^{-1}$. Bars show standard deviation of the three replications of each sample.

4.3.3 Available zinc in soils

The unvegetated soils spiked with ionic zinc ($ZnSO_4$) and ZnO NPs gave similar concentrations of average available zinc (Zn_{DTPA}) when tested, suggesting that the ZnO NPs underwent rapid dissolution. **Figure 4.3** shows that for all ZnO NP and $ZnSO_4$

spiked samples, available zinc concentration at week 18 was lower than week 1, whereas for all ZnS NP and $Zn_3(PO_4)_2$ spiked samples it was slightly higher. This could be due to these species undergoing the processes of dissolution and fixation over different periods of time. The ionic zinc ($ZnSO_4$) and rapidly dissolved ZnO NPs would be fixed within the soil quickly and so become less available over a short time-span, whereas the less soluble and likely aggregated $Zn_3(PO_4)_2$ and ZnS NPs would dissolve more slowly, possibly causing the concentration of Zn_{DTPA} to be maintained over a time period longer than this experiment. For example, Crout et al. [313] added zinc (as dissolved $ZnNO_3$ at 300 mg kg^{-1}) to 23 different soils at 16°C and 80% field capacity for 813 days, and found that an equilibrium was reached with a half-time of 89 days.

In addition, the general trend for the ZnO NP and the $ZnSO_4$ -spiked samples displayed a prominent maximum showing that Zn_{DTPA} in the soil increased during the first 5 weeks after application, followed by the period of rapid fixation for the remaining weeks (**Figure 4.3**). The apparent hump in Zn_{DTPA} was most likely due to the application of zinc causing the soil to acidify, triggering more zinc to become available. This occurs because of exchange between Zn^{2+} ions and H^+ ions adsorbed on soil mineral and organic surfaces. In soils, zinc present as Zn^{2+} cations can be stored in three forms (**Figure 4.4**): in solution, exchangeable and non-exchangeable fractions (also described as labile in solution, labile adsorbed and non-labile). Exchangeable cations weakly bound as a diffuse layer around the negative charges on soil particle surface exchange sites can readily move into the surrounding soil solution or be displaced from the surface by other cations in order to buffer changes in pH and cation availability [314, 315]. Non-exchangeable zinc occurs once it is fixed, for example, between individual clay minerals with permanent charge or fixed within oxides or humics [314].

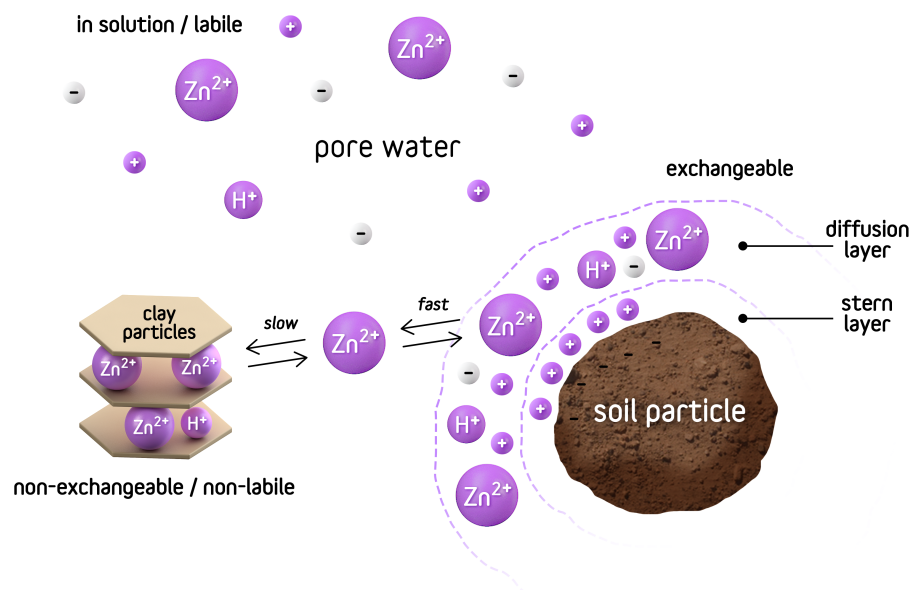


Figure 4.4 Zinc storage in soils, in solution, exchangeable and non-exchangeable. Exchangeable cations weakly bound above soil particle surface exchange sites. Non-exchangeable zinc fixed between individual clay minerals. Source: author

Species	Concentration	Pre-spike	Week 1	Week 18
Blank	0	6.57	6.52	6.45
ZnSO ₄	100	6.57	6.26	5.91
ZnSO ₄	300	6.57	6.05	5.56
ZnSO ₄	600	6.57	5.49	5.45
Zn ₃ (PO ₄) ₂	100	6.57	6.56	6.18
Zn ₃ (PO ₄) ₂	300	6.57	6.46	6.25
Zn ₃ (PO ₄) ₂	600	6.57	6.43	6.16
ZnO NP	100	6.57	6.42	6.11
ZnO NP	300	6.57	6.41	6.19
ZnO NP	600	6.57	6.52	6.38
ZnS NP	100	6.57	6.54	6.11
ZnS NP	300	6.57	6.51	6.11
ZnS NP	600	6.57	6.31	6.05

Table 4.1 Average pH of unvegetated soils from beginning to end of the experiment

This reserve of zinc only becomes available very slowly, however, it has been shown that zinc is particularly sensitive to fluctuations in soil pH and that an increase in soil acidity causes a rapid increase in zinc mobility [316]. The apparent maximum in Zn_{DTPA} hump effect for ZnS NP-spiked samples was still present, which suggests that some dissolution was occurring and it has been shown previously that, given enough time, ZnS NPs applied to soil will eventually dissolve [97]. Indeed, the soil pH at the end of the experiment was lower than that at the beginning for all treatments (**Table 4.1**). Liu et al. [74] spiked soils with 6 concentrations of ZnO NPs between 100 – 3200 mg kg⁻¹ and a comparative treatment of 800 mg kg⁻¹ of ZnSO₄. Maize was grown on the soils and then harvested after 8 weeks of growth, at which point the soil DTPA-extractable zinc was measured. The soils spiked with ZnO NPs were found to have lower available zinc than the ZnSO₄ spiked soils. This contrasts with the current study where by week 8 the 600 mg Zn kg⁻¹ ZnO NP spiked soil gave an average Zn_{DTPA} concentration of 315 mg kg⁻¹ compared to 302 mg kg⁻¹ for the ZnSO₄ spiked soil. Between week 3 to week 18, the soils spiked with 600 mg Zn kg⁻¹ ZnSO₄ and ZnO NP spiked soils both showed a decline in Zn_{DTPA} of 38 and 30%, respectively. In contrast, Zn_{DTPA} in the ZnS NP and Zn₃(PO₄)₂ treatments was low and consistent over the 18 weeks. Concentrations of Zn_{DTPA} followed the sequence ZnO NPs > ZnSO₄ > Zn₃(PO₄)₂ > ZnS NPs. Results clearly showed that pristine ZnO NPs behaved differently to ZnS NPs and Zn₃(PO₄)₂, and therefore are not an appropriate test species to use if the intention is to look at the effect of zinc NPs found in sewage biosolids.

Average Zn_{DTPA} of vegetated and unvegetated soils at week 20 were very closely correlated suggesting that the grass did not have a significant effect on Zn_{DTPA} (**Figure 4.5**), and therefore using data from unvegetated soils to represent vegetated soils is valid.

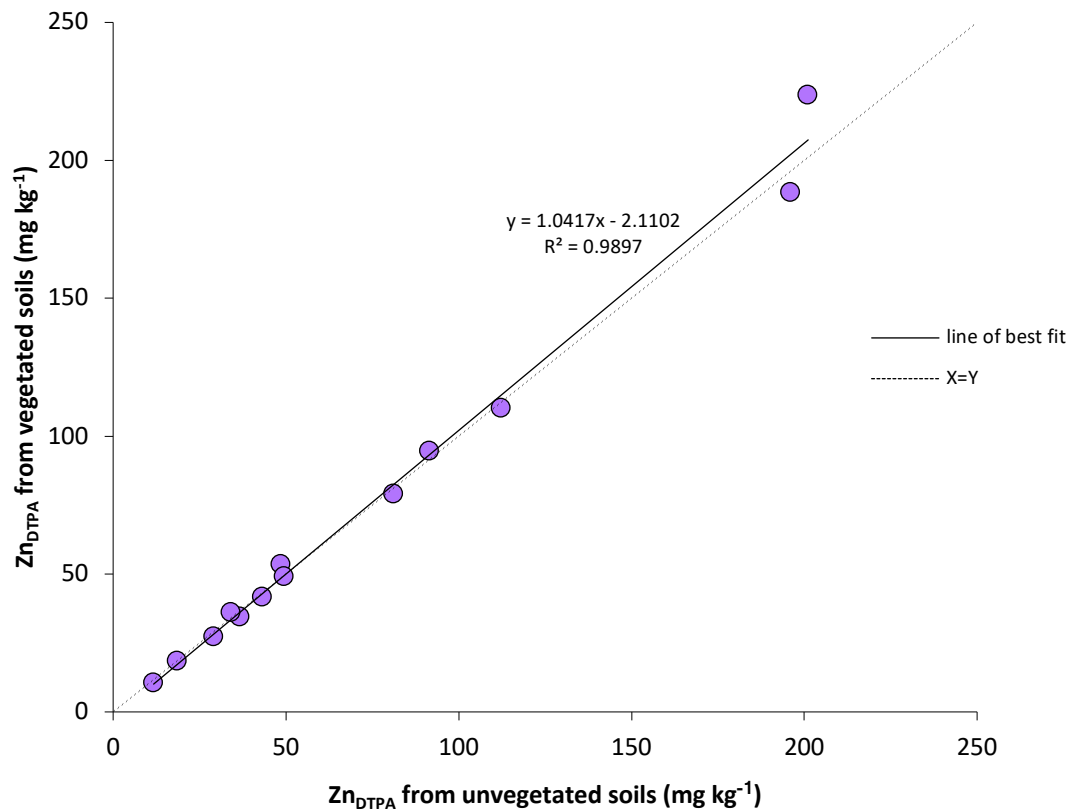


Figure 4.5 Average available zinc (Zn_{DTPA}) concentration of soil from vegetated and unvegetated samples following 20 weeks of incubation.

4.3.4 Weight and length of grass samples

The orthogonal contrasts showed that grass weight (**Table 4.2**) and length (**Table 4.3**) were significantly different between (ZnO NPs and $ZnSO_4$) vs ($Zn_3(PO_4)_2$ and ZnS NPs) spiked samples (C2), ZnO NP and $ZnSO_4$ spiked samples (C3), $Zn_3(PO_4)_2$ and ZnS NP spiked samples (C4), and between harvests (C5). There was also a significant harvest effect between ZnO NP and $ZnSO_4$ spiked samples (C3:C5), and $Zn_3(PO_4)_2$ and ZnS NP spiked samples (C4:C5). The average weight and length of the grass samples increased with each harvest for all spiking species, as the roots of the grass became more established (**Figures 4.6** and **4.7**). At the first harvest, the growth of the grass in the ZnS NP-spiked samples was inhibited in comparison to the other spiking species and

the control samples. However, by the final harvest the average harvest weights of the ZnS NP spiked samples were larger than the samples spiked with ZnO NP, Zn₃(PO₄)₂ and control samples. Liu et al. [74] looked at the zinc content of maize plants after they had been grown on soil spiked with 6 concentrations of ZnO NPs between 100 – 3200 mg kg⁻¹. They found no significant difference between the dry weight of samples spiked with 800 mg kg⁻¹ of ZnO NPs and ZnSO₄, however, the plants were only grown for 8 weeks.

	Num DF	Den DF	F-value	p-value
C2	1	48	12.2587	< 0.001
C3	1	48	35.7285	< 0.0001
C4	1	48	19.2469	< 0.0001
C5	2	103	618.0356	< 0.0001
C3:C5	2	103	35.5786	< 0.0001
C4:C5	2	103	31.4155	< 0.0001

Table 4.2 Significant orthogonal contrasts of grass weight data. DF: Degrees of freedom. Expanded version see Table 7.1

	Num DF	Den DF	F-value	p-value
C2	1	48	19.7217	< 0.0001
C3	1	48	248.2668	< 0.0001
C4	1	48	123.2244	< 0.0001
C5	2	103	962.3427	< 0.0001
C3:C5	2	103	237.5211	< 0.0001
C4:C5	2	103	118.3469	< 0.0001

Table 4.3 Significant orthogonal contrasts of stem length. DF: Degrees of freedom. Expanded version see Table 7.2

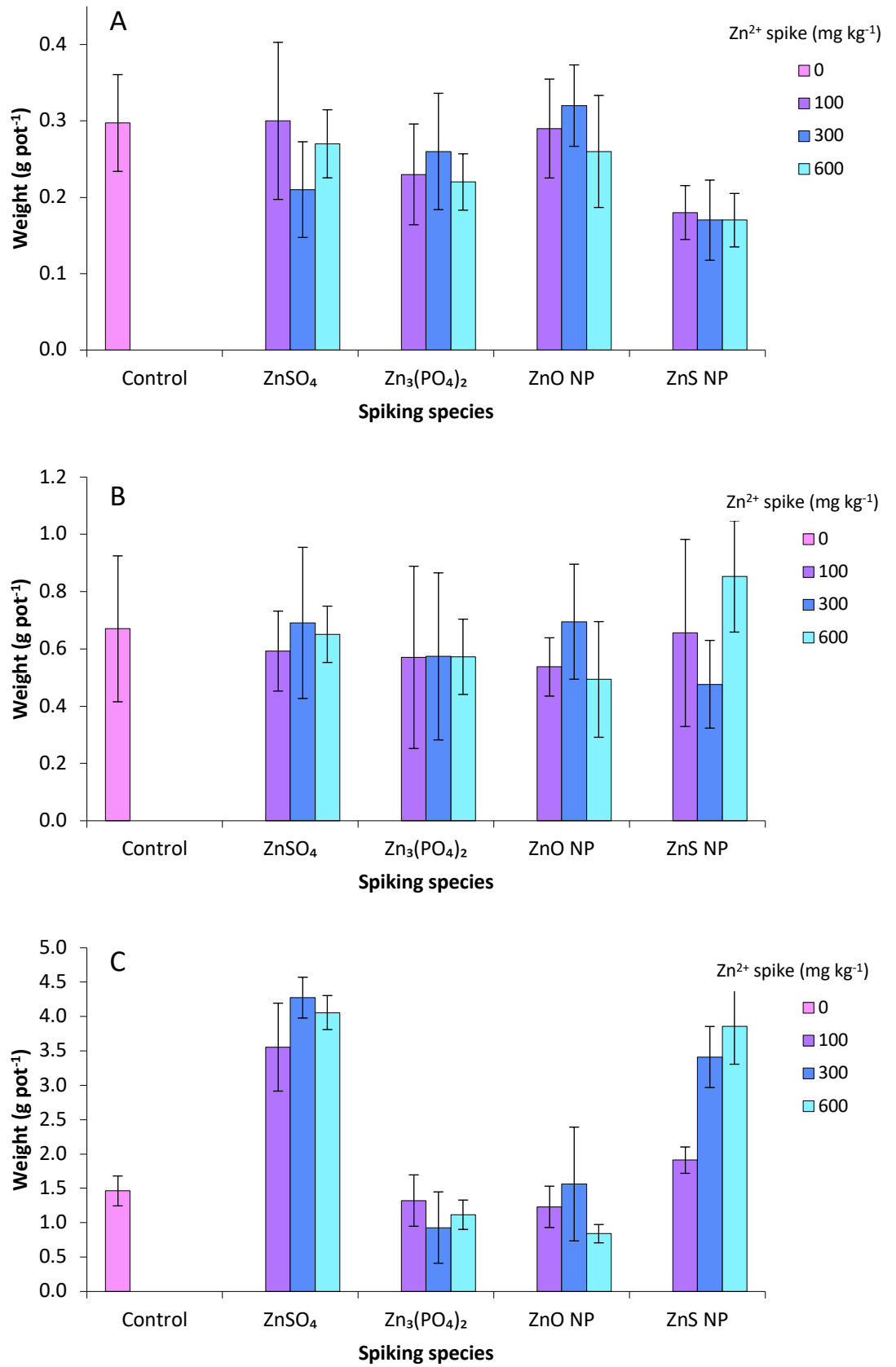


Figure 4.6 Average dry weight of harvested grass. A – first harvest, 01/06/18; B – second harvest, 20/07/18; C – third harvest, 03/09/18. Bars show standard deviation of the five replications of each sample.

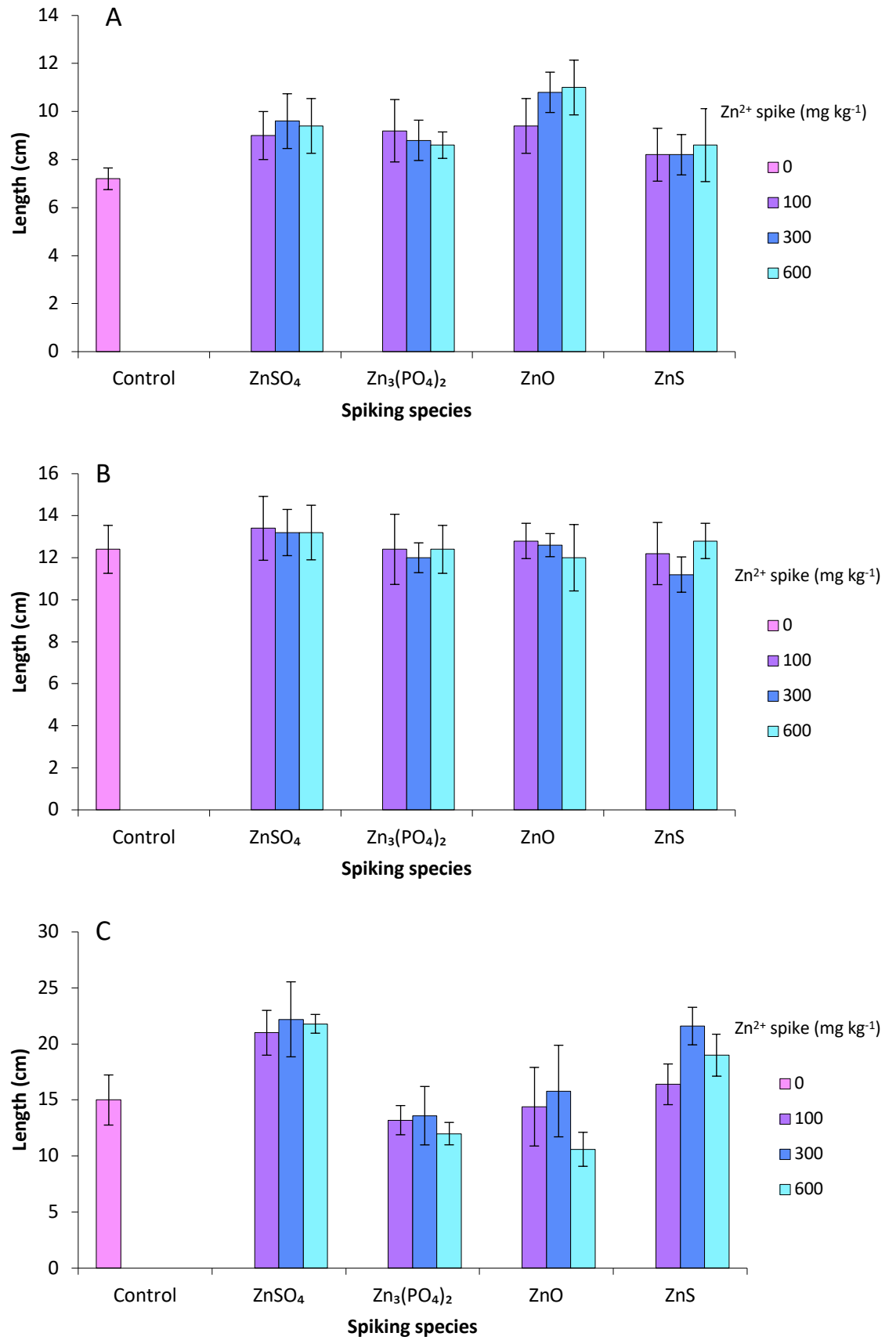


Figure 4.7 Average length of harvested grass. A – first harvest, 01/06/18; B – second harvest, 20/07/18; C – third harvest, 03/09/18. Bars show standard deviation of the five replications of each sample.

Despite the ZnSO_4 and ZnO NP-spiked soil samples containing similar Zn_{DTPA} , the weight of the grass from the final harvest of ZnSO_4 -spiked samples was much greater than the ZnO NP-spiked samples. This has been seen in a previous study looking at ZnO NP phytotoxicity on ryegrass where it was found that ryegrass biomass was significantly reduced when exposed to ZnO NPs compared to ZnSO_4 [80]. Indeed, by the final harvest, the weight of the grass from both the ZnSO_4 and ZnS NP-spiked samples were heavier than those spiked with ZnO NPs, $\text{Zn}_3(\text{PO}_4)_2$ and the control. Sulphur (S) is an essential element for chlorophyll formation so plants that are deficient in S can suffer from stunted growth and chlorosis [317] and because S is not very mobile in plant tissue, it is the younger leaves that will normally be affected first [318]. Sulphur is also a component of the amino acids cysteine, cystine and methionine so an inadequate S supply will limit plant protein production [319]. For these reasons it has been shown that the application of S to ryegrass can substantially increase the harvest yield [320] but that this response tends to not be significant until the third cut [317, 320, 321] and has been shown to be more pronounced on sandy soils [322]. This suggests that the benefit of added S is only seen once the limited soil S supply is exhausted. It has also been shown that S added as sulphide is less available to plants and therefore less effective than S applied as sulphate [321].

4.3.5 Zinc concentration of grass samples

The orthogonal contrasts showed that grass total zinc (Zn_{Total}) concentration (**Table 4.4**) was significantly different between (ZnO NPs and ZnSO_4) vs ($\text{Zn}_3(\text{PO}_4)_2$ and ZnS NPs) spiked samples (C2), ZnO NP and ZnSO_4 spiked samples (C3), $\text{Zn}_3(\text{PO}_4)_2$ and ZnS NP spiked samples (C4), and between harvests (C5). There was also a significant harvest effect between ZnO NP and ZnSO_4 spiked samples (C3:C5), and $\text{Zn}_3(\text{PO}_4)_2$ and ZnS NP spiked samples (C4:C5). The ZnO NP spiked samples contained

the highest average grass Zn_{Total} compared to the equivalent spike concentration samples of the other species, and the ZnS NP spiked samples contained the lowest (**Figure 4.8**). At the first harvest, the average grass Zn_{Total} of the ZnO NP and $ZnSO_4$ spiked samples were similar, however, by the third harvest the ZnO NP spiked samples contained a significantly higher concentration. This is interesting given that ZnO NP and $ZnSO_4$ spiked soil samples showed similar Zn_{DTPA} values throughout all of the harvests and suggests that some observable effects may have been ZnO NP-specific rather than only a result of dissolved Zn^{2+} .

	Num DF	Den DF	F-value	p-value
C2	1	48	12.2587	< 0.001
C3	1	48	35.7285	< 0.0001
C4	1	48	19.2469	< 0.0001
C5	2	103	618.0356	< 0.0001
C3:C5	2	103	35.5786	< 0.0001
C4:C5	2	103	31.4155	< 0.0001

Table 4.4 Significant orthogonal contrasts of grass total zinc. DF: Degrees of freedom. Expanded version see Table 7.3

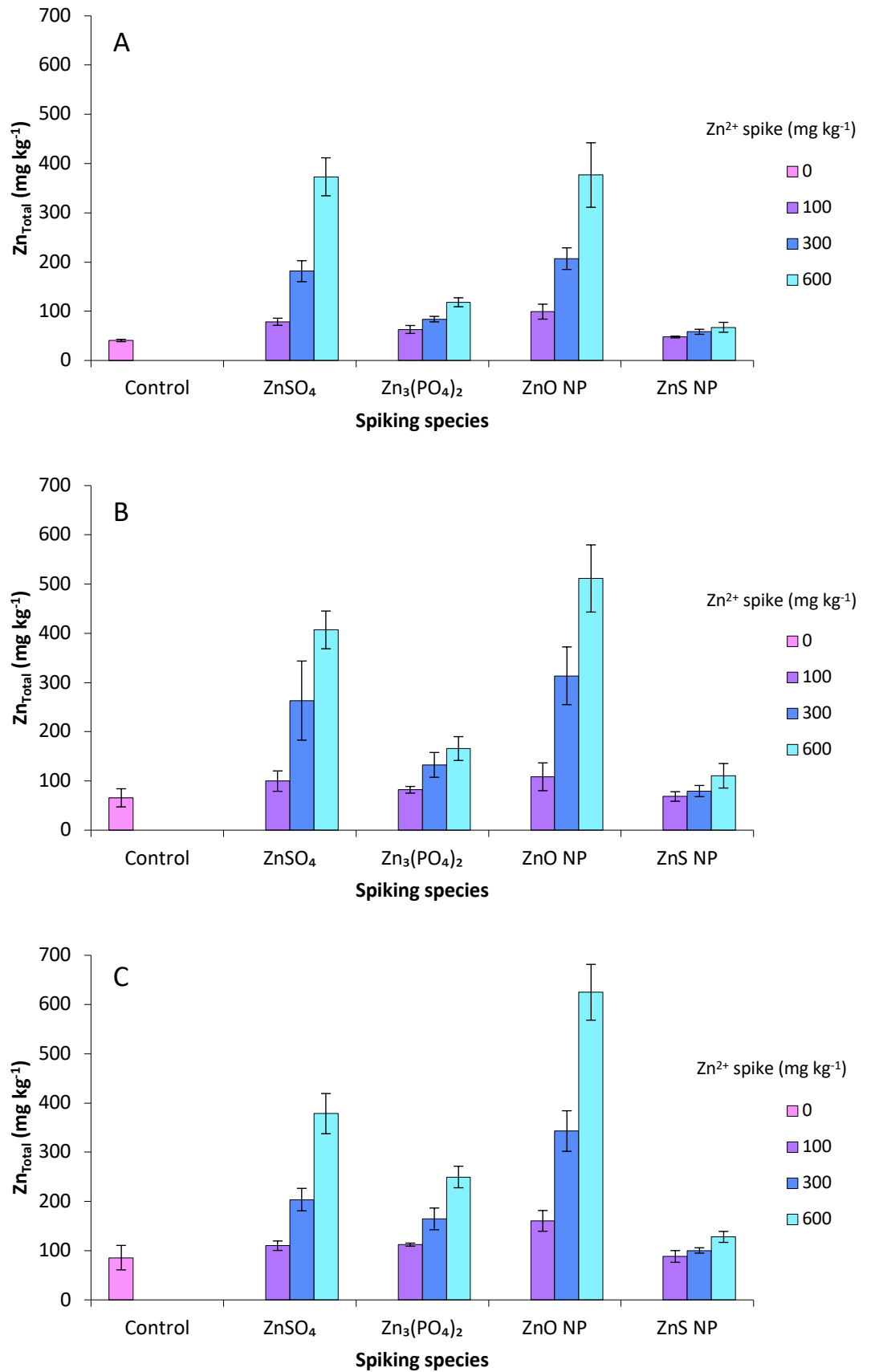


Figure 4.8 Average total zinc (Zn_{Total}) concentration of harvested grass. A – first harvest, 01/06/18; B – second harvest, 20/07/18; C – third harvest, 03/09/18. Bars show standard deviation of the five replications of each sample.

Using one-way analysis of variance (ANOVA) tests to compare the grass Zn_{Total} concentration of the ZnS NP spiked samples with that of the control samples showed that the means were significantly different at all concentrations for the first harvest, but only significantly different at 600 mg kg⁻¹ of zinc for subsequent harvests (**Table 4.5**). The significant result for the first harvest was due to the spread of results for each spiking species being very narrow. The results for harvests two and three could indicate that in order to have a fertilisation effect, application of ZnS NPs would need to exceed the threshold which is somewhere above 300 mg kg⁻¹ of zinc.

Harvest	ZnS NP spike concentration (mg kg ⁻¹ of zinc)	P value
1	100	3.94x10 ⁻⁴
1	300	9.62x10 ⁻⁵
1	600	3.86x10 ⁻⁴
2	100	0.773
2	300	0.193
2	600	0.012
3	100	0.847
3	300	0.234
3	600	0.009

Table 4.5 Results of analysis of variants (ANOVA) tests comparing grass total zinc (Zn_{Total}) concentration of ZnS NP spiked samples with that of control samples.

Plotting the grass Zn_{Total} concentration with the soil Zn_{DTPA} concentration from the weeks corresponding with the grass harvests shows that the grass contained more zinc with successive harvests, indicating that the more established the roots became, the more zinc they were able to take up from the soil (**Figure 4.9**). Plotting the data for each species at each harvest separately highlights that the ZnO NP and the ZnSO₄ spiked samples had similar levels of Zn_{DTPA} and took up very similar concentrations of grass Zn_{Total} , but that by harvest 3 these levels differed to a greater degree (**Figure 4.9**).

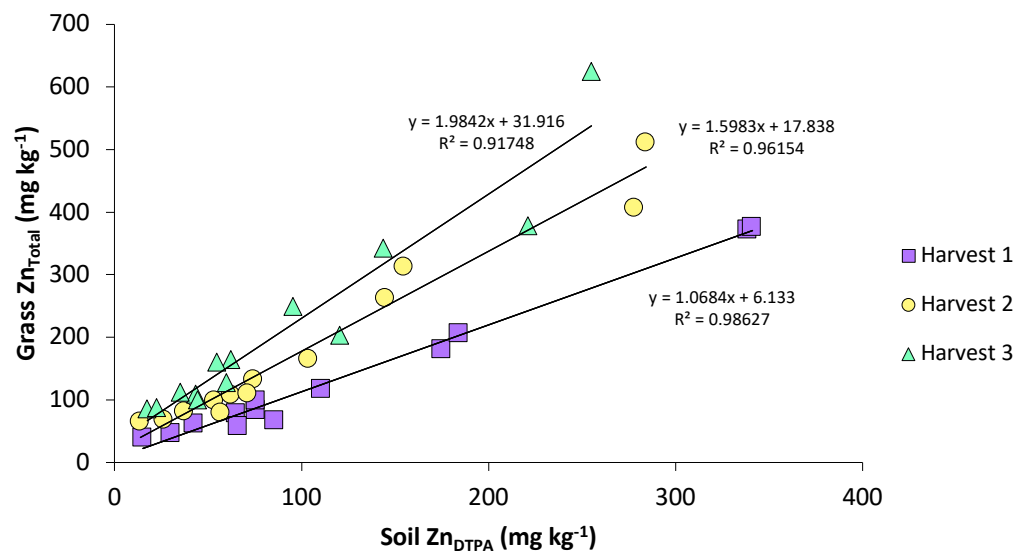
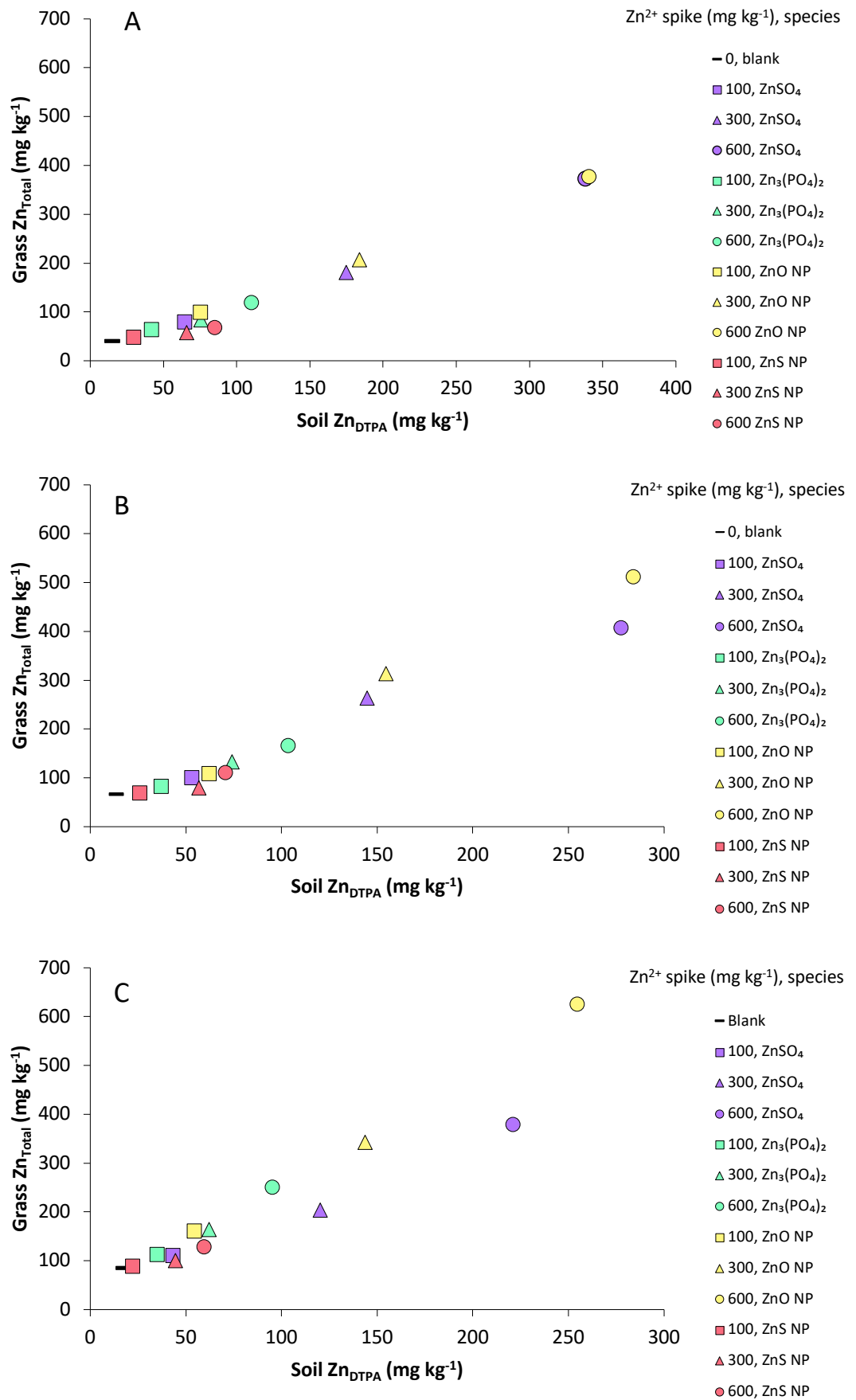


Figure 4.9 Total zinc (Zn_{Total}) concentration of grass compared to available zinc (Zn_{DTPA}) concentration of soil. Harvest 1 - 01/06/18, harvest 2 - 20/07/18, harvest 3 - 03/09/18



4.3.6 Zinc offtake

Multiplying the weight of each grass sample harvest by its Zn_{Total} gives the total amount of zinc taken out of the soil by the grass ($Zn_{Offtake}$). The orthogonal contrasts showed that $Zn_{Offtake}$ (**Table 4.6**) was significantly different between (ZnO NPs and ZnSO₄) vs (Zn₃(PO₄)₂ and ZnS NPs) spiked samples (C2), ZnO NP and ZnSO₄ spiked samples (C3), Zn₃(PO₄)₂ and ZnS NP spiked samples (C4), and between harvests (C5). There was also a significant harvest effect between ZnO NP and ZnSO₄ spiked samples (C3:C5), and Zn₃(PO₄)₂ and ZnS NP spiked samples (C4:C5). Results show that although the ZnO-spiked samples had the highest grass Zn_{Total} concentrations, the low weight of the final harvest meant that the actual amount of $Zn_{Offtake}$ was low (**Figure 4.11**). Conversely, the ZnS-spiked samples had a much lower grass Zn_{Total} concentration but a much higher weight of the final harvest, resulting in the final harvest 600 mg kg⁻¹ samples of ZnO NPs and ZnS NPs having comparable $Zn_{Offtake}$ concentrations.

	Num DF	Den DF	F-value	p-value
C2	1	48	12.2587	< 0.001
C3	1	48	35.7285	< 0.0001
C4	1	48	19.2469	< 0.0001
C5	2	103	618.0356	< 0.0001
C3:C5	2	103	35.5786	< 0.0001
C4:C5	2	103	31.4155	< 0.0001

Table 4.6 Orthogonal contrasts of grass zinc offtake. DF: Degrees of freedom. Expanded version see Table 7.4

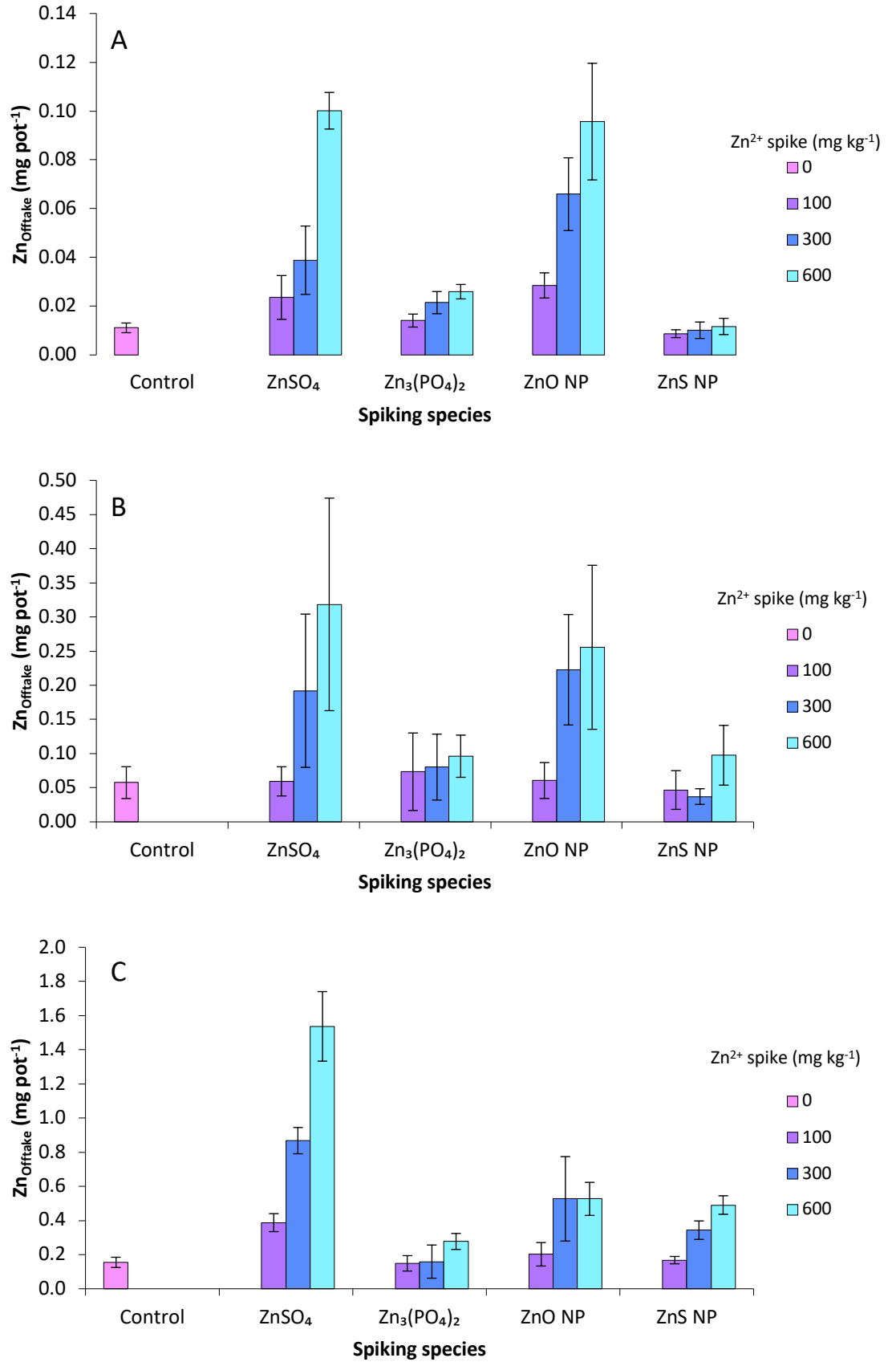


Figure 4.11 Average zinc offtake ($Zn_{Offtake}$) of harvested grass. A – first harvest, 01/06/18; B – second harvest, 20/07/18; C – third harvest, 03/09/18. Bars show standard deviation of the five replications of each sample.

Plotting Zn_{Offtake} for each harvest against soil Zn_{DTPA} shows that the total Zn_{Offtake} rose both with increasing amounts of zinc available in the soil and with increasing maturity of the roots (**Figure 4.12**). Plotting the data for each species at each harvest separately highlights that by harvest 3 the $ZnSO_4$ spiked samples had a much larger offtake than the ZnO NP spiked samples despite similar levels of soil available zinc (**Figure 4.13**). This supports the conclusion that ZnO NPs were not behaving just as ionic zinc and that there was some particle-specific effects occurring.

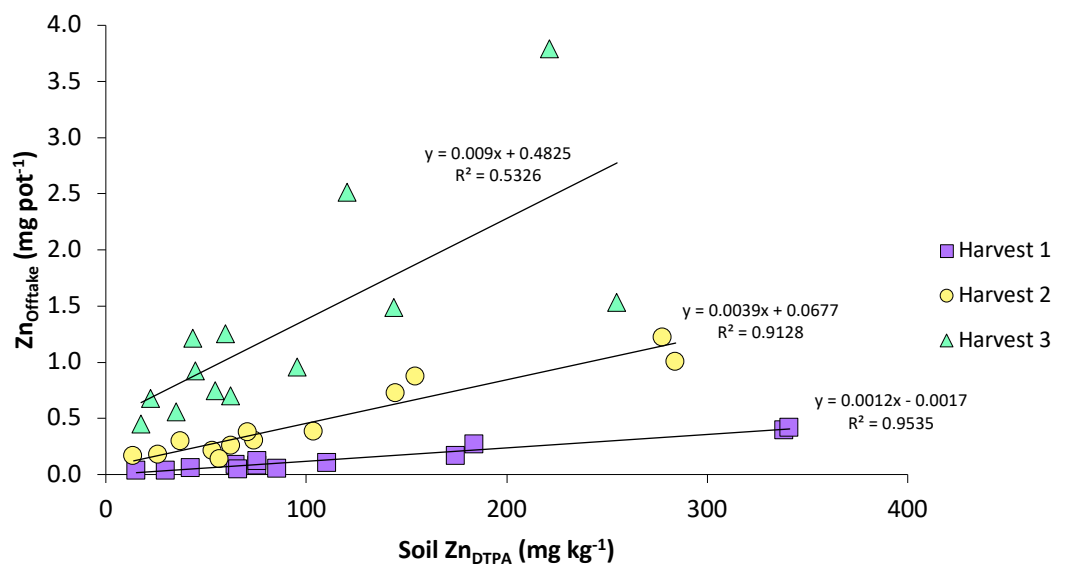
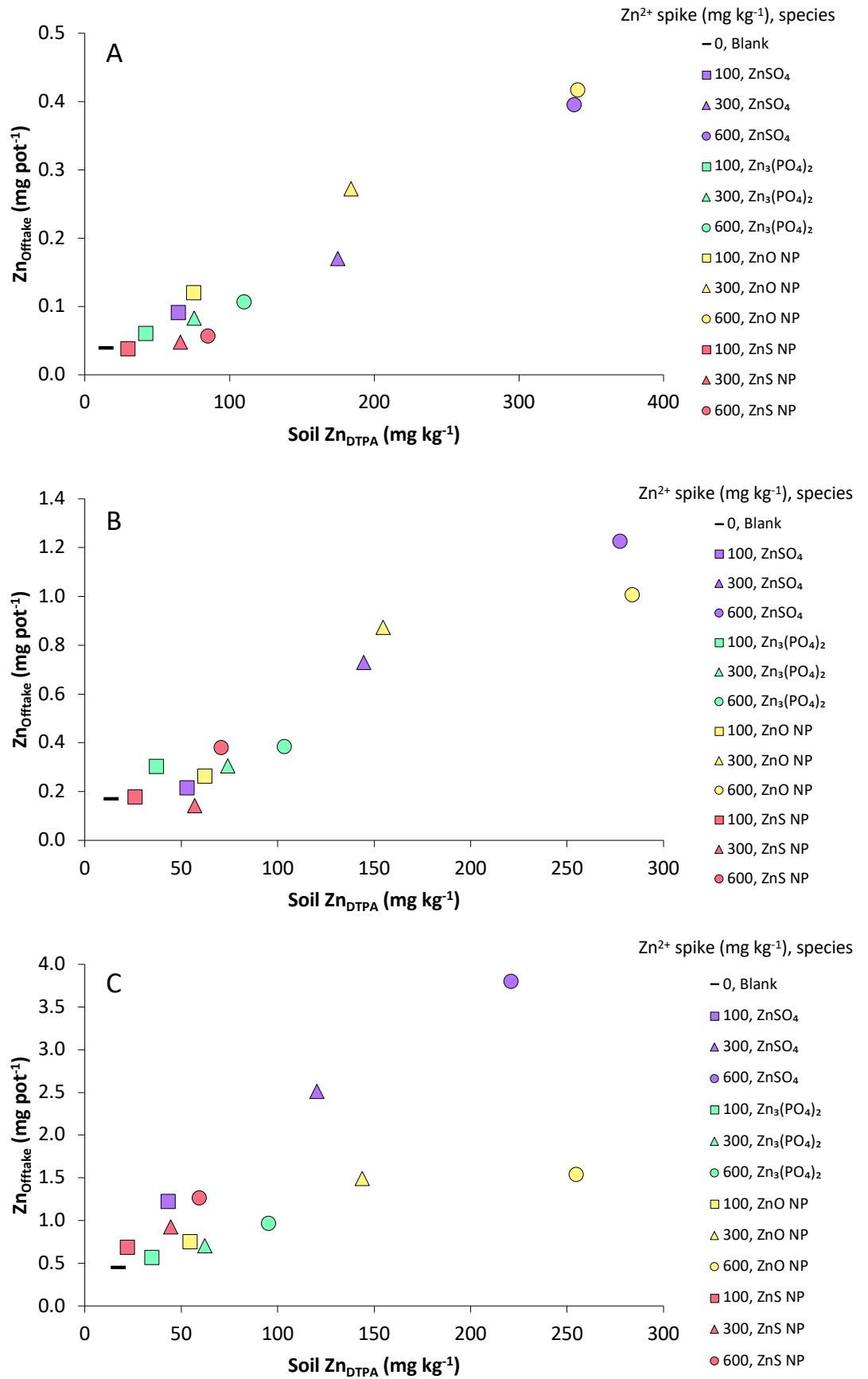


Figure 4.12 Zinc offtake (Zn_{Offtake}) of grass compared to available zinc (Zn_{DTPA}) concentration of soil. Harvest 1 - 01/06/18, harvest 2 - 20/07/18, harvest 3 - 03/09/18



4.3.7 Zinc concentration of roots

The root Zn_{Total} concentration was examined in order to determine any differences in translocation of zinc from roots to shoots between the different spiking species.

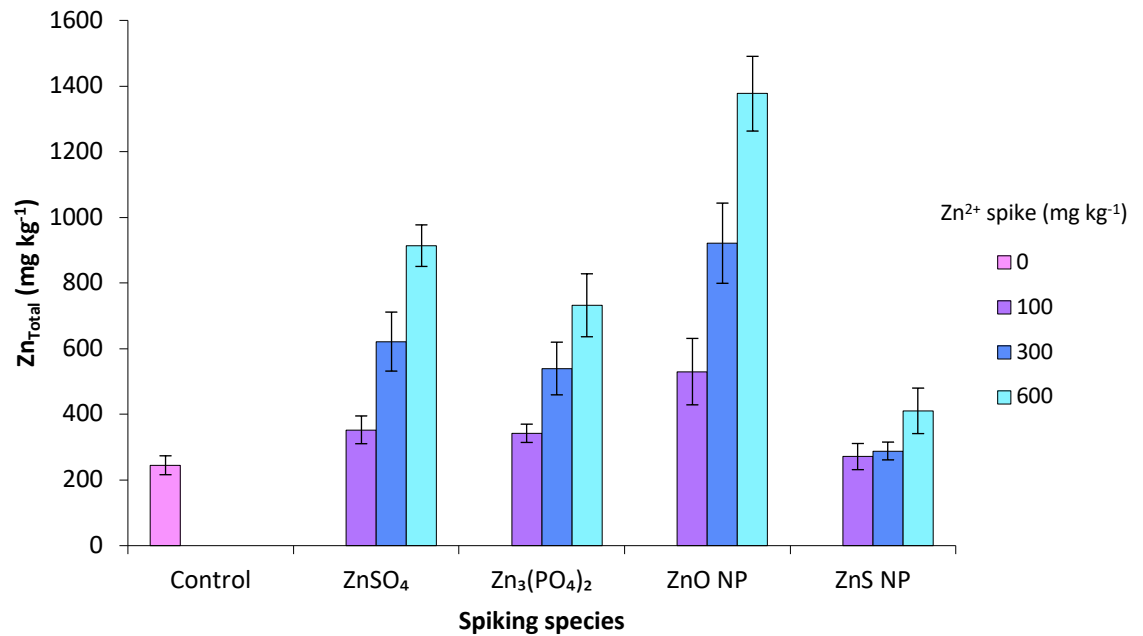


Figure 4.13 Average total zinc (Zn_{Total}) concentration of roots. Bars show standard deviation of the five replications of each sample.

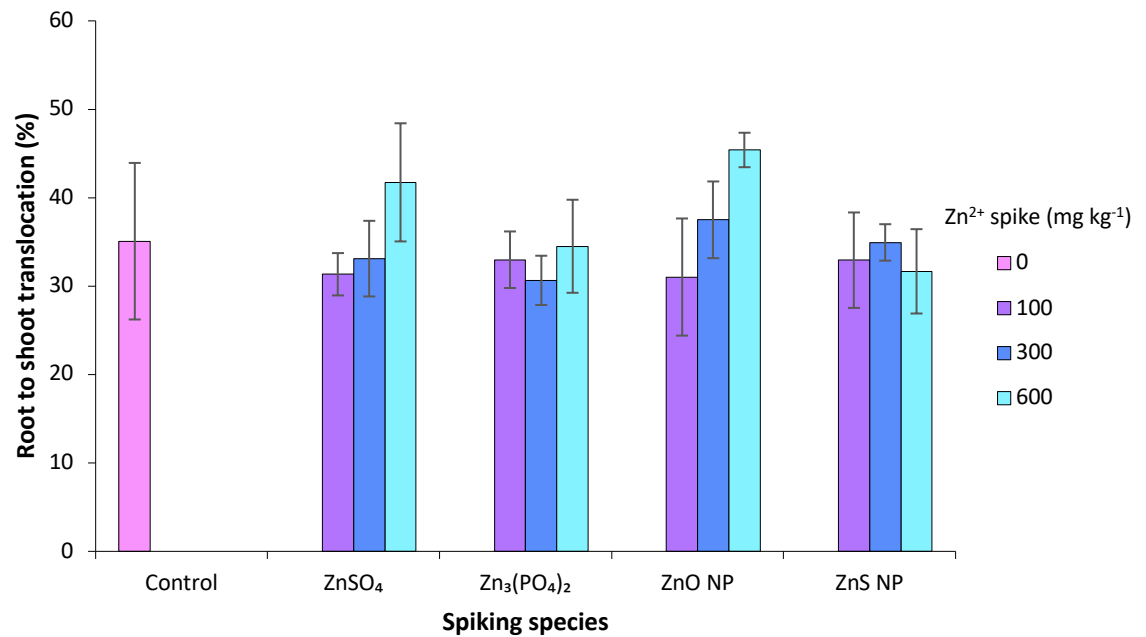


Figure 4.15 Average root to shoot zinc translocation %. Bars show standard deviation of the five replications of each sample.

The root Zn_{Total} concentration was shown to be much higher than the grass Zn_{Total} (Figure 4.14) and the ZnO NP-spiked samples had the highest concentration of zinc. The average root to shoot zinc translocation was highest for 600 mg Zn kg⁻¹ ZnO NP spiked samples, but remained quite consistent across spiking species (Figure 4.15). In contrast, Lin et al. [80] compared the phytotoxicity of ZnO NPs and ZnSO₄ on ryegrass and it was found that zinc translocation from root to shoot was much lower under ZnO NP treatments, than under ZnSO₄ treatments. The difference could possibly be due to the hydroponic culture system that was used in place of soil.

4.3.8 Total zinc in soils

In order to confirm the spiked levels of zinc in the soil samples, the Zn_{Total} of all of the unvegetated soil samples were analysed and then the average concentration of the control samples taken from the concentration of each of the spiked samples (Figure 4.16). Results showed that the ZnO NP and the ZnSO₄ spiked samples were at the anticipated levels with little variation in concentration. Both the Zn₃(PO₄)₂ and the ZnS NP spiked samples showed much more variation between replicates, with the ZnS NP spiked samples containing a lower average concentration than was expected.

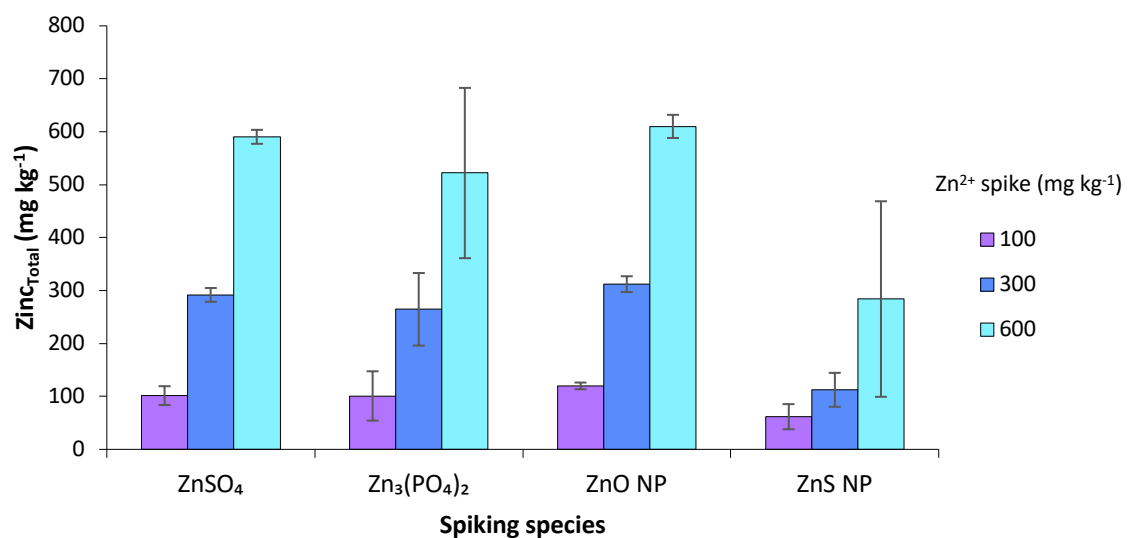


Figure 4.16 Average total zinc (Zn_{Total}) spike of unvegetated soil samples. Bars show standard deviation of the three replications of each sample.

Evenly mixing the ZnO NPs and the ZnSO₄ through the soil at the spiking stage was straight forward, but despite sonication the Zn₃(PO₄)₂ and ZnS NPs were difficult to disperse in the spiking solutions, and therefore the degree of homogenisation in the soil was probably lower. It has been found that breaking apart clumps of low solubility NPs down to primary particles that are < 50 nm may not actually be possible [53, 275, 276] and so the likelihood of the ZnS NPs persisting as small aggregates means that their dispersal within the soil would be incomplete and lead to fluctuations in concentration between samples.

4.3.9 Sequential extraction

In order to compare the speciation and partitioning of the zinc from the different spiking species within the soil, a 5-step sequential extraction was carried out on the unvegetated samples. In sequential extraction schemes, extractants are applied in order of increasing reactivity to obtain decreasingly lower mobility soil fractions. The extractants generally fall into the following groups: (1) unbuffered salts, (2) weak acids, (3) reducing agents, (4) oxidising agents and (5) strong acids [323]. Sequential extraction techniques assume that the reagents used are able to selectively dissolve one phase without any solubilisation of the others, however, matrix effects and analyte re-adsorption can mean that this is not the case [324]. So while it is a useful thing to do to compare differences between the species, the expected recovery rate for zinc is only between 78.5 – 84.5% and the estimated precision of each extraction step is 5 – 10% [312]. The recovery rates for the different spiking species in this experiment are shown in **Table 4.7**. The ZnO NP spiked samples showed recoveries above the expected rate but the ZnS NP spiked sample rates were very low and the Zn₃(PO₄)₂ spiked samples were only slightly higher. As described in section **4.3.8**, this could be due to high levels of aggregation with these spiking species causing poor

Spiking species	Concentration of spike (mg kg ⁻¹ of zinc)		
	100	300	600
ZnSO ₄	65.1	68.3	69.2
Zn ₃ (PO ₄) ₂	55.3	45.6	31.0
ZnO NP	99.3	85.3	94.0
ZnS NP	24.3	18.5	23.2

Table 4.7 Average sequential extraction recovery rates (%)

homogenisation through the soil making accurately sampling the soil difficult. Calculating the data as percentages of total recovered zinc shows the variation between the fractions of each treatment (Figure 4.17). For all treatments, the majority of the soil zinc was found in the Zn_{Oxide} fraction (47 – 59%). The treatment with the smallest percentage of zinc in the Zn_{Resid} fraction was the ZnO NP 600 mg Zn kg⁻¹ spiked sample (6%) and the ZnSO₄ 600 mg Zn kg⁻¹ spiked sample had the largest percentage of zinc (11%) in the Zn_{Ex} fraction. The ZnS NP spiked samples displayed a

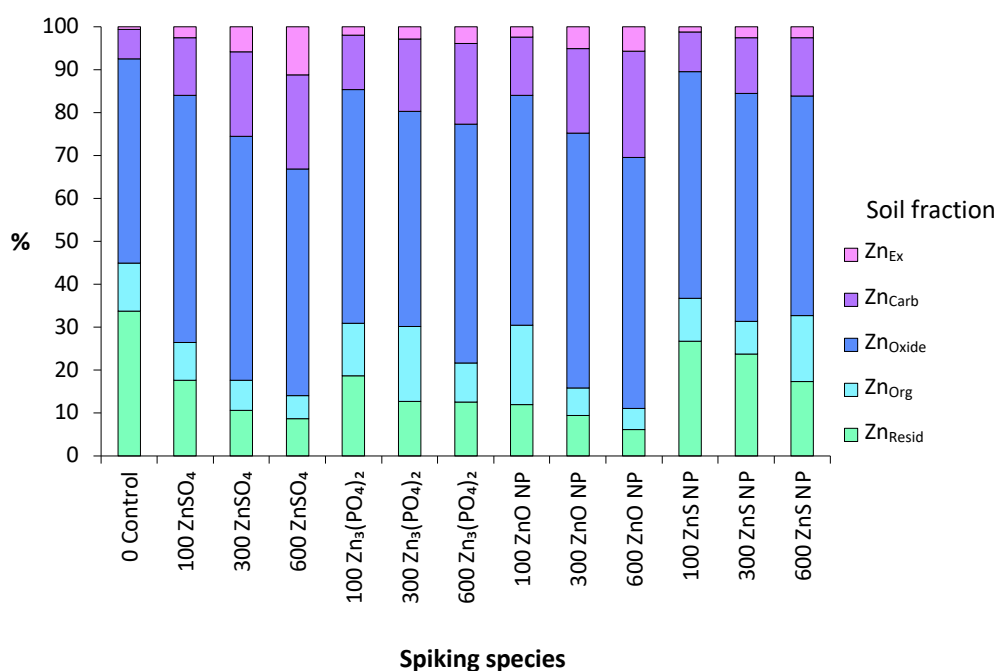
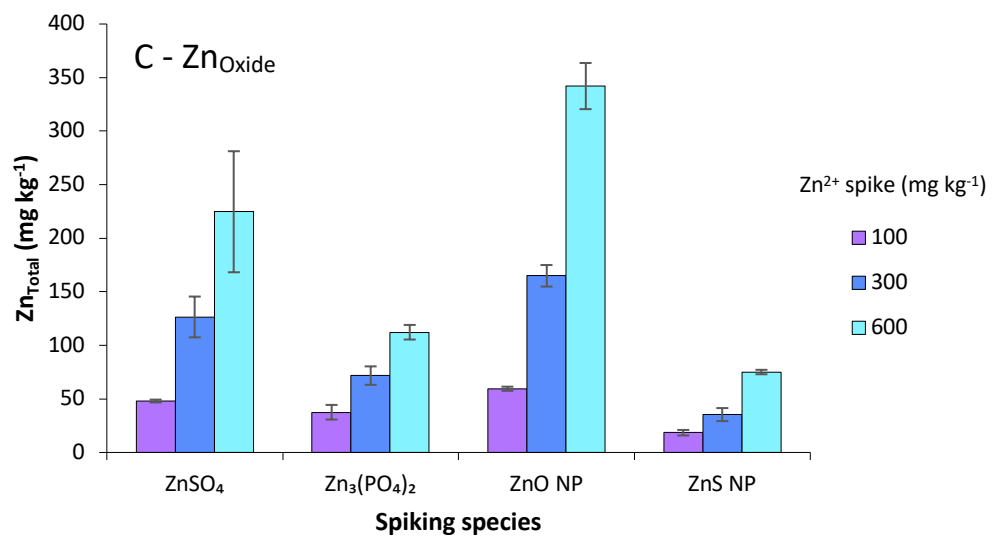
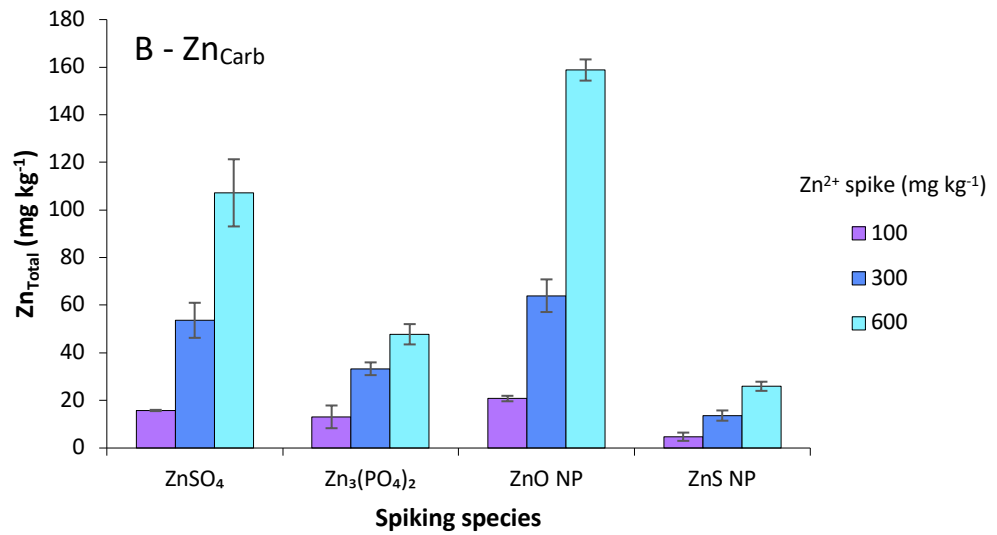
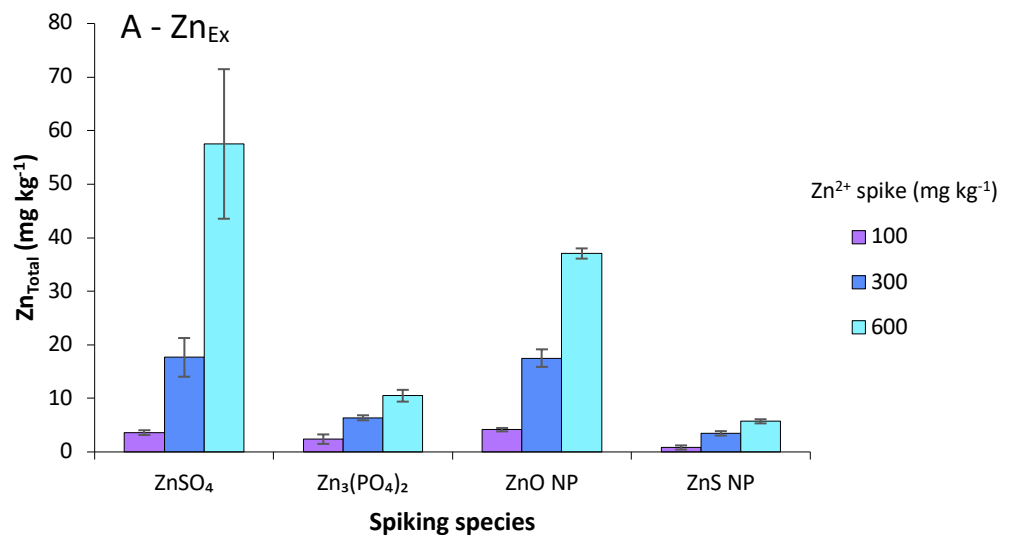


Figure 4.17 Average % of zinc in fractions of unvegetated soils. A – step 1, exchangeable (Zn_{Ex}); B – step 2, bound to carbonate and specifically adsorbed (Zn_{Carb}); C – step 3, bound to Fe–Mn oxides (Zn_{Oxide}); D – step 4, bound to organic matter and sulphide (Zn_{Org}); E – step 5, residual phase (Zn_{Resid}).



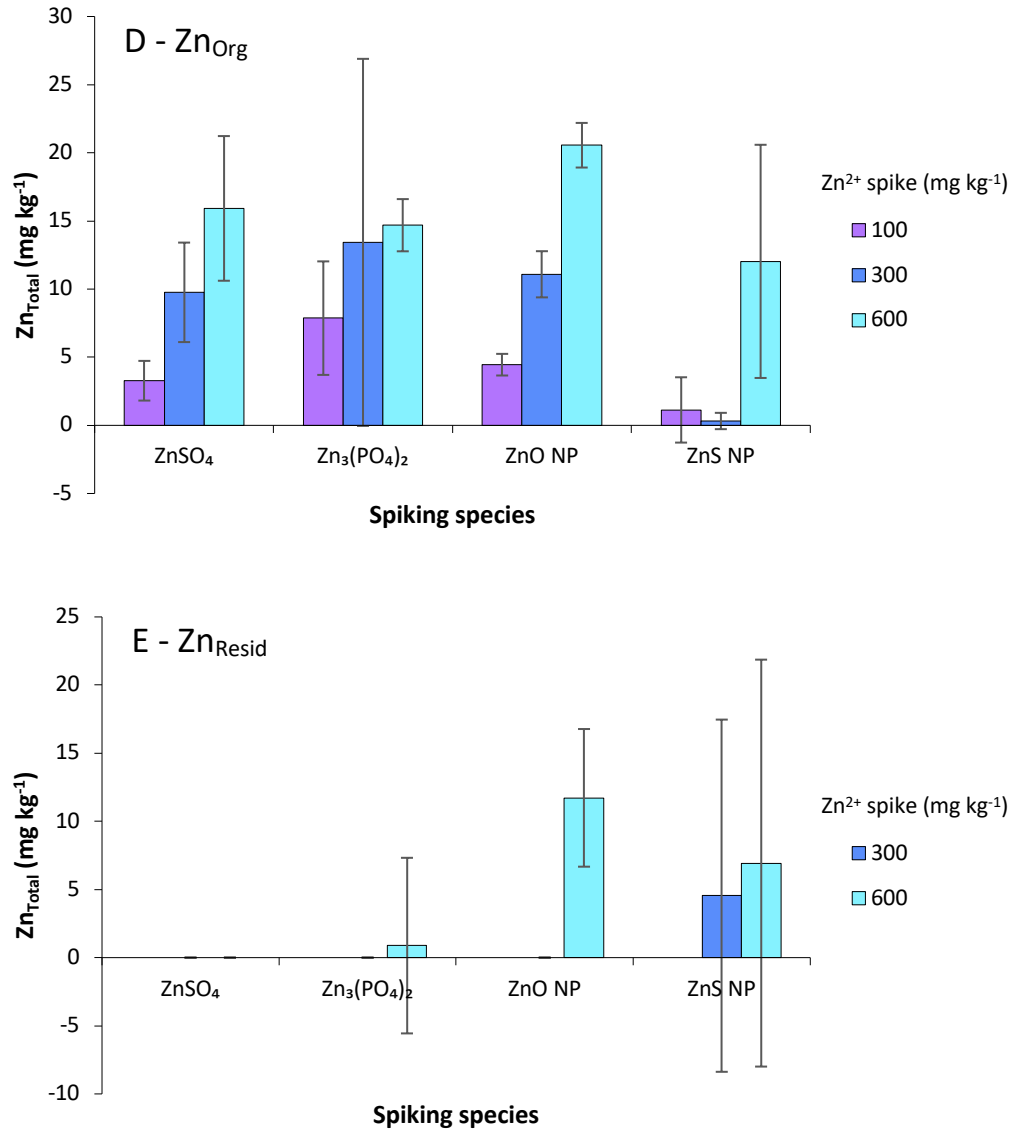


Figure 4.18 Average total zinc (Zn_{Total}) concentration of sequential extraction fractions of unvegetated soils. A – step 1, exchangeable (Zn_{Ex}); B – step 2, bound to carbonate and specifically adsorbed (Zn_{carb}); C – step 3, bound to Fe–Mn oxides (Zn_{oxide}); D – step 4, bound to organic matter and sulphide (Zn_{Org}); E – step 5, residual phase (Zn_{Resid}). Bars show standard deviation of the three replications of each sample.

larger proportion of zinc in the Zn_{Resid} fraction than the ZnO NP spiked samples. The Zn_{Resid} fraction contains mainly crystalline-bound trace elements which are considered to be unavailable under normal environmental conditions.

Subtracting the control Zn_{Total} concentration for each fraction from the corresponding zinc spiked samples highlights a number of things. The ZnS NP spiked samples showed a sharp increase in Zn_{Org} at the 600 mg Zn kg⁻¹ concentration (**Figure 4.18 D**). This could

indicate that the ZnS NPs were contained within the organic matter and were released due to the organic matter decomposing or the H_2O_2 oxidising the NPs. The ZnS NP and ZnO NP spiked samples had a substantial amount of zinc remaining in the Zn_{Resid} fraction at higher spiking levels (**Figure 4.18 E**) indicating a NP-specific effect and the difference in fractionation profiles between the ZnO NP and $ZnSO_4$ spiked samples supports the conclusion that ZnO NPs did not simply dissolve and behave as ionic zinc (**Figure 4.18**). Voegelin et al. [325] investigated zinc fractionation in 49 contaminated soil and found that in soils with a $pH < 6.0$, zinc was mainly found in their mobile and residual fractions whereas in soils with a $pH \geq 6.0$, most zinc was extracted in their intermediate fractions. In contrast, the present study showed that $ZnSO_4$ spiked soil samples had a $pH < 6$ (**Table 4.1**) but did not contain zinc in the Zn_{Resid} fraction, and soil samples spiked with $Zn_3(PO_4)_2$, ZnO NPs and ZnS NPs had a $pH > 6$ and contained varying concentrations of zinc in the Zn_{Resid} fraction at the higher spiking levels (**Figure 4.18 E**). This demonstrates that in addition to pH, species influences the fractionation profile of zinc in soil and therefore the availability of zinc to plants.

4.4 Conclusions

This study looked at the behaviour of ZnO NPs in comparison to ZnS NPs and $Zn_3(PO_4)_2$ when spiked into soil and their effect on the growth of ryegrass.

The unvegetated soils spiked with $ZnSO_4$ and ZnO NPs gave similar high concentrations of average Zn_{DTPA} suggesting that the ZnO NPs underwent rapid dissolution, whereas the ZnS NP and $Zn_3(PO_4)_2$ spiked soils had a low and consistent Zn_{DTPA} concentrations over the 18 weeks. The grass grown on the ZnS NP-spiked samples were slower to germinate and produced the smallest biomass at first harvest, but by the final harvest it was the highest concentration spike of ZnO NP samples that gave the smallest biomass.

The ZnO NP spiked samples had the highest grass Zn_{Total} concentrations but the low weight of the final harvest meant that the actual amount of $Zn_{Offtake}$ was low. Conversely, the ZnS-spiked samples had a much lower grass Zn_{Total} concentration but a much higher weight of the final harvest, resulting in the final harvest 600 mg kg^{-1} samples of ZnO NPs and ZnS NPs having comparable $Zn_{Offtake}$ concentrations. This could indicate that ZnS NPs are safe for crops while still providing nutrition, which would make them useful as a potential fertiliser.

Fractionation results show that although ZnO NPs appeared to dissolve quickly, they still behaved differently to $ZnSO_4$. Some studies investigating ZnO NPs have concluded that toxicity is a result of dissolved zinc [75, 76, 84], but other studies have come to the same conclusion as the present study; that ZnO NPs do not behave solely as ionic zinc and that toxicity cannot be adequately explained by dissolution alone [78-81].

Results clearly showed that pristine ZnO NPs behaved differently to ZnS NPs and $Zn_3(PO_4)_2$, and therefore are not an appropriate species to use if the intention is to investigate the effect of zinc NPs found in sewage biosolids. Studies using ZnO NPs are likely to observe fast NP dissolution and high zinc availability, potentially leading to concerns over zinc toxicity that may not have been raised if appropriately aged particles had been used instead.

Chapter 5

Effects of different zinc nanoparticles on mycorrhizal fungi and wheat

5.1 Background

A plant's requirement for essential micronutrients such as zinc varies over time, and soil concentrations can fluctuate between deficient to toxic levels. As described in section 1.2, zinc NPs can enter agricultural environments via a number of routes, including the use of ZnO NP-containing fertilisers and pesticides [33, 34], and ZnS NP-containing biosolid application onto fields [39, 40]. However, even when abundant, zinc can be present in soils in insoluble and therefore inaccessible forms. In order to cope with this variability, plants have flexible and adaptive strategies that maintain homeostasis. One of the most important strategies is their association with arbuscular mycorrhizal (myco- meaning 'mushroom or fungus' and -rhizal meaning 'related to roots') fungi (AMF). AMF are the most common soil microorganisms and are a crucial component of terrestrial ecosystems. They are obligate biotrophs that form symbiotic associations with nearly 90% of plant species [326]. In these associations, AMF colonise plant roots and develop extensive, branching networks of extraradical hyphae that are able to connect many large areas of forest in a continuous network of cells and transport nutrients between different species of plant [327]. AMF provide plants with enhanced acquisition of phosphorus and other low mobility nutrients such as zinc (**Figure 5.1**). In return they acquire photosynthetic plant-secreted sugars. These are mainly hexoses that fungi convert to sugar alcohols: mannitol, arabitol, and erythritol [327]. This all means that via their hyphal network they facilitate nutrient transfer between plant roots and soil, as well as supporting plant growth and pathogen resistance [328]. As mycologist Paul Stamets says [329]:

"...you can no longer define a plant without its fungal allies. Plants do not exist in absence of fungi."

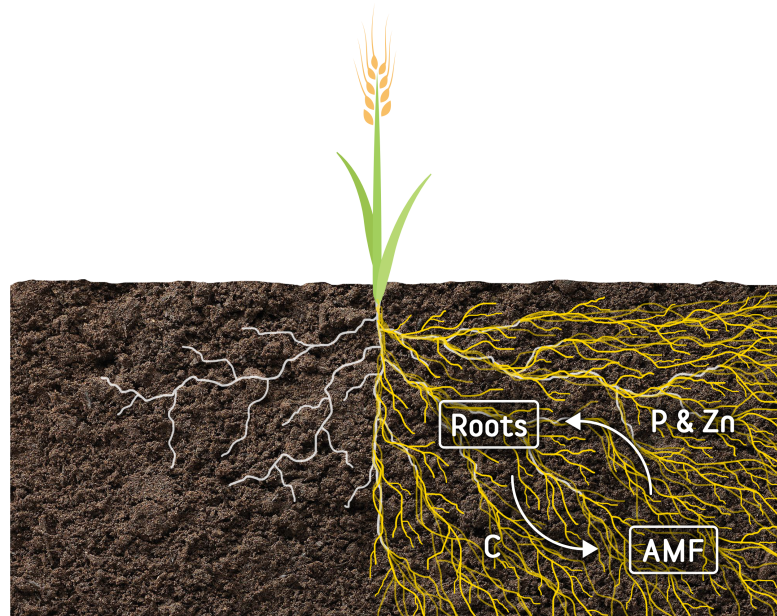


Figure 5.1 AMF form symbiotic associations with plant roots and develop extensive, branching networks of extraradical hyphae that facilitate nutrient transfer between plant roots and soil.

AMF: arbuscular mycorrhizal fungi; C: carbon; P: phosphorus; Zn: zinc. Source: author

AMF can also mediate the effects of heavy metals, potentially allowing plants to grow in contaminated soils [330, 331]. This is in part due to AMF production of glomalin related soil protein (GRSP), which is an operationally defined glycoproteinaceous substance thought to play a key role in metal chelation [332, 333].

In recent years, a number of studies have investigated the effect of ZnO NPs with AMF communities [293, 334-338]. Maize (*Zea mays*) [334, 335, 337], sudan grass (*Sorghum sudanese*) [334], fenugreek (*Trigonella foenum*) [336] and tomato [338] have all been used in AMF microcosm experiments with ZnO NPs. Maize and wheat (*Triticum aestivum*) have been used in AMF experiments with iron oxide (Fe_3O_4) NPs [339, 340] and AMF-inoculated clover (*Trifolium repens*) has been investigated with both Fe_3O_4 NPs and silver (Ag) NPs [341]. As yet there have not been any investigations into the effect of ZnS NPs with AMF communities. The AMF *Glomus caledonium* has been used in a number of experiments using NPs [334, 339, 341] and *Glomus versiforme* [334] has also been investigated. These studies produced their own inoculum by growing fungi in autoclaved sand; however this can take up to 12 months, whereas commercially

available AMF can be bought and used immediately. *Glomus* intraradices (renamed to *Rhizophagus irregularis*) has been used in studies to inoculate wheat [342, 343], barley [343] and tomato [344], where it was reported to have a high % infection rate.

Studies looking at NP effects on AMF often use autoclaved soils [334] or soil is replaced with sand and perlite [336, 341], although fresh soil has also been used [339, 340]. Using sterile media may make processing and analysis more straightforward, however it cannot claim to be representative of what happens in the environment. Some studies have used soil mixed with sand [338] to lower the phosphorus concentration and therefore increase the likelihood of the AMF inoculating the roots while also allowing the easy isolation of root material. Studies typically investigate ZnO NPs with AMF communities [293, 334-338] at concentrations of 3000 mg kg⁻¹ of zinc or more [334, 337] rather than using aged or transformed particles such as ZnS NPs and predicted concentrations. This investigation into AMF, zinc NPs and wheat, aimed to imitate environmental conditions as closely as possible, using agricultural soil and low concentrations of aged particles. The specific objectives of this study were: (i) to assess whether there is a significant difference in the effect of ZnS NPs, Zn₃(PO₄)₂ particles and ionic zinc with ZnO NPs on AMF and wheat, (ii) to evaluate changes in zinc concentration of wheat in response to treatments and (iii) to evaluate changes in AMF colonisation of wheat roots in response to NPs.

5.2 Materials and methods

5.2.1 Zinc species

ZnS NPs were synthesised by the method developed by Ganguly et al. [256] and characterised as described in section 2.1. ZnO NPs (advertised average particle size ≤ 40 nm, 20% wt in H₂O) and Zn₃(PO₄)₂ were purchased from Sigma-Aldrich, and ZnSO₄ salt was purchased from Fisher Scientific.

Solutions (50 mL) of all of the zinc species (ZnS NPs, ZnO NPs, $Zn_3(PO_4)_2$ and $ZnSO_4$) were diluted in Milli-Q water at concentrations intended to produce a spike of either 100, 250 or 500 mg kg^{-1} of zinc to each soil fraction on a dry weight basis.

5.2.2 Arbuscular mycorrhizal fungi species

AMF *Rhizophagus irregularis* and gamma-irradiation sterilized carrier material (powdered diatomite) were purchased from Symplanta, Germany. Diatomite (or diatomaceous earth) is a naturally occurring sedimentary rock made from fossilised unicellular aquatic plants called diatomaceous algae and skeletons of diatoms (a type of hard-shelled protist) found in marine or lacustrine environments. It is composed of approximately 90% silicon dioxide with a honeycomb silica structure that gives it chemical stability, low bulk density, high porosity and a high surface area [345].

5.2.3 Soil sampling, preparation and characterisation

Soil was collected and treated as described in section 2.2 and characterised as described in section 2.8. In order to reduce the level of phosphorus so that the AMF was more likely to colonise the roots, it was then mixed 50:50 with sand (Fisher chemical) and stored at 4°C before use.

Thirteen aliquots of soil were weighed out (20 kg each on a dry weight basis), one aliquot for each zinc spiking species (ZnS NPs, ZnO NPs, $Zn_3(PO_4)_2$ and $ZnSO_4$) and at each concentration level (100, 250 and 500 mg Zn kg^{-1}), with one for the un-spiked control. Zinc species were added to soil fractions as aqueous solutions (50 mL), as described in section 2.3.

Thirteen plant pots (2 L) were filled with 2 kg (dry weight) of spiked (ZnS NPs, ZnO NPs, $Zn_3(PO_4)_2$ and $ZnSO_4$ at 100, 250 and 500 mg Zn kg^{-1}) or un-spiked (control) soil. A layer of AMF inoculum (4 g) was added at approximately 2 cm below surface level. This was

repeated for a further thirteen pots, but adding 2 g of sterilized carrier material instead of the AMF inoculum. The sterilized carrier material was identical to the carrier in the AMF, but contained no water. The AMF inoculum contained 50% water and was therefore applied at a rate twice that of the carrier. Five replications were made of each treatment. Milli-Q water was added to bring each pot up to approximately 80% WHC. Pots were then left to equilibrate in the dark for 24 hr before sowing seeds.

5.2.4 Preparing seeds

Spring wheat seeds (*Triticum aestivum* L., cv. Mulika) were prepared as described in section 2.4. A small batch was germinated and the average germination rate was > 94%. Five seeds were sown in each pot and KNO₃ (0.02 M, Fischer chemicals) was added at a rate of N equivalent to 200 kg ha⁻¹ [310].

5.2.5 Experimental set up

The experiment was set up in a glasshouse as described in section 2.5. Throughout the experiment the temperature varied between a maximum of 38°C and a minimum of 11°C, with an average of 21°C.

The pots were arranged in a randomised block formation with 5 blocks each containing one pot of each treatment. Pots were arranged and watered as described in section 2.5. Seedlings started to appear at week 2, and at week 3 each pot was thinned down to contain only the strongest looking specimen. Blocks 1 – 4 were grown to maturity, but block 5 was sacrificed half way through the growing period to confirm that AMF colonisation had been successful.

5.2.6 Harvesting and processing

In order to confirm that roots had been successfully colonised by AMF, plants in block 5 were harvested at week 10, as described in section 2.6. Plants in blocks 1 – 4

were harvested at week 18. Seed heads were separated from stalks and grains were then separated from the heads. Root samples were cut in half to give two subsamples in order to allow both zinc concentration and AMF colonisation to be assessed. This was done by cutting up the centre of the root ball to ensure that each section included equal amounts of seminal and nodal roots.

Stem/leaf and half of the root samples were dried, and stem/leaf, root and grain samples were weighed and ground, as described in section 2.6. Soil was put into foil trays and air-dried, before being ground using a ball mill (Retsch, Model PM400).

5.2.7 AMF staining

To assess the roots colonised by AMF the staining method developed by Brundrett et al. [346] was followed, with a few adjustments. Roots were removed from the soil and washed thoroughly, cut into sections (2.5 cm) and added to centrifuge tubes. Enough KOH (10% (w/v), Sigma-Aldrich) was added so that roots were covered and the tubes heated to 90°C in a water bath for 20 min. Roots were removed from the tubes and washed with DI water. Roots were then added to clean centrifuge tubes and covered with 0.1% chlorazol black E (equal volumes of 80% lactic acid (Fisher chemicals), glycerol (Fisher chemicals) and Milli-Q water with 0.1% chlorazol black E powder (Alfa Aesar) added). Tubes were then put back into the waterbath (90°C) for 1 hr. Finally, roots were drained of excess solution and suspended in glycerol.

5.2.8 AMF counting

The extent of root colonisation by AMF was determined using the root segment \pm method [347]. Roots were mounted on microscope slides with two slides per sample. Each slide was examined under a microscope (Leitz Laborlux S) by taking fifty views systematically, starting at the top left corner and finishing at the bottom right.

AMF colonisation was calculated as the number of views of the root segments colonised by AMF divided by the total number of views examined.

5.2.9 Microwave digestion of plant material

Stem/leaf, root and grain samples were digested as described in section 2.9. Multi-element analysis was undertaken using ICP-MS as described in section 2.11.

5.2.10 DTPA-extractable zinc of soil

The availability of zinc in soils was evaluated using DTPA-extraction and determined as described in section 2.7. Multi-element analysis was undertaken using ICP-MS as described in section 2.11.

5.2.11 Soil *E* values

In soils, zinc present as Zn^{2+} cations can exist in three forms (**Figure 5.2**): in solution, exchangeable and non-exchangeable fractions (also described as labile in solution, labile adsorbed and non-labile). Isotopic dilution (ID) is a technique that can be used to quantify the labile metal fraction in a soil. This can be achieved by spiking isotopically enriched metal into a soil suspension and leaving it to exchange with the native labile metal, until equilibrium is achieved. The extent of isotopic mixing with the soil zinc by the enriched isotope can then be measured and this is known as the *E* value [348].

Soil (2 g) was added to centrifuge tubes containing $Ca(NO_3)_2$ (0.01 M, 20 mL, Fisher chemicals) and shaken end over end for 24 hr. Enriched ^{70}Zn (Isoflex, USA) was adjusted to pH 4 using ammonium acetate (0.1 M, 500 μ L, VWR chemicals) and 0.4 mL was added to each sample. The samples were again shaken end-over-end for 3 days. Sample pH was verified and then samples were centrifuged (3500 rpm, 15 min).

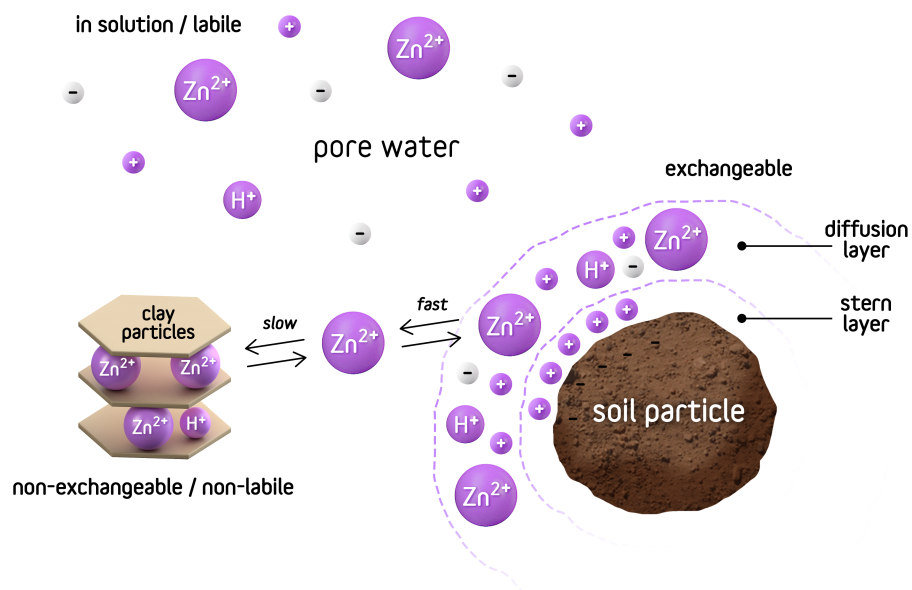


Figure 5.2 Zinc storage in soils, in solution, exchangeable and non-exchangeable. Exchangeable cations weakly bound above soil particle surface exchange sites. Non-exchangeable zinc fixed between individual clay minerals. Source: author

Supernatant was removed, syringe-filtered to < 0.2 μm and added to ICP tubes (9.6 mL) where it was acidified using HNO_3 (50%, 0.4 mL, Fisher 'trace analysis grade'). Analysis was undertaken using ICP-MS as described in section 2.11, with some additions. Intensities for ^{70}Zn were used to calculate E values using the equation:

$$E \text{ value} = \text{Zn}_{\text{sol}} \left[k_d + \frac{v}{w} \right]$$

where k_d is the distribution coefficient of the ^{70}Zn isotope spike, Zn_{sol} is the zinc concentration in solution, v is the solution volume (20.4 mL) and w is the weight of soil (~ 0.2 g). The k_d for each sample was calculated as:

$$k_d = \frac{\text{Zn}_{\text{ads}}}{\text{Zn}_{\text{sol}}}$$

where Zn_{ads} is the concentration of spiked ^{70}Zn adsorbed onto the soil solid phase and Zn_{sol} is the concentration of spiked ^{70}Zn in solution. The measurement of ^{70}Zn in solution from the added spike was corrected for native soil ^{70}Zn by determining the solution concentration of ^{66}Zn and assuming the normal isotopic abundances of ^{66}Zn

and ^{70}Zn applied. Unfortunately, ICP-MS can suffer from spectral interference which can result in analyte concentration being miscalculated. This can occur when species other than the analyte being monitored are present at the same mass-to-charge (m/z) ratio. This then causes an overestimation of the analyte concentration [349]. $^{70}\text{Zn}^+$ analysis is complicated by isobaric interferences from $^{70}\text{Ge}^+$ and $^{140}\text{Ce}^{2+}$. These were mathematically corrected for by running standards. For $^{70}\text{Ge}^+$, a 5 ppb Ge (^{72}Ge , ^{73}Ge and ^{74}Ge) standard was run and the isotopic ratios and sensitivity was checked in order to confirm that ^{70}Ge could be accurately calculated. For Ce, standards were run to examine the 70/140 ratio. ^{140}Ce was monitored for every sample and used to correct the $^{70}\text{Zn}^+$ data.

5.2.12 Statistical analysis

As described in section 2.12, orthogonal contrasts for analysis of variance are an *a priori* (before the fact) statistical approach that makes independent linear comparisons between treatments with at least 3 fixed levels to obtain main effects and interaction effects [259].

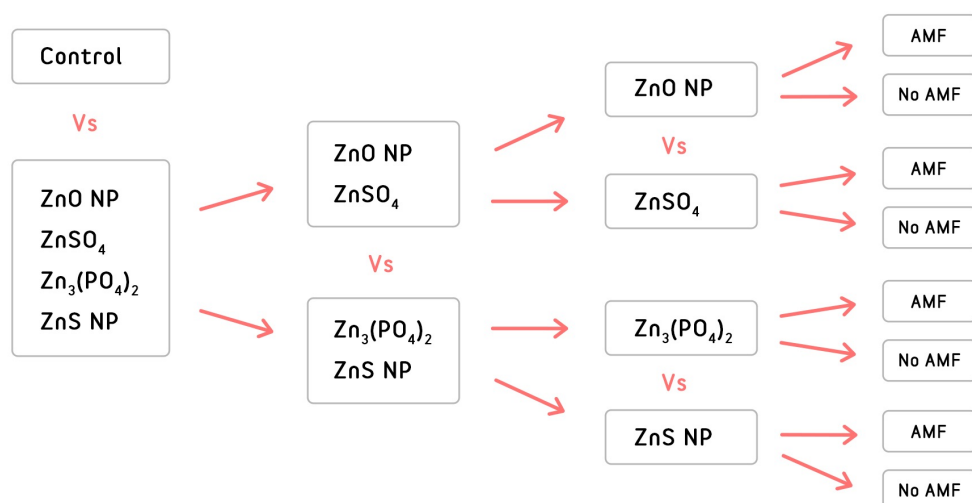


Figure 5.3 Orthogonal contrasts of the different treatments (control, soil spiked with ZnS NPs, ZnO NPs, ZnSO₄ and Zn₃(PO₄)₂)

There were 5 different treatments (control, soil spiked with ZnS NPs, ZnO NPs, ZnSO₄ and Zn₃(PO₄)₂) and therefore four possible independent variables (degrees of freedom) that could be partitioned into simple contrasts (**Figure 5.3**). Orthogonal contrasts were carried out as described in section **2.12**. Data from this experiment was partitioned as follows:

Class comparisons pairs

C1 – Control vs all Zn treatments

C2 – (ZnO NPs and ZnSO₄) vs (Zn₃(PO₄)₂ and ZnS NPs)

C3 – ZnO NPs vs ZnSO₄

C4 – Zn₃(PO₄)₂ vs ZnS NPs

C5 – AMF added vs AMF not added

Trend comparisons

C6 – Linear concentration vs non-linear concentration

C7 – Quadratic concentration vs non-quadratic concentration

Contrasts are orthogonal if the products of their coefficients sum to zero, and a set of more than two contrasts are orthogonal if each and every pair within the set are orthogonal. Contrasts were chosen on the basis that the groups were expected to be different to one another, to assess whether there was a significant average treatment effect and whether treatments were significantly different from one another. For example, ZnO NPs and ZnSO₄ were expected to behave differently to one another (C3), as were Zn₃(PO₄)₂ and ZnS NPs (C4), however, previous experiments showed that ZnO NPs can dissolve rapidly, and so were expected to behave more similarly to ZnSO₄ than Zn₃(PO₄)₂ and ZnS NPs (C2). Contrast 5 was included to see whether there was a significant difference between AMF being added or not. The trend comparison contrasts 6 and 7 were to see whether or not the concentration of the soil spike caused the response to have a significant linear or quadratic trend, respectively. With a linear trend, values tend to rise or fall at a constant rate, whereas with a quadratic trend,

values tend to rise or fall at a rate that is not constant. If both were shown to be significant that would mean that there was an overall linear trend with some non-linear components. Contrasts with $P < 0.05$ were taken to be significant.

If these comparisons are shown to be significant, then they can be combined to look at the interaction comparisons EG – C2:C6, will show whether the linear component to the response differs between the groups.

5.3 Results and discussion

5.3.1 Nanoparticle characterisation

The morphology and size distribution of the NP species were examined using TEM analysis (JEOL, JEM-2100F FEG-TEM); the ZnS NPs were shown to be broadly spherical

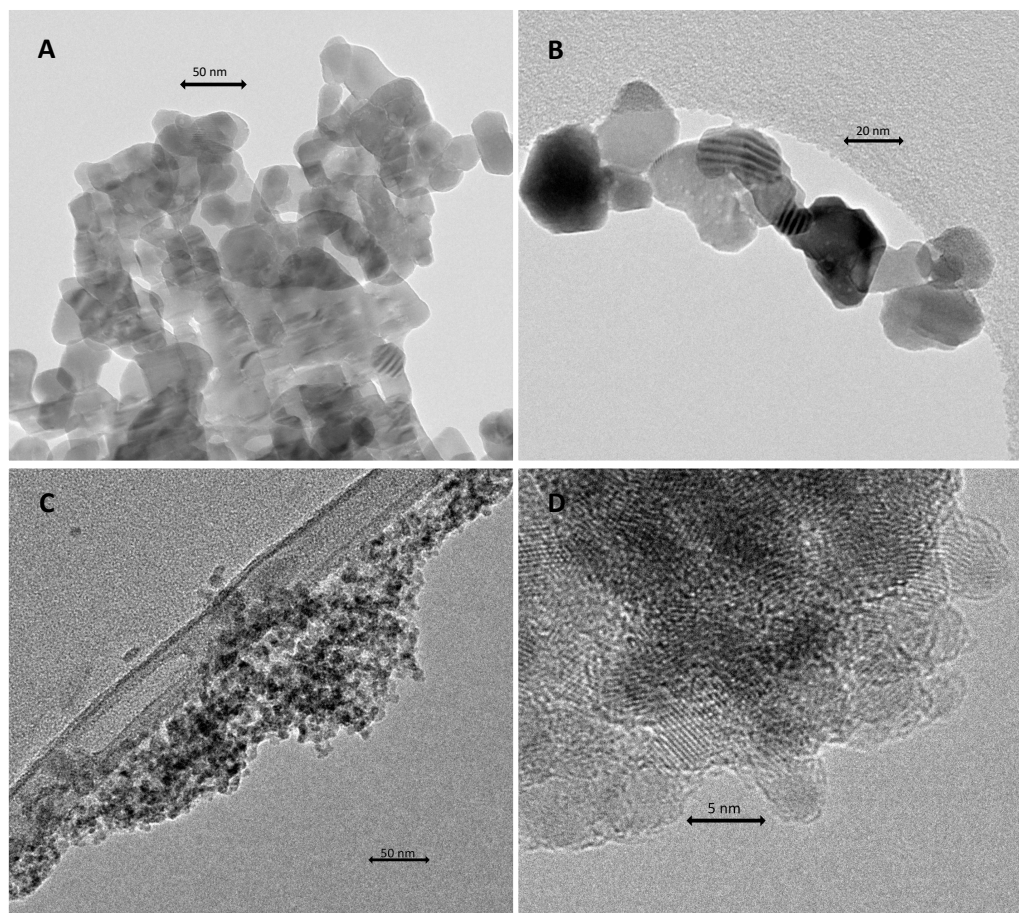


Figure 5.4 Transmission electron microscopy (TEM) images of ZnO NPs at A – 50 nm and B – 20 nm, and ZnS NPs at C – 50 nm and D – 5 nm

with a diameter of approximately 5 nm and results for the ZnO NPs corroborated the advertised average particle size of ≤ 40 nm (**Figure 5.4**).

5.3.2 Soil characteristics

The soil was an arable Wick series sandy loam and the main physico-chemical characteristics of the soil were as follows: pH (water, 1 : 2.5 soil : water ratio) 6.59; LOI of 8.8%; total zinc concentration of 113 mg kg⁻¹; WHC was 25.5%.

5.3.3 Weight of wheat samples

The orthogonal contrast C1 showed that there was a significant difference in weights of stem/leaf and grain between control samples and applied zinc species (**Tables 5.1** and **5.2**), but for roots there was no difference (**Table 5.3**).

The weights of stem/leaf, grain and roots were significantly different between ZnSO₄ and ZnO NPs spiked samples (C3, **Tables 5.1, 5.2** and **5.3**), however, this is not unexpected because the samples spiked with 500 mg kg⁻¹ of ZnSO₄ were toxic to the wheat plants and significantly inhibited their growth (**Figure 5.5**). Du et al. [350] similarly found that, at high concentrations, ZnSO₄ was more toxic than ZnO NPs to wheat plants. There was also a significant difference in the linear component to the responses between ZnO NP and ZnSO₄ spiked samples (C3:C6), again due to the sudden reduction in weight of the 500 mg kg⁻¹ ZnSO₄ spiked samples. The weights of stem/leaf and roots were significantly different between Zn₃(PO₄)₂ and ZnS NPs spiked samples (C4, **Tables 5.1** and **5.3**), but for grain there were no differences (**Table 5.2**).

This study found no correlation between plant biomass, AMF colonisation % and zinc uptake. In contrast, Siani et al. [336] looked at the effect of AMF on ZnO NP toxicity in fenugreek and found that AMF colonisation decreased plant zinc uptake, which increased plant biomass, and Ma et al. [351] reported that AMF inoculation significantly

	DF	Sum Sq	F-value	p-value
C1	1	4.61	5.69	0.0195
C3	1	45.3	55.9	1.18e ⁻¹⁰
C4	1	4.22	5.21	0.0253
C6	1	9.15	11.3	1.22e ⁻³
C7	1	7.22	8.91	3.82e ⁻³
C2:C6	1	11.1	13.7	4.04e ⁻⁴
C3:C6	1	33.9	41.9	8.99e ⁻⁹

Table 5.1 Significant orthogonal contrasts of stem/leaf weight. DF: Degrees of freedom. Expanded version see Table 7.5

	DF	Sum Sq	F-value	p-value
C1	1	34.3	38.4	2.83e ⁻⁸
C2	1	13.2	14.8	2.49e ⁻⁴
C3	1	50.8	57.0	8.64e ⁻¹¹
C6	1	26.2	29.4	6.81e ⁻⁷
C2:C6	1	21.5	24.2	5.08e ⁻⁶
C3:C6	1	41.1	46.1	2.29e ⁻⁹

Table 5.2 Significant orthogonal contrasts of grain weight. DF: Degrees of freedom. Expanded version see Table 7.6

	DF	Sum Sq	F-value	p-value
C2	1	0.654	3.99	0.0493
C3	1	5.64	34.4	1.12e ⁻⁷
C4	1	1.35	8.22	5.38e ⁻³
C6	1	2.09	12.7	6.29e ⁻⁴
C7	1	0.812	4.96	0.0290
C2:C6	1	4.10	25.0	3.64e ⁻⁶
C3:C6	1	2.65	16.2	1.37e ⁻⁴

Table 5.3 Significant orthogonal contrasts of root weight. DF: Degrees of freedom. Expanded version see Table 7.7

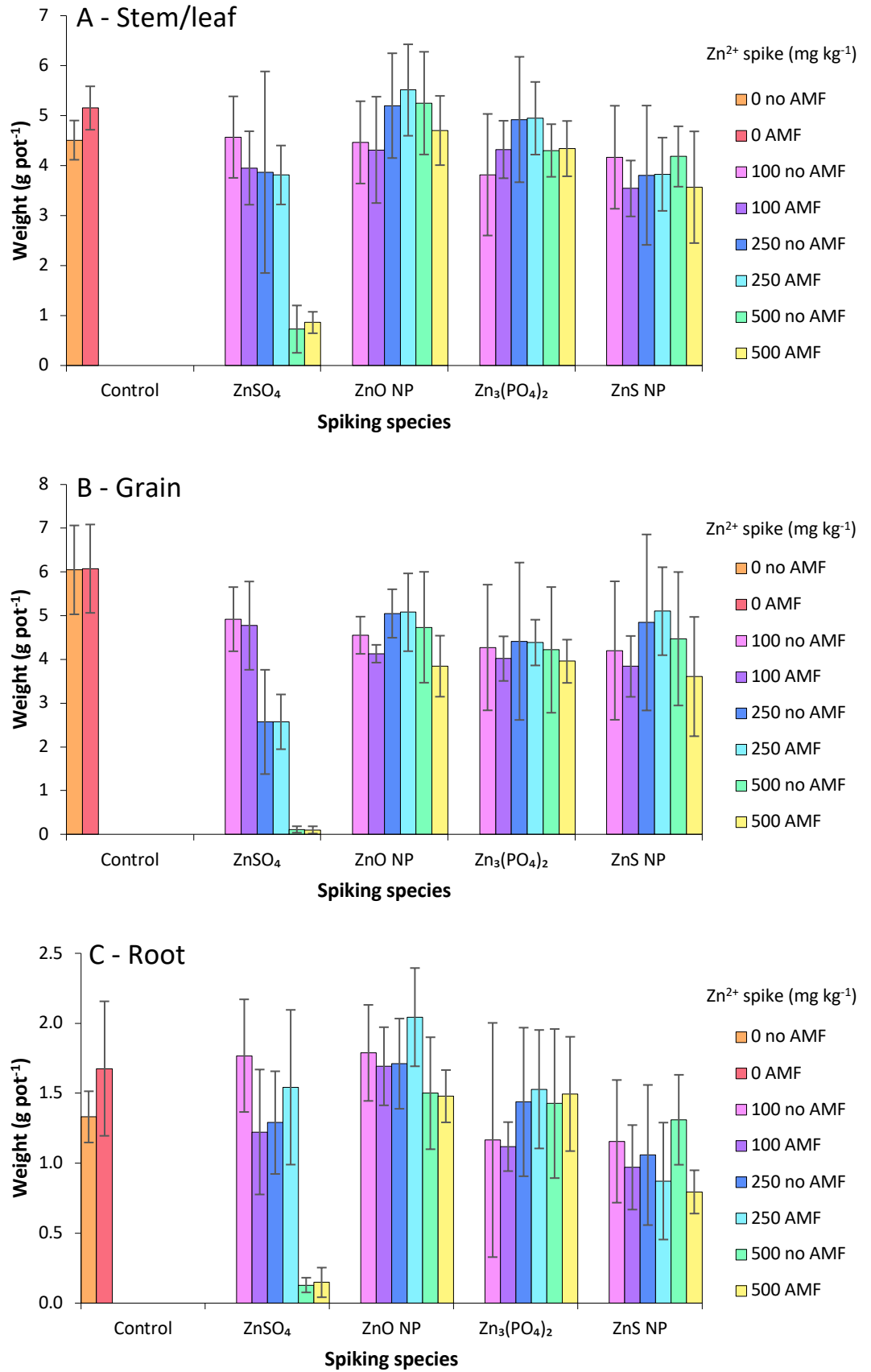


Figure 5.5 Average dry weight of harvested wheat. A - stem/leaf; B - grain; C - root. Bars show standard deviation of the four replications of each sample.

increased grain yield in wheat grown on zinc spiked soils. However, another study by Coccina et al. looking at zinc uptake in wheat via AMF found that biomass did not vary with AMF inoculation [343] and Tran et al. [352] found soil zinc amendments to have a greater effect on plant growth than AMF inoculation.

	DF	Sum Sq	F-value	p-value
C1	1	159	5.31	0.0239
C2	1	207	6.94	0.0103
C3	1	213	7.12	9.35x10 ⁻³
C4	1	147	4.92	0.0295
C6	1	824	27.6	1.34x10 ⁻⁶
C2:C6	1	492	16.5	1.20x10 ⁻⁴
C3:C6	1	747	25.0	3.65x10 ⁻⁶

Table 5.4 Significant orthogonal contrasts of stem length. DF: Degrees of freedom. Expanded version see Table 7.8

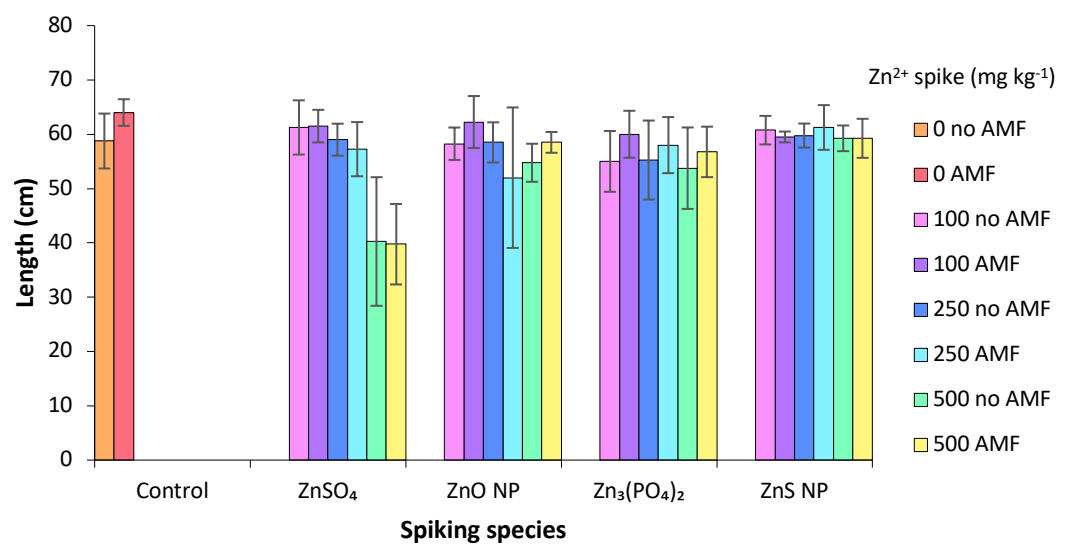


Figure 5.6 Average length of harvested wheat. Bars show standard deviation of the four replications of each sample.

5.3.4 Stem length of wheat samples

The stem length of wheat was significantly different between control samples and all other applied zinc species samples (C1, **Table 5.4**), between (ZnSO₄ and ZnO NPs) vs (Zn₃(PO₄)₂ and ZnS NPs) spiked samples (C2), between ZnSO₄ and ZnO NPs spiked samples (C3), and between Zn₃(PO₄)₂ and ZnS NPs spiked samples (C4). There was also a significant difference in the linear component to the responses between ZnO NP and ZnSO₄ spiked samples (C3:C6, **Figure 5.6**), but again this was due the sudden stunting of the 500 mg kg⁻¹ ZnSO₄ spiked samples.

5.3.5 Number of heads

The production of additional stems from of the main shoot of a plant that occurs in many Poaceae family grasses is called tillering [353]. Tillering means that multiple heads of wheat can be produced by a single plant. For this experiment, the number of heads produced were significantly different between control samples and all other applied zinc species samples (C1, **Table 5.5**), between (ZnSO₄ and ZnO NPs) vs (Zn₃(PO₄)₂ and

	DF	Sum Sq	F-value	p-value
C1	1	0.382	6.93	0.0103
C2	1	0.803	14.6	2.77x10 ⁻⁴
C3	1	3.44	62.4	1.85x10 ⁻¹¹
C4	1	0.723	13.1	5.33x10 ⁻⁴
C6	1	0.695	12.6	6.71x10 ⁻⁴
C7	1	0.530	9.61	2.72x10 ⁻³
C2:C6	1	1.33	24.1	5.25x10 ⁻⁶
C3:C6	1	4.71	85.3	5.31x10 ⁻¹⁴

Table 5.5 Significant orthogonal contrasts of number of heads. DF: Degrees of freedom. Expanded version see Table 7.9

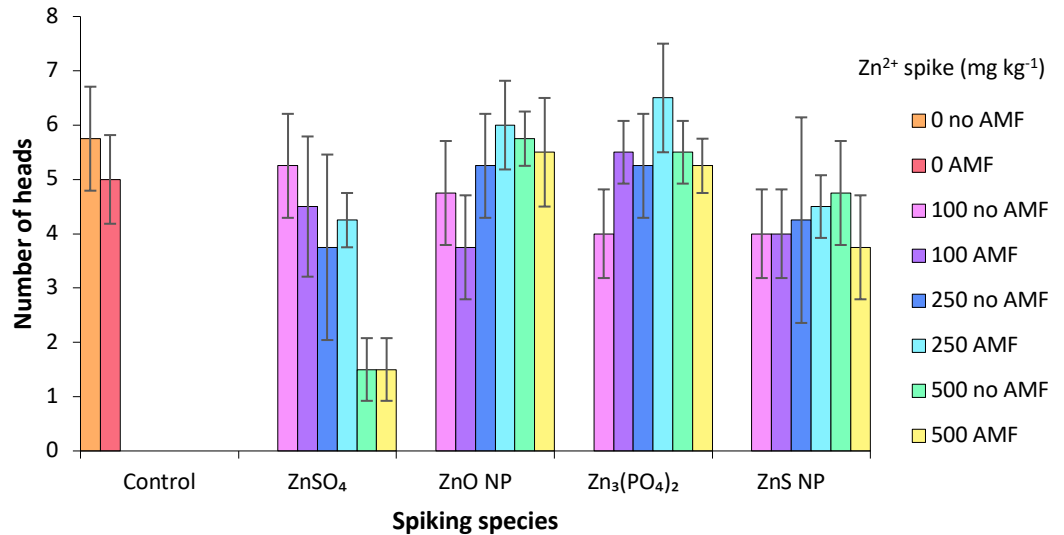


Figure 5.7 Average number of heads of harvested wheat. Bars show standard deviation of the four replications of each sample.

ZnS NPs) spiked samples (C2), between ZnSO₄ and ZnO NPs spiked samples (C3) and between Zn₃(PO₄)₂ and ZnS NPs spiked samples (C4, **Figure 5.7**).

5.3.6 AMF colonisation

There are a number of different stains that can be used to assess AMF colonisation of roots. For this experiment chlorazol black E was selected. Gange et al. [354] compared three different stains on ten different plants. It was found that of the three, chlorazol black E was generally best. However, it was also found that the performance of a stain was dependent on the plant species being examined and therefore the level of colonisation recorded will always be dependent on the combination of stain used and plant being analysed.

Once roots have been stained, the extent of colonisation is normally carried out using qualitative visual microscopy methods. Alternatively, quantitative methods such as WinRHIZO image analysis software [355] or colorimetric methods [356] can be used. Sun and Tang [347] evaluated and compared four frequently used microscopy methods. It was found that regardless of the method used, large divergences between values were

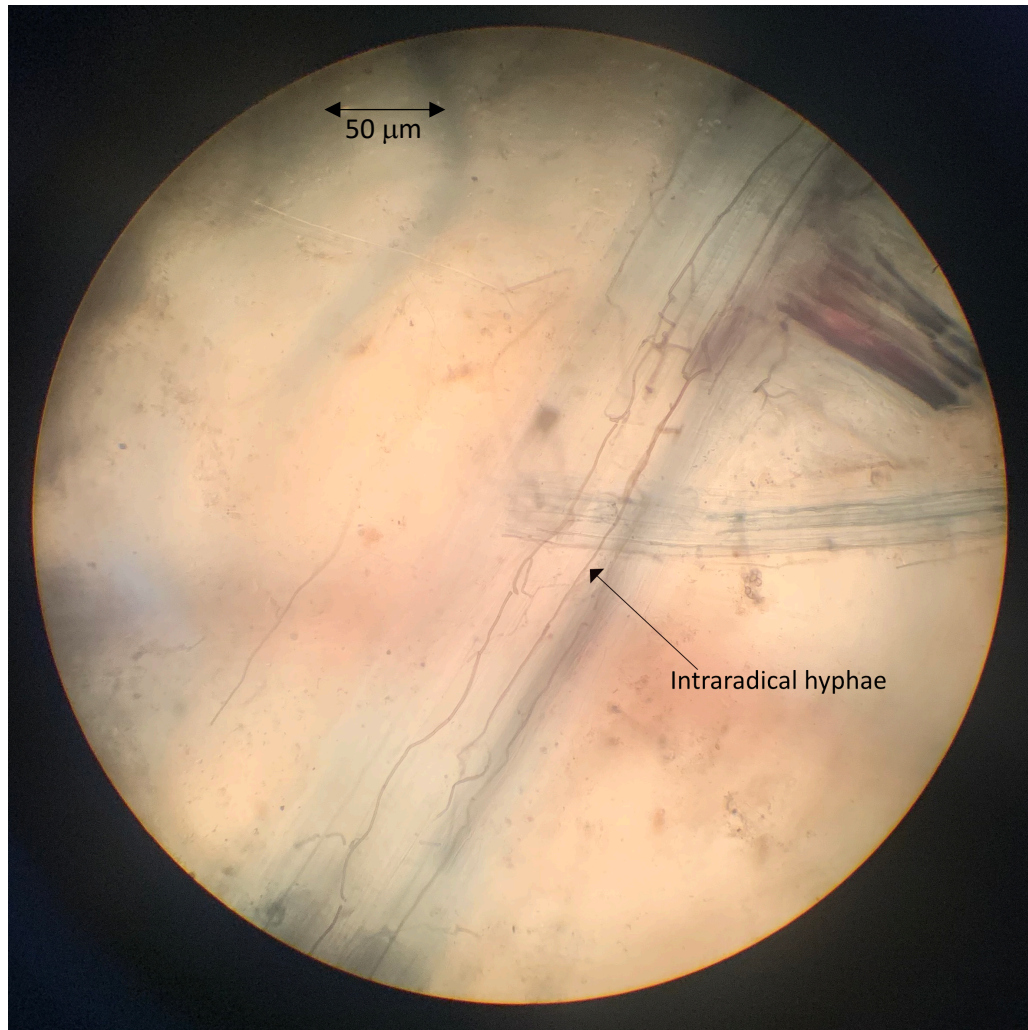


Figure 5.8 Wheat root segment colonised with stained mycorrhizal fungi

found when only fifty root segments were examined and so it was recommended that if possible, up to 150 root segments per root sample should be assessed in order to obtain an accurate value of % colonisation. This experiment looked at 100 root segments per sample (**Figure 5.8**). Results show that although the samples with added AMF had roots with a higher rate of colonisation (%) than those without, all samples had undergone colonisation from AMF occurring naturally in the soil.

There was a significant difference in colonisation rate (%) between samples where AMF had been added and where it had not (C5, **Table 5.6**). **Figure 5.9** shows that in all cases the addition of AMF to the soil resulted in roughly doubling the root colonisation by AMF. In all samples with added AMF, average root colonisation rates were > 30%

for all spiking species at all concentration levels, except for 500 mg kg⁻¹ ZnSO₄. This was presumably due to the toxicity of this spiking species damaging the roots and impeding growth of the plants. Despite not receiving any additional AMF, samples with no added AMF still had average root colonisation rates between 6 – 26% by other AMF present in the soil.

	DF	Sum Sq	F-value	p-value
C5	1	21634	172	< 2.2e ⁻¹⁶
C7	1	2018	16.0	1.46e ⁻⁴

Table 5.6 Significant orthogonal contrasts of AMF colonisation. DF: Degrees of freedom. Expanded version see Table 7.10

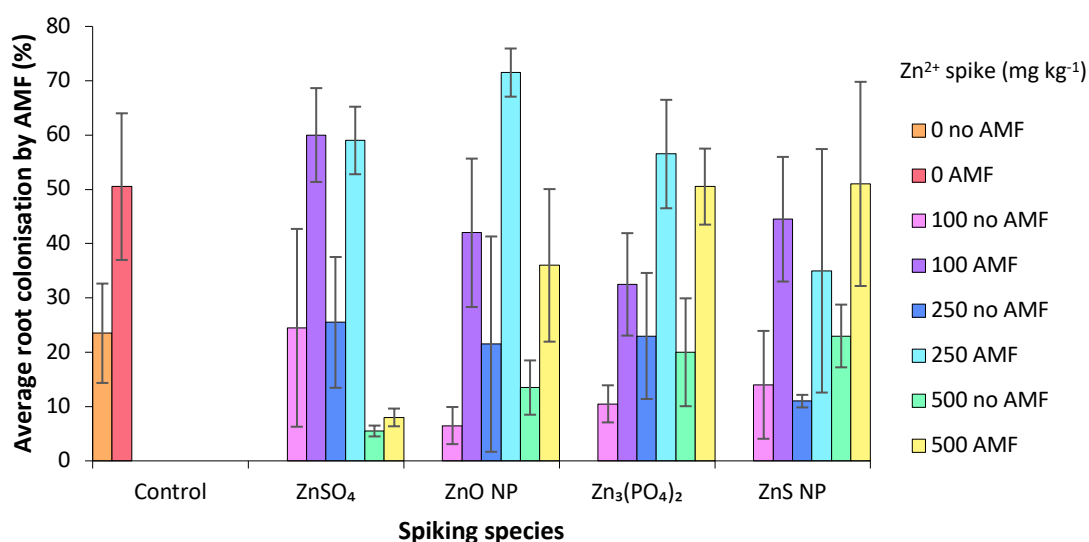


Figure 5.9 Average % wheat root colonisation. Bars show standard deviation of the four replicates of each sample.

With the exception of the 500 mg kg⁻¹ ZnSO₄ treatment which drastically impeded root growth, the present study did not find AMF colonisation of wheat roots to be significantly impacted by the addition of zinc to soil. This is consistent with previous studies looking at the response of AMF to inoculation of *Lygeum spartum*, *Anthyllis cytisoides* [357] and tomatoes under varying zinc concentrations [358].

5.3.7 Zinc concentration of plant samples

The total zinc (Zn_{Total}) concentrations of stem/leaf, grain and roots were significantly different between control samples and all other applied zinc species samples (C1, Tables 5.7, 5.8 and 5.9), between (ZnSO₄ and ZnO NPs) vs (Zn₃(PO₄)₂ and ZnS NPs) spiked samples (C2) and between Zn₃(PO₄)₂ and ZnS NPs spiked samples (C4).

	DF	Sum Sq	F-value	p-value
C1	1	92224	392	< 2.2x10 ⁻¹⁶
C2	1	190346	808	< 2.2x10 ⁻¹⁶
C3	1	74061	314	< 2.2x10 ⁻¹⁶
C4	1	16017	68.0	4.04x10 ⁻¹²
C6	1	199017	845	< 2.2x10 ⁻¹⁶
C7	1	15398	65.4	8.19x10 ⁻¹²
C2:C6	1	25573	109	3.12x10 ⁻¹⁶
C2:C7	1	4122	17.5	7.71x10 ⁻⁵
C3:C6	1	8698	36.9	4.69x10 ⁻⁸
C3:C7	1	9791	41.6	9.87x10 ⁻⁹
C4:C6	1	2820	12.0	8.93x10 ⁻⁴
C4:C7	1	1564	6.64	0.0119

Table 5.7 Significant orthogonal contrasts of stem/leaf total zinc. DF: Degrees of freedom. Expanded version see Table 7.11

	DF	Sum Sq	F-value	p-value
C1	1	15.8	785	$< 2.2 \times 10^{-16}$
C2	1	2.56	125	$< 2.2 \times 10^{-16}$
C3	1	0.511	25.3	3.27×10^{-6}
C4	1	0.699	34.7	1.07×10^{-7}
C6	1	4.02	199	$< 2.2 \times 10^{-16}$
C7	1	0.571	28.3	1.06×10^{-6}
C3:C6	1	0.320	15.9	1.59×10^{-4}

Table 5.8 Significant orthogonal contrasts of grain total zinc. DF: Degrees of freedom. Expanded version see Table 7.12

	DF	Sum Sq	F-value	p-value
C1	1	31673	35.1	9.20×10^{-8}
C2	1	38840	43.0	6.42×10^{-9}
C4	1	16563	18.4	5.44×10^{-5}
C6	1	202223	224	$< 2.2 \times 10^{-16}$
C7	1	5174	5.73	0.0192
C2:C6	1	46101	51.1	5.22×10^{-10}
C2:C7	1	8125	9.00	3.67×10^{-3}
C4:C6	1	4089	4.53	0.0366

Table 5.9 Significant orthogonal contrasts of root total zinc. DF: Degrees of freedom. Expanded version see Table 7.13

The Zn_{Total} concentration of stem/leaf and grain were significantly different between $ZnSO_4$ and ZnO NPs spiked samples (C3), but for roots they were not. Grain samples showed much lower Zn_{Total} concentrations with a much narrower spread than stem/leaf and root samples (**Figure 5.10**). Tran et al. [352] suggested that AMF inoculation may increase the concentration of phytic acid in wheat grain which binds to zinc and therefore reduces the bioavailability of grain zinc. Similarly, Coccina et al. [343] found that the grain from AMF inoculated wheat plants had higher

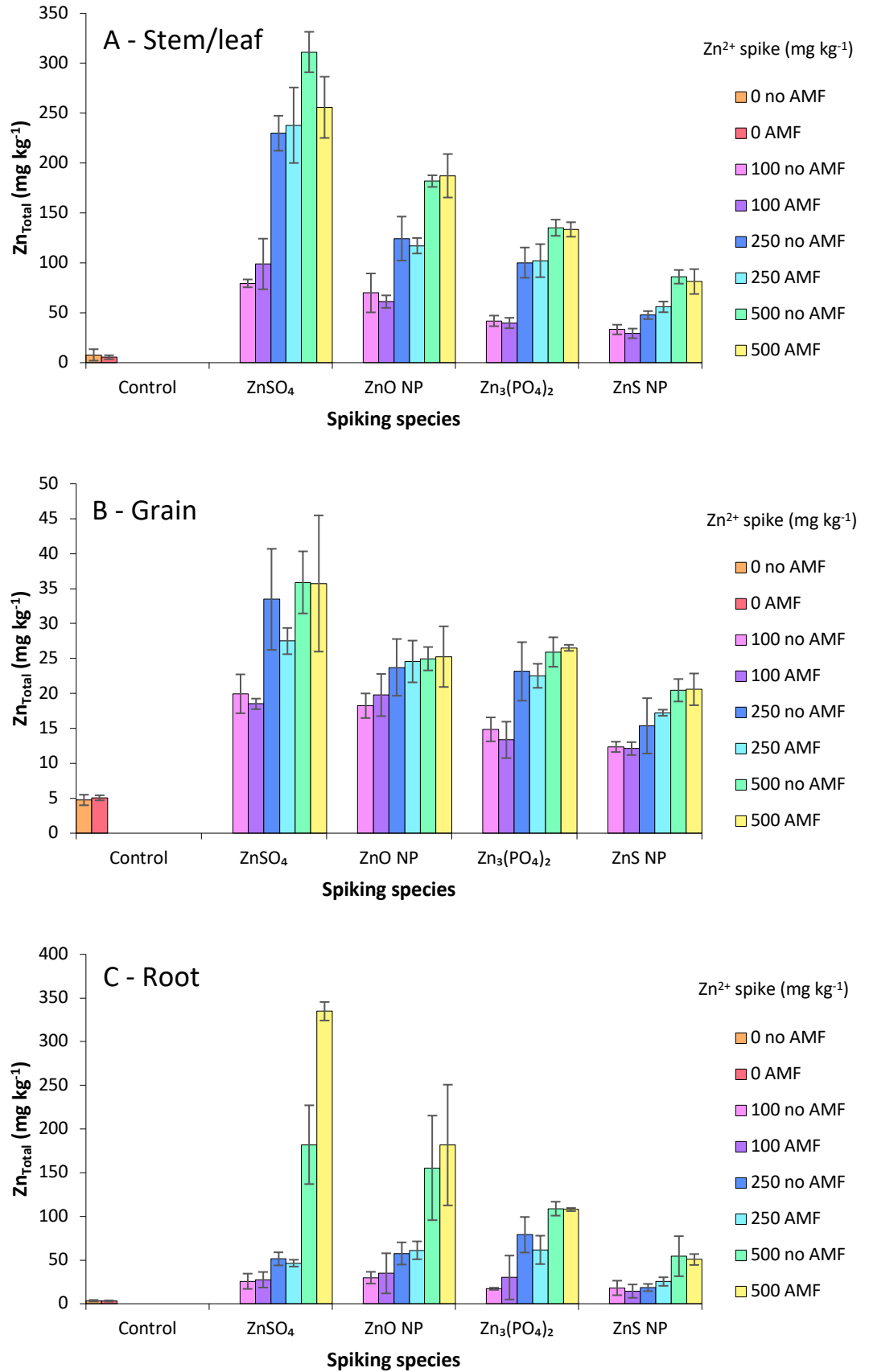


Figure 5.10 Average total zinc (Zn_{Total}) concentration of harvested wheat. A - stem/leaf; B - grain; C - root. Bars show standard deviation of the four replications of each sample.

zinc concentrations than that of non-AMF plants. This could explain the relative consistency in Zn_{Total} concentration across grain samples in comparison to stem/leaf and root samples. However, Ma et al. [351] found that AMF inoculation of wheat had an insignificant effect on grain phytic acid concentrations.

This study did not find evidence of AMF affecting plant tissue Zn_{Total} concentration and previous studies have found soil zinc amendments to have a stronger effect on nutrient responses than AMF [352]. There have been studies that have demonstrated that AMF inoculation increased zinc uptake in papaya [359], cowpea [360], maize [361], orange [362], tomato [363] and wheat grain [351]. However, there have also been studies showing non-mycorrhizal grapevines had higher zinc uptake than mycorrhizal grapevines [364], and that AMF inoculation reduced zinc uptake in faba beans [365], fenugreek [336] and red clover [366]. A meta-analysis of 104 studies examining AMF influence on zinc nutrition in crop plants concluded that AMF has a positive impact on zinc concentration in shoot, root and fruit tissues and found that soil texture was the main regulator of the AMF-mediated effect [367]. In contrast, a later meta-analysis of 93 studies looking at effects of AMF on plants and soils found that AMF had significant positive effects on a number of factors including plant growth, nitrogen and phosphorus uptake, disease resistance and soil aggregation, but no effect was detected on zinc uptake [368]. Many studies omit the germination stage which has been shown to be particularly sensitive to zinc concentration [369-372] and could contribute to the inconsistency of results, as could the wide range of plants, AMF and experimental conditions used.

5.3.8 Zinc offtake

Multiplying the weight of each sample by its zinc concentration gives the total amount of zinc taken out of the soil and into each part of the plant ($Zn_{Offtake}$, **Figure 5.11**). The

	DF	Sum Sq	F-value	p-value
C1	1	47.9	477	$< 2.2 \times 10^{-16}$
C2	1	8.10	80.8	1.58×10^{-13}
C3	1	1.10	11.0	1.42×10^{-3}
C4	1	4.61	45.9	2.42×10^{-9}
C6	1	6.46	64.4	1.06×10^{-11}
C7	1	6.30	62.8	1.64×10^{-11}
C2:C6	1	3.24	32.3	2.42×10^{-7}
C2:C7	1	0.620	6.18	0.0151
C3:C6	1	7.12	71.0	1.83×10^{-12}
C3:C7	1	1.20	12.0	8.79×10^{-4}
C4:C7	1	0.681	6.79	0.0110

Table 5.10 Significant orthogonal contrasts of stem/leaf zinc offtake. DF: Degrees of freedom. Expanded version see Table 7.14

	DF	Sum Sq	F-value	p-value
C1	1	0.0190	54.3	1.88×10^{-10}
C3	1	0.0256	73.0	1.11×10^{-12}
C4	1	3.63×10^{-3}	10.4	1.91×10^{-3}
C7	1	9.79×10^{-3}	27.9	1.19×10^{-6}

Table 5.11 Significant orthogonal contrasts of grain zinc offtake. DF: Degrees of freedom. Expanded version see Table 7.15

	DF	Sum Sq	F-value	p-value
C1	1	0.0393	28.9	8.28×10^{-7}
C2	1	0.0216	15.9	1.54×10^{-4}
C3	1	0.105	76.9	4.11×10^{-13}
C4	1	0.0490	36.0	6.42×10^{-8}
C6	1	0.125	91.9	1.14×10^{-14}
C3:C6	1	0.0927	68.2	3.89×10^{-12}
C4:C6	1	0.0166	12.2	7.94×10^{-4}

Table 5.12 Significant orthogonal contrasts of root zinc offtake (Zn_{offtake}). DF: Degrees of freedom. Expanded version see Table 7.16

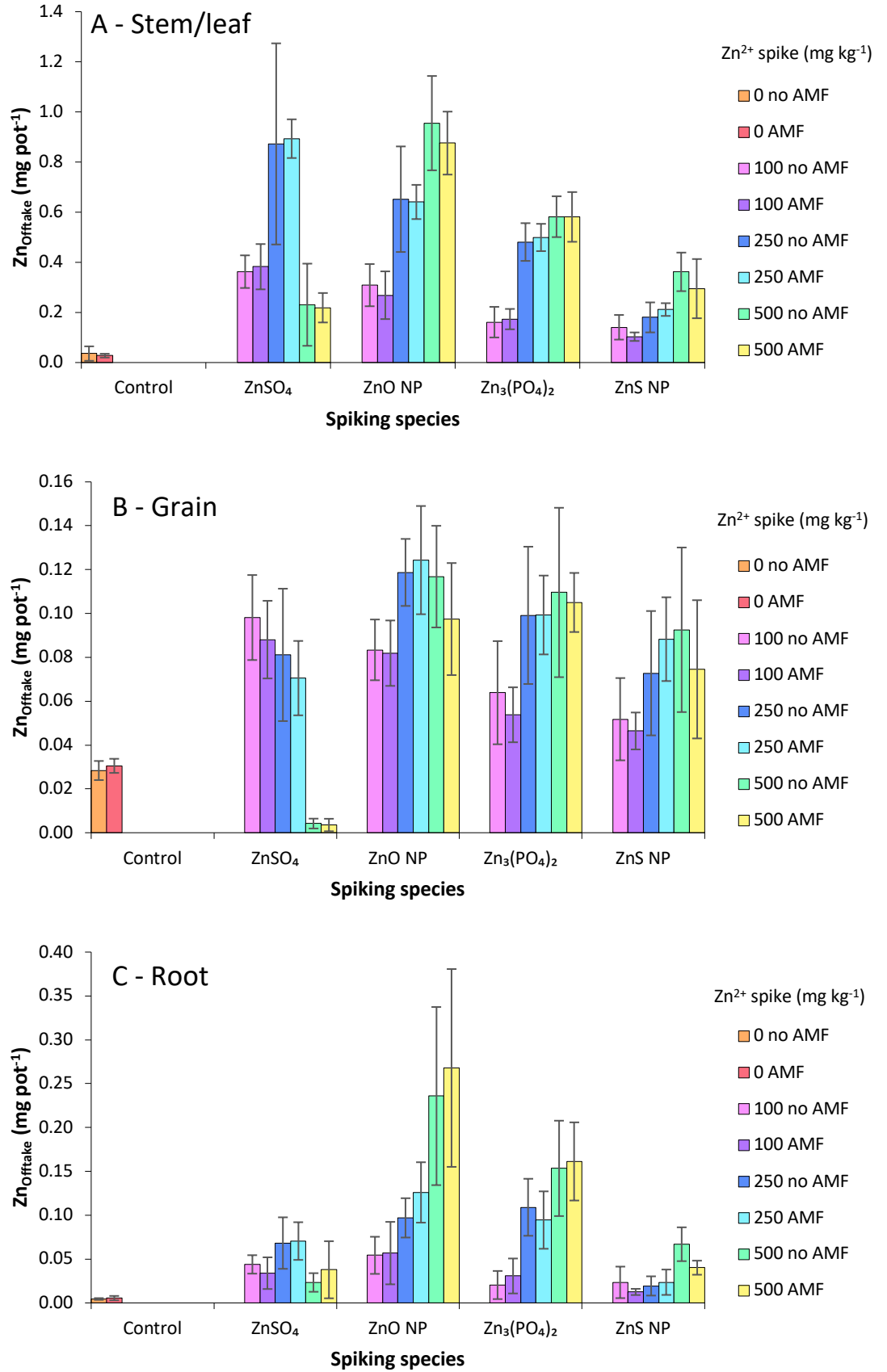


Figure 5.11 Average zinc off-take ($Zn_{Offtake}$) of harvested wheat. A - stem/leaf; B - grain; C - root. Bars show standard deviation of the four replications of each sample.

Zn_{Offtake} of stem/leaf, grain and roots were significantly different between control samples and all other applied zinc species samples, between $ZnSO_4$ and ZnO NPs spiked samples and between $Zn_3(PO_4)_2$ and ZnS NPs spiked samples (**Tables 5.10, 5.11 and 5.12**). Zn_{Offtake} was not found to be correlated to % AMF colonisation.

5.3.9 Soil pH

Prior to the experiment being set up the soil pH was 6.59. The soil pH of all sample species was reduced over the growth period; the 500 mg kg^{-1} $ZnSO_4$ spike concentration produced the greatest fall in pH whereas the 500 mg kg^{-1} ZnO NP spike produced the smallest reduction in pH (**Figure 5.12**). The $ZnSO_4$ and ZnO NP spiked samples show predictable trends in pH; the $ZnSO_4$ spiked treatments show a decline in pH due to $Zn^{2+} - H^+$ exchange on soil humus and oxide surfaces, whereas the ZnO NP treatments show a rise in pH because the ZnO NP oxygen neutralises H^+ . It is possible that the lack of any noticeable pH effects with the ZnS NP and $Zn_3(PO_4)_2$ spiked samples was due to their low solubility.

AMF colonisation was not found to affect pH. In contrast, Bi et al. [366] looked at the influence of AMF on zinc uptake in red clover and found that, at the end of the experiment, soil pH was higher in AMF-treated samples than in controls but that soil pH decreased with increasing zinc application rate. It was suggested that this could affect plant zinc uptake by altering soil zinc availability.

The soil pH after harvest was significantly different between $ZnSO_4$ vs ZnO NPs spiked samples and between $Zn_3(PO_4)_2$ and ZnS NPs spiked samples (**Table 5.13**). Plotting soil pH against grain Zn_{Offtake} shows a slight positive correlation (**Figure 5.13**). However, a modest effect is to be expected because although lower pH increases zinc solubility [373], it also increases H^+ competition with Zn^{2+} on root surfaces, potentially causing two opposing effects. Hough et al. [311] found that the transfer of zinc from soil solution

	DF	Sum Sq	F-value	p-value
C3	1	1.02	148	$< 2.2 \times 10^{-16}$
C4	1	0.030	4.39	0.0396
C6	1	0.0212	3.09	0.0827
C3:C6	1	0.414	60.6	3.09×10^{-11}

Table 5.13 Significant orthogonal contrasts of soil pH. DF: Degrees of freedom. Expanded version see Table 7.17

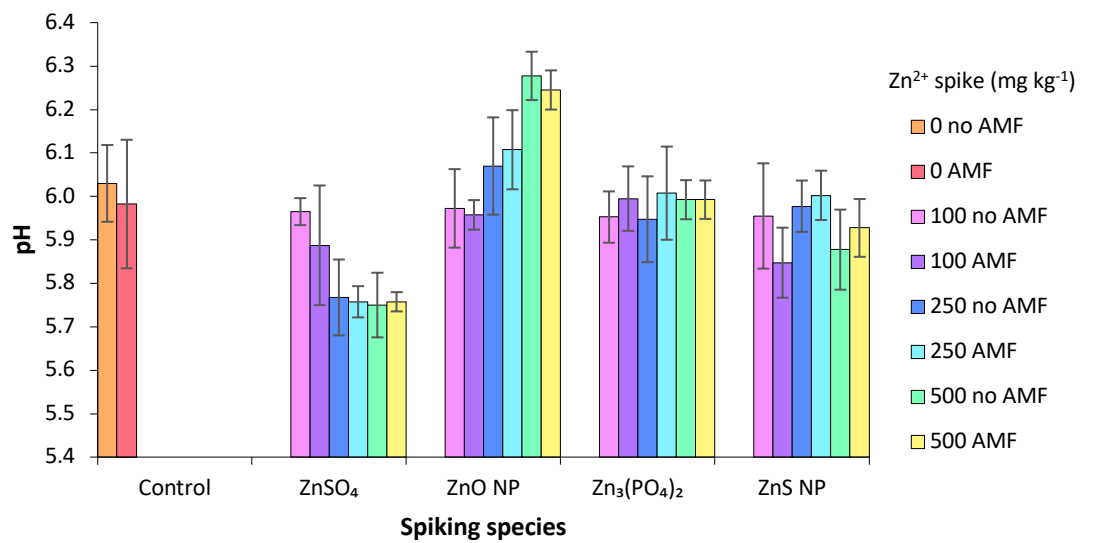


Figure 5.12 Average soil pH. Bars show standard deviation of the four replications of each sample.

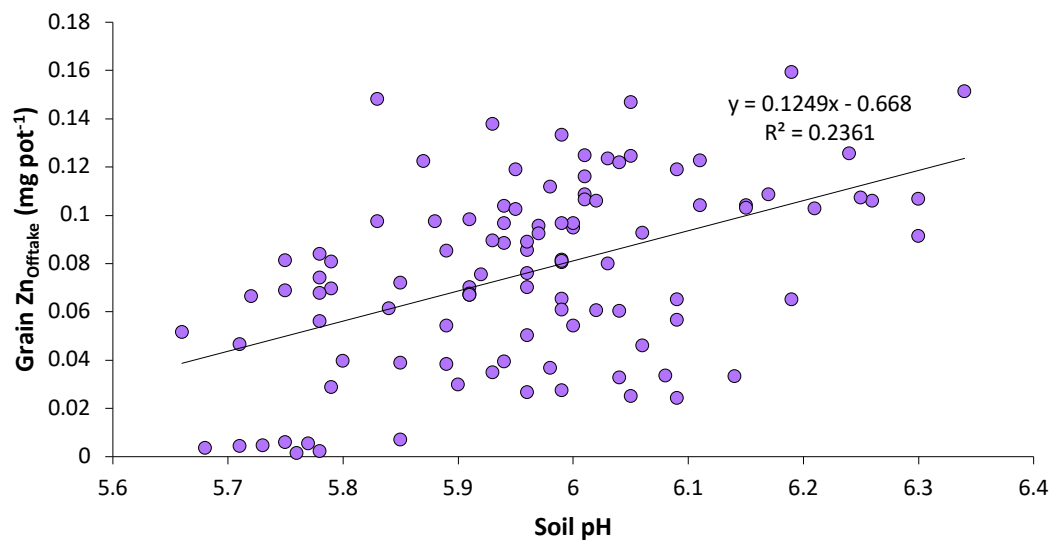


Figure 5.13 Soil pH verses grain zinc offtake (Zn_{Offtake})

	DF	Sum Sq	F-value	p-value
C1	1	100	4864	$< 2.2 \times 10^{-16}$
C2	1	20.5	995	$< 2.2 \times 10^{-16}$
C3	1	1.53	73.9	8.77×10^{-13}
C4	1	19.1	923	$< 2.2 \times 10^{-16}$
C6	1	35.5	1716	$< 2.2 \times 10^{-16}$
C7	1	3.21	155	8.19×10^{-12}
C2:C6	1	0.193	9.35	3.09×10^{-3}
C3:C6	1	0.291	14.1	3.42×10^{-4}
C3:C7	1	0.0660	3.19	0.0781
C4:C6	1	0.245	11.9	9.41×10^{-4}
C4:C7	1	1.04	50.1	6.56×10^{-10}

Table 5.14 Significant orthogonal contrasts of average available zinc (Zn_{DTPA}). DF: Degrees of freedom. Expanded version see Table 7.18

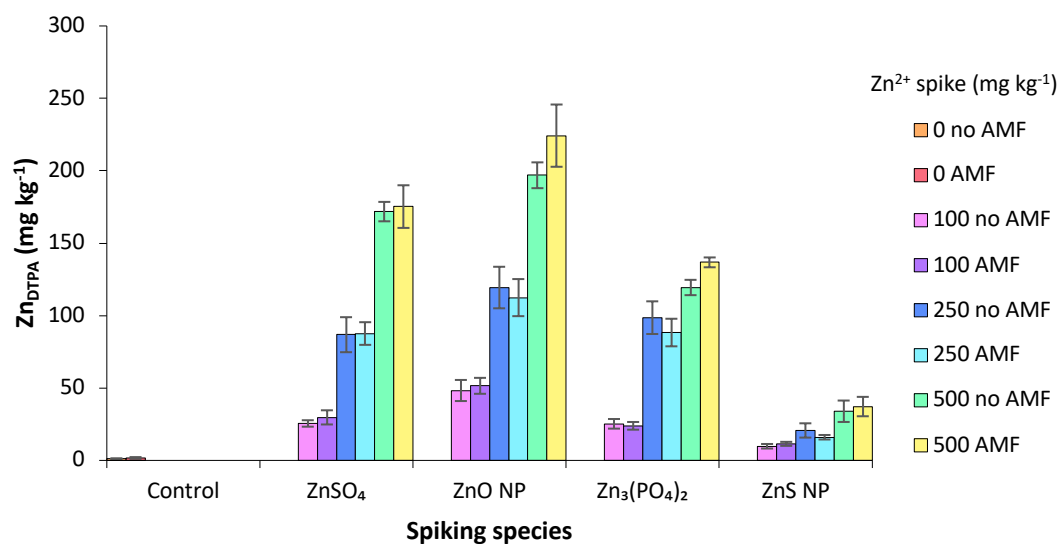


Figure 5.14 Post harvest average available zinc (Zn_{DTPA}) of soil. Bars show standard deviation of the four replications of each sample.

to plant was highly pH-dependent and suggested that this might be due to competition between trace metals and protons for sorption sites on roots but stated that it was not possible to separate the influence of pH from the effect of changing metal ion activity on uptake rate.

5.3.10 DTPA-extractable zinc in soil

The soil Zn_{DTPA} concentration was significantly different between control samples and all other applied zinc species samples, between ($ZnSO_4$ and ZnO NPs) vs ($Zn_3(PO_4)_2$ and ZnS NPs) spiked samples, between $ZnSO_4$ and ZnO NPs spiked samples and between $Zn_3(PO_4)_2$ and ZnS NPs spiked samples (**Table 5.14, Figure 5.14**). For the $ZnSO_4$ and ZnO NPs spiked samples, it is possible that the $ZnSO_4$ had longer to react with the soil and therefore allowed a greater proportion to become fixed, producing a higher solubility of zinc in the ZnO NP spiked samples. The trends shown in **Figure 5.14** between the $ZnSO_4$ and ZnO NP, and the $Zn_3(PO_4)_2$ and ZnS NP spiked treatments are to be expected considering their relative solubilities.

5.3.11 Soil *E* values

ID has been used to quantify zinc lability in soils in a variety of situations, such as following minespoil contamination [374] or in anaerobic rice-paddy fields [375], but as yet it has not been used to investigate zinc NPs. Ayoub et al. [376] used ID to see whether a hyperaccumulating plant was able to access more zinc than two other plant species in two different soils, one of which had been amended with sewage sludge. The spike amount used was based on the amount that could be extracted by 0.43 M ethanoic acid, with the aim to change the $^{66}Zn/^{67}Zn$ ratio from 6.76 to 6.10. However, this method led to the size of the labile zinc fraction in one of the soils being considerably underestimated possibly because the amount of spike introduced to the soil was too low. Other methods that have been used for estimating the amount of

stable zinc isotope spike to administer have been calculated by using one third of the EDTA-extractable zinc content of the soil [252] and the total zinc content extracted by DTPA [254].

The equilibrating electrolyte selected should ideally reflect the composition of soil pore water but also solubilise sufficient zinc to allow robust analytical measurement without extracting non-exchangeable zinc from soils. Care must be taken not to alter the soil suspension pH and release non-labile zinc or to add substances that will cause zinc to precipitate out of the solution.

Izquierdo et al. [377] looked at the use of 0.0005 M EDTA and 0.01 M $\text{Ca}(\text{NO}_3)_2$ as electrolytes and found that for soils where the zinc concentration was $< 400 \text{ mg kg}^{-1}$, 0.0005 M EDTA extracted both labile and non-labile zinc, but that 0.01 M $\text{Ca}(\text{NO}_3)_2$ could not always solubilise enough zinc to obtain accurate isotope measurements, resulting in neither electrolyte providing reliable results for three of the samples tested. However, studies using other soils have found dilute salts such as 0.01 M CaCl_2 [378, 379], 0.01 M $\text{Ca}(\text{NO}_3)_2$ [252, 380] or even just deionised water [376, 381] to be sufficiently effective.

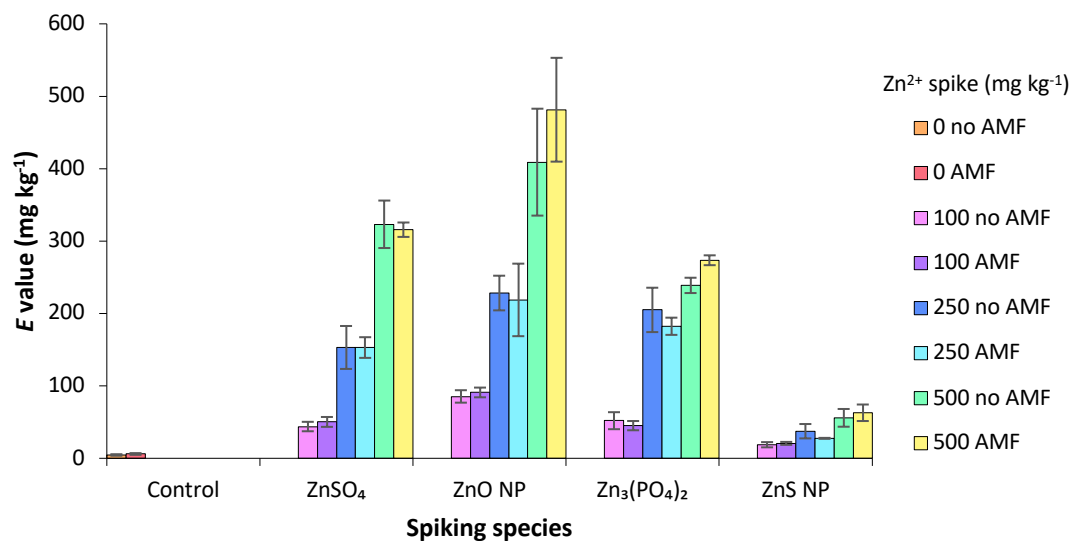


Figure 5.15 Average E value of soil. Bars show standard deviation of the four replications of each sample.

	DF	Sum Sq	F-value	p-value
C1	1	66.6	2872	$< 2.2 \times 10^{-16}$
C2	1	19.6	846	$< 2.2 \times 10^{-16}$
C3	1	2.37	102	1.23×10^{-15}
C4	1	23.3	1003	$< 2.2 \times 10^{-16}$
C6	1	37.3	1607	$< 2.2 \times 10^{-16}$
C7	1	3.41	147	$< 2.2 \times 10^{-16}$
C2:C6	1	0.603	26.0	2.48×10^{-6}
C3:C6	1	0.173	7.48	7.80×10^{-3}
C4:C6	1	0.444	19.2	3.84×10^{-5}
C3:C7	1	1.24	53.6	2.34×10^{-10}

Table 5.15 Significant orthogonal contrasts of soil *E* values. DF: Degrees of freedom. Expanded version see Table 7.19

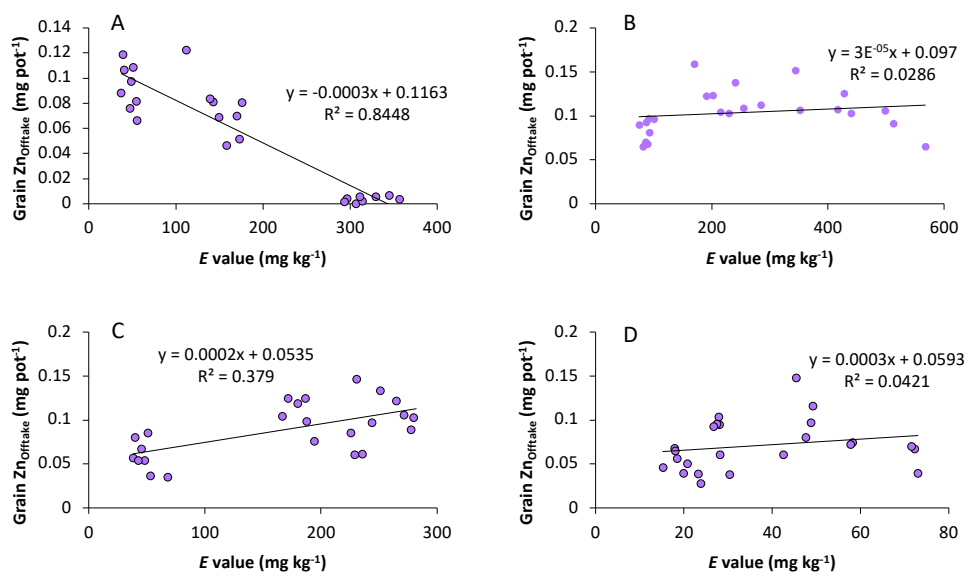


Figure 5.16 Soil *E* value vs grain zinc offtake (Zn_{Offtake}). A: $ZnSO_4$ spiked samples; B: ZnO NP spiked samples; C: $Zn_3(PO_4)_2$ spiked samples; D: ZnS NP spiked samples.

The E value of soil was significantly different between control samples and all other applied zinc species samples, between (ZnSO_4 and ZnO NPs) vs ($\text{Zn}_3(\text{PO}_4)_2$ and ZnS NPs) spiked samples, between ZnSO_4 and ZnO NPs spiked samples and between $\text{Zn}_3(\text{PO}_4)_2$ and ZnS NPs spiked samples (Table 5.15, Figure 5.15).

Plotting E values against grain $\text{Zn}_{\text{Offtake}}$ shows that, for the ZnSO_4 spiked samples, there was an inverse correlation which reflects the toxic response of wheat grown in the ZnSO_4 spiked treatment, whereas for samples spiked with the other zinc species there were slight positive correlations (Figure 5.16).

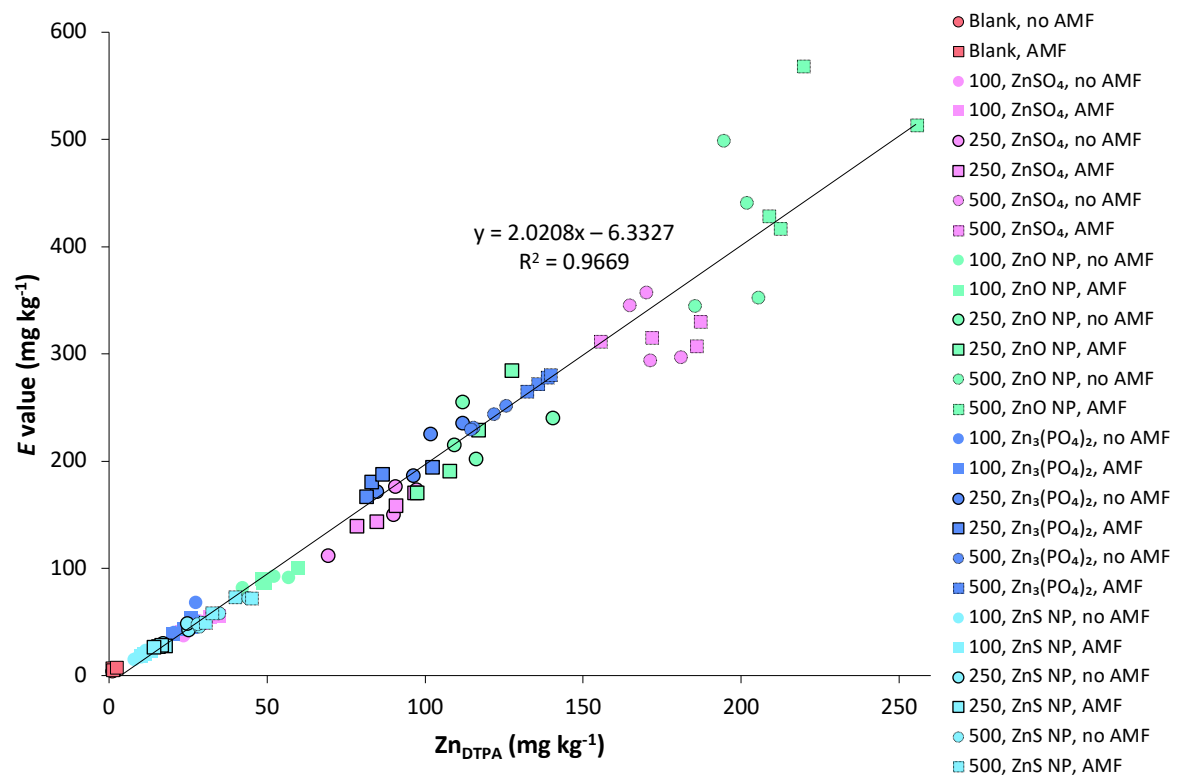


Figure 5.17 Soil E value vs soil available zinc (Zn_{DTPA})

Comparing the Zn_{DTPA} and E values shows that they are very closely correlated, with the Zn_{DTPA} estimates of the available metal concentration in the soil samples approximately half that of the E values (**Figure 5.17**). It may be that the concentration of DTPA used (0.005 M) was too low to extract all of the available zinc, however, using a higher concentration may have risked non-labile zinc to be released and intact NPs to be dissolved. The E value should only include zinc which has been released from the NPs and has joined the soil-adsorbed labile pool, and so is perhaps a better index of available zinc.

5.3.12 Biological concentration ratio

Biological concentration ratio (BCR) was calculated as plant sample Zn_{Total} concentration minus the average control plant sample Zn_{Total} divided by the soil E value (**Figure 5.18**). This showed that the ratio of zinc in grain was larger for the ZnS NP spiked samples than for the other zinc treatments. This is significant because increasing zinc transfer to grain is an important research area that has received a lot of attention [382, 383].

Wheat grain Zn_{Total} concentration currently has an approximate average value of 28 – 30 mg kg⁻¹, with the aim to increase it to 40 – 50 mg kg⁻¹ [382]. Studies have looked into achieving this in many different ways, including: enriching seeds with zinc [384-386]; the addition of biostimulants such as fulvic acid, seaweed extract and amino acids [387]; the use of green manure [388, 389]; biofortification and selective breeding of wheat cultivars [390]; and inoculation with non-indigenous AMF strains [388]. Other investigations into wheat grain zinc enhancement have explored the effect of different soil nutrients [391], sewage sludge application [392], the impact of different farming systems [393, 394], zinc application rate to soil [395] and the mode of zinc application

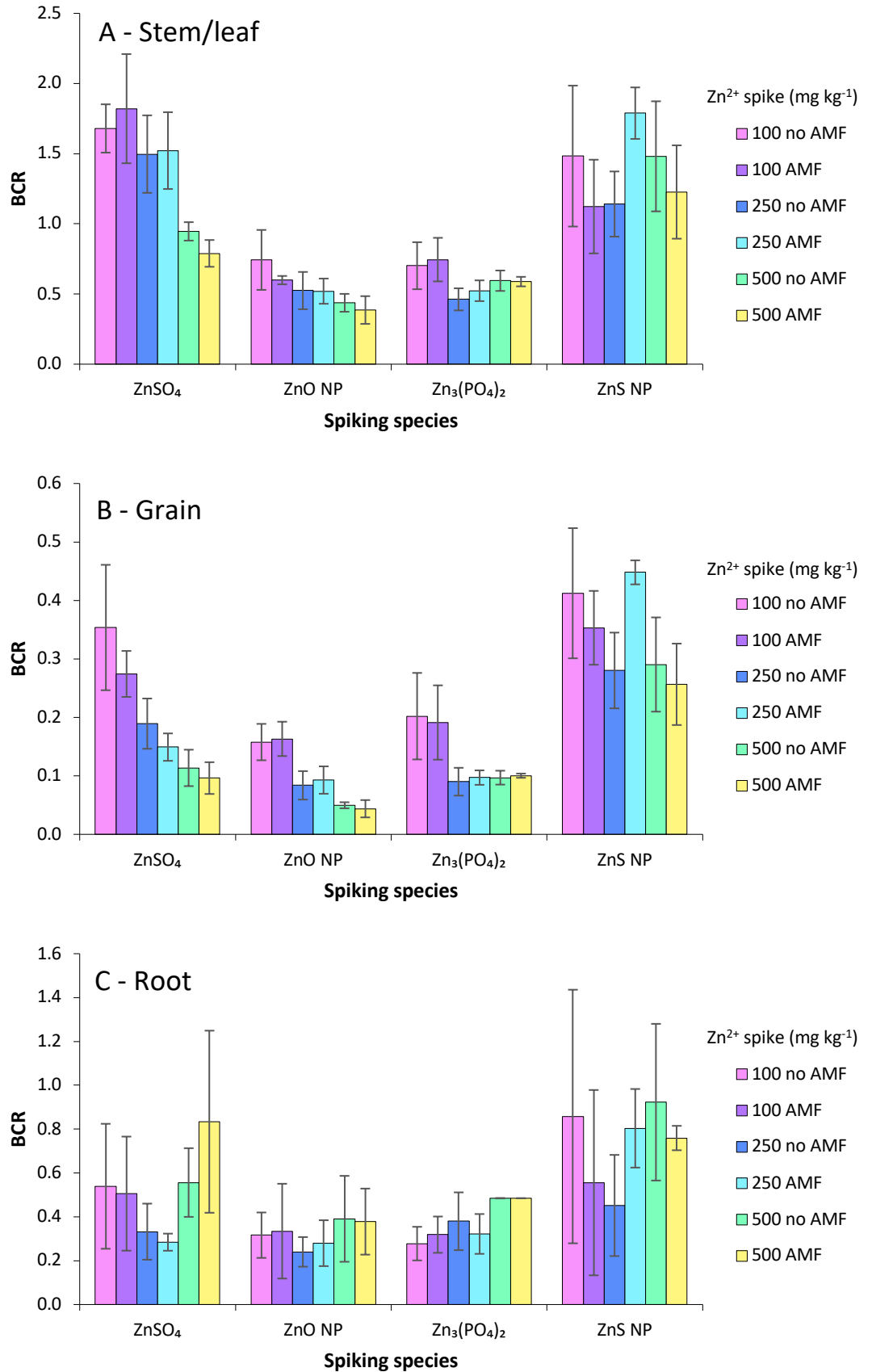


Figure 5.18 Average biological concentration ratio (BCR). A - stem/leaf; B - grain; C - root. Bars show standard deviation of the four replications of each sample.

[396-399]. Many studies have examined foliar application of zinc to enhance grain concentration, generally using ZnSO_4 as the treatment species [387, 400-404].

A disadvantage to this method is the potential for leaf damage due to the rapid release of concentrated Zn^{2+} into leaf tissues [405], although it has been suggested that plants may overcome this localised zinc toxicity by complexing Zn^{2+} with phytate in the leaves [403]. Doolette et al. investigated using ZnO NPs as an alternative foliar treatment but found that it was not as efficient as ZnEDTA at translocating applied zinc to wheat grain [405]. It has been found that increasing leaf/stem Zn_{Total} concentration is achievable, but that the subsequent transfer into grain is more strictly regulated by plants, which can result in the overuse of applied zinc and eventual toxicity to wheat plants at approximately 300 mg kg^{-1} [382]. If the application of ZnS NPs has the potential to increase the transfer of zinc to wheat grain without causing toxic side-effects to the plant, that could be of huge benefit to cereal growers.

5.4 Conclusions

This study looked at the differences in the effects of ZnS NPs, $\text{Zn}_3(\text{PO}_4)_2$ particles and ionic zinc with ZnO NPs on AMF and wheat when spiked into soil.

The BCR results shown in **Figure 5.17** suggests that the application of ZnS NPs to soils may have the ability to increase the transfer of zinc to grain. Overall, the present study indicates that ZnS NPs could potentially provide a long-term supply of zinc that supports the biofortification of cereal grains while also avoiding issues of toxicity with ZnSO_4 or ZnO NP fertilisers. However, for this to be successful, an appropriate application method would need to be developed and risk assessments would need to be generated.

Figure 5.9 shows that in all cases the addition of AMF to soil resulted in roughly doubling the % root colonisation. There was more variability in the amount of root

colonisation in plants treated with ZnO NPs than in the other species or the control but it is not clear what the reason for this is. The % root colonisation across all species ranged from 6 – 72%. While there were distinct differences in plant zinc concentration between different spiking species and different concentrations, there was no evidence that the differences between AMF root colonisation % had any effect. Since it has been established that AMF root colonisation plays an important role in plants' uptake of zinc [343], this could suggest that there is a very low threshold level of root colonisation which will enable plants to acquire the zinc they need as long as it is present in the soil. The anomalous results for samples spiked with ZnSO₄ at 500 mg kg⁻¹ of zinc were due to the toxicity to plants at high concentration.

There have been studies that have shown AMF inoculation to increase plant zinc uptake [359-363], however, there have also been studies indicating the opposite [364-366] or finding no effect at all [406]. Large scale meta analyses have had similarly conflicting results, with one reporting that AMF increases plant zinc concentration [367] and another finding no effect [368]. These differences could be due to the attention of the studies, with the one finding an increase solely focusing on plant zinc concentration and the one finding no increase in zinc uptake investigating many aspects of plant health. Perhaps the variety of results is indicative of the myriad subtle functions and relationships that are inadvertently being investigated. It has been shown that AMF can shift from increasing plant zinc concentration in low soil zinc conditions, to protecting plants from toxic zinc levels in high soil zinc conditions [352, 357, 358, 366]. It is becoming clear that the interdependency of plants and AMF means that understanding the effects of NPs on plant-AMF systems will require plant and fungal reactions to be considered conjointly.

Chapter 6

Conclusions and next steps for understanding zinc nanoparticle behaviour in soils

6.1 Current issues and project conclusions

The present project has highlighted many factors concerning zinc NPs in soil environments. A large pool of literature assessing the environmental fate and toxicity of zinc NPs in the environment has begun to develop. However, the bulk of this literature has been focused on the short-term behaviour of high concentrations of pristine ZnO NPs in simplified media. These experimental issues are generally a result of the lack of viable methods that allow aged zinc NPs to be detected and analysed under realistic environmental conditions. Chapter 3 illustrates some of the difficulties associated with working with zinc NPs which partly explain why this work is still ongoing. Analytical techniques that could potentially be useful such as SEC and dialysis need to be developed to overcome the issues that NPs pose for them to become used routinely. The need for standardised analytical techniques and methods for characterising NPs in complex media like soils means that implementation of regulatory safety procedures such as product labelling and risk assessment are currently very challenging [407]. At the time of writing, there are still no definitive internationally agreed definitions for nanotechnologies [408], standardised protocols for evaluating toxicity and environmental impact of NPs or certified standard zinc NP reference materials [409].

Chapter 3 determined that NPs can exhibit different behaviours in different solutions and can readily adsorb to equipment surfaces. It is therefore critically important to check the stability of a NP sample in the test matrices. Similarly, Pradhan et al. [67] found that measuring NP concentration in each individual sample is necessary because unpredictable disaggregation can cause NP concentration to be significantly lower than expected. The present study also found that SEC suffered severely from zinc NP column adsorption which persisted despite many attempts to rectify the issue. For SEC

to become a viable technique for monitoring zinc NP behaviour, a great deal more method development would need to be undertaken. Attempts to use dialysis experienced similar issues. Dialysis has the potential to be a useful way of monitoring zinc NP dissolution, but NP adsorption to tubing and equipment prevented the present study from accomplishing this.

Chapter 4 investigated the different behaviours of ZnO NPs, ZnSO₄, ZnS NPs and Zn₃(PO₄)₂ in soil and ryegrass. Pristine ZnO NPs were shown to dissolve quickly in soil and followed a similar pattern to ZnSO₄ for Zn_{DTPA}, but sequential fractionation results revealed that they behaved differently to ZnSO₄. ZnO NPs also reacted differently to aged ZnS NP and Zn₃(PO₄)₂ particles, which did dissolve, but very slowly. This experiment indicated that ZnS NPs could potentially be safe for crops while still providing nutrition, which would make them useful as a potential method of fertilisation. It also highlighted that it is not applicable to test ZnO NPs and subsequently apply the results to aged particles. Studies using ZnO NPs are likely to observe fast NP dissolution and high zinc availability, potentially leading to concerns over zinc toxicity that may not have been raised if appropriately aged particles had been used instead.

Chapter 5 examined the same four zinc species with AMF and wheat. Results suggested that ZnS NPs could potentially provide a long-term supply of zinc that supports the biofortification of cereal grains while also avoiding issues of toxicity that can be associated with ZnSO₄ or ZnO NP fertilisers. Concerning AMF, no evidence was found that AMF root colonisation % had any effect on plant biomass or zinc uptake. All plants were colonised whether they were spiked with AMF or not which could suggest that there is a very low threshold level of root colonisation which can enable plants to acquire the zinc they need as long as it is present in the soil. A holistic understanding

of fungal ecology suggests that fungi are likely keystone species in all habitats and nutrient cycles [410] and that the relationships between plants and AMF are fundamental to the functioning of ecosystems [411]. Despite this, mycology is a greatly underexamined discipline; fungi are predicted to outnumber plants at a ratio of at least 6 to 1 but only a tiny fraction of species have been identified [412]. What is understood is that AMF are critical for plant, animal and soil health [410], and so much more research is needed to discover what the environmental impacts of NPs on AMF are.

6.2 New avenues for future research

Alongside the experimental variables described in section 1.4, there are a number of unexplored areas of NP research that require future investigation.

6.2.1 Long term low dose exposures

As this thesis has highlighted, there is a need for soil-based experiments using low doses of NP spike concentration ranges that cover relevant environmental levels. Aged/relevant species need to be used and time scales need to be extended. Typically, short-term toxicity tests are used for the ecological hazard assessments of bulk pollutants. Many studies have looked at acute NP toxicity in a wide range of species and NP fate hours and days after introduction into soil, but there has been very little research into long-term chronic toxicity and NP fate over periods of months and years. Processes such as dissolution, aggregation/agglomeration and adsorption which affect NP bioavailability and toxicity in soils in the short-term, could also greatly affect long-term bioavailability, toxicity and bioaccumulation by supplying the soil solution with a steady slow flow of dissolved ions and/or particles. Of the few studies that have looked at NPs in soil over an extended time period, silver NP toxicity to earthworms was shown to increase [188] whereas ZnO NP toxicity to *F. candida* was found to reduce [116] over the course of a year. Both of these studies introduced pristine particles into

soil so extending these experiments using aged particles as a starting point would be a useful progression.

6.2.2 Poly nanoparticle systems

The mechanistic modelling of NP homoaggregation and heteroaggregation in environmental waters has indicated that homoaggregation may not contribute to the NPs' overall fate, due to their presence at such low concentrations [142]. Instead it may be heteroaggregation between the naturally occurring colloids and the combination of NPs present that dominates.

While many studies look at a number of different NPs, they are rarely looked at in combination with one another. Joško et al. [413] assessed the toxicity of mixtures of NPs on 4 different plant species and found that ZnO NPs were considerably more phytotoxic when administered alone than in mixtures containing other NPs. Zinc NPs are likely to come into contact with multiple other species of NPs and pollutants in biosolids and elsewhere in the environment, potentially resulting in many co-contaminant effects, so this is an area that requires further investigation.

6.2.3 Different soil types

It is known that for bulk ZnO and ZnS, the long-term speciation of zinc is strongly influenced by soil type [105] and it has been shown that ZnO NPs inhibit plant root growth [414] and soil enzyme activity [122] differently depending on soil type. However, studies using multiple soil types are currently very rare and future investigations are needed in order to determine the effect that soil type has on zinc NP behaviour.

6.2.4 Trans-generational transfer

It is possible that zinc NPs may be taken up by plants and translocated to seeds [141, 415]. So far, the long-term impacts on seed integrity and food safety across plant

generations have not been studied. Investigating any potential trans-generational effects in progeny produced from plants exposed to zinc NPs is another area that requires development.

6.2.5 Trophic transfer

The potential trophic transfer of NPs within terrestrial food webs is one of the least examined aspects of NP fate and behaviour [416]. Lammel et al. [417] exposed worms to sediment spiked with $^{65}\text{CuCl}_2$ or ^{65}CuO NPs at environmentally relevant concentrations and subsequently fed them to fish. It was found that worms accumulated ^{65}Cu but that ^{65}Cu accumulation in fish was limited. The trophic transfer of some metal NPs from soils to plants to insects or animals has been explored [418-421]. As yet this has not included zinc NPs, although, trophic transfer of ZnO NPs from crustaceans to zebrafish has been investigated [422]. The potential bioaccumulation of zinc NPs in food webs is an important area that requires attention.

6.3 Promising analytical techniques

6.3.1 Field flow fractionation

Field-flow fractionation (FFF) is the sequential separation of analytes in a mobile phase pumped through a long and narrow channel, with a force field applied in a perpendicular direction [423]. Many different fields can be used, including, hydraulic where an asymmetrical flow (AF4) is applied through a semi-permeable membrane, gravitational, centrifugal, thermal, electrical or magnetic. The separation mechanism is based on the laminar flow of particles in a solution and produced by size-dependent differences in particle mobility in the applied force field (**Figure 6.1**). FFF has a very wide analytical range, allowing separation of particles and dissolved molecules in a single run [423]. Fractions can be collected for offline processing but it is also possible

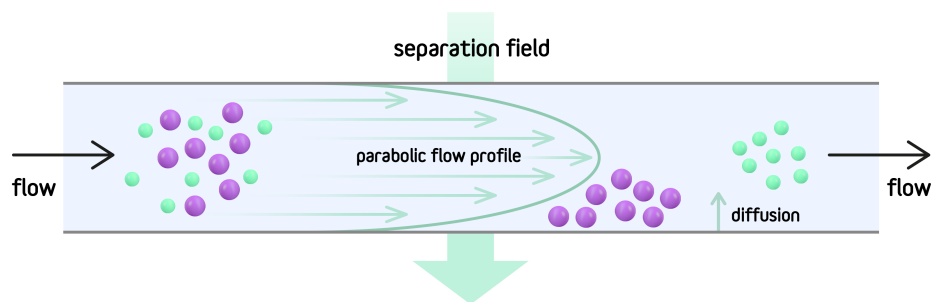


Figure 6.1 Field Flow Fractionation (FFF). Source: author

to hyphenate to many different online detectors, including multi-angle light scattering, DLS, UV-Vis spectrophotometry and fluorescence detectors. For elemental analysis, coupling with ICP-MS is possible as well [424].

FFF is particularly suited to analysing environmental samples containing aggregates and fragile analytes due to the lack of a stationary phase [425] and therefore does not suffer from analyte adsorption as with SEC. AF4 has been used to measure ZnO NP size distribution in soil suspensions [126] and environmental water samples [426]. Jang et al. [427] used AF4 coupled with UV-Vis to characterise silver NPs in natural waters. The effects of organic matter on NP size and stability were evaluated and it was found that stability and hydrodynamic diameter increased with increasing concentration of HA, suggesting that HA was adsorbed onto the NP surface.

FFF-ICP-MS could offer a promising analytical approach to carry out some of the analysis attempted in chapter 3, however, their scarce availability in environmental research labs [425] means that it was not possible to attempt this for the present project.

6.3.2 Single particle ICP-MS

Single particle (sp) ICP-MS is a mode of ICP-MS operation that has recently been demonstrated to be a potentially very useful tool for NP analysis [428-432]. As the name suggests, single particles are analysed individually rather than as a cluster as in conventional ICP-MS analysis. Ideally, sp ICP-MS data is collected in fast continuous acquisition mode where dwell time is set at a high enough speed so that multiple points can be measured from a single particle and there is no settling time, meaning no particles are missed (**Figure 6.2**). Various studies have been carried out to look into optimising sp ICP-MS parameters [433-440] and when accurate data is obtained it is possible to use sp ICP-MS for NP characterisation at low concentrations [211] and in place of other characterisation techniques [441]. For example, the particle concentration can be determined directly from the number of peaks per second and the flow rate if the sample is introduced via a monodisperse droplet generator. More common is sample introduction via a pneumatic nebuliser. In this case, if the nebuliser efficiency is known or can be calibrated, then the particle concentration of the sample can be determined from the number of pulses over time. NP size can also be determined if the particle composition and geometry are known [438]. Short run times mean that another advantage of sp ICP-MS analysis is that data is acquired much faster than with other characterisation techniques [211, 442].

Hineman et al. [437] used a PerkinElmer NexION to carry out sp ICP-MS on gold NPs to test the effect altering dwell times had on the spectra and reported that in order to obtain reliable information the dwell time must be ≤ 0.1 ms. Despite this, many sp ICP-MS dwell times reported in literature are 3 – 10 ms long [428, 435, 438, 439, 441]. It was also predicted that any dwell times ≥ 0.5 ms would result in ≥ 10 % of the resulting data being due to coincidences. The consequence of which would result in NP sizes

being recorded as larger and NP number being recorded as lower than they actually are (Figure 6.2).

The sp ICP-MS size detection limits for 40 different elements were assessed [443] and the values were found to vary considerably depending on the element, with zinc reported to be around 70 nm. Reed et al. found that rapid dissolution of ZnO NPs in deionised water meant that sp ICP-MS analysis was not possible [442], however, a subsequent study characterised and quantified ZnO NPs using sp ICP-MS by coupling the instrument to an ion exchange column [221]. For nanoparticles that undergo dissolution, removing the ionic fraction has been shown to lower the sp ICP-MS particle size detection limit and increase repeatability [221, 440, 444]. This led to Frechette-Viens et al. recommending the following approach to NP quantification by sp ICP-MS [440]:

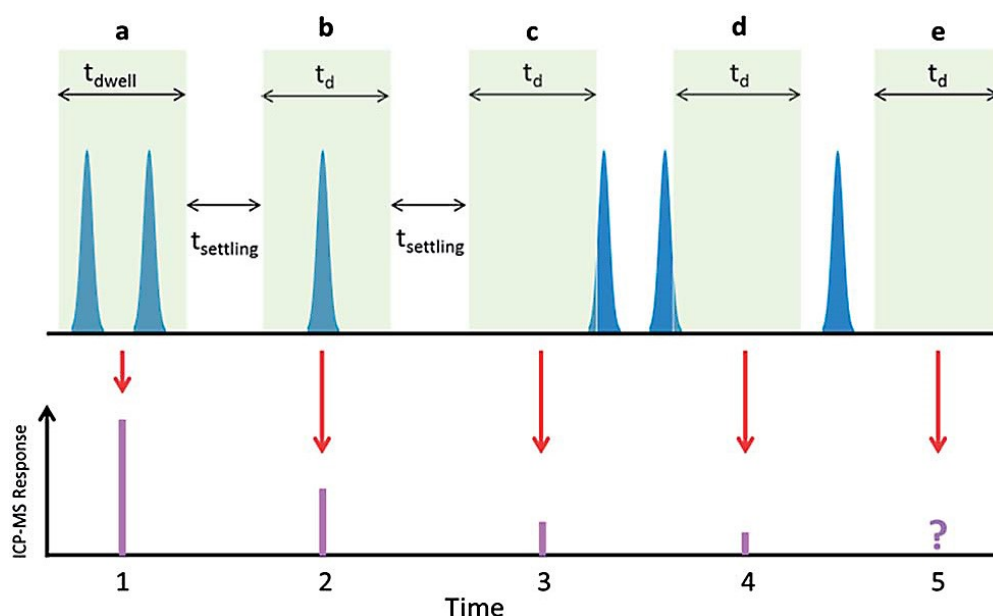


Figure 6.2. Single particle ICP-MS – effect of dwell and settling times. From [437]. a: Dwell time is too long. More than one particle is detected. Recorded as one large particle; b: Ideal; c and d: Settling time is too long. Particle partially detected. Recorded as small particle; e: Settling time is too long. Particle not detected.

“(i) measure the concentration and size distribution of the NP using sp ICP-MS coupled to an ion exchange resin; (ii) quantify the total concentration of the metal following acidification/digestion; (iii) determine the concentration of the dissolved metal by difference.”

sp ICP-MS is usually carried out with Q analysers [435, 437-439, 441, 443, 444], although typical Q-based MS instruments do not have detection electronics that are designed to measure at fast enough speeds. It is possible to carry out sp ICP-MS with SF instruments [428, 445] with size limits of detection reported to be much lower when compared with Q-based instruments [428].

6.3.3 Multi collector ICP-MS

High precision isotopic ratio measurements with multiple collector (MC) ICP-MS using SF-based MS and several detectors gives high analytical sensitivity and low limits of detection so that small isotope ratio differences can be resolved. This allows cheaper zinc stable isotope tracers to be used and in smaller quantities which reduces the cost of analyses. It also enables the detection of more than one isotope at the same time rather than with single collector SF-based or Q-based ICP-MS where ions are monitored sequentially [446].

MC ICP-MS has been used to determine that small amounts of zinc from topically applied suncreams containing ZnO NPs are absorbed through the skin and transfer to the blood and urine [249, 447, 448]. The technique has also been used to discover that ionic zinc from ZnO NPs is ingested by mudshrimp [214] and Estuarine snails [449] mainly via adsorption on sediment particles.

The use of MC ICP-MS and isotopically labelled ^{68}ZnO NPs allowed Laycock et al. [144] to track the uptake routes and rates of ZnO NP added to soil at 5 mg kg^{-1} into earthworms. This concentration is considerably lower than previous studies have been

able to trace [195, 450] and emphasises that it is possible to study environmentally realistic concentrations if the analytical techniques and instruments used are sensitive and specific enough for the analyte under observation.

MC ICP-MS was also used in combination with a technique where a ^{64}Zn - ^{67}Zn double spike was added to soil samples and then extracted with a mild acid in order to estimate the isotopic pool of plant-available zinc [182].

6.4 Overall Conclusions

The aim of this thesis was to enhance knowledge about the application of biosolids containing zinc NPs onto soils and despite a number of setbacks, this has been achieved. The aims to develop methods for sampling zinc NP-spiked soil pore waters using dialysis and monitoring zinc NPs with humic acid using SEC proved unsuccessful, however the experiments provided insight into the handling of zinc NPs, and this could support future research into the separation of zinc NPs from complex mediums.

The experiments using grass and wheat with zinc NPs gave some interesting results. ZnO NPs were shown to follow similar patterns as ionic ZnSO_4 in some capacities but not in others. Pristine ZnO NPs demonstrated very different patterns to aged ZnS NPs and $\text{Zn}_3(\text{PO}_4)_2$. Indications are that aged ZnS NPs and $\text{Zn}_3(\text{PO}_4)_2$ contained in biosolids are safe for soil application, and ZnS NPs may even be able to enhance the proportion of zinc taken into wheat grain. Although this thesis was not able to draw any new understanding concerning AMF, it is clear that AMF need to be considered in future investigations into plant–NP systems. As stated by Lynn Margulis [451]:

“The idea of species itself requires symbiosis.....Symbiosis is not a marginal or rare phenomenon. It is natural and common. We abide in a symbiotic world”

It therefore follows that the future of research into the impact of NPs on the environment needs to recognise that there is little hope of success for an approach that focusses in or attempts to isolate particular processes or substances and that in order to gain an understanding of the dynamics involved it must utilise a variety of analytical techniques and take a holistic approach.

References

1. Center for responsible nanotechnology. *What is nanotechnology?* 2008 [cited 2020 16/03]; Available from: <http://www.crnano.org/whatis.htm>.
2. Bleeker, E.A.J., et al., *Considerations on the EU definition of a nanomaterial: science to support policy making*. Regulatory Toxicology and Pharmacology, 2013. **65**(1): p. 119-125.
3. Boholm, M. and R. Arvidsson, *A definition framework for the terms nanomaterial and nanoparticle*. NanoEthics, 2016. **10**(1): p. 25-40.
4. Boverhof, D.R., et al., *Comparative assessment of nanomaterial definitions and safety evaluation considerations*. Regulatory Toxicology and Pharmacology, 2015. **73**(1): p. 137-150.
5. EC, *Commission recommendation on the definition of nanomaterial*. 2011, Official Journal of the European Union.
6. Lövestam, G., et al., *Considerations on a definition of nanomaterial for regulatory purposes*. Joint Research Centre Reference Reports, 2010.
7. Maynard, A.D., *Don't define nanomaterials*. Nature, 2011. **475**(7354): p. 31-31.
8. Jurewicz, M., *Controversy around the definition of nanomaterial in European Union law*. CHEMIK, 2014. **68**(12): p. 1090-1095.
9. Auffan, M., et al., *Towards a definition of inorganic nanoparticles from an environmental, health and safety perspective*. Nature Nanotechnology, 2009. **4**(10): p. 634-641.
10. Handy, R.D., et al., *The ecotoxicology and chemistry of manufactured nanoparticles*. Ecotoxicology, 2008. **17**(4): p. 287-314.
11. Höck, J., et al., *Guidelines on the precautionary matrix for synthetic nanomaterials*, 2008, Federal Office for Public Health, Federal Office for the Environment: Berne. p. 1 - 26.
12. House of Lords, *Nanotechnologies and food*, S.a.t. committee, Editor. 2010, House of Lords.
13. The Royal Society, *Nanoscience and nanotechnologies: opportunities and uncertainties*. 2004, The Royal Society: London. p. 1 - 127.
14. Kreyling, W.G., M. Semmler-Behnke, and Q. Chaudhry, *A complementary definition of nanomaterial*. Nano Today, 2010. **5**(3): p. 165-168.
15. Royal Academy of Engineering, *Nanoscience and nanotechnologies: opportunities and uncertainties*. 2004, Royal Society. p. 116.
16. Baalousha, M., et al., *The concentration-dependent behaviour of nanoparticles*. Environmental Chemistry, 2016. **13**(1): p. 1-3.
17. Misra, S.K., et al., *The complexity of nanoparticle dissolution and its importance in nanotoxicological studies*. Science of the Total Environment, 2012. **438**: p. 225-232.
18. Jiang, W., H. Mashayekhi, and B. Xing, *Bacterial toxicity comparison between nano- and micro-scaled oxide particles*. Environmental Pollution, 2009. **157**(5): p. 1619-1625.
19. Nagarajan, P. and V. Rajagopalan, *Enhanced bioactivity of ZnO nanoparticles - an anti-microbial study*. Science and Technology of Advanced Materials, 2008. **9**(3).
20. Rajendran, R., et al., *Use of zinc oxide nano particles for production of antimicrobial textiles*. International Journal of Engineering, Science and Technology, 2010. **2**: p. 202-208.

21. Subash, A.A., et al., *Preparation, characterization, and functional analysis of zinc oxide nanoparticle-coated cotton fabric for antibacterial efficacy*. The Journal of The Textile Institute, 2012. **103**(3): p. 298-303.
22. Chattopadhyay, D.P. and B.H. Patel, *Modification of cotton textiles with nanostructural zinc particles*. Journal of Natural Fibers, 2011. **8**(1): p. 39-47.
23. Rathnayake, W.G.I.U., et al., *Enhancement of the antibacterial activity of natural rubber latex foam by the incorporation of zinc oxide nanoparticles*. Journal of Applied Polymer Science, 2014. **131**(1)
24. Khan, S.T., A.A. Al-Khedhairi, and J. Musarrat, *ZnO and TiO₂ nanoparticles as novel antimicrobial agents for oral hygiene: a review*. Journal of Nanoparticle Research, 2015. **17**(6).
25. Espitia, P.J.P., et al., *Zinc oxide nanoparticles: synthesis, antimicrobial activity and food packaging applications*. Food and Bioprocess Technology, 2012. **5**(5): p. 1447-1464.
26. Tankhiwale, R. and S.K. Bajpai, *Preparation, characterization and antibacterial applications of ZnO-nanoparticles coated polyethylene films for food packaging*. Colloids and Surfaces B: Biointerfaces, 2012. **90**(Supplement C): p. 16-20.
27. Goh, E.G., X. Xu, and P.G. McCormick, *Effect of particle size on the UV absorbance of zinc oxide nanoparticles*. Scripta Materialia, 2014. **78–79**: p. 49-52.
28. Joni, I.M., et al., *Intense UV-light absorption of ZnO nanoparticles prepared using a pulse combustion-spray pyrolysis method*. Chemical Engineering Journal, 2009. **155**(1-2): p. 433-441.
29. Kessler, R., *Engineered nanoparticles in consumer products: understanding a new ingredient*. Environmental Health Perspectives, 2011. **119**(3): p. 120-125.
30. Project on emerging nanotechnologies. *Consumer products inventory*. 2013 [cited 2020 18/03]; Available from: <http://www.nanotechproject.org/cpi/>.
31. The Nanodatabase. *Search the nanodatabase*. 2013 [cited 2020 18/03]; Available from: <http://nanodb.dk/en/>.
32. Gondikas, A.P., et al., *Release of TiO₂ nanoparticles from sunscreens into surface waters: a one-year survey at the old Danube recreational Lake*. Environmental Science and Technology, 2014. **48**(10): p. 5415-5422.
33. Singh, N.B., et al., *Zinc oxide nanoparticles as fertilizer for the germination, growth and metabolism of vegetable crops*. Journal of Nanoengineering and Nanomanufacturing, 2013. **3**(4): p. 353-364.
34. Sabir, S., M. Arshad, and S.K. Chaudhari, *Zinc oxide nanoparticles for revolutionizing agriculture: synthesis and applications*. The Scientific World Journal, 2014. **2014**:
35. Bolyard, S.C., D.R. Reinhart, and S. Santra, *Behavior of engineered nanoparticles in landfill leachate*. Environmental Science and Technology, 2013. **47**(15): p. 8114-8122.
36. Sakallioğlu, T., et al., *Leaching of nano-ZnO in municipal solid waste*. Journal of Hazardous Materials, 2016. **317**: p. 319-326.
37. Som, C., et al., *Environmental and health effects of nanomaterials in nanotextiles and facade coatings*. Environ Int, 2011. **37**(6): p. 1131-1142.
38. Westerhoff, P.K., A. Kiser, and K. Hristovski, *Nanomaterial removal and transformation during biological wastewater treatment*. Environmental Engineering Science, 2013. **30**(3): p. 109-117.
39. Lombi, E., et al., *Fate of zinc oxide nanoparticles during anaerobic digestion of wastewater and post-treatment processing of sewage sludge*. Environmental science and technology, 2012. **46**(16): p. 9089-9096.

40. Ma, R., et al., *Fate of zinc oxide and silver nanoparticles in a pilot wastewater treatment plant and in processed biosolids*. Environmental science and technology, 2014. **48**(1): p. 104-112.
41. Brunetti, G., et al., *Fate of zinc and silver engineered nanoparticles in sewerage networks*. Water Research, 2015. **77**: p. 72-84.
42. Kim, B., et al., *Integrated approaches of x-ray absorption spectroscopic and electron microscopic techniques on zinc speciation and characterization in a final sewage sludge product*. Journal of environmental quality, 2014. **43**(3): p. 908-916.
43. Garcia-Gomez, C., M.D. Fernandez, and M. Babin, *Ecotoxicological evaluation of sewage sludge contaminated with zinc oxide nanoparticles*. Archives of Environmental Contamination and Toxicology, 2014. **67**(4): p. 494-506.
44. Gottschalk, F., et al., *Modeled environmental concentrations of engineered nanomaterials (TiO₂, ZnO, Ag, CNT, Fullerenes) for different regions*. Environmental science and technology, 2009. **43**(24): p. 9216-9222.
45. Chai, H., et al., *The effect of metal oxide nanoparticles on functional bacteria and metabolic profiles in agricultural soil*. Bulletin of Environmental Contamination and Toxicology, 2015. **94**(4): p. 490-495.
46. Corinaldesi, C., et al., *Impact of inorganic UV filters contained in sunscreen products on tropical stony corals (Acropora spp.)*. Science of The Total Environment, 2018. **637**: p. 1279-1285.
47. Soil Association. *Organic standards food and drink*. Revision 17.5 2016 [cited 2020 22/06].
48. Lowry, G.V., et al., *Transformations of nanomaterials in the environment*. Environmental Science and Technology, 2012. **46**(13): p. 6893-6899.
49. Heidmann, I., *Metal oxide nanoparticle transport in porous media – an analysis about (un)certainities in environmental research*. Journal of Physics: Conference Series, 2013. **429**(1)
50. Nichols, G., et al., *A review of the terms agglomerate and aggregate with a recommendation for nomenclature used in powder and particle characterization*. Journal of Pharmaceutical Sciences, 2002. **91**(10): p. 2103-2109.
51. International Organization for Standardization. *Nano-objects*. Nanotechnologies 2015 [cited 2020 20/09]; Available from: <https://www.iso.org/standard/54440.html>.
52. Sokolov, S.V., et al., *Reversible or not? distinguishing agglomeration and aggregation at the nanoscale*. Analytical Chemistry, 2015. **87**(19): p. 10033-10039.
53. Chung, S.J., et al., *Characterization of ZnO nanoparticle suspension in water: effectiveness of ultrasonic dispersion*. Powder Technology, 2009. **194**(1): p. 75-80.
54. Taurozzi, J.S., V.A. Hackley, and M.R. Wiesner, *Ultrasonic dispersion of nanoparticles for environmental, health and safety assessment - issues and recommendations*. Nanotoxicology, 2011. **5**(4): p. 711-729.
55. Kusters, K.A., et al., *Ultrasonic fragmentation of agglomerate powders*. Chemical Engineering Science, 1993. **48**(24): p. 4119-4127.
56. Cao, G. and Y. Wang, *Physical Chemistry of Solid Surfaces*, in *Nanostructures and Nanomaterials*. 2012, World Scientific. p. 19-60.
57. Hotze, E.M., T. Phenrat, and G.V. Lowry, *Nanoparticle aggregation: challenges to understanding transport and reactivity in the environment*. Journal of Environmental Quality, 2010. **39**(6): p. 1909-1924.

58. Peng, Y.-H., et al., *The effect of electrolytes on the aggregation kinetics of three different ZnO nanoparticles in water*. Science of The Total Environment, 2015. **530–531**: p. 183-190.
59. Sun, P., et al., *Distinguishable transport behavior of zinc oxide nanoparticles in silica sand and soil columns*. Science of The Total Environment, 2015. **505**: p. 189-198.
60. Zhu, X., et al., *Aggregation kinetics of natural soil nanoparticles in different electrolytes*. European Journal of Soil Science, 2014. **65**(2): p. 206-217.
61. Jiang, X., et al., *Deposition kinetics of zinc oxide nanoparticles on natural organic matter coated silica surfaces*. Journal of Colloid and Interface Science, 2010. **350**(2): p. 427-434.
62. Bian, S.W., et al., *Aggregation and dissolution of 4 nm ZnO nanoparticles in aqueous environments: influence of pH, ionic strength, size, and adsorption of humic acid*. Langmuir : the ACS journal of surfaces and colloids, 2011. **27**(10): p. 6059-6068.
63. Kurlanda-Witek, H., B.T. Ngwenya, and I.B. Butler, *Transport of bare and capped zinc oxide nanoparticles is dependent on porous medium composition*. Journal of Contaminant Hydrology, 2014. **162**: p. 17-26.
64. Zhou, D. and A.A. Keller, *Role of morphology in the aggregation kinetics of ZnO nanoparticles*. Water Research, 2010. **44**(9): p. 2948-2956.
65. Wang, X., et al., *Roles of pH, cation valence, and ionic strength in the stability and aggregation behavior of zinc oxide nanoparticles*. Journal of Environmental Management, 2020. **267**.
66. Deonarine, A., et al., *Effects of humic substances on precipitation and aggregation of zinc sulfide nanoparticles*. Environmental Science and Technology, 2011. **45**(8): p. 3217-3223.
67. Pradhan, S., et al., *Effect of sonication on particle dispersion, administered dose and metal release of non-functionalized, non-inert metal nanoparticles*. Journal of Nanoparticle Research, 2016. **18**(9): p. 285.
68. Majedi, S.M., B.C. Kelly, and H.K. Lee, *Role of combinatorial environmental factors in the behavior and fate of ZnO nanoparticles in aqueous systems: a multiparametric analysis*. Journal of Hazardous Material, 2014. **264**: p. 370-379.
69. Nguyen, V.S., D. Rouxel, and B. Vincent, *Dispersion of nanoparticles: From organic solvents to polymer solutions*. Ultrasonics Sonochemistry, 2014. **21**(1): p. 149-153.
70. Wang, X., et al., *Roles of pH, cation valence, and ionic strength in the stability and aggregation behavior of zinc oxide nanoparticles*. Journal of Environmental Management, 2020. **267**.
71. Wu, J., et al., *Dissolution kinetics of oxidative etching of cubic and icosahedral platinum nanoparticles revealed by in situ liquid transmission electron microscopy*. ACS Nano, 2017. **11**(2): p. 1696-1703.
72. Raliya, R., et al., *Mechanistic evaluation of translocation and physiological impact of titanium dioxide and zinc oxide nanoparticles on the tomato (Solanum lycopersicum L.) plant*. Metallomics, 2015. **7**(12): p. 1584-1594.
73. Mukherjee, A., et al., *A soil mediated phyto-toxicological study of iron doped zinc oxide nanoparticles (Fe@ZnO) in green peas (Pisum sativum L.)*. Chemical Engineering Journal, 2014. **258**: p. 394-401.
74. Liu, X., et al., *Bioavailability of Zn in ZnO nanoparticle-spiked soil and the implications to maize plants*. Journal of Nanoparticle Research, 2015. **17**(4): p. 1-11.

75. Rousk, J., et al., *Comparative toxicity of nanoparticulate CuO and ZnO to soil bacterial communities*. PLoS One, 2012. **7**(3)
76. Franklin, N.M., et al., *Comparative toxicity of nanoparticulate ZnO, Bulk ZnO, and ZnCl₂ to a freshwater microalga (*Pseudokirchneriella subcapitata*): the importance of particle solubility*. Environmental Science and Technology, 2007. **41**(24): p. 8484-8490.
77. Adam, N., et al., *The chronic toxicity of ZnO nanoparticles and ZnCl₂ to *Daphnia magna* and the use of different methods to assess nanoparticle aggregation and dissolution*. Nanotoxicology, 2014. **8**(7): p. 709-717.
78. Wang, H., R.L. Wick, and B. Xing, *Toxicity of nanoparticulate and bulk ZnO, Al₂O₃ and TiO₂ to the nematode *Caenorhabditis elegans**. Environmental Pollution, 2009. **157**(4): p. 1171-1177.
79. Waalewijn-Kool, P.L., et al., *The effect of pH on the toxicity of zinc oxide nanoparticles to *Folsomia candida* in amended field soil*. Environmental Toxicology and Chemistry, 2013. **32**(10): p. 2349-2355.
80. Lin, D. and B. Xing, *Root uptake and phytotoxicity of ZnO nanoparticles*. Environmental Science and Technology, 2008. **42**(15): p. 5580-5585.
81. Lin, D. and B. Xing, *Phytotoxicity of nanoparticles: inhibition of seed germination and root growth*. Environmental Pollution, 2007. **150**(2): p. 243-250.
82. Xu, M., et al., *Challenge to assess the toxic contribution of metal cation released from nanomaterials for nanotoxicology - the case of ZnO nanoparticles*. Nanoscale, 2013. **5**(11): p. 4763-4769.
83. Chen, X., J. O'Halloran, and M.A. Jansen, *The toxicity of zinc oxide nanoparticles to *Lemna minor* (L.) is predominantly caused by dissolved Zn*. Aquatic Toxicology, 2016. **174**: p. 46-53.
84. Kool, P.L., M.D. Ortiz, and C.A.M. van Gestel, *Chronic toxicity of ZnO nanoparticles, non-nano ZnO and ZnCl₂ to *Folsomia candida* (Collembola) in relation to bioavailability in soil*. ENPO Environmental Pollution, 2011. **159**(10): p. 2713-2719.
85. Du, W., et al., *TiO₂ and ZnO nanoparticles negatively affect wheat growth and soil enzyme activities in agricultural soil*. Journal of Environmental Monitoring, 2011. **13**(4): p. 822-828.
86. Lee, C.W., et al., *Developmental phytotoxicity of metal oxide nanoparticles to *Arabidopsis thaliana**. Environmental Toxicology and Chemistry, 2010. **29**(3): p. 669-675.
87. Shchekin, A.K. and A.I. Rusanov, *Generalization of the Gibbs–Kelvin–Köhler and Ostwald–Freundlich equations for a liquid film on a soluble nanoparticle*. The Journal of Chemical Physics, 2008. **129**(15)
88. Mudunkotuwa, I.A. and V.H. Grassian, *The devil is in the details (or the surface): impact of surface structure and surface energetics on understanding the behavior of nanomaterials in the environment*. J Environ Monit, 2011. **13**(5): p. 1135-1144.
89. Bandyopadhyay, S., et al., *Comparative phytotoxicity of ZnO NPs, bulk ZnO, and ionic zinc onto the alfalfa plants symbiotically associated with *Sinorhizobium meliloti* in soil*. Science of The Total Environment, 2015. **515**: p. 60-69.
90. Milani, N., et al., *Dissolution kinetics of macronutrient fertilizers coated with manufactured zinc oxide nanoparticles*. Journal of Agricultural and Food Chemistry, 2012. **60**(16): p. 3991-3998.

91. David, C.A., et al., *Dissolution kinetics and solubility of ZnO nanoparticles followed by AGNES*. The Journal of Physical Chemistry C, 2012. **116**(21): p. 11758-11767.
92. Zhang, H., B. Chen, and J.F. Banfield, *Particle size and pH effects on nanoparticle dissolution*. The Journal of Physical Chemistry C, 2010. **114**(35): p. 14876-14884.
93. Mudunkotuwa, I.A., et al., *Dissolution of ZnO nanoparticles at circumneutral pH: a study of size effects in the presence and absence of citric acid*. Langmuir, 2012. **28**(1): p. 396-403.
94. Dokoumetzidis, A. and P. Macheras, *A century of dissolution research: from Noyes and Whitney to the Biopharmaceutics Classification System*. International Journal of Pharmaceutics, 2006. **321**(1–2): p. 1-11.
95. Borm, P., et al., *Research strategies for safety evaluation of nanomaterials, part V: role of dissolution in biological fate and effects of nanoscale particles*. Toxicological Sciences, 2006. **90**(1): p. 23-32.
96. Ma, R., et al., *Sulfidation mechanism for zinc oxide nanoparticles and the effect of sulfidation on their solubility*. Environmental Science and Technology, 2013. **47**(6): p. 2527-2534.
97. Formentini, T.A., et al., *Radical change of Zn speciation in pig slurry amended soil: key role of nano-sized sulfide particles*. Environmental Pollution, 2017. **222**: p. 495-503.
98. Lv, J., et al., *Dissolution and microstructural transformation of ZnO nanoparticles under the influence of phosphate*. Environmental Science and Technology, 2012. **46**(13): p. 7215-7221.
99. Rathnayake, S., et al., *Multitechnique investigation of the pH dependence of phosphate induced transformations of ZnO nanoparticles*. Environmental science and technology, 2014. **48**(9): p. 4757-4764.
100. Farzana, R., et al., *Zinc oxide nanoparticles from waste Zn-C battery via thermal route: characterization and properties*. Nanomaterials (Basel), 2018. **8**(9).
101. Fernandez, M.D., et al., *Evaluation of zinc oxide nanoparticle toxicity in sludge products applied to agricultural soil using multispecies soil systems*. Science of the Total Environment, 2014. **497**: p. 688-696.
102. Judy, J.D., et al., *Nanomaterials in biosolids inhibit nodulation, shift microbial community composition, and result in increased metal uptake relative to bulk/dissolved metals*. Environmental Science and Technology, 2015. **49**(14): p. 8751-8758.
103. Donner, E., et al., *X-ray absorption and micro X-ray fluorescence spectroscopy investigation of copper and zinc speciation in biosolids*. Environmental science and technology, 2011. **45**(17): p. 7249-7257.
104. Salt Lake metals. *Solubility products of selected compounds*. [cited 2020 20/09]; Available from: <http://www.saltlakemetals.com/SolubilityProducts.htm>.
105. Voegelin, A., et al., *Time-dependent changes of zinc speciation in four soils contaminated with zincite or sphalerite*. Environmental science and technology, 2011. **45**(1): p. 255-261.
106. Nowack, B., et al., *Meeting the needs for aged and released nanomaterials required for further testing – the SUN approach*. Environmental Science and Technology, 2016.
107. Valsami-Jones, E. and I. Lynch, *Nanosafety. How safe are nanomaterials?* Science, 2015. **350**(6259): p. 388-389.

108. Nowack, B. and D.M. Mitrano, *Procedures for the production and use of synthetically aged and product released nanomaterials for further environmental and ecotoxicity testing*. *NanoImpact*, 2018. **10**: p. 70-80.
109. Mitrano, D.M. and B. Nowack, *The need for a life-cycle based aging paradigm for nanomaterials: importance of real-world test systems to identify realistic particle transformations*. *Nanotechnology*, 2017. **28**(7)
110. Mitrano, D.M., et al., *Review of nanomaterial aging and transformations through the life cycle of nano-enhanced products*. *Environment International*, 2015. **77**(Supplement C): p. 132-147.
111. Waalewijn-Kool, P.L., et al., *Effect of soil organic matter content and pH on the toxicity of ZnO nanoparticles to Folsomia candida*. *Ecotoxicology and Environmental Safety*, 2014. **108**: p. 9-15.
112. Goldberg, S., *Equations and models describing adsorption processes in soils*. *Chemical processes in soils*. 2005.
113. Cornelis, G., et al., *A method for determination of retention of silver and cerium oxide manufactured nanoparticles in soils*. *Environmental Chemistry*, 2010. **7**(3): p. 298-308.
114. Domingos, R.F., et al., *Agglomeration and dissolution of zinc oxide nanoparticles: role of pH, ionic strength and fulvic acid*. *Environmental Chemistry*, 2013. **10**(4): p. 306-312.
115. Mohd Omar, F., H. Abdul Aziz, and S. Stoll, *Aggregation and disaggregation of ZnO nanoparticles: influence of pH and adsorption of Suwannee River humic acid*. *Science of The Total Environment*, 2014. **468**: p. 195-201.
116. Waalewijn-Kool, P.L., et al., *Sorption, dissolution and pH determine the long-term equilibration and toxicity of coated and uncoated ZnO nanoparticles in soil*. *Environmental Pollution*, 2013. **178**: p. 59-64.
117. Heggelund, L.R., et al., *Soil pH effects on the comparative toxicity of dissolved zinc, non-nano and nano ZnO to the earthworm Eisenia fetida*. *Nanotoxicology*, 2014. **8**(5): p. 559-572.
118. Watson, J.-L., et al., *The phytotoxicity of ZnO nanoparticles on wheat varies with soil properties*. *BioMetals*, 2014. **28**(1): p. 101-112.
119. Garcia-Gomez, C., et al., *Comparative study of the phytotoxicity of ZnO nanoparticles and Zn accumulation in nine crops grown in a calcareous soil and an acidic soil*. *Science of the Total Environment*, 2018. **644**: p. 770-780.
120. Shen, Z., et al., *Ecotoxicological effect of zinc oxide nanoparticles on soil microorganisms*. *Frontiers of Environmental Science and Engineering*, 2015. **9**(5): p. 912-918.
121. Read, D.S., et al., *Soil pH effects on the interactions between dissolved zinc, non-nano- and nano-ZnO with soil bacterial communities*. *Environmental Science and Pollution Research*, 2015: p. 1-9.
122. Joško, I., P. Oleszczuk, and B. Futa, *The effect of inorganic nanoparticles (ZnO, Cr₂O₃, CuO and Ni) and their bulk counterparts on enzyme activities in different soils*. *Geoderma*, 2014. **232**: p. 528-537.
123. Reed, R.B., et al., *Solubility of nano-zinc oxide in environmentally and biologically important matrices*. *Environmental Toxicology and Chemistry*, 2012. **31**(1): p. 93-99.
124. Mukherjee, A., et al., *Differential toxicity of bare and hybrid ZnO nanoparticles in green pea (Pisum sativum L.): a life cycle study*. *Frontiers in Plant Science*, 2016. **6**.
125. Merdzan, V., et al., *The effects of different coatings on zinc oxide nanoparticles and their influence on dissolution and bioaccumulation by the*

- green alga, C. reinhardtii*. Science of the Total Environment, 2014. **488**: p. 316-324.
126. Gimbert, L.J., et al., *Partitioning and stability of engineered ZnO nanoparticles in soil suspensions using flow field-flow fractionation*. Environmental Chemistry, 2007. **4**(1): p. 8-10.
 127. Grillo, R., A.H. Rosa, and L.F. Fraceto, *Engineered nanoparticles and organic matter: a review of the state-of-the-art*. Chemosphere, 2015. **119**(415): p. 608-619.
 128. GÜNGÖR, E.B.Ö. and M. Bekbölet, *Zinc release by humic and fulvic acid as influenced by pH, complexation and DOC sorption*. Geoderma, 2010. **159**(1-2): p. 131-138.
 129. Jiang, C., G.R. Aiken, and H. Hsu-Kim, *Effects of natural organic matter properties on the dissolution kinetics of zinc oxide nanoparticles*. Environmental Science and Technology, 2015. **49**(19): p. 11476-11484.
 130. Peng, Y.-H., et al., *Influence of water chemistry on the environmental behaviors of commercial ZnO nanoparticles in various water and wastewater samples*. Journal of Hazardous Materials, 2017. **322, Part B**: p. 348-356.
 131. Keller, A.A., et al., *Stability and aggregation of metal oxide nanoparticles in natural aqueous matrices*. Environmental Science and Technology, 2010. **44**(6): p. 1962-1967.
 132. Lau, B.L. and H. Hsu-Kim, *Precipitation and growth of zinc sulfide nanoparticles in the presence of thiol-containing natural organic ligands*. Environmental Science and Technology, 2008. **42**(19): p. 7236-7241.
 133. Akhil, K., P. Chandran, and S. Sudheer Khan, *Influence of humic acid on the stability and bacterial toxicity of zinc oxide nanoparticles in water*. Journal of Photochemistry and Photobiology B: Biology, 2015. **153**: p. 289-295.
 134. Moghaddasi, S., et al., *Effects of coated and non-coated ZnO nano particles on cucumber seedlings grown in gel chamber*. Archives of Agronomy and Soil Science, 2017. **63**(8): p. 1108-1120.
 135. Tso, C.P., et al., *Stability of metal oxide nanoparticles in aqueous solutions*. Water Science and Technology, 2010. **61**(1): p. 127-133.
 136. Han, Y., et al., *Aggregation and dissolution of ZnO nanoparticles synthesized by different methods: influence of ionic strength and humic acid*. Colloids and Surfaces A: Physicochemical and Engineering Aspects, 2014. **451**: p. 7-15.
 137. Jiang, C. and H. Hsu-Kim, *Direct in situ measurement of dissolved zinc in the presence of zinc oxide nanoparticles using anodic stripping voltammetry*. Environmental Science: Processes and Impacts, 2014. **16**(11): p. 2536-2544.
 138. Notter, D.A., D.M. Mitrano, and B. Nowack, *Are nanosized or dissolved metals more toxic in the environment? A meta-analysis*. Environmental Toxicology and Chemistry, 2014. **33**(12): p. 2733-2739.
 139. Khare, P., et al., *Size dependent toxicity of zinc oxide nano-particles in soil nematode Caenorhabditis elegans*. Nanotoxicology, 2015. **9**(4): p. 423-432.
 140. Mukherjee, A., et al., *Physiological effects of nanoparticulate ZnO in green peas (Pisum sativum L.) cultivated in soil*. Metallomics, 2014. **6**(1): p. 132-138.
 141. Servin, A.D. and J.C. White, *Nanotechnology in agriculture: next steps for understanding engineered nanoparticle exposure and risk*. NanoImpact, 2016. **1**(Supplement C): p. 9-12.
 142. Quik, J.T.K., D. van De Meent, and A.A. Koelmans, *Simplifying modeling of nanoparticle aggregation-sedimentation behavior in environmental systems: a theoretical analysis*. Water Research, 2014. **62**: p. 193-201.
 143. Holden, P.A., et al., *Considerations of environmentally relevant test conditions for improved evaluation of ecological hazards of engineered*

- nanomaterials*. Environmental Science and Technology, 2016. **50**(12): p. 6124-6145.
144. Laycock, A., et al., *Earthworm uptake routes and rates of ionic Zn and ZnO nanoparticles at realistic concentrations, traced using stable isotope labeling*. Environmental Science and Technology, 2016. **50**(1): p. 412-419.
 145. García-Gómez, C., et al., *Integrating ecotoxicity and chemical approaches to compare the effects of ZnO nanoparticles, ZnO bulk, and ZnCl₂ on plants and microorganisms in a natural soil*. Environmental Science and Pollution Research, 2015. **22**(21): p. 16803-16813.
 146. Dybowska, A., S.K. Misra, and E. Valsami-Jones, *Labelling nanoparticles with non-radioactive isotopes*, in *Isotopes in nanoparticles*. 2016, Pan Stanford. p. 455-492.
 147. Hernandez, F., et al., *Current use of high-resolution mass spectrometry in the environmental sciences*. Analytical and Bioanalytical Chemistry, 2012. **403**(5): p. 1251-1264.
 148. Mahajan, P., S.K. Dhoke, and A.S. Khanna, *Effect of nano-ZnO particle suspension on growth of mung (Vigna radiata) and gram (Cicer arietinum) seedlings using plant agar method*. Journal of Nanotechnology, 2011. **2011**: p. 7.
 149. Mousavi Kouhi, S.M., et al., *Comparative effects of ZnO nanoparticles, ZnO bulk particles, and Zn²⁺ on Brassica napus after long-term exposure: changes in growth, biochemical compounds, antioxidant enzyme activities, and Zn bioaccumulation*. Water, Air, and Soil Pollution, 2015. **226**(11): p. 1-11.
 150. Mousavi Kouhi, S.M., et al., *Long-term exposure of rapeseed (Brassica napus L.) to ZnO nanoparticles: anatomical and ultrastructural responses*. Environmental Science and Pollution Research, 2015. **22**(14): p. 10733-10743.
 151. Hernandez-Viezcas, J.A., et al., *Spectroscopic verification of zinc absorption and distribution in the desert plant Prosopis juliflora-velutina (velvet mesquite) treated with ZnO nanoparticles*. Chemical Engineering Journal, 2011. **170**(1-3): p. 346-352.
 152. Xiang, L., et al., *Effects of the size and morphology of zinc oxide nanoparticles on the germination of Chinese cabbage seeds*. Environmental Science and Pollution Research, 2015. **22**(14): p. 10452-10462.
 153. Boonyanitipong, P., et al., *Toxicity of ZnO and TiO₂ nanoparticles on germinating rice seed Oryza sativa L.* International Journal of Bioscience, Biochemistry and Bioinformatics, 2011. **1**(4): p. 282-285.
 154. Judy, J.D. and P.M. Bertsch, *Bioavailability, toxicity, and fate of manufactured nanomaterials in terrestrial ecosystems*, in *Advances in Agronomy*, L.S. Donald, Editor. 2014, Academic Press. p. 1-64.
 155. Joško, I. and P. Oleszczuk, *Phytotoxicity of nanoparticles - problems with bioassay choosing and sample preparation*. Environmental Science and Pollution Research, 2014. **21**(17): p. 10215-10224.
 156. Wang, P., et al., *Fate of ZnO nanoparticles in soils and cowpea (Vigna unguiculata)*. Environmental Science and Technology, 2013. **47**(23): p. 13822-13830.
 157. Thunugunta, T., et al., *Impact of zinc oxide nanoparticles on eggplant (S. melongena): studies on growth and the accumulation of nanoparticles*. IET Nanobiotechnology, 2018. **12**(6): p. 706-713.
 158. Ben-Moshe, T., I. Dror, and B. Berkowitz, *Transport of metal oxide nanoparticles in saturated porous media*. Chemosphere, 2010. **81**(3): p. 387-393.

159. Jiang, X., et al., *Transport and deposition of ZnO nanoparticles in saturated porous media*. Colloids and Surfaces A: Physicochemical and Engineering Aspects, 2012. **401**: p. 29-37.
160. Kanel, S.R. and S.R. Al-Abed, *Influence of pH on the transport of nanoscale zinc oxide in saturated porous media*. Journal of Nanoparticle Research, 2011. **13**(9): p. 4035-4047.
161. Petosa, A.R., et al., *Transport of two metal oxide nanoparticles in saturated granular porous media: role of water chemistry and particle coating*. Water Research, 2012. **46**(4): p. 1273-1285.
162. Wang, Y.X., A. Specht, and W.J. Horst, *Stable isotope labelling and zinc distribution in grains studied by laser ablation ICP-MS in an ear culture system reveals zinc transport barriers during grain filling in wheat*. New Phytologist, 2011. **189**(2): p. 428-437.
163. Adhikari, T., et al., *Characterization of zinc oxide nano particles and their effect on growth of maize (Zea mays L.) plant*. Journal of Plant Nutrition, 2015. **38**(10): p. 1505-1515.
164. Zhao, L., et al., *ZnO nanoparticle fate in soil and zinc bioaccumulation in corn plants (Zea mays) influenced by alginate*. Environmental Science: Processes and Impacts, 2013. **15**(1): p. 260-266.
165. Zhao, L., et al., *Transport of Zn in a sandy loam soil treated with ZnO NPs and uptake by corn plants: electron microprobe and confocal microscopy studies*. Chemical Engineering Journal, 2012. **184**: p. 1-8.
166. López-Moreno, M.L., et al., *Evidence of the differential biotransformation and genotoxicity of ZnO and CeO₂ nanoparticles on soybean (Glycine max) plants*. Environmental Science and Technology, 2010. **44**(19): p. 7315-7320.
167. Priester, J.H., et al., *Soybean susceptibility to manufactured nanomaterials with evidence for food quality and soil fertility interruption*. Proc Natl Acad Sci USA, 2012. **109**(37): p. 2451-2456.
168. Priester, J.H., et al., *Damage assessment for soybean cultivated in soil with either CeO₂ or ZnO manufactured nanomaterials*. Science of The Total Environment, 2017. **579**: p. 1756-1768.
169. Yoon, S.-J., et al., *Zinc oxide nanoparticles delay soybean development: a standard soil microcosm study*. Ecotoxicology and Environmental Safety, 2014. **100**: p. 131-137.
170. Stampoulis, D., S.K. Sinha, and J.C. White, *Assay-dependent phytotoxicity of nanoparticles to plants*. Environmental Science and Technology, 2009. **43**(24): p. 9473-9479.
171. Lee, S., et al., *Assessment of phytotoxicity of ZnO NPs on a medicinal plant, Fagopyrum esculentum*. Environmental Science Pollution Research, 2013. **20**(2): p. 848-854.
172. Faizan, M., et al., *Zinc oxide nanoparticle-mediated changes in photosynthetic efficiency and antioxidant system of tomato plants*. PHOTOSYNTHETICA, 2018. **56**(2): p. 678-686.
173. Kumari, M., et al., *Cytogenetic and genotoxic effects of zinc oxide nanoparticles on root cells of Allium cepa*. Journal of Hazardous Material, 2011. **190**(1-3): p. 613-621.
174. Zhao, L., et al., *CeO₂ and ZnO nanoparticles change the nutritional qualities of cucumber (Cucumis sativus)*. Journal of Agricultural Food Chemistry, 2014. **62**(13): p. 2752-2759.
175. De la Rosa, G., et al., *Toxicity and biotransformation of ZnO nanoparticles in the desert plants Prosopis juliflora-velutina, Salsola tragus and Parkinsonia florida*. International Journal of Nanotechnology, 2011. **8**(6-7): p. 492-506.

176. Rao, S. and G.S. Shekhawat, *Toxicity of ZnO engineered nanoparticles and evaluation of their effect on growth, metabolism and tissue specific accumulation in Brassica juncea*. Journal of Environmental Chemical Engineering, 2014. **2**(1): p. 105-114.
177. Zafar, H., et al., *CuO and ZnO nanoparticle application in synthetic soil modulates morphology, nutritional contents, and metal analysis of Brassica nigra*. ACS Omega 2020. **5**: p. 13566-13577.
178. Reddy, P.V.L., et al., *Lessons learned: are engineered nanomaterials toxic to terrestrial plants?* Science of The Total Environment, 2016. **568**: p. 470-479.
179. Miralles, P., T.L. Church, and A.T. Harris, *Toxicity, uptake, and translocation of engineered nanomaterials in vascular plants*. Environmental Science and Technology, 2012. **46**(17): p. 9224-9239.
180. Chen, C.S., et al., *Toxicogenomic responses of the model legume Medicago truncatula to aged biosolids containing a mixture of nanomaterials (TiO₂, Ag, and ZnO) from a pilot wastewater treatment Plant*. Environmental Science and Technology, 2015. **49**(14): p. 8759-8768.
181. Miglietta, M.L., et al., *Methodological issues about techniques for the spiking of standard OECD soil with nanoparticles: evidence of different behaviours*. Journal of Nanoparticle Research, 2015. **17**(7): p. 1-12.
182. Arnold, T., et al., *Measurement of zinc stable isotope ratios in biogeochemical matrices by double-spike MC-ICPMS and determination of the isotope ratio pool available for plants from soil*. Analytical and Bioanalytical Chemistry, 2010. **398**(7-8): p. 3115-3125.
183. Sun, T.Y., et al., *Comprehensive probabilistic modelling of environmental emissions of engineered nanomaterials*. Environmental Pollution, 2014. **185**: p. 69-76.
184. Caballero-Guzman, A. and B. Nowack, *A critical review of engineered nanomaterial release data: are current data useful for material flow modeling?* Environmental Pollution, 2016. **213**: p. 502-517.
185. Qafoku, N.P., *Terrestrial nanoparticles and their controls on soil-/geo-processes and reactions*, in *Advances in Agronomy*, L.S. Donald, Editor. 2010, Academic Press. p. 33-91.
186. Rabajczyk, A., *Possibilities for analysis of selected nanometals in solid environmental samples*. Desalination and Water Treatment, 2016. **57**(3): p. 1598-1610.
187. Holden, P.A., et al., *Evaluation of exposure concentrations used in assessing manufactured nanomaterial environmental hazards: are they relevant?* Environmental Science and Technology, 2014. **48**(18): p. 10541-10551.
188. Diez-Ortiz, M., et al., *Short-term soil bioassays may not reveal the full toxicity potential for nanomaterials; bioavailability and toxicity of silver ions (AgNO₃) and silver nanoparticles to earthworm Eisenia fetida in long-term aged soils*. Environmental Pollution, 2015. **203**: p. 191-198.
189. Laborda, F., et al., *Detection, characterization and quantification of inorganic engineered nanomaterials: A review of techniques and methodological approaches for the analysis of complex samples*. Analytica Chimica Acta.
190. Linsinger, T., et al., *Requirements on measurements for the implementation of the European Commission definition of the term 'nanomaterial'*. 2012, Publications Office of the European Union.
191. Valsami-Jones, E., I. Lynch, and C.A. Charitidis, *Nanomaterial ontologies for nanosafety: a rose by any other name*. Journal of Nanomedical Research, 2016. **3**(5).

192. Petersen, E.J., et al., *Identification and avoidance of potential artifacts and misinterpretations in nanomaterial ecotoxicity measurements*. Environmental Science and Technology, 2014. **48**(8): p. 4226-4246.
193. van der Ploeg, M.J.C., et al., *Effects of C60 nanoparticle exposure on earthworms (*Lumbricus rubellus*) and implications for population dynamics*. ENPO Environmental Pollution, 2011. **159**(1): p. 198-203.
194. Heggelund, L.R., et al., *Soil pH effects on the comparative toxicity of dissolved zinc, non-nano and nano ZnO to the earthworm *Eisenia fetida**. 2014.
195. Hooper, H.L., et al., *Comparative chronic toxicity of nanoparticulate and ionic zinc to the earthworm *Eisenia veneta* in a soil matrix*. Environment International, 2011. **37**(6): p. 1111-1117.
196. Tourinho, P.S., et al., *Influence of soil pH on the toxicity of zinc oxide nanoparticles to the terrestrial isopod *Porcellionides pruinosus**. Environmental Toxicology and Chemistry, 2013. **32**(12): p. 2808-2815.
197. Akanbi-Gada, M.A., et al., *Phytotoxicity of nano-zinc oxide to tomato plant (*Solanum lycopersicum* L.): Zn uptake, stress enzymes response and influence on non-enzymatic antioxidants in fruits*. Environmental Technology and Innovation, 2019. **14**: p. 100325.
198. Waalewijn-Kool, P.L., M. Diez Ortiz, and C.A.M. van Gestel, *Effect of different spiking procedures on the distribution and toxicity of ZnO nanoparticles in soil*. Ecotoxicology, 2012. **21**(7): p. 1797-1804.
199. Yang, K., D. Lin, and B. Xing, *Interactions of humic acid with nanosized inorganic oxides*. Langmuir, 2009. **25**(6): p. 3571-3576.
200. Tuoriniemi, J., et al., *In situ characterisation of physicochemical state and concentration of nanoparticles in soil ecotoxicity studies using environmental scanning electron microscopy*. Environmental Chemistry, 2014. **11**(4): p. 367-376.
201. Hasselov, M., et al., *Nanoparticle analysis and characterization methodologies in environmental risk assessment of engineered nanoparticles*. Ecotoxicology, 2008. **17**(5): p. 344-361.
202. Di Bonito, M., et al., *Overview of selected soil pore water extraction methods for the determination of potentially toxic elements in contaminated soils : operational and technical aspects*. Environmental geochemistry, 2008: p. 213-249.
203. Gimbert, L.J., et al., *Comparison of centrifugation and filtration techniques for the size fractionation of colloidal material in soil suspensions using sedimentation field-flow fractionation*. Environmental Science and Technology, 2005. **39**(6): p. 1731-1735.
204. Gimbert, L., et al., *The influence of sample preparation on observed particle size distributions for contrasting soil suspensions using flow field-flow fractionation*. Vol. 3. 2006.
205. Van Koetsem, F., et al., *Use of filtration techniques to study environmental fate of engineered metallic nanoparticles: factors affecting filter performance*. Journal of Hazardous Materials, 2017. **322**: p. 105-117.
206. Majedi, S.M., H.K. Lee, and B.C. Kelly, *Chemometric analytical approach for the cloud point extraction and inductively coupled plasma mass spectrometric determination of zinc oxide nanoparticles in water samples*. Analytical Chemistry, 2012. **84**(15): p. 6546-52.
207. Boverhof, D.R. and R.M. David, *Nanomaterial characterization: considerations and needs for hazard assessment and safety evaluation*. Analytical and Bioanalytical Chemistry, 2010. **396**(3): p. 953-961.

208. Bouwmeester, H., et al., *Minimal analytical characterization of engineered nanomaterials needed for hazard assessment in biological matrices*. *Nanotoxicology*, 2011. **5**(1): p. 1-11.
209. MINChar, i. *Recommended minimum physical and chemical parameters for characterizing nanomaterials on toxicology studies*. 2008 [cited 2019 31/05]; Available from: <https://characterizationmatters.wordpress.com/parameters/>.
210. Pettitt, M.E. and J.R. Lead, *Minimum physicochemical characterisation requirements for nanomaterial regulation*. *Environment International*, 2013. **52**: p. 41-50.
211. Domingos, R.F., et al., *Characterizing manufactured nanoparticles in the environment: multimethod determination of particle sizes*. *Environmental Science and Technology*, 2009. **43**(19): p. 7277-7284.
212. Pyrz, W.D. and D.J. Buttrey, *Particle size determination using TEM: a discussion of image acquisition and analysis for the novice microscopist*. *Langmuir*, 2008. **24**(20): p. 11350-11360.
213. Hassan, P.A., S. Rana, and G. Verma, *Making sense of brownian motion: colloid characterization by dynamic light scattering*. *Langmuir*, 2015. **31**(1): p. 3-12.
214. Larner, F., et al., *Tracing bioavailability of ZnO nanoparticles using stable isotope labeling*. *Environmental science and technology*, 2012. **46**(21): p. 12137-12145.
215. Merkus, H.G., *Particle size measurements: fundamentals, practice, quality*. Particle Technology Series. Vol. 17. 2009: Springer Netherlands. 534.
216. Hoo, C.M., et al., *A comparison of atomic force microscopy (AFM) and dynamic light scattering (DLS) methods to characterize nanoparticle size distributions*. *Journal of Nanoparticle Research*, 2008. **10**: p. 89.
217. Hall, B.D., D. Zanchet, and D. Ugarte, *Estimating nanoparticle size from diffraction measurements*. *Journal of Applied Crystallography*, 2000. **33**(6): p. 1335-1341.
218. Lechner, M.D. and W. Mächtle, *Determination of the particle size distribution of 5–100 nm nanoparticles with the analytical ultracentrifuge: consideration and correction of diffusion effects*, in *Analytical Ultracentrifugation V*, H. Cölfen, Editor. 1999, Springer Berlin Heidelberg: Berlin, Heidelberg. p. 37-43.
219. Wiench, K., et al., *Acute and chronic effects of nano- and non-nano-scale TiO₂ and ZnO particles on mobility and reproduction of the freshwater invertebrate *Daphnia magna**. *Chemosphere*, 2009. **76**(10): p. 1356-1365.
220. Fabricius, A.-L., et al., *ICP-MS-based characterization of inorganic nanoparticles - sample preparation and off-line fractionation strategies*. *Analytical and Bioanalytical Chemistry*, 2014. **406**(2): p. 467-479.
221. Hadioui, M., V. Merdzan, and K.J. Wilkinson, *Detection and characterization of ZnO nanoparticles in surface and waste waters using single particle ICPMS*. *Environmental science and technology*, 2015. **49**(10): p. 6141-6148.
222. Pitkänen, L. and A.M. Striegel, *Size-exclusion chromatography of metal nanoparticles and quantum dots*. *Trends in Analytical Chemistry*, 2016. **80**: p. 311-320.
223. Liu, F.-K. and G.-T. Wei, *Effect of mobile-phase additives on separation of gold nanoparticles by size-exclusion chromatography*. *Chromatographia*, 2004. **59**(1): p. 115-119.
224. Wei, G.-T. and F.-K. Liu, *Separation of nanometer gold particles by size exclusion chromatography*. *Journal of Chromatography A*, 1999. **836**(2): p. 253-260.

225. Chatterjee, A., et al., *Thermodynamics of micelle formation of ionic surfactants: a critical assessment for sodium dodecyl sulfate, cetyl pyridinium chloride and dioctyl sulfosuccinate (Na salt) by microcalorimetric, conductometric, and tensiometric measurements*. The Journal of Physical Chemistry B, 2001. **105**(51): p. 12823-12831.
226. Liu, G., et al., *Tetraalkylammonium interactions with dodecyl sulfate micelles: a molecular dynamics study*. Physical Chemistry Chemical Physics, 2016. **18**(2): p. 878-885.
227. Pletnev, M.Y., *Chemistry of surfactants*, in *Studies in Interface Science*. 2001. p. 1-97.
228. Wei, G.-T., F.-K. Liu, and C.R.C. Wang, *Shape separation of nanometer gold particles by size-exclusion chromatography*. Analytical Chemistry, 1999. **71**(11): p. 2085-2091.
229. Liu, F.-K., *Using SEC for analyzing the sizes of Au/Pt core/shell nanoparticles*. Chromatographia, 2010. **72**(5): p. 473-480.
230. Liu, F.-K., *Using size-exclusion chromatography to monitor variations in the sizes of microwave-irradiated gold nanoparticles*. ISRN Chromatography, 2012. **2012**: p. 7.
231. Liu, F.-K., *Using size-exclusion chromatography to monitor the stabilization of Au nanoparticles in the presence of salt and organic solvent*. Chromatographia, 2012. **75**(19): p. 1099-1105.
232. Liu, F.-K., *Monitoring the synthesis of Au nanoparticles using SEC*. Chromatographia, 2008. **68**(1): p. 81-87.
233. Liu, F.-K., *SEC characterization of Au nanoparticles prepared through seed-assisted synthesis*. Chromatographia, 2007. **66**(9): p. 791-796.
234. Liu, F.-K. and Y.-C. Chang, *Using size-exclusion chromatography to evaluate changes in the sizes of Au and Au/Pd core/shell nanoparticles under thermal treatment*. Chromatographia, 2011. **74**(11): p. 767-775.
235. Al-Sid-Cheikh, M., et al., *Robust method using online steric exclusion chromatography-ultraviolet-inductively coupled plasma mass spectrometry to investigate nanoparticle fate and behavior in environmental samples*. Analytical Chemistry, 2015. **87**(20): p. 10346-10353.
236. Zhou, X.-X., J.-F. Liu, and F.-L. Geng, *Determination of metal oxide nanoparticles and their ionic counterparts in environmental waters by size exclusion chromatography coupled to ICP-MS*. NanoImpact, 2016. **1**: p. 13-20.
237. Siebrands, T., et al., *Steric exclusion chromatography of nanometer-sized gold particles*. Langmuir, 1993. **9**(9): p. 2297-2300.
238. Philippe, A., et al., *Evaluation of hydrodynamic chromatography coupled with inductively coupled plasma mass spectrometry detector for analysis of colloids in environmental media - effects of colloid composition, coating and shape*. Analytical Methods, 2014. **6**(21): p. 8722-8728.
239. Philippe, A. and G.E. Schaumann, *Evaluation of hydrodynamic chromatography coupled with UV-visible, fluorescence and inductively coupled plasma mass spectrometry detectors for sizing and quantifying colloids in environmental media*. PLoS ONE, 2014. **9**(2)
240. Rakcheev, D., A. Philippe, and G.E. Schaumann, *Hydrodynamic chromatography coupled with single particle-inductively coupled plasma mass spectrometry for investigating nanoparticles agglomerates*. Analytical Chemistry, 2013. **85**(22): p. 10643-10647.
241. Proulx, K., M. Hadioui, and K.J. Wilkinson, *Separation, detection and characterization of nanomaterials in municipal wastewaters using*

- hydrodynamic chromatography coupled to ICPMS and single particle ICPMS*. Analytical and Bioanalytical Chemistry, 2016. **408**(19): p. 5147-5155.
242. Proulx, K. and K.J. Wilkinson, *Separation, detection and characterisation of engineered nanoparticles in natural waters using hydrodynamic chromatography and multi-method detection (light scattering, analytical ultracentrifugation and single particle ICP-MS)*. Environmental Chemistry, 2014. **11**(4): p. 392-401.
243. Tiede, K., et al., *A robust size-characterisation methodology for studying nanoparticle behaviour in 'real' environmental samples, using hydrodynamic chromatography coupled to ICP-MS*. Journal of Analytical Atomic Spectrometry, 2009. **24**(7): p. 964-972.
244. Pergantis, S.A., T.L. Jones-Lepp, and E.M. Heithmar, *Hydrodynamic chromatography online with single particle-inductively coupled plasma mass spectrometry for ultratrace detection of metal-containing nanoparticles*. Analytical chemistry, 2012. **84**(15): p. 6454-6462.
245. Olesik, J.W., *Elemental Analysis Using ICP-OES and ICP/MS*. Analytical Chemistry, 1991. **63**(1): p. 12A-21A.
246. Gulson, B. and H. Wong, *Stable isotopic tracing - a way forward for nanotechnology*. Environmental Health Perspectives, 2006. **114**(10): p. 1486-1488.
247. Buffet, P.E., et al., *Fate of isotopically labeled zinc oxide nanoparticles in sediment and effects on two endobenthic species, the clam *Scrobicularia plana* and the ragworm *Hediste diversicolor**. Ecotoxicology Environmental Safety, 2012. **84**: p. 191-198.
248. Rodgers, D.W., et al., *An enriched stable isotope technique to estimate the availability of soil zinc to *Lumbricus terrestris* (L.) across a salinization gradient*. Environmental Toxicology and Chemistry, 2011. **30**(3): p. 607-615.
249. Gulson, B., et al., *Comparison of dermal absorption of zinc from different sunscreen formulations and differing UV exposure based on stable isotope tracing*. Science of the Total Environment, 2012. **420**: p. 313-318.
250. Dybowska, A.D., et al., *Synthesis of isotopically modified ZnO nanoparticles and their potential as nanotoxicity tracers*. Environmental Pollution, 2011. **159**(1): p. 266-273.
251. Croteau, M.N., et al., *Stable metal isotopes reveal copper accumulation and loss dynamics in the freshwater bivalve *Corbicula**. Environmental science and technology, 2004. **38**(19): p. 5002-5009.
252. Gäbler, H.E., et al., *Enriched stable isotopes for determining the isotopically exchangeable element content in soils*. European Journal of Soil Science, 2007. **58**(3): p. 746-757.
253. Croteau, M.N., S.N. Luoma, and B. Pellet, *Determining metal assimilation efficiency in aquatic invertebrates using enriched stable metal isotope tracers*. AQTQX Aquatic Toxicology, 2007. **83**(2): p. 116-125.
254. Marzouk, E.R., S.R. Chenery, and S.D. Young, *Measuring reactive metal in soil: a comparison of multi-element isotopic dilution and chemical extraction*. European Journal of Soil Science, 2013. **64**(4): p. 526-536.
255. Croteau, M.N., et al., *A novel approach reveals that zinc oxide nanoparticles are bioavailable and toxic after dietary exposures*. Nanotoxicology, 2011. **5**(1): p. 79-90.
256. Ganguly, S., S. Das, and S.G. Dastidar, *Study of the antimicrobial effects of the anticancer drug oxaliplatin and its interaction with synthesized ZnS nanoparticles*. International Journal Of Pharmacy and Therapeutics, 2014. **5**(3): p. 230-234.

257. Sverdrup, L.E., et al., *Toxicity of eight polycyclic aromatic compounds to red clover (Trifolium pratense), ryegrass (Lolium perenne), and mustard (Sinapsis alba)*. Chemosphere, 2003. **53**(8): p. 993-1003.
258. Lindsay, W.L. and W.A. Norvell, *Development of a DTPA soil test for zinc, iron, manganese, and copper*. Soil Science Society of America Journal, 1978. **42**(3): p. 421-428.
259. Nogueira, M.C.S., *Orthogonal contrasts: definitions and concepts*. Scientia Agricola, 2004. **61**: p. 118-124.
260. Scherber, C. *Working with orthogonal contrasts in R* 2019 [cited 2020 12/03]; Available from: <http://www.christoph-scherber.de/content/Statistics%20Course%20files/Working%20with%20orthogonal%20contrasts%20in%20R.pdf>.
261. Seyedbagheri, M.M., *Influence of humic products on soil health and potato production*. Potato Research, 2010. **53**: p. 341-349.
262. Kaya, C., et al., *Sulfur-enriched Leonardite and humic acid soil amendments enhance tolerance to drought and phosphorus deficiency stress in maize (Zea mays L.)*. Scientific Reports, 2020. **10**.
263. Liu, M., et al., *Saline-alkali soil applied with vermicompost and humic acid fertilizer improved macroaggregate microstructure to enhance salt leaching and inhibit nitrogen losses*. Applied Soil Ecology, 2020. **156**.
264. Swift, R.S., *Organic Matter Characterization, in Methods of Soil Analysis Part 3 - Chemical Methods*, D.L. Sparks, et al., Editors. 1996, Soil Science Society of America, American Society of Agronomy: Madison, WI. p. 1011-1069.
265. Dolan, J.W., *Attacking carryover problems*. Lc Gc North America, 2001. **19**(10): p. 1050-1054.
266. Soto-Alvaredo, J., M. Montes-Bayón, and J. Bettmer, *Speciation of silver nanoparticles and silver(I) by reversed-phase liquid chromatography coupled to ICPMS*. Analytical Chemistry, 2013. **85**(3): p. 1316-1321.
267. Sevenich, G.J. and J.S. Fritz, *Addition of complexing agents in ion chromatography for separation of polyvalent metal ions*. Analytical Chemistry, 1983. **55**(1): p. 12-16.
268. Tanaka, T., *Ion-chromatographic determination of divalent metal ions (Co, Ni, Cu, Zn, Cd) using EDTA as complexing agent*. Fresenius' Zeitschrift für analytische Chemie, 1985. **320**(2): p. 125-127.
269. Hajós, P., et al., *The simultaneous analysis of metal-EDTA complexes and inorganic anions by suppressed ion chromatography*. Journal of Chromatographic Science, 1996. **34**(6): p. 291-299.
270. Sötebier, C.A., et al., *Separation and quantification of silver nanoparticles and silver ions using reversed phase high performance liquid chromatography coupled to inductively coupled plasma mass spectrometry in combination with isotope dilution analysis*. Journal of Chromatography A, 2016. **1468**: p. 102-108.
271. Panda, S.K., A. Datta, and S. Chaudhuri, *Nearly monodispersed ZnS nanospheres: synthesis and optical properties*. Chemical Physics Letters, 2007. **440**(4-6): p. 235-238.
272. Chae, W.-S., *Fabrication of 50 to 1000 nm Monodisperse ZnS Colloids*. Bulletin of the Korean Chemical Society, 2009. **30**(1): p. 129-132.
273. Yamashita, A.C. and K. Sakurai, *Dialysis membranes – physico-chemical structures and features*, in *Updates in Hemodialysis*, H. Suzuki, Editor. 2015, Intech. p. 163-189.
274. Auld, D.S., *Metal-free dialysis tubing*, in *Methods in Enzymology*. 1988, Academic Press. p. 13-14.

275. Mandzy, N., E. Grulke, and T. Druffel, *Breakage of TiO₂ agglomerates in electrostatically stabilized aqueous dispersions*. Powder Technology, 2005. **160**(2): p. 121-126.
276. Pacek, A.W., P. Ding, and A.T. Utomo, *Effect of energy density, pH and temperature on de-aggregation in nano-particles/water suspensions in high shear mixer*. Powder Technology, 2007. **173**(3): p. 203-210.
277. Bowles, L.C., et al., *Synthesis and characterization of metal sulfide clusters for toxicological studies*. Environ Toxicol Chem, 2002. **21**(4): p. 693-699.
278. Royal Society of Chemistry. *Chemical Methods Ontology*. 2017 [cited 2020 29/08]; Available from: <http://www.rsc.org/publishing/journals/prospect/ontology.asp?id=CMO:0001708>.
279. Roebben, G., et al., *Interlaboratory comparison of size and surface charge measurements on nanoparticles prior to biological impact assessment*. Journal of Nanoparticle Research, 2011. **13**(7): p. 2675.
280. Nguyen, V.S., et al., *Effect of ultrasonication and dispersion stability on the cluster size of alumina nanoscale particles in aqueous solutions*. Ultrasonic Sonochemistry, 2011. **18**(1): p. 382-388.
281. Taurozzi, J.S., V.A. Hackley, and M.R. Wiesner, *Preparation of nanoparticle dispersions from powdered material using ultrasonic disruption*. NIST special publication, 2012. **1200**(2): p. 1200-1202.
282. Koczkur, K.M., et al., *Polyvinylpyrrolidone (PVP) in nanoparticle synthesis*. Dalton transactions, 2015(44): p. 17883-17905.
283. Dhumale, V.A., et al., *Reversible aggregation control of polyvinylpyrrolidone capped gold nanoparticles as a function of pH*. Materials express, 2012. **2**(4): p. 311-318.
284. Huynh, K.A. and K.L. Chen, *Aggregation kinetics of citrate and polyvinylpyrrolidone coated silver nanoparticles in monovalent and divalent electrolyte solutions*. Environmental Science & Technology, 2011. **45**(13): p. 5564-5571.
285. Garcia-Gomez, C., et al., *Study of Zn availability, uptake, and effects on earthworms of zinc oxide nanoparticle versus bulk applied to two agricultural soils: acidic and calcareous*. Chemosphere, 2020. **239**: p. 124814.
286. Hafeez, B., Y.M. Khanif, and M. Saleem, *Role of zinc in plant nutrition - a review* American Journal of Experimental Agriculture, 2013. **3**(2).
287. Tsonev, T. and F.J.C. Lidon, *Zinc in plants - an overview*. Emirates Journal of Food and Agriculture, 2012. **24**(4): p. 322-333.
288. Bouain, N., et al., *Phosphate and zinc transport and signalling in plants: toward a better understanding of their homeostasis interaction*. Journal of Experimental Botany, 2014. **65**(20): p. 5725-5741.
289. Van Assche, F. and H. Clijsters, *Effects of metals on enzyme activity in plants*. Plant, Cell and Environment, 1990. **13**(3): p. 195-206.
290. Dimkpa, C.O., et al., *Bioactivity and biomodification of Ag, ZnO, and CuO nanoparticles with relevance to plant performance in agriculture*. Industrial Biotechnology, 2012. **8**(6): p. 344-357.
291. Collins, D., et al., *Assessing the impact of copper and zinc oxide nanoparticles on soil: a field study*. PLoS One, 2012. **7**(8)
292. Wang, F., et al., *Combined effects of ZnO NPs and Cd on sweet sorghum as influenced by an arbuscular mycorrhizal fungus*. Chemosphere, 2018. **209**: p. 421-429.

293. Wang, F., et al., *Decreased ZnO nanoparticle phytotoxicity to maize by arbuscular mycorrhizal fungus and organic phosphorus*. Environmental Science and Pollution Research, 2018. **25**(24): p. 23736-23747.
294. Xu, J., et al., *Evaluation of zinc oxide nanoparticles on lettuce (*Lactuca sativa* L.) growth and soil bacterial community*. Environmental Science and Pollution Research, 2018. **25**(6): p. 6026-6035.
295. Mazaheri-Tirani, M. and S. Dayani, *In vitro effect of zinc oxide nanoparticles on *Nicotiana tabacum* callus compared to ZnO micro particles and zinc sulfate ($ZnSO_4$)*. Plant Cell, Tissue and Organ Culture (PCTOC), 2019.
296. Akaighe, N., et al., *Humic acid-induced silver nanoparticle formation under environmentally relevant conditions*. Environmental science and technology, 2011. **45**(9): p. 3895-3901.
297. Thapa, M., et al., *Zinc sulphide nanoparticle (nZnS): a novel nano-modulator for plant growth*. Plant Physiology and Biochemistry, 2019. **142**: p. 73-83.
298. Singh, M.D. and B.N.A. Kumar, *Bio efficacy of nano zinc sulphide (ZnS) on growth and yield of sunflower (*Helianthus annuus* L.) and nutrient status in the soil*. International Journal of Agricultural Sciences, 2017. **9**(6): p. 3795-3798.
299. García-Gómez, C., et al., *Comparative effect of ZnO NPs, ZnO bulk and $ZnSO_4$ in the antioxidant defences of two plant species growing in two agricultural soils under greenhouse conditions*. Science of The Total Environment, 2017. **589**: p. 11-24.
300. Singh, N.B., et al., *Zinc oxide nanoparticles as fertilizer for the germination, growth and metabolism of vegetable crops*. Journal of Nanoengineering and Nanomanufacturing, 2013. **3**(4): p. 353-364.
301. Khanm, H., B.A. Vaishnavi, and A.G. Shankar. *Raise of nano-fertilizer era: effect of nano scale zinc oxide particles on the germination, growth and yield of tomato (*Solanum lycopersicum*)*. International Journal of Current Microbiology and Applied Sciences, 2018. **7**(5): p. 1861-1871.
302. Kheyri, N., et al., *Effects of silicon and zinc nanoparticles on growth, yield, and biochemical characteristics of rice*. Agronomy, 2019. **11**(6): p. 3084-3090.
303. Baranowska-Korczyn, A., et al., *ZnS coating for enhanced environmental stability and improved properties of ZnO thin films*. RSC Advances, 2018. **8**: p. 24411-24421.
304. Patel, S.S., et al., *Foliar application of green synthesized zinc sulphide and zinc oxide nano particles enhances growth, root attributes, yield and oil quality of sunflower (*Helianthus Annuus* L.)*. Global Journal of Science Frontier Research: Agriculture and Veterinary, 2019. **19**(4).
305. Zulfiqar, F., et al., *Nanofertilizer use for sustainable agriculture: advantages and limitations*. Plant science, 2019. **289**.
306. Chhipa, H. and P. Joshi, *Nanofertilisers, nanopesticides and nanosensors in agriculture*, in *Nanoscience in Food and Agriculture*. 2016. p. 247-282.
307. NRCS. *Plants database*. 2019 [cited 2020 22/07]; Available from: <https://plants.usda.gov/core/profile?symbol=LOPE>.
308. Zhu, Z.-J., et al., *Effect of surface charge on the uptake and distribution of gold nanoparticles in four plant species*. Environmental Science and Technology, 2012. **46**(22).
309. Sun, R.-J., et al., *Effect of nanoparticle hydroxyapatite on the immobilization of Cu and Zn in polluted soil*. Environmental Science and Pollution Research, 2018. **25**(1): p. 73-80.

310. Liu, C.-W., et al., *Effects of Nitrogen Fertilizers on the Growth and Nitrate Content of Lettuce (Lactuca sativa L.)*. International Journal of Environmental Research and Public Health, 2014: p. 4427-4440.
311. Hough, R.L., et al., *Evaluating a 'free ion activity model' applied to metal uptake by Lolium perenne L. grown in contaminated soils*. Plant and Soil, 2005. **270**(1): p. 1-12.
312. Li, X., et al., *Sequential extraction of soils for multielement analysis by ICP-AES*. Chemical Geology, 1995. **124**(1): p. 109-123.
313. Crout, N.M., et al., *Kinetics of metal fixation in soils: measurement and modeling by isotopic dilution*. Environmental Toxicology and Chemistry, 2006. **25**(3): p. 659-663.
314. Ashman, M.R. and G. Puri, *Essential soil science*. 2002, Blackwell science.
315. Schaetzl, R.J. and M.L. Thompson, *Soils: genesis and geomorphology*. 2015, Cambridge University Press.
316. Anderson, P.R. and T.H. Christensen, *Distribution coefficients of Cd, Co, Ni, and Zn in soils*. European Journal of Soil Science, 1988. **39**(1).
317. Murphy, M.D. and J.M. Boggan, *Sulphur deficiency in herbage in Ireland: 1. Causes and extent*. Irish Journal of Agricultural Research, 1988. **27**(1): p. 83-90.
318. Mahler, R.L., *Nutrients plants require for growth*. University of Idaho. College of Agricultural and Life Science. CIS, 2004. **1124**.
319. Rendig, V.V., C. Oputa, and E.A. McComb, *Effects of sulfur deficiency on non-protein nitrogen, soluble sugars, and N/S ratios in young corn (Zea mays L.) plants*. Plant and Soil, 1976. **44**(2): p. 423-437.
320. Scott, N.M., et al., *Response of grassland to the application of sulphur at two sites in north-east Scotland*. Journal of the Science of Food and Agriculture, 1983. **34**(4): p. 357-361.
321. Murphy, M.D. and T. O'Donnell, *Sulphur deficiency in herbage in Ireland: 2. Sulphur fertilisation and its effect on yield and quality of herbage*. Irish Journal of Agricultural Research, 1989. **28**(1): p. 79-90.
322. Mathot, M., et al., *Positive effects of sulphur fertilisation on grasslands yields and quality in Belgium*. European journal of agronomy, 2008. **28**(4): p. 655-658.
323. Laing, G.D., *Redox metal processes and controls in estuaries: sequential extraction procedures*, in *Treatise on Estuarine and Coastal Science*. 2011.
324. Martin, J.M., P. Nirel, and A.J. Thomas, *Sequential extraction techniques: promises and problems*. Marine Chemistry, 1987. **22**(2): p. 313-341.
325. Voegelin, A., et al., *Zinc fractionation in contaminated soils by sequential and single extractions: influence of soil properties and zinc content*. Journal of Environmental Quality, 2008. **37**(3): p. 1190-1200.
326. Begum, N., et al., *Role of arbuscular mycorrhizal fungi in plant growth regulation: Implications in abiotic stress tolerance*. Frontiers in Plant Science, 2019. **10**(1068).
327. Stamets, P., *Mycelium running*. 2004, Ten Speed Press p. 256.
328. Smith, S.E. and D.J. Read, *Introduction*, in *Mycorrhizal Symbiosis (Second Edition)*, S.E. Smith and D.J. Read, Editors. 1997, Academic Press: London. p. 1-8.
329. Stamets, P., *Can mushrooms help save the world?* Explore (NY), 2006. **2**(2): p. 152-161.
330. Bano, S.A. and D. Ashfaq, *Role of mycorrhiza to reduce heavy metal stress*. Natural Science, 2013. **5**(12): p. 16.

331. Yang, Y., et al., *The effects of arbuscular mycorrhizal fungi on glomalin-related soil protein distribution, aggregate stability and their relationships with soil properties at different soil depths in lead-zinc contaminated area*. PLOS ONE, 2017. **12**(8)
332. Vodnik, D., et al., *The contribution of glomalin-related soil protein to Pb and Zn sequestration in polluted soil*. Science of The Total Environment, 2008. **392**(1): p. 130-136.
333. Saraswat, S. and J.P.N. Rai, *Mechanism of metal tolerance and detoxification in mycorrhizal fungi*, in *Bio-management of Metal-Contaminated Soils*, M.S. Khan, et al., Editors. 2011, Springer Netherlands: Dordrecht. p. 225-240.
334. Wang, F., et al., *Arbuscular mycorrhizae alleviate negative effects of zinc oxide nanoparticle and zinc accumulation in maize plants - a soil microcosm experiment*. Chemosphere, 2016. **147**: p. 88-97.
335. Li, S., et al., *Effects of ZnO nanoparticles, ZnSO₄ and arbuscular mycorrhizal fungus on the growth of maize*. Huan Jing Ke Xue, 2015. **36**(12): p. 4615-4622.
336. Ghasemi Siani, N., et al., *Natural amelioration of zinc oxide nanoparticle toxicity in fenugreek (Trigonella foenum-gracum) by arbuscular mycorrhizal (Glomus intraradices) secretion of glomalin*. Plant Physiol Biochem, 2017. **112**: p. 227-238.
337. Wang, W.-Z., et al., *Arbuscular mycorrhizal symbiosis influences the biological effects of Nano-ZnO on maize*. Huan Jing Ke Xue, 2014. **35**: p. 3135-3141.
338. Watts-Williams, S.J., et al., *Uptake of zinc and phosphorus by plants is affected by zinc fertiliser material and arbuscular mycorrhizas*. Plant and Soil, 2014. **376**(1): p. 165-175.
339. Cao, J., et al., *Arbuscular mycorrhizal fungi alleviate the negative effects of iron oxide nanoparticles on bacterial community in rhizospheric soils*. Frontiers in Environmental Science, 2016. **4**(10).
340. Cao, J., et al., *Iron oxide magnetic nanoparticles deteriorate the mutual interaction between arbuscular mycorrhizal fungi and plant*. Journal of Soils and Sediments, 2017. **17**(3): p. 841-851.
341. Feng, Y., et al., *The role of metal nanoparticles in influencing arbuscular mycorrhizal fungi effects on plant growth*. Environmental Science and Technology, 2013. **47**(16): p. 9496-9504.
342. Jan, J., M. Ahmad, and F. Emmanuel, *Long-distance transport of P and Zn through the hyphae of an arbuscular mycorrhizal fungus in symbiosis with maize*. Agronomie, 2003. **23**(5-6): p. 481-488.
343. Coccina, A., et al., *The mycorrhizal pathway of zinc uptake contributes to zinc accumulation in barley and wheat grain*. BMC Plant Biology, 2019. **19**.
344. Watts-Williams, S.J., et al., *How important is the mycorrhizal pathway for plant Zn uptake?* Plant and Soil, 2015. **390**(1): p. 157-166.
345. Zahajská, P., et al., *What is diatomite?* Quaternary Research, 2020. **96**: p. 48-52.
346. Brundrett, M.C., Y. Piché, and R.L. Peterson, *A new method for observing the morphology of vesicular–arbuscular mycorrhizae*. Canadian Journal of Botany, 1984. **62**(10): p. 2128-2134.
347. Sun, X.-G. and M. Tang, *Comparison of four routinely used methods for assessing root colonization by arbuscular mycorrhizal fungi*. Botany, 2012. **90**(11): p. 1073-1083.
348. Hamon, R.E., D.R. Parker, and E. Lombi, *Advances in Isotopic dilution techniques in trace element research: a review of methodologies, benefits, and limitations*, in *Advances in Agronomy*. 2008, Academic Press. p. 289-343.

349. Lum, T.-S. and K. Sze-Yin Leung, *Strategies to overcome spectral interference in ICP-MS detection*. Journal of Analytical Atomic Spectrometry, 2016. **31**(5): p. 1078-1088.
350. Du, W., et al., *Comparison study of zinc nanoparticles and zinc sulphate on wheat growth: from toxicity and zinc biofortification*. Chemosphere, 2019. **227**: p. 109-116.
351. Ma, X., et al., *Arbuscular mycorrhizal fungi increase both concentrations and bioavailability of Zn in wheat (*Triticum aestivum* L) grain on Zn-spiked soils*. Applied Soil Ecology, 2019. **135**: p. 91-97.
352. Tran, B.T.T., T.R. Cavagnaro, and S.J. Watts-Williams, *Arbuscular mycorrhizal fungal inoculation and soil zinc fertilisation affect the productivity and the bioavailability of zinc and iron in durum wheat*. Mycorrhiza, 2019. **29**(5): p. 445-457.
353. Jewiss, O.R., *Tillering in grasses - its significance and control*. Grass and Forage Science, 1972. **27**(2): p. 65-82.
354. Gange, A.C., et al., *A comparison of visualization techniques for recording arbuscular mycorrhizal colonization*. New Phytologist, 1999. **142**(1): p. 123-132.
355. Deguchi, S., et al., *Proposal of a new estimation method of colonization rate of arbuscular mycorrhizal fungi in the roots of *Chengioplanax sciadophylloides**. Mycobiology, 2017. **45**(1): p. 15-19.
356. Becker, W.N. and J.W. Gerdemann, *Colorimetric quantification of vesicular-arbuscular mycorrhizal infection in onion*. New Phytologist, 1977. **78**(2): p. 289-295.
357. Díaz, G., C. Azcón-Aguilar, and M. Honrubia, *Influence of arbuscular mycorrhizae on heavy metal (Zn and Pb) uptake and growth of *Lygeum spartum* and *Anthyllis cytisoides**. Plant and Soil, 1996. **180**: p. 241-249.
358. Cavagnaro, T., S. Dickson, and F.A. Smith, *Arbuscular mycorrhizas modify plant responses to soil zinc addition*. Plant and Soil, 2010. **329**(1): p. 307-313.
359. Mohandas, S., *Effect of VAM inoculation on plant growth, nutrient level and root phosphatase activity in papaya (*Carica papaya* cv. Coorg Honey Dew)*. Fertilizer research, 1992. **31**: p. 263-267.
360. Bagayoko, M.G., E. Römheld, V. Buerkert, A., *Effects of mycorrhizae and phosphorus on growth and nutrient uptake of millet, cowpea and sorghum on a West African soil*. The Journal of Agricultural Science, 2000. **135**(4).
361. Alloush, G. and R.B. Clark, *Maize response to phosphate rock and arbuscular mycorrhizal fungi in acidic soil*. Communications in Soil Science and Plant Analysis, 2001. **32**(1): p. 231-254.
362. Ortas, I., et al., *Mycorrhizal dependency of sour orange in relation to phosphorus and zinc nutrition*. Journal of Plant Nutrition, 2002. **25**(6): p. 1263-1279.
363. Cavagnaro, T.R., et al., *Growth, nutrition, and soil respiration of a mycorrhiza-defective tomato mutant and its mycorrhizal wild-type progenitor*. Functional Plant Biology, 2008. **35**: p. 228-235.
364. Karagiannidis, N., et al., *Effects of different N fertilizers on the activity of *Glomus mosseae* and on grapevine nutrition and berry composition*. Mycorrhiza, 2007. **18**(1): p. 43-50.
365. Abdel-Aziz, R.A. and R. Samir, *Reducing the heavy metals toxicity in sludge amended soil using VA mycorrhizae*. Egyptian Journal of Microbiology, 1997. **32**(2): p. 217-234.
366. Bi, Y.L., X.L. Li, and P. Christie, *Influence of early stages of arbuscular mycorrhiza on uptake of zinc and phosphorus by red clover from a low-*

- phosphorus soil amended with zinc and phosphorus*. Chemosphere, 2003. **50**(6): p. 831-837
367. Lehmann, A., et al., *Arbuscular mycorrhizal influence on zinc nutrition in crop plants – a meta-analysis*. Soil Biology and Biochemistry, 2014. **69**: p. 123-131.
368. Delavaux, C.S., L.M. Smith-Ramesh, and S.E. Kuebbing, *Beyond nutrients: a meta-analysis of the diverse effects of arbuscular mycorrhizal fungi on plants and soils*. Ecology, 2017. **98**(8): p. 2111-2119.
369. Upadhyaya, H., et al., *Physiological impact of zinc nanoparticle on germination of rice (Oryza sativa L) seed*. Journal of Plant Science and Phytopathology, 2017. **1**: p. 62-70.
370. Stanković, M., et al., *Influence of zinc (Zn) on germination of wheat (Triticum Aestivum L.)*. Biotechnology & Biotechnological Equipment, 2010. **24**(1): p. 236-239.
371. Gokak, I.B. and T.C. Taranath, *Seed germination and growth responses of Macrotyloma uniflorum (Lam.) Verdc. exposed to zinc and zinc nanoparticles*. International Journal Of Environmental Sciences 2015. **5**(4): p. 840-847.
372. Bae, J., D.L. Benoit, and A.K. Watson, *Effect of heavy metals on seed germination and seedling growth of common ragweed and roadside ground cover legumes*. Environmental Pollution, 2016. **213**: p. 112-118.
373. Saeed, M.F., R. L., *Relations between suspension pH and zinc solubility in acid and calcareous soils*. Soil Science, 1977. **124**(4): p. 199-204.
374. Marzouk, E.R., S.R. Chenery, and S.D. Young, *Predicting the solubility and lability of Zn, Cd, and Pb in soils from a minespoil-contaminated catchment by stable isotopic exchange*. Geochimica et Cosmochimica Acta, 2013. **123**: p. 1-16.
375. Izquierdo, M., et al., *Measurement of isotopically-exchangeable Zn in Zn-deficient paddy soil*. European Journal of Soil Science, 2016. **67**(1): p. 51-59.
376. Ayoub, A.S., et al., *Phytoavailability of Cd and Zn in soil estimated by stable isotope exchange and chemical extraction*. Plant and Soil, 2003. **252**(2): p. 291-300.
377. Izquierdo, M., A.M. Tye, and S.R. Chenery, *Lability, solubility and speciation of Cd, Pb and Zn in alluvial soils of the River Trent catchment UK*. Environmental Science: Processes and Impacts, 2013. **15**(10): p. 1844-1858.
378. Degryse, F., et al., *Soil solution concentration of Cd and Zn can be predicted with a CaCl₂ soil extract*. European Journal of Soil Science, 2003. **54**(1): p. 149-158.
379. Sterckeman, T., et al., *Quantifying the effect of rhizosphere processes on the availability of soil cadmium and zinc*. Plant and Soil, 2005. **276**(1): p. 335-345.
380. Stacey, S., G. Merrington, and M.J. McLaughlin, *The effect of aging biosolids on the availability of cadmium and zinc in soil*. European Journal of Soil Science, 2001. **52**(2): p. 313-321.
381. Hamon, R.E., M.J. McLaughlin, and G. Cozens, *Mechanisms of attenuation of metal availability in in situ remediation treatments*. Environmental Science and Technology, 2002. **36**(18): p. 3991-3996.
382. Xia, H., et al., *Elucidating the source–sink relationships of zinc biofortification in wheat grains: a review*. Food and Energy Security, 2020. **9**(4).
383. Velu, G., et al., *Biofortification strategies to increase grain zinc and iron concentrations in wheat*. Journal of Cereal Science, 2014. **59**(3): p. 365-372.
384. Rashid, A., et al., *Effect of zinc-biofortified seeds on grain yield of wheat, rice, and common bean grown in six countries*. Journal of Plant Nutrition and Soil Science, 2019. **182**(5): p. 791-804.

385. Hassan, N., et al., *Potential of zinc seed treatment in improving stand establishment, phenology, yield and grain biofortification of wheat*. Journal of Plant Nutrition, 2019. **42**(14).
386. Rehman, A. and M. Farooq, *Zinc seed coating improves the growth, grain yield and grain biofortification of bread wheat*. Acta Physiologiae Plantarum, 2016. **38**.
387. Wang, S., X. Tian, and Q. Liu, *The effectiveness of foliar applications of zinc and biostimulants to increase zinc concentration and bioavailability of wheat grain*. Agronomy, 2020. **10**(2).
388. Aghili, F., et al., *Green manure addition to soil increases grain zinc concentration in bread wheat*. PLoS One, 2014. **9**(7).
389. Grüter, R., et al., *Green manure effects on zinc and cadmium accumulation in wheat grains (Triticum aestivum L.) on high and low zinc soils*. Plant and Soil volume, 2018. **422**: p. 437-453.
390. Gupta, P.K., et al., *Biofortification and bioavailability of Zn, Fe and Se in wheat: present status and future prospects*. Theoretical and Applied Genetics, 2020.
391. Huang, T., et al., *Grain zinc concentration and its relation to soil nutrient availability in different wheat cropping regions of China*. Soil and Tillage Research, 2019. **191**: p. 57-65.
392. McGrath, S.P., et al., *Biofortification of zinc in wheat grain by the application of sewage sludge*. Plant and Soil, 2012. **361**: p. 97-108.
393. Schweizer, S.A., et al., *Impact of organic and conventional farming systems on wheat grain uptake and soil bioavailability of zinc and cadmium*. Science of The Total Environment, 2018. **639**: p. 608-616.
394. Helfenstein, J., et al., *Organic wheat farming improves grain zinc concentration*. PLoS One, 2016. **11**(8).
395. Das, S., et al., *Zinc biofortification in the grains of two wheat (Triticum aestivum L.) varieties through fertilization*. Acta Agrobotanica, 2020. **73**(1): p. 1-13.
396. Zhao, A.-Q., et al., *Comparison of soil and foliar zinc application for enhancing grain zinc content of wheat when grown on potentially zinc-deficient calcareous soils*. Journal of the Science of Food and Agriculture, 2014. **94**(10): p. 2016-2022.
397. Hussain, S., et al., *Biofortification and estimated human bioavailability of zinc in wheat grains as influenced by methods of zinc application*. Plant and Soil, 2012. **361**: p. 279-290.
398. Wang, J., et al., *Different increases in maize and wheat grain zinc concentrations caused by soil and foliar applications of zinc in Loess Plateau, China*. Field Crops Research, 2012. **135**: p. 89-96.
399. Yang, X., et al., *Effect of soil and foliar zinc application on zinc concentration and bioavailability in wheat grain grown on potentially zinc-deficient soil*. Cereal Research Communications, 2011. **39**(4): p. 535-543.
400. Wang, X.-Z., et al., *An effective strategy to improve grain zinc concentration of winter wheat, aphids prevention and farmers' income*. Field Crops Research, 2015. **184**: p. 74-79.
401. Ning, P., et al., *Enhancing zinc accumulation and bioavailability in wheat grains by integrated zinc and pesticide application*. Agronomy, 2019. **9**(9).
402. Jalal, A., et al., *Agro-biofortification of zinc and iron in wheat grains*. Gesunde Pflanzen, 2020. **72**: p. 227-236.

403. Doolette, C.L., et al., *Foliar application of zinc sulfate and Zinc EDTA to wheat leaves: differences in mobility, distribution and speciation*. Journal of Experimental Botany, 2018.
404. Yang, X.-W., et al., *Foliar zinc fertilization improves the zinc nutritional value of wheat (*Triticum aestivum* L.) grain*. African Journal of Biotechnology, 2011. **10**(66): p. 14778-14785.
405. Doolette, C.L., et al., *Zinc from foliar-applied nanoparticle fertiliser is translocated to wheat grain: a ⁶⁵Zn radiolabelled translocation study comparing conventional and novel foliar fertilisers*. Science of The Total Environment, 2020. **749**.
406. Diatterich, L.H., C. Gonneau, and B.B. Casper, *Arbuscular mycorrhizal colonization has little consequence for plant heavy metal uptake in contaminated field soils*. Ecological Applications: a Publication of the Ecological Society of America, 2017. **27**(6): p. 1862-1875.
407. Rauscher, H., K. Rasmussen, and B. Sokull-Klüttgen, *Regulatory aspects of nanomaterials in the EU*. Chemie Ingenieur Technik, 2017. **89**(3): p. 224-231.
408. Murphy, F., et al., *Insuring nanotech requires effective risk communication*. Nature Nanotechnology, 2017. **12**: p. 717.
409. Stefaniak, A.B., et al., *Nanoscale reference materials for environmental, health and safety measurements: needs, gaps and opportunities*. Nanotoxicology, 2013. **7**(8): p. 1325-1337.
410. McCoy, P., *Radical mycology: a treatise on seeing & working with fungi*. 2016: Chthaeus Press.
411. Sheldrake, M., *Entangled life*. 2020: The Bodley Head.
412. Stamets, P., *Mycelium running*. 2004, Ten Speed Press.
413. Josko, I., P. Oleszczuk, and E. Skwarek, *Toxicity of combined mixtures of nanoparticles to plants*. J Hazard Mater, 2017. **331**: p. 200-209.
414. Joško, I. and P. Oleszczuk, *Influence of soil type and environmental conditions on ZnO, TiO₂ and Ni nanoparticles phytotoxicity*. Chemosphere, 2013. **92**(1): p. 91-99.
415. Lv, J., P. Christie, and S. Zhang, *Uptake, translocation, and transformation of metal-based nanoparticles in plants: recent advances and methodological challenges*. Environmental science. Nano, 2019. **6**: p. 41-59.
416. Gardea-Torresdey, J.L., C.M. Rico, and J.C. White, *Trophic transfer, transformation, and impact of engineered nanomaterials in terrestrial environments*. Environmental Science and Technology, 2014. **48**(5): p. 2526-2540.
417. Lammel, T., et al., *Trophic transfer of CuO NPs from sediment to worms (*Tubifex tubifex*) to fish (*Gasterosteus aculeatus*): a comparative study of dissolved Cu and NPs enriched with a stable isotope tracer (⁶⁵Cu)*. Environmental science: Nano, 2020.
418. Judy, J., J.M. Unrine, and P.M. Bertsch, *Evidence for biomagnification of gold nanoparticles within a terrestrial food chain*. Environmental Science and Technology, 2011. **45**: p. 776-781.
419. Unrine, J.M., et al., *Trophic transfer of Au nanoparticles from soil along a simulated terrestrial food chain*. Environmental Science and Technology, 2012. **46**: p. 9753-9760.
420. Hawthorne, J., et al., *Particle-size dependent accumulation and trophic transfer of cerium oxide through a terrestrial food chain*. Environmental Science and Technology, 2014. **48**: p. 13102-13109.

421. De La Torre-Roche, R., et al., *Terrestrial trophic transfer of bulk and nanoparticle La₂O₃ does not depend on particle size*. Environmental Science and Technology, 2015. **49**: p. 11866-11874.
422. Skjolding, L.M., M. Winther-Nielsen, and A. Baun, *Trophic transfer of differently functionalized zinc oxide nanoparticles from crustaceans (Daphnia magna) to zebrafish (Danio rerio)*. Aquatic Toxicology, 2014. **157**: p. 101-108.
423. Schimpf, M.E., K. Caldwell, and J.C. Giddings, *Field-flow fractionation handbook*. 2000: John Wiley & Sons.
424. Pornwilard, M.-M. and A. Siripinyanond, *Field-flow fractionation with inductively coupled plasma mass spectrometry: past, present, and future*. Journal of Analytical Atomic Spectrometry, 2014. **29**(10): p. 1739-1752.
425. Contado, C., *Field flow fractionation techniques to explore the "nano-world"*. 2017. **409**: p. 2501-2518.
426. Amde, M., Z.-Q. Tan, and J. Liu, *Separation and size characterization of zinc oxide nanoparticles in environmental waters using asymmetrical flow field-flow fractionation*. Talanta, 2019. **200**: p. 357-365.
427. Jang, M.-H., S. Lee, and Y.S. Hwang, *Characterization of silver nanoparticles under environmentally relevant conditions using asymmetrical flow field-flow fractionation (AF4)*. Plos one, 2015. **10**(11).
428. Peters, R., et al., *Single particle ICP-MS combined with a data evaluation tool as a routine technique for the analysis of nanoparticles in complex matrices*. Journal of Analytical Atomic Spectrometry, 2015. **30**(6): p. 1274-1285.
429. Laborda, F., E. Bolea, and J. Jiménez-Lamana, *Single particle inductively coupled plasma mass spectrometry: a powerful tool for nanoanalysis*. Analytical Chemistry, 2014. **86**(5): p. 2270-2278.
430. Kutscher, D., J.D. Wills, and S. McSheehy Ducos. *Nanoparticle characterization via single particle inductively coupled plasma – mass spectrometry (spICP-MS) using a dedicated plug-in for Qtegra ISDS software*. 2016 [cited 2020 20 June]; Available from: <https://tools.thermofisher.com/content/sfs/brochures/TN-43279-LC-MS-nanoparticles-spICP-MS-npQuant-Qtegra-TN43279-EN.pdf>.
431. Stephan, C. and K. Neubauer. *Single particle inductively coupled plasma mass spectrometry: understanding how and why*. 2014 [cited 2020 20 June]; Available from: <https://www.perkinelmer.com/lab-solutions/resources/docs/NanoSingleParticleICPMSTheory.pdf>.
432. Sannac, S. *Single particle analysis of nanomaterials using the Agilent 7900 ICP-MS*. 2015 [cited 2020 20 June]; Available from: https://www.agilent.com/cs/library/applications/5991-4401EN_AppNote_ICP-MS7900_nanoparticles.pdf.
433. Lee, W.W. and W.T. Chan, *Calibration of single-particle inductively coupled plasma-mass spectrometry (SP-ICP-MS)*. Journal of Analytical Atomic Spectrometry, 2015. **30**(6): p. 1245-1254.
434. Montañó, M.D., et al., *Improvements in the detection and characterization of engineered nanoparticles using spICP-MS with microsecond dwell times*. Environmental Science: Nano, 2014. **1**(4): p. 338-346.
435. Laborda, F., et al., *Critical considerations for the determination of nanoparticle number concentrations, size and number size distributions by single particle ICP-MS*. Journal of Analytical Atomic Spectrometry, 2013. **28**(8): p. 1220.
436. Olesik, J.W. and P.J. Gray, *Considerations for measurement of individual nanoparticles or microparticles by ICP-MS: determination of the number of*

- particles and the analyte mass in each particle*. Journal of Analytical Atomic Spectrometry, 2012. **27**(7): p. 1143-1155.
437. Hineman, A. and C. Stephan, *Effect of dwell time on single particle inductively coupled plasma mass spectrometry data acquisition quality*. Journal of Analytical Atomic Spectrometry, 2014. **29**(7): p. 1252-1257.
438. Pace, H.E., et al., *Determining transport efficiency for the purpose of counting and sizing nanoparticles via single particle inductively coupled plasma mass spectrometry*. Analytical chemistry, 2011. **83**(24): p. 9361-9369.
439. Ho, K.S., et al., *Considerations of particle vaporization and analyte diffusion in single-particle inductively coupled plasma-mass spectrometry*. Spectrochimica Acta Part B: Atomic Spectroscopy, 2013. **89**: p. 30-39.
440. Fréchette-Viens, L., M. Hadioui, and K.J. Wilkinson, *Practical limitations of single particle ICP-MS in the determination of nanoparticle size distributions and dissolution: case of rare earth oxides*. Talanta, 2016.
441. Pace, H.E., et al., *Single particle inductively coupled plasma-mass spectrometry: a performance evaluation and method comparison in the determination of nanoparticle size*. Environmental science and technology, 2012. **46**(22): p. 12272-12280.
442. Reed, R.B., et al., *Overcoming challenges in analysis of polydisperse metal-containing nanoparticles by single particle inductively coupled plasma mass spectrometry*. Journal of Analytical Atomic Spectrometry, 2012. **27**(7): p. 1093-1100.
443. Lee, S., et al., *Nanoparticle size detection limits by single particle ICP-MS for 40 elements*. Environmental science and technology, 2014. **48**(17): p. 10291-10300.
444. Hadioui, M., C. Peyrot, and K.J. Wilkinson, *Improvements to single particle ICPMS by the online coupling of ion exchange resins*. Analytical chemistry, 2014. **86**(10): p. 4668-4674.
445. Tuoriniemi, J., G. Cornelis, and M. Hasselov, *A new peak recognition algorithm for detection of ultra-small nano-particles by single particle ICP-MS using rapid time resolved data acquisition on a sector-field mass spectrometer*. Journal Of Analytical Atomic Spectrometry, 2015. **30**(8): p. 1723-1729.
446. Larner, F. and M. Rehkämper, *Evaluation of stable isotope tracing for ZnO nanomaterials - new constraints from high precision isotope analyses and modeling*. Environmental science and technology, 2012. **46**(7): p. 4149-4158.
447. Gulson, B., et al., *Small amounts of zinc from zinc oxide particles in sunscreens applied outdoors are absorbed through human skin*. Toxicological sciences : an official journal of the Society of Toxicology, 2010. **118**(1): p. 140-149.
448. Larner, F., et al., *An inter-laboratory comparison of high precision stable isotope ratio measurements for nanoparticle tracing in biological samples*. Journal of Analytical Atomic Spectrometry, 2014. **29**(3): p. 471-477.
449. Khan, F.R., et al., *Stable isotope tracer to determine uptake and efflux dynamics of ZnO nano- and bulk particles and dissolved Zn to an estuarine snail*. Environmental science and technology, 2013. **47**(15): p. 8532-8539.
450. Li, L.-Z., et al., *Toxicity of zinc oxide nanoparticles in the earthworm, Eisenia fetida and subcellular fractionation of Zn*. Environment International, 2011. **37**(6): p. 1098-1104.
451. Margulis, L., *Symbiotic planet: a new look at evolution*. 1998.

Appendix

7.1 Additional information for chapter 4

Contrasts

C1 – Control vs all Zn treatments

C2 – (ZnO NPs and ZnSO₄) vs (Zn₃(PO₄)₂ and ZnS NPs)

C3 – ZnO NPs vs ZnSO₄

C4 – Zn₃(PO₄)₂ vs ZnS NPs

C5 – Harvest effect vs no harvest effect

C6 – Linear concentration vs non-linear concentration

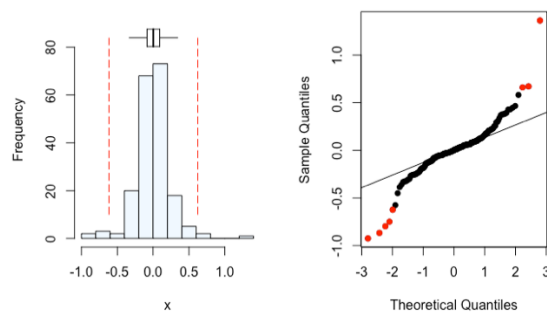
C7 – Quadratic concentration vs non-quadratic concentration

7.1.1 Grass dry weight

Unlogged data

Exp model AIC – 211.834

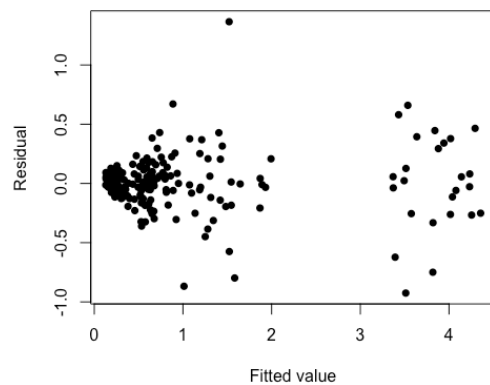
Sp model AIC – 209.834



8 outliers

Skewness – 0.2744484

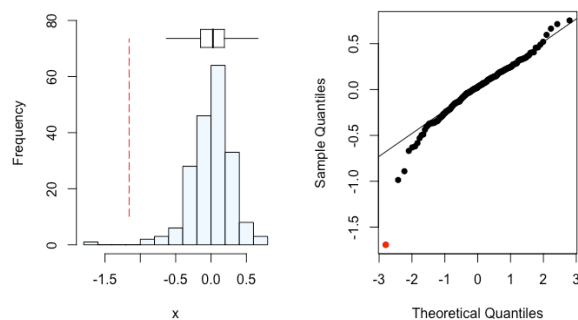
Octile skewness – -0.06401878



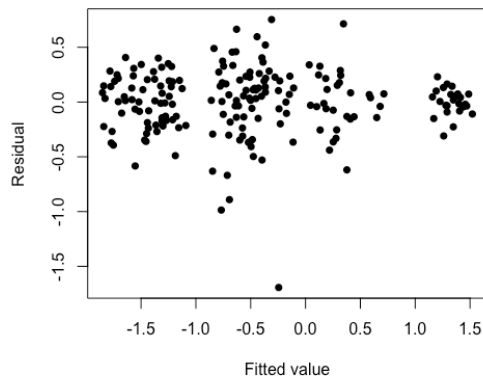
Logged data

Exp model AIC – 266.6414

Sp model AIC – 264.6414



1 outlier – looks normal
 Skewness – -1.210766
 Octile skewness – -0.1355239



Logged and Sp model data chosen for orthogonal contrasts

Table 7.1 Grass dry weight

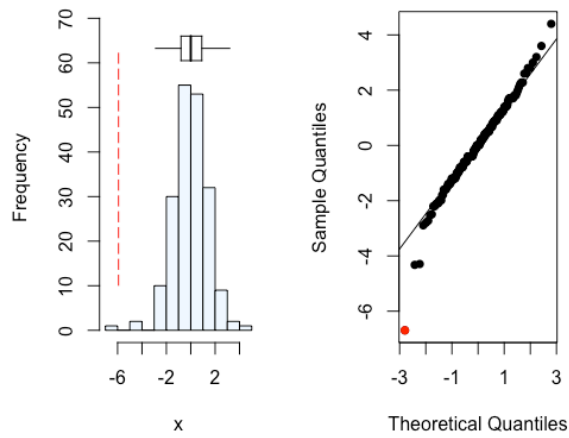
	numDF	denDF	F-value	p-value
(Intercept)	1	103	360.1398	< 0.0001
Rep	4	48	1.2600	0.2987
C1	1	48	0.8381	0.3645
C2	1	48	12.2587	0.0010
C3	1	48	35.7285	< 0.0001
C4	1	48	19.2469	0.0001
C5	2	103	618.0356	< 0.0001
C6	1	48	0.3924	0.5340
C7	1	48	0.0049	0.9444
C2:C6	1	48	4.4359	0.0404
C2:C7	1	48	3.7132	0.0599
C3:C6	1	48	3.5010	0.0674
C3:C7	1	48	3.4570	0.0691
C4:C6	1	48	3.5911	0.0641
C4:C7	1	48	0.3170	0.5761
C1:C5	2	103	2.7068	0.0715
C2:C5	2	103	2.1131	0.1261
C3:C5	2	103	35.5786	< 0.0001
C4:C5	2	103	31.4155	< 0.0001
C6:C5	2	103	0.7702	0.4656
C7:C5	2	103	0.2742	0.7608
C2:C6:C5	2	103	0.8614	0.4256
C2:C7:C5	2	103	2.4371	0.0924
C3:C6:C5	2	103	0.4291	0.6522
C3:C7:C5	2	103	0.3396	0.7128
C4:C6:C5	2	103	1.6929	0.1891
C4:C7:C5	2	103	5.7015	0.0045

7.1.2 Stem length

Unlogged data

Exp model AIC – 748.4434

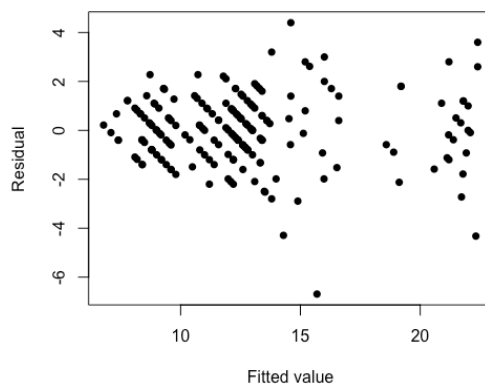
Sp model AIC – 746.4715



1 outlier – looks normal

Skewness - -0.4659144

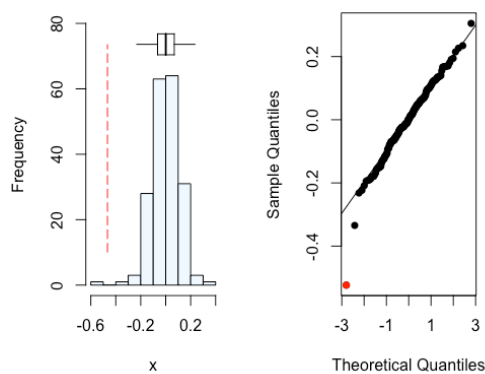
Octile skewness – 0.05699482



Logged data

Exp model AIC – -32.70200

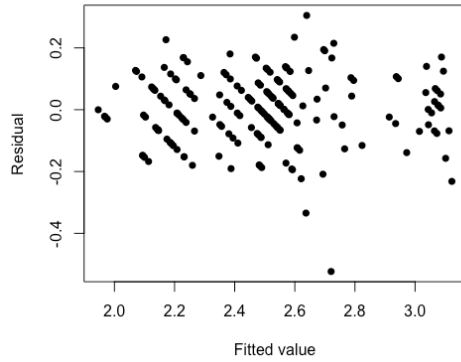
Sp model AIC – -34.63217



1 outlier – same as unlogged data

Skewness – -0.5891962

Octile skewness – -0.01537912



Unlogged and Sp model data chosen for orthogonal contrasts

Table 7.2 Stem length

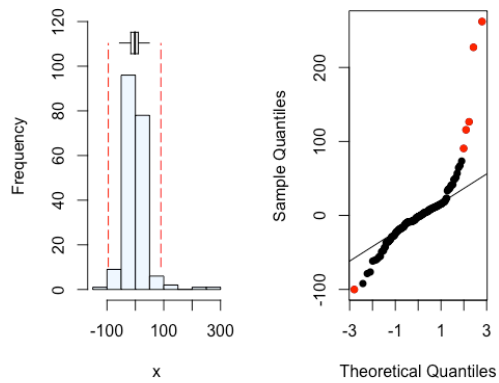
	numDF	denDF	F-value	p-value
(Intercept)	1	103	2719.1978	< 0.0001
Rep	4	48	1.4914	0.2196
C1	1	48	7.6059	0.0082
C2	1	48	19.7217	0.0001
C3	1	48	248.2668	< 0.0001
C4	1	48	123.2244	< 0.0001
C5	2	103	962.3427	< 0.0001
C6	1	48	8.7671	0.0048
C7	1	48	6.8661	0.0117
C2:C6	1	48	10.6704	0.0020
C2:C7	1	48	3.7455	0.0589
C3:C6	1	48	5.6822	0.0211
C3:C7	1	48	0.2366	0.6289
C4:C6	1	48	27.2686	< 0.0001
C4:C7	1	48	3.7505	0.0587
C1:C5	2	103	16.6305	< 0.0001
C2:C5	2	103	14.0082	< 0.0001
C3:C5	2	103	237.5211	< 0.0001
C4:C5	2	103	118.3469	< 0.0001
C6:C5	2	103	7.0738	0.0013
C7:C5	2	103	7.0794	0.0013
C2:C6:C5	2	103	6.6908	0.0019
C2:C7:C5	2	103	1.3455	0.2650
C3:C6:C5	2	103	3.6510	0.0294
C3:C7:C5	2	103	0.1318	0.8767
C4:C6:C5	2	103	19.6951	< 0.0001
C4:C7:C5	2	103	10.0030	0.0001

7.1.3 Grass total zinc concentration

Unlogged data

Exp model AIC – 1737.470

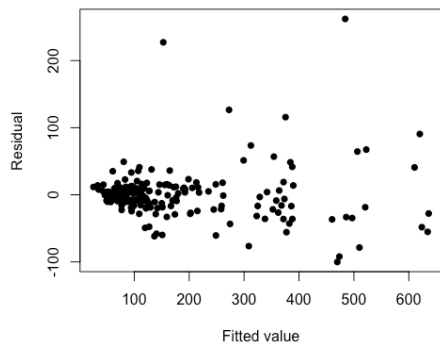
Sp model AIC – 1735.686



6 outliers

Skewness – 2.756332

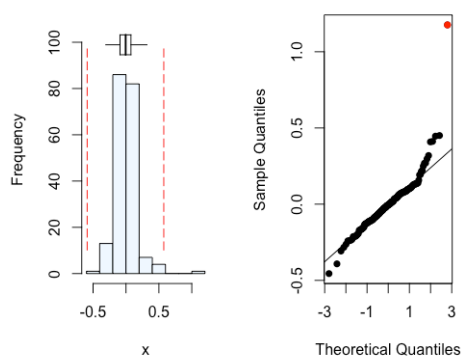
Octile skewness – -0.1478611



Logged data

Exp model AIC – 79.21544

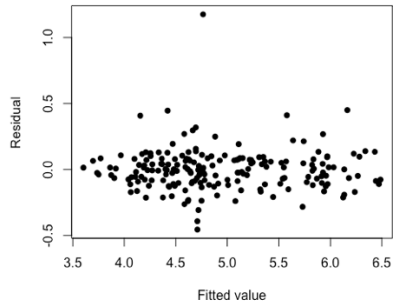
Sp model AIC – 77.49283



1 outlier

Skewness – 2.154314

Octile skewness – -0.07012689



Logged and Sp model data chosen for orthogonal contrasts

Table 7.3 Grass total zinc concentration

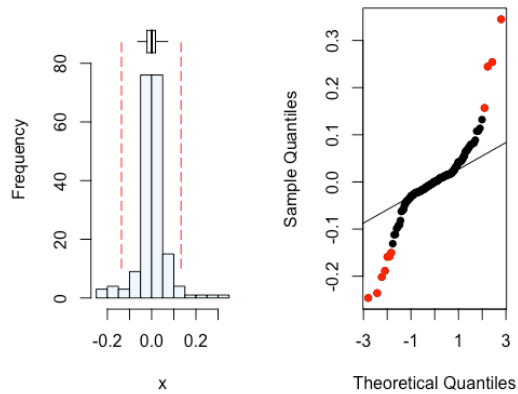
	numDF	denDF	F-value	p-value
(Intercept)	1	103	360.1398	< 0.0001
Rep	4	48	1.2600	0.2987
C1	1	48	0.8381	0.3645
C2	1	48	12.2587	0.0010
C3	1	48	35.7285	< 0.0001
C4	1	48	19.2469	0.0001
C5	2	103	618.0356	< 0.0001
C6	1	48	0.3924	0.5340
C7	1	48	0.0049	0.9444
C2:C6	1	48	4.4359	0.0404
C2:C7	1	48	3.7132	0.0599
C3:C6	1	48	3.5010	0.0674
C3:C7	1	48	3.4570	0.0691
C4:C6	1	48	3.5911	0.0641
C4:C7	1	48	0.3170	0.5761
C1:C5	2	103	2.7068	0.0715
C2:C5	2	103	2.1131	0.1261
C3:C5	2	103	35.5786	< 0.0001
C4:C5	2	103	31.4155	< 0.0001
C6:C5	2	103	0.7702	0.4656
C7:C5	2	103	0.2742	0.7608
C2:C6:C5	2	103	0.8614	0.4256
C2:C7:C5	2	103	2.4371	0.0924
C3:C6:C5	2	103	0.4291	0.6522
C3:C7:C5	2	103	0.3396	0.7128
C4:C6:C5	2	103	1.6929	0.1891
C4:C7:C5	2	103	5.7015	0.0045

7.1.4 Grass zinc offtake

Unlogged data

Exp model AIC – -190.8758

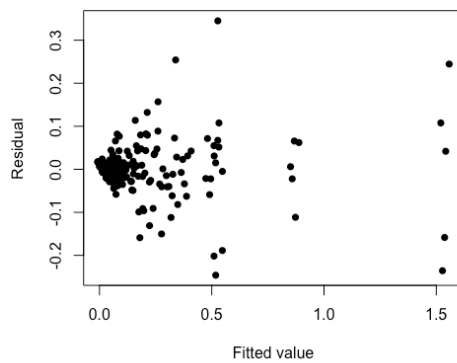
Sp model AIC – -191.8057



11 outliers

Skewness – 0.4320683

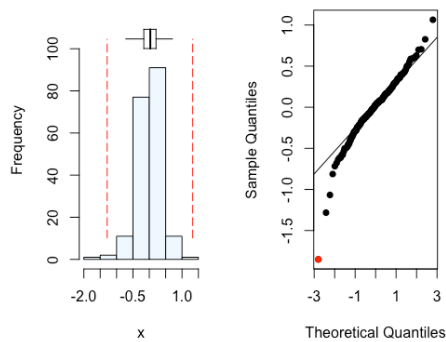
Octile skewness – 0.07143221



Logged data

Exp model AIC – 322.059

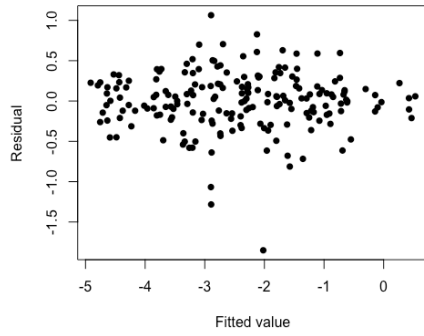
Sp model AIC – 320.059



1 outlier

Skewness – -0.9331245

Octile skewness – -0.09040364



Logged and Sp model data chosen for orthogonal contrasts

Table 7.4 Grass zinc offtake

	numDF	denDF	F-value	p-value
(Intercept)	1	103	360.1398	< 0.0001
Rep	4	48	1.2600	0.2987
C1	1	48	0.8381	0.3645
C2	1	48	12.2587	0.0010
C3	1	48	35.7285	< 0.0001
C4	1	48	19.2469	0.0001
C5	2	103	618.0356	< 0.0001
C6	1	48	0.3924	0.5340
C7	1	48	0.0049	0.9444
C2:C6	1	48	4.4359	0.0404
C2:C7	1	48	3.7132	0.0599
C3:C6	1	48	3.5010	0.0674
C3:C7	1	48	3.4570	0.0691
C4:C6	1	48	3.5911	0.0641
C4:C7	1	48	0.3170	0.5761
C1:C5	2	103	2.7068	0.0715
C2:C5	2	103	2.1131	0.1261
C3:C5	2	103	35.5786	< 0.0001
C4:C5	2	103	31.4155	< 0.0001
C6:C5	2	103	0.7702	0.4656
C7:C5	2	103	0.2742	0.7608
C2:C6:C5	2	103	0.8614	0.4256
C2:C7:C5	2	103	2.4371	0.0924
C3:C6:C5	2	103	0.4291	0.6522
C3:C7:C5	2	103	0.3396	0.7128
C4:C6:C5	2	103	1.6929	0.1891
C4:C7:C5	2	103	5.7015	0.0045

7.2 Additional information for chapter 5

Contrasts

C1 – Control vs all Zn treatments

C2 – (ZnO NPs and ZnSO₄) vs (Zn₃(PO₄)₂ and ZnS NPs)

C3 – ZnO NPs vs ZnSO₄

C4 – Zn₃(PO₄)₂ vs ZnS NPs

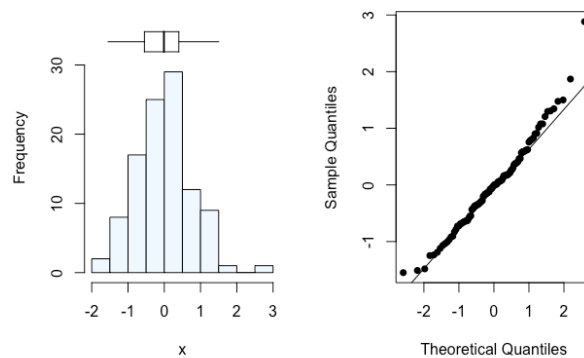
C5 – AMF added vs AMF not added

C6 – Linear concentration vs non-linear concentration

C7 – Quadratic concentration vs non-quadratic concentration

7.2.1 Stem/Leaf dry weight

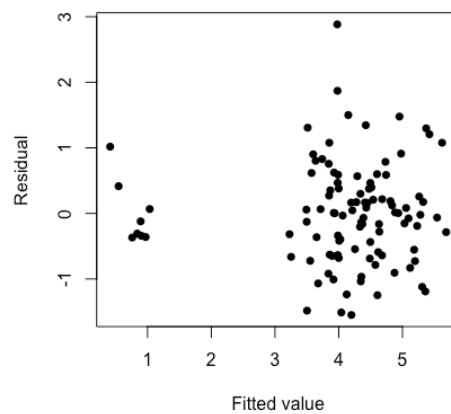
unlogged data



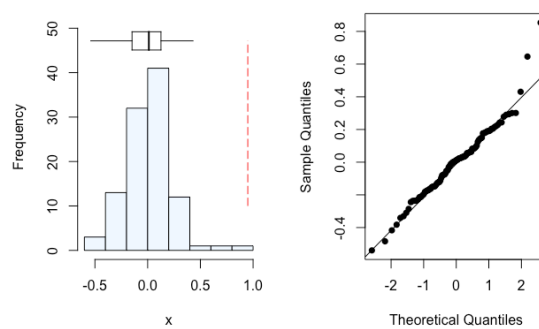
0 outliers

Skewness – 0.5694008

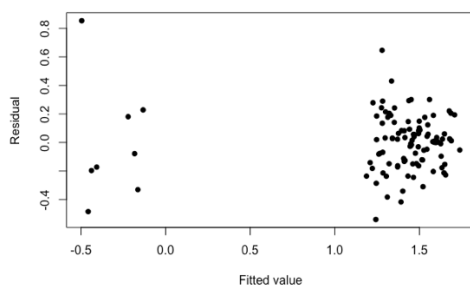
Octile skewness – 0.01019765



logged data



0 outliers
 Skewness – 0.5592889
 Octile skewness – -0.07709273



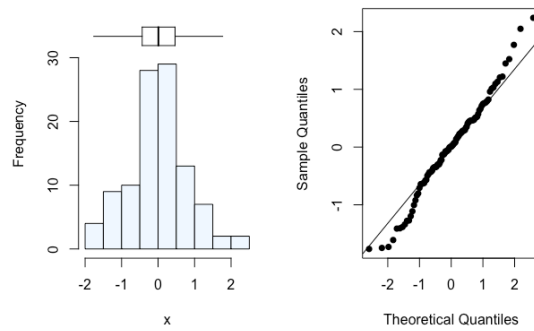
Unlogged data chosen for orthogonal contrasts

Table 7.5 Stem/Leaf dry weight

	Df	Sum Sq	Mean Sq	F value	Pr(>F)
Rep	3	3.699	1.233	1.5219	0.2157622
C1	1	4.612	4.612	5.6938	0.0195481
C2	1	1.052	1.052	1.2988	0.2580605
C3	1	45.280	45.280	55.8962	1.176e ⁻¹⁰
C4	1	4.219	4.219	5.2077	0.0253238
C5	1	0.134	0.134	0.1660	0.6848244
C6	1	9.150	9.150	11.2954	0.0012248
C7	1	7.221	7.221	8.9138	0.0038206
C1:C5	1	1.106	1.106	1.3652	0.2463466
C2:C6	1	11.113	11.113	13.7183	0.0004035
C2:C7	1	1.057	1.057	1.3051	0.2569163
C3:C6	1	33.910	33.910	41.8607	8.985e ⁻⁹
C3:C7	1	0.046	0.046	0.0567	0.8123618
C4:C6	1	0.020	0.020	0.0242	0.8767045
C4:C7	1	1.738	1.738	2.1461	0.1471165
C5:C2	1	0.012	0.012	0.0153	0.9019600
C5:C3	1	0.008	0.008	0.0099	0.9210634
C5:C4	1	1.065	1.065	1.3148	0.2551778
C5:C6	1	0.024	0.024	0.0294	0.8642187
C5:C7	1	0.494	0.494	0.6092	0.4375395
C5:C2:C6	1	0.132	0.132	0.1629	0.6876038
C5:C2:C7	1	0.101	0.101	0.1247	0.7249592
C5:C3:C6	1	0.737	0.737	0.9095	0.3433123
C5:C3:C7	1	0.071	0.071	0.0880	0.7676071
C5:C4:C6	1	0.053	0.053	0.0658	0.7983128
C5:C4:C7	1	0.584	0.584	0.7214	0.3983980
Residuals	75	60.755	0.810		

7.2.2 Grain weight

Unlogged data



0 outliers

Skewness – 0.04787442

Octile skewness – -0.08843443

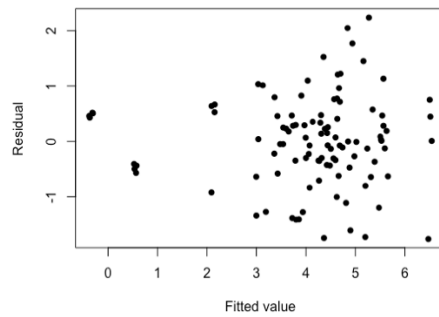


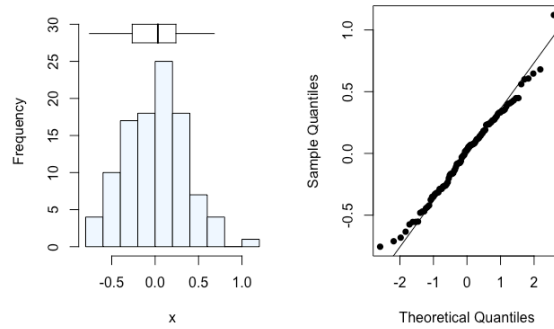
Table 7.6 Grain weight

	Df	Sum Sq	Mean Sq	F value	Pr(>F)
Rep	3	20.855	6.952	7.7947	0.0001346
C1	1	34.268	34.268	38.4238	2.825e ⁻⁸
C2	1	13.202	13.202	14.8027	0.0002488
C3	1	50.800	50.800	56.9606	8.638e ⁻¹¹
C4	1	0.216	0.216	0.2422	0.6240552
C5	1	1.319	1.319	1.4784	0.2278372
C6	1	26.248	26.248	29.4311	6.812e ⁻⁷
C7	1	2.810	2.810	3.1506	0.0799572
C1:C5	1	0.138	0.138	0.1551	0.6948000
C2:C6	1	21.546	21.546	24.1593	5.079e ⁻⁶
C2:C7	1	1.248	1.248	1.3989	0.2406408
C3:C6	1	41.119	41.119	46.1059	2.291e ⁻⁹
C3:C7	1	4.008	4.008	4.4946	0.0373091
C4:C6	1	0.002	0.002	0.0025	0.9603598
C4:C7	1	1.169	1.169	1.3106	0.2559330
C5:C2	1	0.001	0.001	0.0011	0.9742215
C5:C3	1	0.426	0.426	0.4773	0.4918016
C5:C4	1	0.060	0.060	0.0675	0.7957088
C5:C6	1	0.323	0.323	0.3620	0.5492265
C5:C7	1	1.010	1.010	1.1329	0.2905678
C5:C2:C6	1	0.013	0.013	0.0149	0.9030970
C5:C2:C7	1	0.032	0.032	0.0355	0.8509760
C5:C3:C6	1	0.244	0.244	0.2733	0.6026758
C5:C3:C7	1	0.181	0.181	0.2033	0.6533916

C5:C4:C6	1	0.179	0.179	0.2009	0.6553022
C5:C4:C7	1	0.221	0.221	0.2477	0.6201818
Residuals	75	66.888	0.892		

7.2.3 Root weight

Unlogged data



0 outliers

Skewness – 0.1145844

Octile skewness – -0.1621814

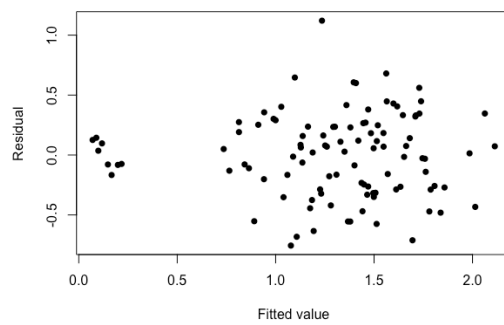


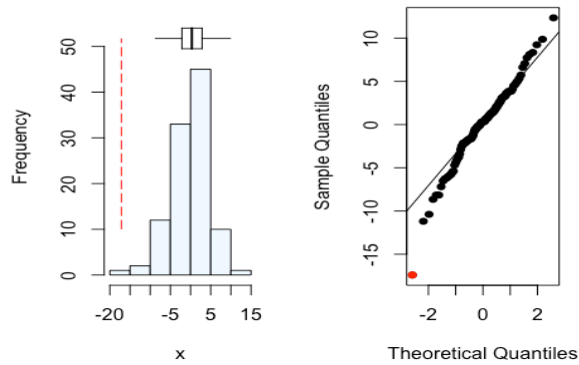
Table 7.7 Root weight

	Df	Sum Sq	Mean Sq	F value	Pr(>F)
Rep	3	0.2479	0.0826	0.5046	0.6803081
C1	1	0.3790	0.3790	2.3137	0.1324430
C2	1	0.6542	0.6542	3.9944	0.0492763
C3	1	5.6410	5.6410	34.4412	1.117e ⁻⁷
C4	1	1.3460	1.3460	8.2182	0.0053801
C5	1	0.0366	0.0366	0.2237	0.6376147
C6	1	2.0864	2.0864	12.7386	0.0006289
C7	1	0.8122	0.8122	4.9590	0.0289558
C1:C5	1	0.3175	0.3175	1.9384	0.1679615
C2:C6	1	4.0962	4.0962	25.0096	3.644e ⁻⁶
C2:C7	1	0.3711	0.3711	2.2659	0.1364503
C3:C6	1	2.6471	2.6471	16.1619	0.0001372
C3:C7	1	0.1029	0.1029	0.6282	0.4305035
C4:C6	1	0.1576	0.1576	0.9623	0.3297566
C4:C7	1	0.2602	0.2602	1.5887	0.2114215
C5:C2	1	0.0856	0.0856	0.5228	0.4719125
C5:C3	1	0.0800	0.0800	0.4881	0.4869154
C5:C4	1	0.3333	0.3333	2.0352	0.1578457
C5:C6	1	0.0133	0.0133	0.0810	0.7766719

C5:C7	1	0.4739	0.4739	2.8935	0.0930820
C5:C2:C6	1	0.1348	0.1348	0.8229	0.3672395
C5:C2:C7	1	0.1931	0.1931	1.1787	0.2811028
C5:C3:C6	1	0.1078	0.1078	0.6581	0.4197855
C5:C3:C7	1	0.0227	0.0227	0.1387	0.7106401
C5:C4:C6	1	0.1035	0.1035	0.6322	0.4290757
C5:C4:C7	1	0.0005	0.0005	0.0032	0.9549174
Residuals	75	12.2839	0.1638		

7.2.4 Stem length

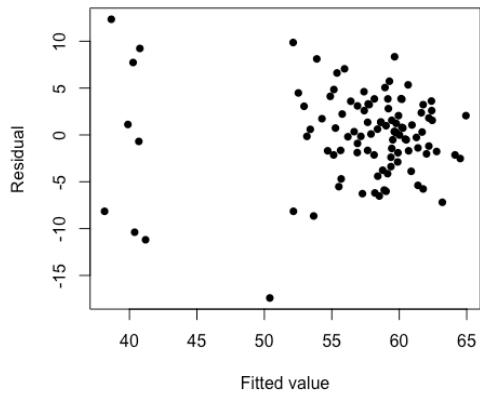
Unlogged data



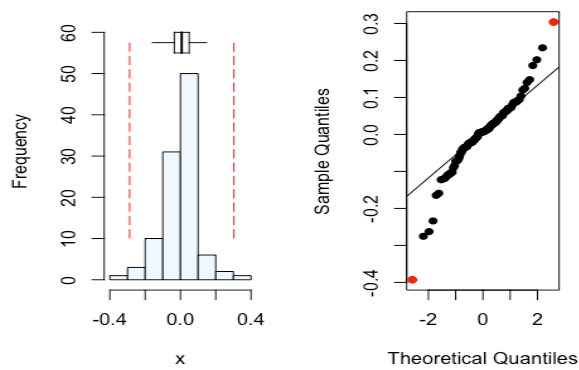
1 outlier

Skewness -- -0.4636124

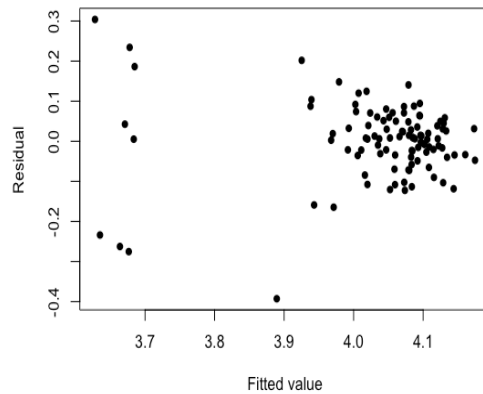
Octile skewness -- -0.1698565



Logged data



2 outliers
 Skewness – -0.6449122
 Octile skewness – -0.1590791



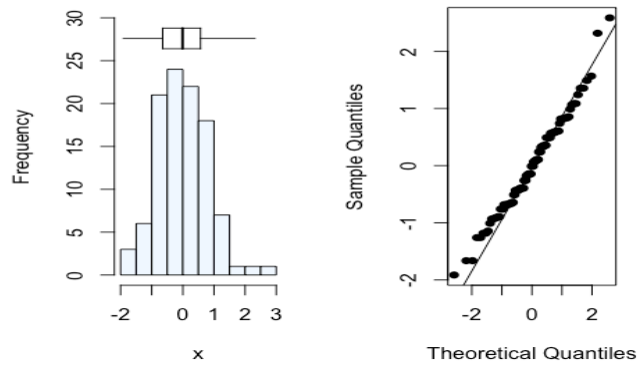
Unlogged data chosen

Table 7.8 Stem length

	Df	Sum Sq	Mean Sq	F value	Pr(>F)
Rep	3	96.81	32.27	1.0808	0.3624778
C1	1	158.67	158.67	5.3147	0.0239137
C2	1	207.09	207.09	6.9364	0.0102529
C3	1	212.52	212.52	7.1182	0.0093457
C4	1	147.00	147.00	4.9237	0.0295160
C5	1	36.96	36.96	1.2380	0.2694109
C6	1	824.43	824.43	27.6136	1.344e ⁻⁶
C7	1	4.22	4.22	0.1413	0.7081021
C1:C5	1	35.67	35.67	1.1949	0.2778483
C2:C6	1	491.79	491.79	16.4723	0.0001199
C2:C7	1	0.27	0.27	0.0090	0.9247461
C3:C6	1	746.57	746.57	25.0059	3.650e ⁻⁶
C3:C7	1	184.59	184.59	6.1828	0.0151239
C4:C6	1	3.22	3.22	0.1077	0.7436648
C4:C7	1	1.41	1.41	0.0472	0.8286229
C5:C2	1	23.01	23.01	0.7707	0.3827994
C5:C3	1	3.52	3.52	0.1179	0.7322540
C5:C4	1	36.75	36.75	1.2309	0.2707744
C5:C6	1	0.00	0.00	0.0001	0.9924977
C5:C7	1	42.02	42.02	1.4074	0.2392387
C5:C2:C6	1	0.88	0.88	0.0295	0.8641335
C5:C2:C7	1	54.39	54.39	1.8218	0.1811625
C5:C3:C6	1	1.88	1.88	0.0629	0.8026316
C5:C3:C7	1	49.29	49.29	1.6509	0.2027944
C5:C4:C6	1	3.54	3.54	0.1185	0.7316412
C5:C4:C7	1	9.34	9.34	0.3127	0.5776650
Residuals	75	2239.19	29.86		

7.2.5 Number of heads

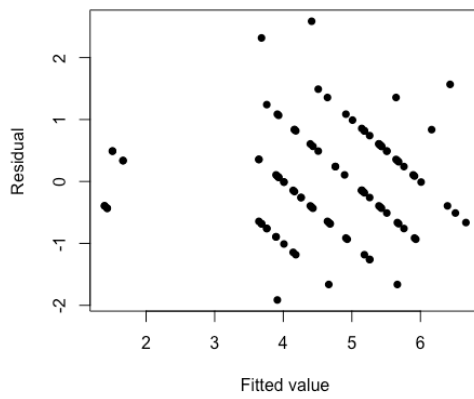
Unlogged data



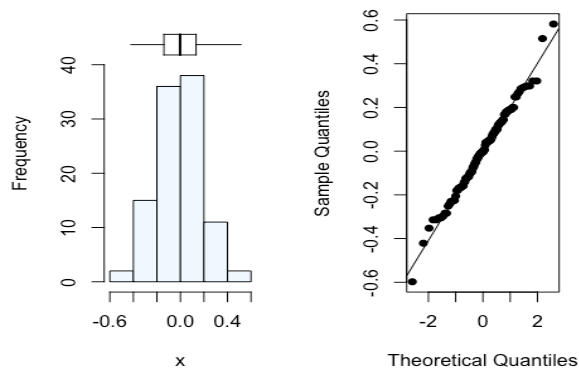
0 outliers

Skewness -- 0.3509044

Octile skewness -- -0.02357836



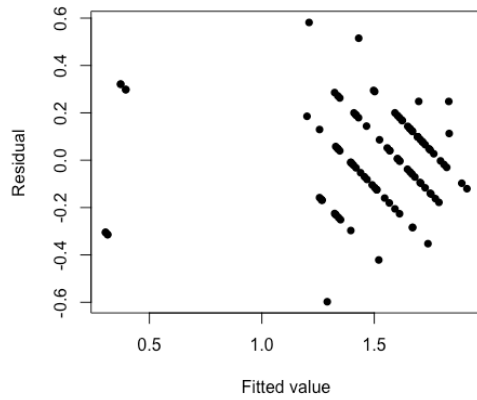
Logged data



0 outliers

Skewness -- 0.01904197

Octile skewness -- -0.0418058



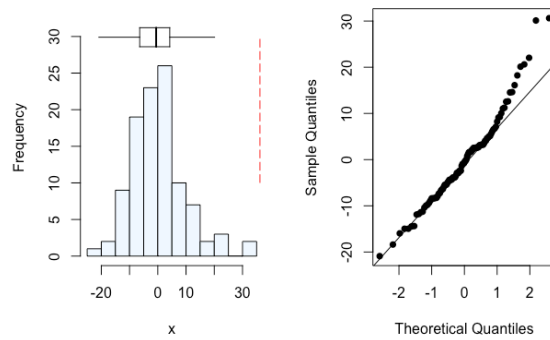
Logged data chosen

Table 7.9 Number of heads

	Df	Sum Sq	Mean Sq	F value	Pr(>F)
Rep	3	0.1499	0.0500	0.9059	0.4423717
C1	1	0.3824	0.3824	6.9319	0.0102769
C2	1	0.8032	0.8032	14.5596	0.0002771
C3	1	3.4428	3.4428	62.4058	1.851e ⁻¹¹
C4	1	0.7229	0.7229	13.1035	0.0005327
C5	1	0.0015	0.0015	0.0275	0.8686433
C6	1	0.6949	0.6949	12.5968	0.0006710
C7	1	0.5304	0.5304	9.6137	0.0027204
C1:C5	1	0.0472	0.0472	0.8550	0.3581017
C2:C6	1	1.3282	1.3282	24.0752	5.250e ⁻⁶
C2:C7	1	0.0546	0.0546	0.9894	0.3230904
C3:C6	1	4.7059	4.7059	85.3013	5.306e ⁻¹⁴
C3:C7	1	0.0082	0.0082	0.1488	0.7007396
C4:C6	1	0.0109	0.0109	0.1975	0.6580328
C4:C7	1	0.0343	0.0343	0.6209	0.4331970
C5:C2	1	0.0431	0.0431	0.7820	0.3793493
C5:C3	1	0.0117	0.0117	0.2123	0.6463339
C5:C4	1	0.1337	0.1337	2.4243	0.1236772
C5:C6	1	0.0406	0.0406	0.7355	0.3938243
C5:C7	1	0.2409	0.2409	4.3665	0.0400434
C5:C2:C6	1	0.2165	0.2165	3.9245	0.0512531
C5:C2:C7	1	0.0484	0.0484	0.8778	0.3518011
C5:C3:C6	1	0.0001	0.0001	0.0021	0.9634130
C5:C3:C7	1	0.0000	0.0000	0.0004	0.9831825
C5:C4:C6	1	0.0053	0.0053	0.0958	0.7578103
C5:C4:C7	1	0.0207	0.0207	0.3752	0.5420476
Residuals	75	4.1376	0.0552		

7.2.6 AMF colonisation

Unlogged data



0 outliers

Skewness – 0.6921325

Octile skewness – 0.07636714

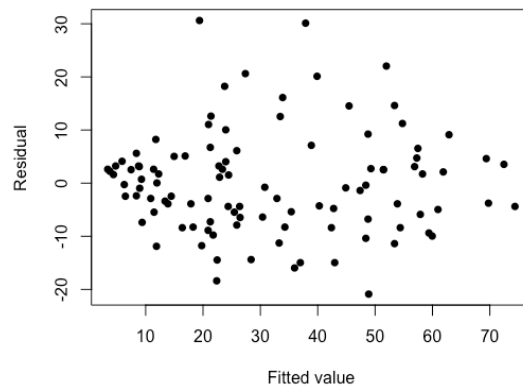


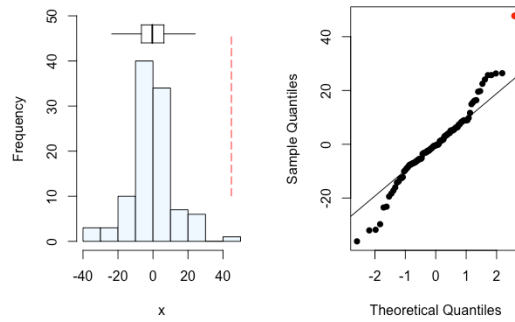
Table 7.10 AMF colonisation

	Df	Sum Sq	Mean Sq	F value	Pr(>F)
Rep	3	434.6	144.9	1.1491	0.3349416
C1	1	262.2	262.2	2.0795	0.1534517
C2	1	0.7	0.7	0.0053	0.9422236
C3	1	24.1	24.1	0.1910	0.6633177
C4	1	70.1	70.1	0.5559	0.4582472
C5	1	21634.6	21634.6	171.6055	< 2.2e ⁻¹⁶
C6	1	405.0	405.0	3.2125	0.0771101
C7	1	2018.6	2018.6	16.0113	0.0001464
C1:C5	1	7.4	7.4	0.0586	0.8094236
C2:C6	1	3877.7	3877.7	30.7580	4.182e ⁻⁷
C2:C7	1	1290.9	1290.9	10.2391	0.0020161
C3:C6	1	2440.2	2440.2	19.3554	3.534e ⁻⁵
C3:C7	1	200.0	200.0	1.5864	0.2117472
C4:C6	1	11.4	11.4	0.0908	0.7640479
C4:C7	1	1293.2	1293.2	10.2578	0.0019982
C5:C2	1	20.2	20.2	0.1600	0.6903286
C5:C3	1	444.1	444.1	3.5225	0.0644319
C5:C4	1	4.1	4.1	0.0324	0.8576620
C5:C6	1	523.9	523.9	4.1552	0.0450326
C5:C7	1	344.9	344.9	2.7357	0.1023066
C5:C2:C6	1	812.0	812.0	6.4411	0.0132260

C5:C2:C7	1	238.0	238.0	1.8881	0.1735049
C5:C3:C6	1	175.3	175.3	1.3902	0.2420933
C5:C3:C7	1	52.9	52.9	0.4196	0.5191217
C5:C4:C6	1	38.9	38.9	0.3089	0.5800170
C5:C4:C7	1	125.7	125.7	0.9972	0.3211891
Residuals	75	9455.4	126.1		

7.2.7 Stem/leaf total zinc concentration

Unlogged data



1 outlier

Skewness – 0.1715431

Octile skewness – 0.009773889

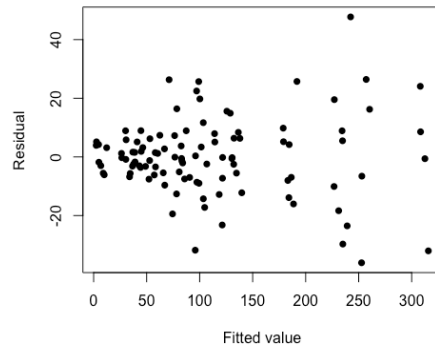


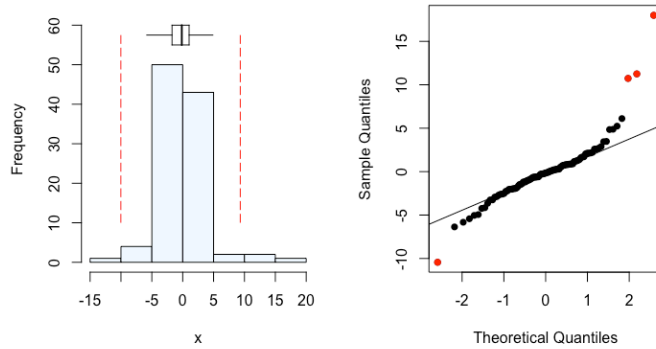
Table 7.11 Stem/leaf total zinc concentration

	Df	Sum Sq	Mean Sq	F value	Pr(>F)
Rep	3	1025	342	1.4509	0.2348278
C1	1	92224	92224	391.6042	< 2.2e ⁻¹⁶
C2	1	190346	190346	808.2474	< 2.2e ⁻¹⁶
C3	1	74061	74061	314.4791	< 2.2e ⁻¹⁶
C4	1	16017	16017	68.0127	4.042e ⁻¹²
C5	1	285	285	1.2107	0.2747151
C6	1	199017	199017	845.0696	< 2.2e ⁻¹⁶
C7	1	15398	15398	65.3830	8.187e ⁻¹²
C1:C5	1	2	2	0.0100	0.9205309
C2:C6	1	25573	25573	108.5889	3.117e ⁻¹⁶
C2:C7	1	4122	4122	17.5021	7.710e ⁻⁵
C3:C6	1	8698	8698	36.9353	4.693e ⁻⁸
C3:C7	1	9791	9791	41.5762	9.866e ⁻⁹
C4:C6	1	2820	2820	11.9745	0.0008933

C4:C7	1	1564	1564	6.6402	0.0119344
C5:C2	1	219	219	0.9313	0.3376347
C5:C3	1	100	100	0.4254	0.5162514
C5:C4	1	1	1	0.0032	0.9551944
C5:C6	1	1115	1115	4.7342	0.0327182
C5:C7	1	279	279	1.1849	0.2798563
C5:C2:C6	1	908	908	3.8562	0.0532677
C5:C2:C7	1	4	4	0.0174	0.8955171
C5:C3:C6	1	4345	4345	18.4498	5.162e ⁻⁵
C5:C3:C7	1	271	271	1.1526	0.2864498
C5:C4:C6	1	4	4	0.0151	0.9024423
C5:C4:C7	1	46	46	0.1974	0.6581169
Residuals	75	17663	236		

7.2.8 Grain total zinc concentration

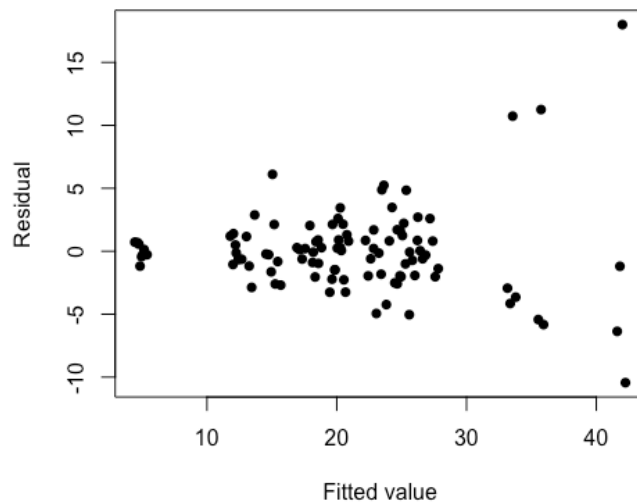
Unlogged data



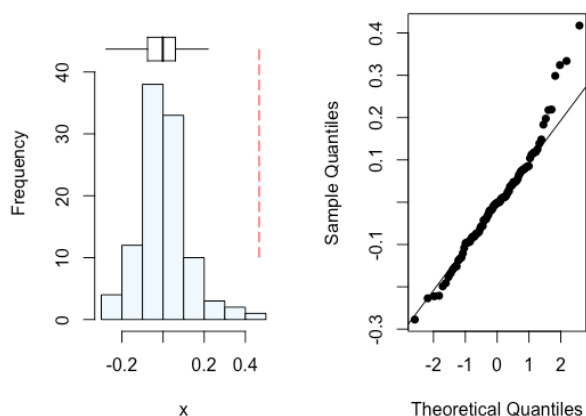
4 outliers

Skewness – 1.638808

Octile skewness – -0.02541846



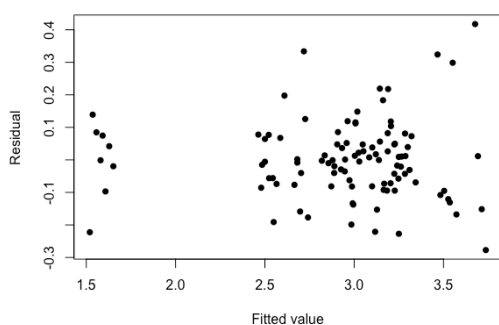
Logged data



0 outliers

Skewness – 0.6394915

Octile skewness – -0.05215117



Logged data chosen

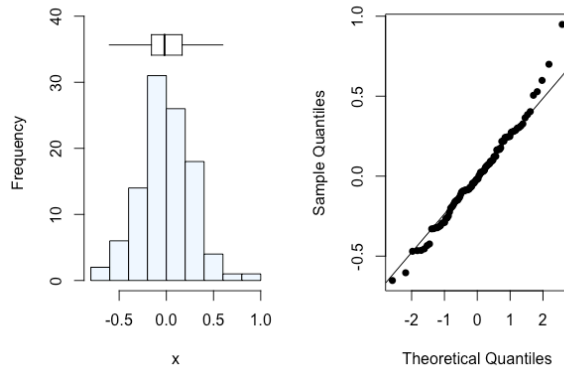
Table 7.12 Grain total zinc concentration

	Df	Sum Sq	Mean Sq	F value	Pr(>F)
Rep	3	0.0237	0.0079	0.3919	0.7591699
C1	1	15.8149	15.8149	784.5398	< 2.2e ⁻¹⁶
C2	1	2.5164	2.5164	124.8331	< 2.2e ⁻¹⁶
C3	1	0.5109	0.5109	25.3457	3.267e ⁻⁶
C4	1	0.6987	0.6987	34.6626	1.069e ⁻⁷
C5	1	0.0163	0.0163	0.8106	0.3708616
C6	1	4.0193	4.0193	199.3887	< 2.2e ⁻¹⁶
C7	1	0.5706	0.5706	28.3057	1.062e ⁻⁶
C1:C5	1	0.0162	0.0162	0.8053	0.3724213
C2:C6	1	0.0357	0.0357	1.7710	0.1873456
C2:C7	1	0.0000	0.0000	0.0000	0.9965892
C3:C6	1	0.3195	0.3195	15.8501	0.0001587
C3:C7	1	0.0090	0.0090	0.4489	0.5049626
C4:C6	1	0.0154	0.0154	0.7639	0.3849238
C4:C7	1	0.0723	0.0723	3.5844	0.0622327
C5:C2	1	0.0122	0.0122	0.6071	0.4383485
C5:C3	1	0.0842	0.0842	4.1750	0.0445852
C5:C4	1	0.0175	0.0175	0.8658	0.3551587
C5:C6	1	0.0000	0.0000	0.0005	0.9830809
C5:C7	1	0.0033	0.0033	0.1639	0.6867479
C5:C2:C6	1	0.0182	0.0182	0.9011	0.3455698

C5:C2:C7	1	0.0271	0.0271	1.3462	0.2496674
C5:C3:C6	1	0.0001	0.0001	0.0031	0.9558971
C5:C3:C7	1	0.0040	0.0040	0.2004	0.6557457
C5:C4:C6	1	0.0091	0.0091	0.4501	0.5043831
C5:C4:C7	1	0.0070	0.0070	0.3450	0.5587648
Residuals	74	1.4917	0.0202		

7.2.8 Root total zinc concentration

Logged data



0 outlier

Skewness – 0.3617072

Octile skewness – 0.01717944

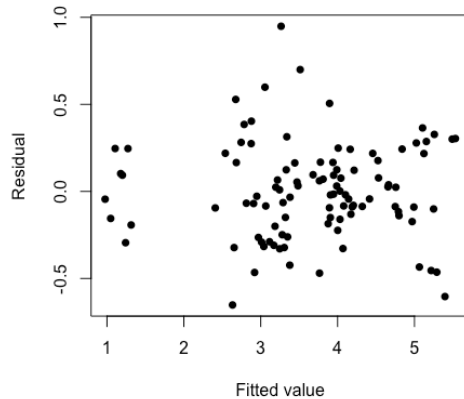


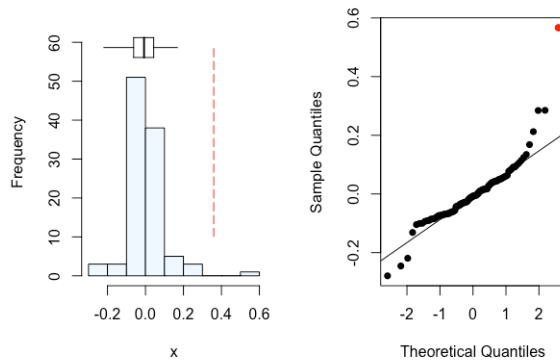
Table 7.13 Root total zinc concentration

	Df	Sum Sq	Mean Sq	F value	Pr(>F)
Rep	3	8246	2749	3.0459	0.033965
C1	1	31673	31673	35.0955	9.195e ⁻⁸
C2	1	38840	38840	43.0370	6.418e ⁻⁹
C3	1	313	313	0.3467	0.557789
C4	1	16563	16563	18.3534	5.444e ⁻⁵
C5	1	470	470	0.5213	0.472568
C6	1	202223	202223	224.0774	< 2.2e ⁻¹⁶
C7	1	5174	5174	5.7335	0.019177
C1:C5	1	88	88	0.0970	0.756329
C2:C6	1	46101	46101	51.0832	5.219e ⁻¹⁰
C2:C7	1	8125	8125	9.0032	0.003671
C3:C6	1	6388	6388	7.0787	0.009560
C3:C7	1	1596	1596	1.7685	0.187650

C4:C6	1	4089	4089	4.5310	0.036615
C4:C7	1	1367	1367	1.5148	0.222313
C5:C2	1	1906	1906	2.1114	0.150430
C5:C3	1	353	353	0.3911	0.533655
C5:C4	1	8	8	0.0088	0.925721
C5:C6	1	1909	1909	2.1158	0.150010
C5:C7	1	1068	1068	1.1833	0.280216
C5:C2:C6	1	3243	3243	3.5939	0.061896
C5:C2:C7	1	282	282	0.3125	0.577848
C5:C3:C6	1	1763	1763	1.9536	0.166379
C5:C3:C7	1	451	451	0.4999	0.481764
C5:C4:C6	1	32	32	0.0359	0.850303
C5:C4:C7	1	828	828	0.9172	0.341321
Residuals	74	66783	902		

7.2.9 Stem/leaf zinc offtake

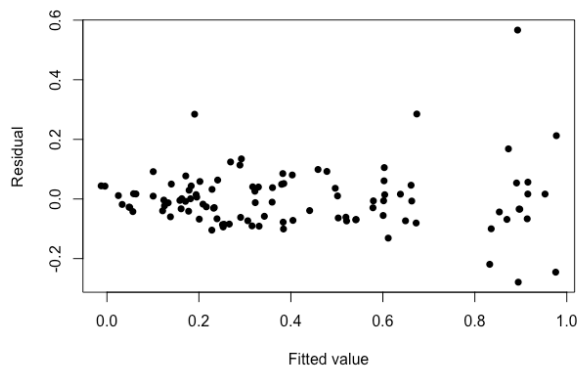
Unlogged data



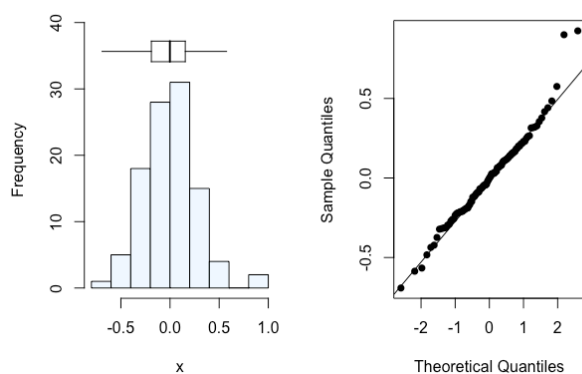
1 outlier

Skewness – -0.2327737

Octile skewness – 0.08414634



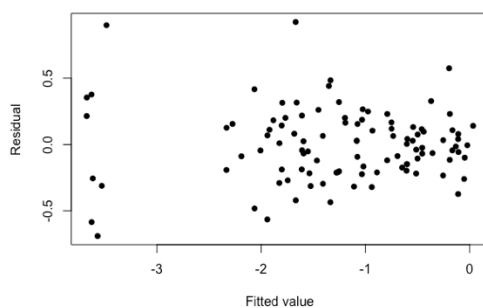
Logged data



0 outliers

Skewness – 0.4766405

Octile skewness – -0.01737672



Logged data chosen

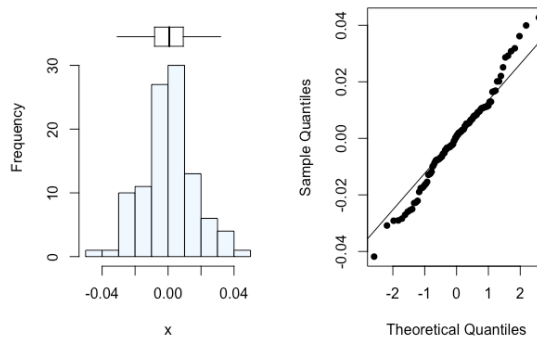
Table 7.14 Stem/leaf zinc offtake

	Df	Sum Sq	Mean Sq	F value	Pr(>F)
Rep	3	0.358	0.119	1.1891	0.319721
C1	1	47.872	47.872	477.3001	< 2.2e ⁻¹⁶
C2	1	8.100	8.100	80.7606	1.578e ⁻¹³
C3	1	1.101	1.101	10.9787	0.001421
C4	1	4.607	4.607	45.9361	2.417e ⁻⁹
C5	1	0.008	0.008	0.0843	0.772350
C6	1	6.462	6.462	64.4325	1.060e ⁻¹¹
C7	1	6.302	6.302	62.8378	1.643e ⁻¹¹
C1:C5	1	0.002	0.002	0.0164	0.898428
C2:C6	1	3.236	3.236	32.2674	2.420e ⁻⁷
C2:C7	1	0.620	0.620	6.1833	0.015120
C3:C6	1	7.124	7.124	71.0324	1.827e ⁻¹²
C3:C7	1	1.204	1.204	12.0093	0.000879
C4:C6	1	0.089	0.089	0.8910	0.348241
C4:C7	1	0.681	0.681	6.7925	0.011036
C5:C2	1	0.004	0.004	0.0428	0.836600
C5:C3	1	0.061	0.061	0.6088	0.437703
C5:C4	1	0.077	0.077	0.7648	0.384632
C5:C6	1	0.002	0.002	0.0240	0.877190
C5:C7	1	0.118	0.118	1.1783	0.281188
C5:C2:C6	1	0.016	0.016	0.1607	0.689619
C5:C2:C7	1	0.021	0.021	0.2115	0.646938

C5:C3:C6	1	0.000	0.000	0.0037	0.951912
C5:C3:C7	1	0.007	0.007	0.0734	0.787262
C5:C4:C6	1	0.002	0.002	0.0163	0.898902
C5:C4:C7	1	0.154	0.154	1.5337	0.219428
Residuals	75	7.522	0.100		

7.2.10 Grain zinc offtake

Unlogged data



0 outliers

Skewness – 0.1188919

Octile skewness – -0.0809649

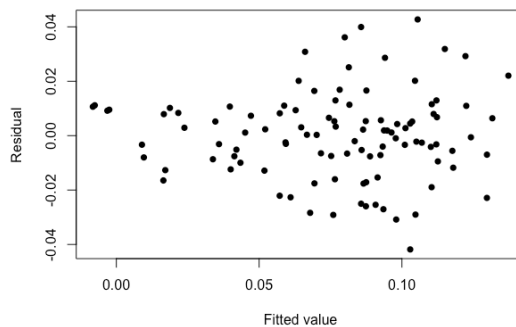


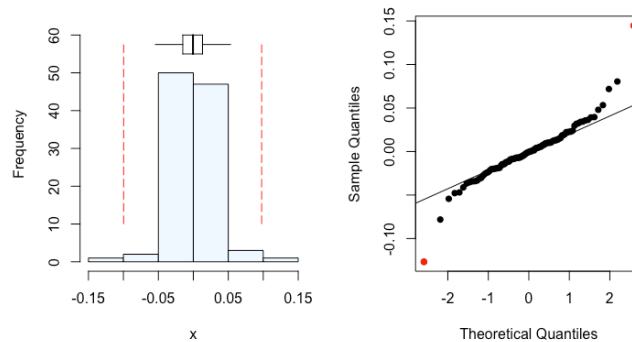
Table 7.15 Grain zinc offtake

	Df	Sum Sq	Mean Sq	F value	Pr(>F)
Rep	3	0.0098754	0.0032918	9.3875	2.420e ⁻⁵
C1	1	0.0190410	0.0190410	54.3011	1.878e ⁻¹⁰
C2	1	0.0000206	0.0000206	0.0589	0.808980
C3	1	0.0255837	0.0255837	72.9592	1.110e ⁻¹²
C4	1	0.0036319	0.0036319	10.3573	0.001906
C5	1	0.0004962	0.0004962	1.4150	0.237975
C6	1	0.0000163	0.0000163	0.0466	0.829691
C7	1	0.0097942	0.0097942	27.9311	1.192e ⁻⁶
C1:C5	1	0.0000916	0.0000916	0.2613	0.610699
C2:C6	1	0.0225204	0.0225204	64.2234	1.123e ⁻¹¹
C2:C7	1	0.0000346	0.0000346	0.0986	0.754372
C3:C6	1	0.0253959	0.0253959	72.4239	1.274e ⁻¹²
C3:C7	1	0.0004779	0.0004779	1.3629	0.246726
C4:C6	1	0.0003674	0.0003674	1.0476	0.309346
C4:C7	1	0.0000360	0.0000360	0.1026	0.749630
C5:C2	1	0.0000338	0.0000338	0.0965	0.756979

C5:C3	1	0.0000124	0.0000124	0.0354	0.851349
C5:C4	1	0.0000145	0.0000145	0.0415	0.839161
C5:C6	1	0.0001314	0.0001314	0.3748	0.542246
C5:C7	1	0.0006201	0.0006201	1.7684	0.187608
C5:C2:C6	1	0.0000018	0.0000018	0.0050	0.943839
C5:C2:C7	1	0.0001890	0.0001890	0.5391	0.465113
C5:C3:C6	1	0.0004650	0.0004650	1.3260	0.253178
C5:C3:C7	1	0.0002086	0.0002086	0.5949	0.442939
C5:C4:C6	1	0.0002254	0.0002254	0.6429	0.425211
C5:C4:C7	1	0.0001992	0.0001992	0.5680	0.453410
Residuals	75	0.0262993	0.0003507		

7.2.11 Root zinc offtake

Unlogged data



2 outliers

Skewness – 0.4060524

Octile skewness – 0.05162943

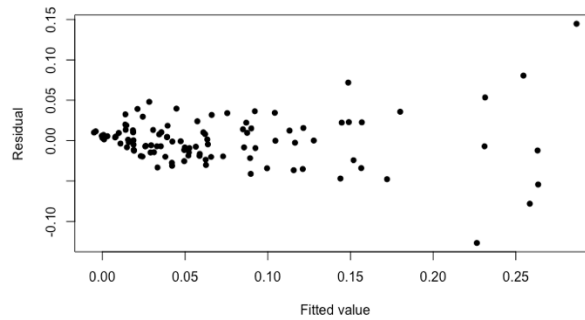


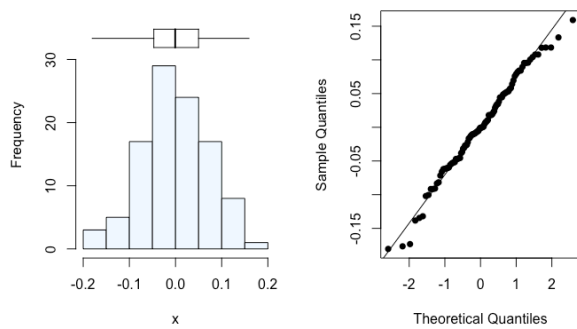
Table 7.16 Root zinc offtake

	Df	Sum Sq	Mean Sq	F value	Pr(>F)
Rep	3	0.012575	0.004192	3.0824	0.0324042
C1	1	0.039306	0.039306	28.9045	8.284e ⁻⁷
C2	1	0.021609	0.021609	15.8907	0.0001543
C3	1	0.104551	0.104551	76.8844	4.107e ⁻¹³
C4	1	0.048994	0.048994	36.0291	6.415e ⁻⁸
C5	1	0.000267	0.000267	0.1960	0.6592547
C6	1	0.125030	0.125030	91.9436	1.139e ⁻¹⁴
C7	1	0.001409	0.001409	1.0363	0.3119500
C1:C5	1	0.000010	0.000010	0.0077	0.9304155
C2:C6	1	0.000441	0.000441	0.3242	0.5707771
C2:C7	1	0.000001	0.000001	0.0010	0.9750214

C3:C6	1	0.092684	0.092684	68.1575	$3.889e^{-12}$
C3:C7	1	0.006874	0.006874	5.0550	0.0274932
C4:C6	1	0.016631	0.016631	12.2303	0.0007939
C4:C7	1	0.003501	0.003501	2.5747	0.1127905
C5:C2	1	0.001672	0.001672	1.2295	0.2710460
C5:C3	1	0.001075	0.001075	0.7902	0.3768751
C5:C4	1	0.000458	0.000458	0.3371	0.5632511
C5:CoL	1	0.000281	0.000281	0.2070	0.6504561
C5:CoQ	1	0.000079	0.000079	0.0583	0.8098496
C5:C2:C6	1	0.001205	0.001205	0.8864	0.3494798
C5:C2:C7	1	0.000150	0.000150	0.1101	0.7409371
C5:C3:C6	1	0.000005	0.000005	0.0034	0.9534374
C5:C3:C7	1	0.000099	0.000099	0.0725	0.7884832
C5:C4:C6	1	0.000221	0.000221	0.1628	0.6877662
C5:C4:C7	1	0.001327	0.001327	0.9757	0.3264299
Residuals	75	0.101989	0.001360		

7.2.12 Soil pH

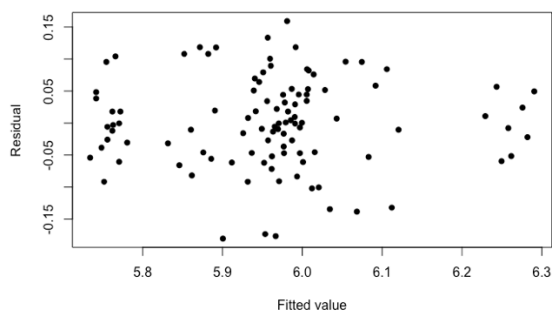
Unlogged data



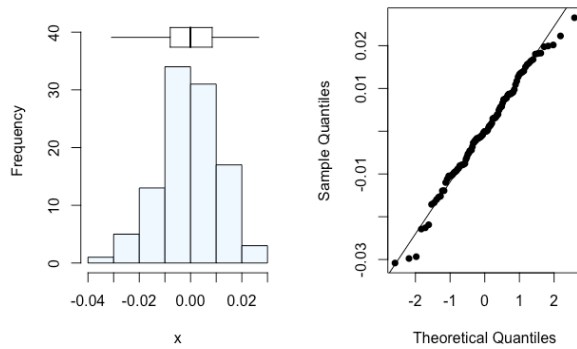
0 outlier

Skewness – -0.2327737

Octile skewness – 0.08414634



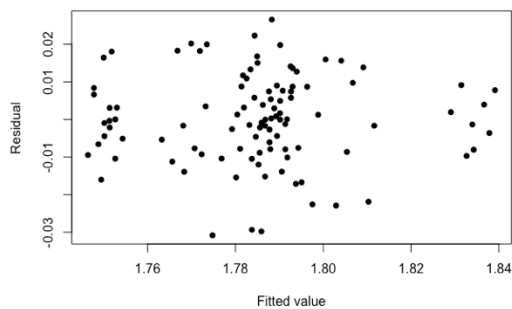
Logged data



0 outlier

Skewness – -0.2427952

Octile skewness – 0.07911044



Unlogged data chosen

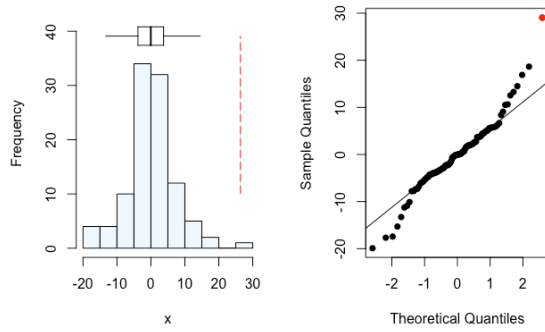
Table 7.17 Soil pH

	Df	Sum Sq	Mean Sq	F value	Pr(>F)
Rep	3	0.01153	0.00384	0.5616	0.64203
C1	1	0.01725	0.01725	2.5216	0.11650
C2	1	0.00027	0.00027	0.0390	0.84402
C3	1	1.01501	1.01501	148.3644	< 2.2e ⁻¹⁶
C4	1	0.03000	0.03000	4.3851	0.03963
C5	1	0.00070	0.00070	0.1025	0.74979
C6	1	0.02116	0.02116	3.0933	0.08270
C7	1	0.00000	0.00000	0.0004	0.98455
C1:C5	1	0.00388	0.00388	0.5669	0.45386
C2:C6	1	0.01772	0.01772	2.5895	0.11178
C2:C7	1	0.03837	0.03837	5.6092	0.02044
C3:C6	1	0.41438	0.41438	60.5695	3.09e ⁻¹¹
C3:C7	1	0.03260	0.03260	4.7657	0.03216
C4:C6	1	0.00215	0.00215	0.3142	0.57677
C4:C7	1	0.02190	0.02190	3.2012	0.07762
C5:C2	1	0.00427	0.00427	0.6237	0.43218
C5:C3	1	0.00163	0.00163	0.2387	0.62654
C5:C4	1	0.00608	0.00608	0.8880	0.34905
C5:C6	1	0.00571	0.00571	0.8348	0.36382
C5:C7	1	0.01327	0.01327	1.9391	0.16788
C5:C2:C6	1	0.00053	0.00053	0.0773	0.78181
C5:C2:C7	1	0.00005	0.00005	0.0071	0.93312
C5:C3:C6	1	0.00577	0.00577	0.8435	0.36135

C5:C3:C7	1	0.00036	0.00036	0.0524	0.81950
C5:C4:C6	1	0.01911	0.01911	2.7926	0.09887
C5:C4:C7	1	0.00104	0.00104	0.1527	0.69704
Residuals	75	0.51310	0.00684		

7.2.13 Soil DTPA

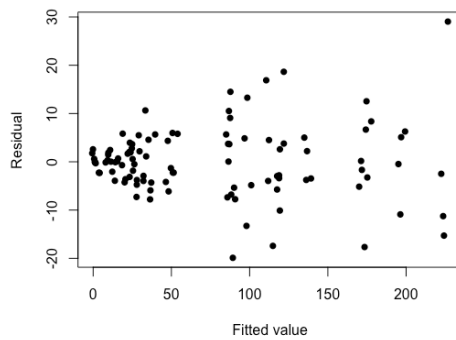
Unlogged data



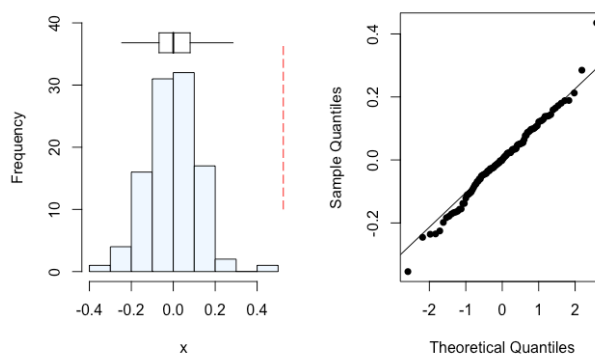
1 outlier

Skewness – 0.4339246

Octile skewness – -0.02528432



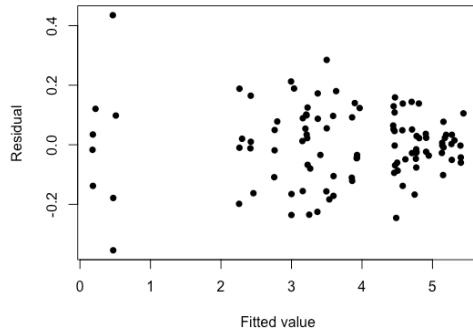
Logged data



0 outliers

Skewness – 0.09776272

Octile skewness – -0.08999039



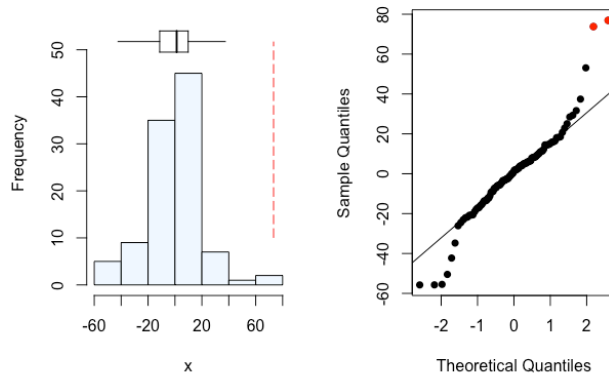
Logged data chosen

Table 7.18 Soil DTPA

	Df	Sum Sq	Mean Sq	F value	Pr(>F)
Rep	3	0.030	0.010	0.4871	0.6922583
C1	1	100.484	100.484	4864.5152	< 2.2e ⁻¹⁶
C2	1	20.544	20.544	994.5557	< 2.2e ⁻¹⁶
C3	1	1.526	1.526	73.8788	8.773e ⁻¹³
C4	1	19.071	19.071	923.2281	< 2.2e ⁻¹⁶
C5	1	0.054	0.054	2.6075	0.1105614
C6	1	35.452	35.452	1716.2729	< 2.2e ⁻¹⁶
C7	1	3.205	3.205	155.1686	< 2.2e ⁻¹⁶
C1:C5	1	0.128	0.128	6.1745	0.0151900
C2:C6	1	0.193	0.193	9.3499	0.0030902
C2:C7	1	0.002	0.002	0.0817	0.7758591
C3:C6	1	0.291	0.291	14.0889	0.0003418
C3:C7	1	0.066	0.066	3.1902	0.0781214
C4:C6	1	0.245	0.245	11.8625	0.0009408
C4:C7	1	1.036	1.036	50.1311	6.563e ⁻¹⁰
C5:C2	1	0.017	0.017	0.8401	0.3623143
C5:C3	1	0.001	0.001	0.0249	0.8750379
C5:C4	1	0.001	0.001	0.0330	0.8563517
C5:C6	1	0.008	0.008	0.3920	0.5331716
C5:C7	1	0.176	0.176	8.5381	0.0045935
C5:C2:C6	1	0.014	0.014	0.6999	0.4054847
C5:C2:C7	1	0.023	0.023	1.1317	0.2908364
C5:C3:C6	1	0.020	0.020	0.9498	0.3329115
C5:C3:C7	1	0.003	0.003	0.1476	0.7019591
C5:C4:C6	1	0.023	0.023	1.1372	0.2896600
C5:C4:C7	1	0.040	0.040	1.9563	0.1660318
Residuals	75	1.549	0.021		

7.2.14 Soil E values

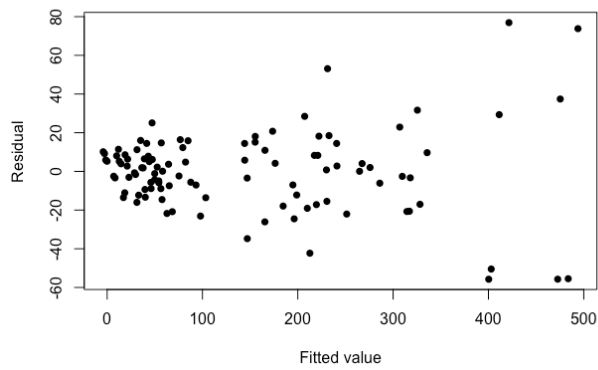
Unlogged data



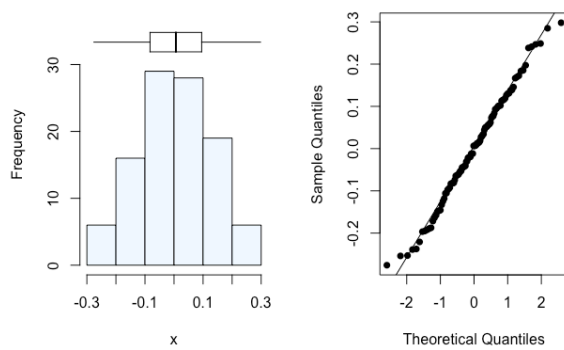
2 outliers

Skewness – 0.3306726

Octile skewness – -0.1762258



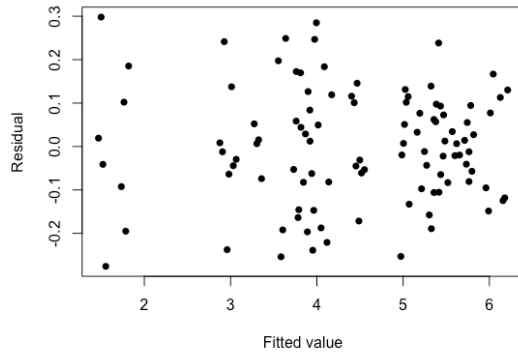
Logged data



0 outlier

Skewness – 0.0318437

Octile skewness – -0.1059572



Logged data chosen

Table 7.19 Soil E values

	Df	Sum Sq	Mean Sq	F value	Pr(>F)
Rep	3	0.098	0.033	1.4133	0.245550
C1	1	66.589	66.589	2871.9039	< 2.2e ⁻¹⁶
C2	1	19.615	19.615	845.9904	< 2.2e ⁻¹⁶
C3	1	2.366	2.366	102.0426	1.232e ⁻¹⁵
C4	1	23.259	23.259	1003.1388	< 2.2e ⁻¹⁶
C5	1	0.026	0.026	1.1236	0.292551
C6	1	37.270	37.270	1607.4004	< 2.2e ⁻¹⁶
C7	1	3.408	3.408	146.9664	< 2.2e ⁻¹⁶
C1:C5	1	0.118	0.118	5.0810	0.027110
C2:C6	1	0.603	0.603	26.0032	2.482e-06
C2:C7	1	0.005	0.005	0.2133	0.645560
C3:C6	1	0.173	0.173	7.4758	0.007798
C3:C7	1	0.052	0.052	2.2310	0.139465
C4:C6	1	0.444	0.444	19.1582	3.837e ⁻⁵
C4:C7	1	1.242	1.242	53.5618	2.337e ⁻¹⁰
C5:C2	1	0.035	0.035	1.5092	0.223095
C5:C3	1	0.001	0.001	0.0290	0.865216
C5:C4	1	0.001	0.001	0.0383	0.845441
C5:C6	1	0.030	0.030	1.2970	0.258392
C5:C7	1	0.159	0.159	6.8631	0.010645
C5:C2:C6	1	0.037	0.037	1.5746	0.213437
C5:C2:C7	1	0.020	0.020	0.8418	0.361836
C5:C3:C6	1	0.039	0.039	1.6606	0.201481
C5:C3:C7	1	0.006	0.006	0.2478	0.620067
C5:C4:C6	1	0.020	0.020	0.8609	0.356469
C5:C4:C7	1	0.063	0.063	2.7367	0.102248
Residuals	75	1.739	0.023		